UNIVERSITÀ
DEGLI STUDI
DI MILANO

DEPARTMENT OF PHARMACEUTICAL SCIENCES

Doctoral School in Pharmaceutical Sciences

XXXI Cycle

Analytical Strategies for the Identification and Characterization of RAGE Binders of Proinflammatory Mediators, AGEs and ALEs

SECTOR CHIM/08 – PHARMACEUTICAL CHEMISTRY

Marco Mol

R11506

Tutor: Prof. Giancarlo Aldini

PhD coordinator: PROF. GIANCARLO ALDINI

Academic year 2018/2019

Declaration of originality

I declare that all of the work presented in this thesis is my own, and that all else, figures, images, ideas, quotations, data, results, published or unpublished, have been acknowledged and referenced.

This thesis contains some modified material from my deliverables, milestones and progress reports submitted for MASSTRPLAN.

Marco Mol
August 2019

Funding

This work has been funded by the European Union's Horizon 2020 research and innovation programme under the Marie Sklowdowska- Curie grant agreement number 675132 (http://cordis.europa.eu/ project/rcn/198275_en.html).

Scientific contributions

Publications

Mol, M., Regazzoni, L., Altomare, A., Degani, G., Carini, M., Vistoli, G., & Aldini, G. (2017). Enzymatic and non-enzymatic detoxification of 4-hydroxynonenal: methodological aspects and biological consequences. Free Radical Biology and Medicine, 111, 328-344.

Mol, M., Degani, G., Coppa, C., Baron, G., Popolo, L., Carini, M., ... & Altomare, A. (2018). Advanced lipoxidation end products (ALEs) as RAGE binders: Mass spectrometric and computational studies to explain the reasons why. Redox biology, 101083.

Degani, G., Baron, G., **Mol, M.**, Carini, M., Aldini, G. and Altomare, A., 2019. 'Methods for detection and quantification of non-enzymatic protein modifications', in Sadowska-Bartosz, I. (ed.) *Non-Enzymatic Protein Modifications in Health, Disease and Ageing*. Elsevier. (Submitted)

Mol, M., Baron, G., Carini, M., Aldini, G. & Altomare, A. (2019) Identification of low-abundant AGEs/ALEs in plasma of heart-failure patients using Orbitrap Fusion. Manuscript under preparation.

Oral communications

Mol, M., Altomare, A., Degani, G., D'Amato, A., Vistoli, G., Banfi, C., Carini, M., Popolo, L. & Aldini, G. (2019). Mass spectrometry and VC-1 affinity chromatography as an integrated strategy to identify pro-inflammatory AGEs and ALEs. In: *Advances in the study of lipid and protein oxidation: from methods to targets*, 13-15 March 2019, Ghent, Belgium.

Mol, M., Altomare, A., Degani, G., D'Amato, A., Vistoli, G., Banfi, C., Carini, M., Popolo, L. & Aldini, G. (2019). Mass spectrometry and VC-1 affinity chromatography as an integrated strategy to identify pro-inflammatory AGEs and ALEs. In: *OMICS Integration*, 5 April 2019, Milan, Italy.

Poster presentations

Mol, M. Degani, G. Altomare, A. Popolo, L. and Aldini, G. Analytical strategies for the identification and characterization of protein adducts with HNE and related compounds. In: *International HNE Club Meeting*, 14-15 September 2017, Graz, Austria.

Mol, M., Altomare, A., Degani, G., Popolo, L., Vistoli, G., Raucci, A., & Aldini, G. (2018). Identification and characterization of pro-inflammatory AGEs and ALEs by VC1-affinity chromatography and mass spectrometry. In: *SFRR-International Meeting*, 4-7 June 2018, Lisbon, Portugal.

Acknowledgements

Without the following people, this work would not have been possible.

Massive thanks to my supervisor Prof. Aldini, for giving me the opportunity to undertake my PhD part of an ITN-network. Also, lots of gratitude for the support, guidance, inspiration, patience and understanding, of both the scientific and personal kind.

I would like to thank everybody that was/is part of the analytical research group on the first floor of the Department of Pharmaceutical Sciences under the supervision of Prof Aldini and Prof. Carini. Special thanks to Luca for helping me around during my first weeks, to Cristina for helping me with any kind of paperwork, to Alessandra, Genny, Giovanna and Ettore for answering my many questions about research. Lastly, I would like to thank Sarath, with whom I had the pleasure to share offices with for the past three years. Dr. Raucci for providing the cell line and advice on cellular techniques. Dr. Widera for providing the lentiviral vectors. Dr. Banfi for proving us plasma samples of healthy subjects and heart failure patients.

My sincere thanks to the European joint doctoral program MASSTRPLAN and to its funding entity, the Marie Skłodowska-Curie EU Framework for Research and Innovation Horizon 2020 (Grant agreement number 675132) and to all the people involved. In particular, Prof. Spickett for the outstanding work in managing this network and for support during my secondment. Debbie Toomeoks for constant support throughout the project and easing our lives in Birmingham during my secondment. Prof. Domingues, for giving me the introduction to the lipidomics field and support during my secondment. And to all the ESRs involved, making every training and network event a success.

My family and friends, who have supported and sustained me throughout. My children, Ethan and Alba, for always keeping me positive and for the very few times they let me work. But most of all my lovely wife Maria, for unconditional care, support, encouragement, inspiration and perspective.

Abbreviations

AAPH	2,2'-Azobis(2-amidinopropane) dihydrochloride
ACR	Acrolein
ADH	Alcoholdehydrogenase
AGE	Advanced glycoxidation end products
AGER	Advanced glycation end products specific receptor
AKR	Aldo-keto reductase
ALDH	Aldehydedehydrogenase
ALE	Advanced lipoxidation end products
APCI	Atmospheric pressure chemical ionization
ARP	Aldehyde reactive probe
CEL	Carboxy-ethyllysine
CID	Collision-induced dissociation
CML	Carboxy-methyllysine
CYP	Cytochromes P450
DHN	1,4-dihydroxy-2-nonene
DHP	Di-hydropyridine adduct
DNPH	2,4-Dinitrophenylhydrazine
ECD	Electron-capture dissociation
ELISA	Enzyme-linked immunosorbent assay
ESI	Electrospray ionization
ETD	Electron-transfer dissociation
FDP	N-(3-formyl-3,4-dehydro-piperidinyl)
FITCR	Fourier-transform ion cyclotron resonance
GC	Gas chromatography
GO	Glyoxal
GSH	Glutathion
GST	Glutathione S-transferase
HCD	Higher-energy collisional dissociation
HHE	4-hydroxy-2-hexenal
HNA	4-hydroxynonenoic acid
HNE	4-hydroxy-(2)-nonenal
HPLC	High-performance liquid chromatography

HR-MS	High-resolution mass spectrometry
HSA	Human serum albumin
HTPO	N−2-(4 hydroxy-tetrahydro-pyrimidyl) ornitine (propane-arginine)
iTRAQ	Isobaric tags for relative and absolute quantitation
LC	Liquid chromatography
MA	Michael adduct
MALDI	Matrix-assisted laser desorption/ionization
MDA	Malondialdehyde
MG	Methylglyoxal
MP	Nε-(3-methylpyridinium)
MRM	Multiple reaction monitoring
MS	Mass spectrometry
NADP	Nicotinamide adenine dinucleotide phosphate
NADPH	Dihydronicotinamide-adenine dinucleotide phosphate
nePTM	Non-enzymatic post-translational modification
NF-κB	Nuclear factor kappa-light-chain-enhancer of activated B cells
NP	N-propenal adduct
NPO	N-2-pyrimidyl-ornithine adduct
nrf2	Nuclear factor erythroid 2-related factor 2
PCO	Protein carbonyl
PP	2-pentyl-pyrrole
PTM	Post-translational modification
PUFA	Polyunsaturated fatty acid
PVDF	Polyvinylidene fluoride or polyvinylidene difluoride
RAGE	Receptor for advanced glycation end products
RCS	Reactive carbonyl species
RNS	Reactive nitrogen species
ROS	Reactive oxygen species
SB	Schiff’s base
SILAC	Stable Isotope Labeling by/with Amino acids in Cell culture
SIM	Selected ion monitoring
SRM	Selected reaction monitoring
TMT	Tandem Mass Tag

Table of Contents

Declaration of originality *2*
Funding *2*
Scientific contributions *3*
Abbreviations *5*
Table of Contents *7*
List of figures *11*
Chapter I 11
Chapter III 11
Chapter IV 11
Chapter V 13
Chapter VI 15
Chapter VII 16
Appendix I 17
List of tables *18*
Chapter III 18
Chapter IV 18
Chapter V 18
Chapter VI 19
List of appendices *19*
Chapter I: Introduction *21*
1.1 Oxidative stress 21
1.2 Advanced Glycation End Products 22
1.3 Advanced lipoxidation end products 23
1.4 Biological significance of AGEs and ALEs 24
1.5 Identification and characterization 25
1.6 Receptor for advanced glycation end products (RAGE) 25
1.7 NF-κB pathway 26
References 26
Chapter II: Aim of the project *30*
Chapter III: Enzymatic and non-enzymatic detoxification of 4-hydroxynonenal: Methodological aspects and biological consequences *33*
Abstract 33
3 1. Introduction 33

3.2. Enzymatic detoxification 34
3.2.1. Phase I Metabolism 34
3.2.1.1. Oxidation 34
3.2.1.2. Reduction 35
3.2.1.3. Oxidation and reduction 36
3.2.2. Phase II metabolism 36
2.2.1. Glutathione conjugation 36
3.2.2.2. Putative phase II metabolites from uncharacterized pathways 37
3.2.3. Quantitative aspects of HNE phase I and phase II metabolism 37
3.2.4. Transport and excretion of HNE metabolites 38
3.2.5. Enantioselectivity of phase I and phase II reactions 39
3.2.6. Analytical aspects of HNE metabolism tracking 39
3.2.7. Biological activity of phase I and II HNE metabolites 40

3.3. Non-enzymatic detoxification 40
3.3.1. Protein adducts 40
3.3.1.1. HNE induced protein carbonylation: general aspects 40
3.3.1.2. Biological effects of HNE protein modification 41
3.3.1.2.1. Damaging effects. 41
3.3.1.3. Proteomic study for identifying HNE protein targets 43
3.3.1.4. HNE Protein adduct stability and metabolic turnover 43
3.3.2. Adducts with nucleic acids 44
3.3.3. Adducts with endogenous peptides 45
3.3.4. HNE and small endogenous molecules 45
3.3.4.1. Reactions with cofactors and vitamins 45
3.3.4.2. Reaction with hydrogen sulphide (H_2S) 45
3.3.4.3. Reaction with aminophospholipids 45

3.4. Conclusion and future perspectives 46

Acknowledgements 46

References 46

Chapter IV: Methods for detection and quantification of non-enzymatic protein modifications 51

Abstract 51

4.1 Introduction 51

4.2 Analytical methods for qualitative identification of nePTMs 54
4.2.1 MS top down 56
4.2.2 MS Bottom UP 58
4.2.3 Chemical derivatization and enrichment methods 59

4.3 Overview of the analytical methods for the measurements of specific nePTM 61
4.3.1 Carbonylation 61
4.3.2 Glycation (Early and Advanced Glycation end Products) 65
4.3.3 Deamidation, isomerization or racemization 68
4.3.4 Methionine and cysteine oxidation 72
4.3.5 Protein nitration 79

4.4 MS Quantification 81

References 85

Chapter V: Advanced lipoxidation end products (ALEs) as RAGE binders: Mass spectrometric and computational studies to explain the reasons why 97

Abstract ... **97**

5.1. Introduction ... **97**

5.2. Materials and methods ... **98**
5.2.1. Reagents ... 98
5.2.2. In vitro generation of ALEs-HSA ... 98
5.2.3. Intact protein analysis by MS ... 98
5.2.4. VC1 pull-down assay ... 99
5.2.5. Electrophoretic procedures ... 99
5.2.6. ALE-HSA in-gel digestion ... 99
5.2.7. Mass spectrometry analyses ... 100
5.2.8. Identification and localization of protein adducts ... 100
5.2.9. Semi-quantitative analysis of ALE-HSA adducts ... 100
5.2.10. Computational studies ... 100

5.3. Results ... **101**
5.3.1. Intact protein analysis of HSA and ALEs-HSA by MS ... 101
5.3.2. Pull-down assay with modified albumins ... 102
5.3.3. Identification and localization of protein adducts by mass spectrometry ... 102
5.3.4. Semi-quantitative analysis of ALE-HSA adducts ... 102
5.3.5. Computational results ... 102

5.4. Discussion ... **107**

5.5. Conclusions ... **108**

Acknowledgements ... **109**

Conflict of interest ... **109**

References ... **109**

Appendix A ... **110**

Chapter VI – Analysis of AGEs/ALEs in plasma samples ... ***117***

Abstract ... **117**

6.1. Introduction ... **117**

6.2. Materials and methods ... **119**
6.2.1. Reagents ... 119
6.2.3 Blood collection ... 119
6.2.4 In-vitro oxidation of plasma ... 119
6.2.5 Plasma incubation with RCS ... 120
6.2.6 Measurement of plasma oxidation ... 120
6.2.7 Protein carbonyl measurement ... 120
6.2.8 VC1 pull-down assay ... 120
6.2.9 HSA extraction ... 121
6.2.10 Reduction with sodium borohydride ... 121
6.2.11 Intact protein analysis by MS ... 121
6.2.12 In-gel and in-solution digestion ... 122
6.2.13 Mass spectrometry analyses ... 122
6.2.14 Identification and localization of protein adducts ... 123
6.2.15 pFind ... 123

6.3. Results ... **124**
6.3.1 Oxidizability of healthy human plasma ... 124
6.3.2 Longer incubations with AAPH ... 125
6.3.3 Intact protein analysis ... 126

6.3.4 Spectral counting 127
6.3.5 Plasma incubation with RCS 128
6.3.6 VC1 Pull-Down assay 130
6.3.7 HSA extraction 130
6.3.8 Heart failure stage III samples 131
6.3.9 Validation of identified AGEs/ALEs 133
6.4. Discussion 133
References 135
Appendix 137
Chapter VII: Effect of AGEs and ALEs on NF-κB activity 142
Abstract 142
7.1. Introduction 142
7.2. Materials and Methods 143
7.2.1 Chemicals and reagents 143
7.2.2 Cell Culture and Lentiviral Transduction 143
7.2.3 Western blot 144
7.2.4 Preparation of AGE/ALE albumins and natural extracts 144
7.2.5 Stimulation of Cells 144
7.2.6 NF-κB luciferase activity assay 144
7.2.7 RealTime-Glo assay 145
7.2.8 MTT assay 145
7.3. Results 145
7.3.1 Transduction of the cell line 145
7.3.2 Validating a RAGE-dependent mechanism 146
7.3.3 Effects of AGEs/ALEs on control cells 147
7.3.4 Proliferating effect of ALEs on control cells 149
7.4. Discussion 150
References 152
Chapter VIII: General discussion 156
References 158
Appendix I: Anti-inflammatory activity 162
1. Introduction 162
2. Material and Methods 162
2.1 Chemicals and reagents 162
2.2 Cell Culture 162
2.3 Preparation of natural extracts 163
2.4 Stimulation of Cells 163
2.5 NF-κB luciferase activity assay 163
2.6 RealTime-Glo assay 163
2.7 MTT assay 163
3. Results 164
3.1 Rosiglitazone as NF-κB inhibitor 164
3.2 Natural compounds 164
4. Discussion 167

References 167

List of figures

Chapter I

Figure 1: Overview of the different oxidation pathways of biomolecules…….22

Chapter III

Fig. 1. Brief overview of the detoxification pathways of HNE. HNE is a toxic product of lipid peroxidation and can be detoxified enzymatically or non-enzymatically……34

Fig. 2. Phase I and II metabolism of HNE. Any known pathway of HNE is depicted in this figure. Blue structures represent original HNE, whereas the red structures show the modifications. The enzymatic processes are shown in green. ……35

Fig. 3. Metabolites of HNE from uncharacterized pathways. …….38

Fig. 4. HNE adduction on different protein side chains. ……..41

Fig. 5. Key contacts explaining the marked acidity of Cys34 in human albumin. ……..41

Fig. 6. Reaction mechanism for the cross-talk between Lys6 and His68 of ubiquitin. Right figure depicts proximity between Lys6 and His68. Reproduced from ref. [110] with the permission of Elsevier. ……..42

Fig. 7. Multifaceted biological effects exerted by HNE carbonylation. ……..42

Fig. 8. Reaction scheme between protein adduct involving HNE containing an alkynyl tail and biotin azide using click chemistry. So adducted proteins can then be separated using avidin….44

Fig. 9. Derivatizing agents to identify HNE adducts based on biotin hydrazide and aldehyde/keto reactive probe. ……..44

Chapter IV

Figure 1. Schematic of bottom-up vs. top-down approaches in proteomics. ……56

Figure 2. Enrichment strategy to reverse this dynamic range in favour of the protein adducts. …60

Figure 3. Primary and secondary protein carbonyls generated by direct oxidation of amino acid side chains (i.e., Lys, Arg, Pro, Thr, His, and others) – Panel A; hydrogen atom abstraction from alpha carbons causing crosslinking or breakdown of proteins – Panel B; and Michael addition reactions of His, Lys, and Cys residues with products of lipid peroxidation – Panel C. ……..62

Figure 4. Summary of the selected protein-carbonylation detection methods. Depending on the sample type, experimental aims and instrumentation available analysis of protein-carbonylation may be carried out via DNPH labelling (Spectrophotometric, ELISA, Western blot, APCI-MS) – Panel A; or by using Affinity chromatography to enrich the protein-carbonyl adducts, subsequently

analyzed by MS – Panel B. Depending on the depth of the analysis, the techniques might be used individually or in combination. ……..63
Figure 5. Early-stage glycation adducts and advanced glycation end products (AGEs) mainly derived from the glycation pathway. Carbonyl groups of sugars react with the free amino groups of amino acids (mostly occuring at lysine residue side chains) to form a Schiff base that rapidly undergoes molecular rearrangement to form a stable ketoamine called an Amadori product. …..65
Figure 6. Schematic representation of the pull-down assay strategy. ……..68
Figure 7. Deamidation proceeds through the formation of a five-membered succinimide ring intermediate by the condensation of the side-chain amide group of asparagine with the carbonyl group of the following amino acid. The L-succinimidyl intermediate then undergoes a relatively rapid hydrolysis at either the α- or β-carbonyl group to generate L-isoaspartate (L-iso-Asp) and normal L-aspartate (L-Asp). The free α-carbonyl group of L-iso-Asp can be methylated by the enzyme L-isoaspartyl O-methyltransferase (PIMT) with S-adenosylmethionine (SAM) as the methyl donor which is transformed to S-adenosylhomocysteine (SAH). Enzymatic methylation is usually followed by spontaneous ester hydrolysis leads to reformation of the L-succinimide intermediate. The formation of L-succinimide can also be accompanied by enhanced racemization at the α-carbon to generate a mixture of D-succinimidyl, D-aspartyl, and D-isoaspartyl compounds…….69
Figure 8. The neutral loss of 64 Da, due to the ejection of methanesulfenic acid (CH3SOH, 64 Da) from the side chain of Met(O), is unique and particularly useful to differentiate between Met(O) and phenylalanine (same nominal mass of 147 Da) in peptide mass fingerprint analysis. …….74
Figure 9. Common oxidative cysteine modifications: physiologically reversible and irreversible oxidative post-translational modifications that can occur to the thiol side chain of a Cys. ……..75
Figure 10. The most studied RNS-induced modifications: tyrosine and tryptophan nitration, and cysteine S-nitrosylation (also known as S-nitrosation). ……80
Figure 11. Summary of the main quantitative MS methods. Panel-A. Stable isotope labelling by amino acids in cell culture (SILAC) approach (Panel-A1) or chemical (isotopic or isobaric) labelling procedures, e.g. trypsin-catalyzed 18O labelling, iTRAQ, TMT (Panel-A2); Panel-B. Absolute quantitation of peptides and proteins by B1. Multiple reactions monitoring (MRM) or Single / selected reaction monitoring (SRM) (Panel-B1), or by spiking known amounts of heavy-labelled standards into the sample prior to LC–MS/MS analysis and subsequently comparing the intensities of such standards with the analyte (Panel-B2). ……82

Chapter V

Fig. 1. Work flow of the study. ALEs-lipox were firstly prepared by incubating HSA with lipid peroxidation derived RCS (HNE, ACR and MDA) and then fully characterized by MS. The RAGE binding ability of each identified ALE was then determined by using the VC1 assay as previously reported [20]. Computation studies were then carried out to explain the factors governing the affinity of the adducted moieties and the site of interaction on adducted HSA for VC1-binding…..99

Fig. 2. Direct infusion ESI-MS analysis of native and HNE-modified HSA. Mass spectra of HSA recorded in a mass range between m/z 1400 and 1500. A) Native HSA shows sharp intense peaks referred to the charge ions 47 + , 46 + and 45 + ; the deconvoluted spectrum reports a MW 66,455 Da (H). When HSA is reacted with HNE at increasing molar ratios 1:1 (B), 1:5 (C), 1:10 (D), additional peaks relative to HNE adducts appear. At higher molar ratios 1:100 (E), 1:200 (F) and 1:1000 (G) the MS spectra lose resolution and become flat due to the presence of multiple adducts. H) Deconvoluted spectra showing the MS of HSA and protein adducts. MS spectra relative to HSA incubated with HNE at 1:100 M ratio and higher cannot be deconvoluted due to the extent of modification. ……..101

Fig. 3. Modified albumin obtained by incubation of recombinant HSA in the presence of different molar ratio of RCS and VC1 pull-down assay. A) VC1 pull-down assay with untreated HSA. SDS PAGE analysis followed by Coomassie staining of the modified HSA obtained by 72 h incubation with the indicated molar ratio of RCS (panel B: MDA; panel D: ACR; panel F: HNE). The highest molar ratio of HSA-MDA (1:12,600), HSA-ACR (1:5000) or HSA-HNE (1:2000) were used as input (IN) in the pull-down assays with the VC1 and control (CTRL)-resins. The IN fractions, the unbound fractions (UNB) and eluates (E) were analysed by SDS-PAGE followed by Coomassie staining. The gels show that untreated HSA does not bind VC1 (panel A), whereas high MW species of HSA- MDA (panel C), HSA-ACR (panel E) and HSA-HNE (panel G) are retained by the VC1-resin, but not by the CTRL-resin. Since the elution is performed in denaturing conditions, this step removes any associated molecule from the resin, including the two VC1 glycovariants (34 and 36 kDa) and streptavidin (Stv, 14 kDa), indicated by arrows. ……103

Fig. 4. Venn diagrams of the identified ALEs as reported in Table 1 and 2. ALEs are reported as the modified amino acid residues. The upper diagram refers to ALEs obtained by treating HSA with MDA, the middle with ACR and the lower with HNE. The input reports ALEs not retained by VC1 and present only in the input samples; VC1 are the ALEs identified only after VC1-enrich-ment; the intersections report the ALEs found both in the input and VC1-enriched samples..……105

Fig. 5. Enrichment Factor (EF) graphical distribution. Enrichment Factor (EF) graphical distribution by means of vertical scatter plot overviewing the affinity of each identified ALEs towards VC1; all

EF values spotted have been calculated as the differences between the relative abundance in the enriched sample minus the amount in the untreated one (Enrichment factor= %VC1-% NoVC1), and graphically grouped as: MDA-adducts (panel A), ACR-adducts (panel B) and HNE-adducts (panel C). ……105
Fig. 6. Chemical structures of ALEs-lipox formed by incubating HSA with MDA, ACR and HNE and identified by MS. For some ALEs the pK values are reported in brackets. ……106
Fig. 7. Putative RAGE-HSA complex as computed by protein-protein docking and induced by RP-Arg472 (6 A), DHPK-Lys436 (6B) and FDP-Lys262 (6 C). For each simulated adduct, the right panel shows the entire RAGE-HSA complex while the left panel focuses on key interactions stabilized by the adduct and its surrounding residues. ……..107
Fig. 8. Mechanism explaining AGEs/ALEs and ALEs-lipox binding to VC1. A) VC1 engagement based on the acid residues of the protein ligand. Such a mechanism occurs when RCS, such as GO and MGO react with the basic residue forming a carboxylated adduct (CML and CEL) which directly contacts the RAGE residues. B) Panel B summarizes the mechanism described in the present paper for explaining the binding of ALEs-lipox to VC1 and called the “flowering effect”. It is based on a two-step process and involves exposed basic residues (mainly Lys and Arg) which in the non-adducted protein form a set of ionic bridges with the carboxylic groups of sur- rounding aspartate and glutamate residues. Lipid peroxidation derived RCS react with the basic residue and abolish or greatly reduce their basicity. Consequently, the adducted residues shift in a neutral form and such a change in the ionization state destabilizes the ionic bridges and renders the surrounding anionic residues more accessible and available to stabilize ion-pairs with the positive RAGE residues. ……..108

Supplementary Figure 1. Direct infusion ESI-MS analysis of native and ACR-modified HSA. Spectra of HSA with charge 47 + , 46 + and 45 + are shown. A) Native HSA shows a sharp intense peak with multiple low abundant peaks. When HSA is reacted with increasing concentrations of ACR, 1: 10 (B), 1: 100 (C), 1: 1000 (D), 1: 2500 (E) and 1: 5000 (F), the sharp peak diminishes and new peaks appear, confirming that HSA has been modified with different adducts of ACR..110
Supplementary Figure 2. Direct infusion ESI-MS analysis of native and MDA-modified HSA. Spectra of HSA with charge 47 + , 46 + and 45 + are shown. A) Native HSA shows a sharp intense peak with multiple low abundant peaks. When HSA is reacted with increasing concentrations of MDA, 1: 6.3 (B), 1: 63 (C), 1: 630 (D), 1: 6.300 (E) and 1: 12.600 (F), the sharp peak diminishes and new peaks appear, confirming that HSA has been modified with different adducts of MDA..111
Supplementary Figure 3. Time course analysis of the dose-dependent modification of HSA by ACR. Recombinant HSA was incubated with increasing concentrations of ACR (molar ration HSA-

ACR from 1:10–1:5000) as reported in Materials and methods. At 24, 48 and 72 h of incubation, aliquots were withdrawn and after removal of free acrolein, pull-down assays with the VC1-resin or control (CTRL)-resin were performed. A specific binding of both the monomer of modified HSA and of the HMW-species to the VC1-resin was detected at increasing concentrations, starting from the molar ratio 1:1000……..112

Supplementary Figure 4. Analysis of the dose-dependent modification of HSA by HNE. Recombinant HSA was incubated with increasing concentrations of HNE (molar ration HSA-HNE from 1:10–1:2000) as reported in Materials and methods. At 24, 48 and 72 h of incubation, aliquots were withdrawn and after removal of free HNE, pull-down assays with the VC1-resin or control (CTRL)-resin were performed. A specific binding of modified HSA to the VC1-resin was detected at increasing concentrations, starting from the molar ratio 1:200. At 1:1000 is evident the interaction with VC1 of both the monomer of modified HSA and the HMW-species……..113

Chapter VI

Figure 1. Oxidation of plasma content using AAPH. A) Oxidation of DCFH to DCF induced by AAPH. The reaction mixture consisted of DCFH, the azo-compound and human plasma (1:5 with PBS). Samples were incubated at 37°C in the dark and at fixed times the DCF content was measured by fluorescence (λex 485 nm, λem 535 nm). Values are mean ± SEM. B and C) At different timepoints protein carbonyl content was measured using a fluorometric assay (B, values are mean ± SEM) and by western blot (C). D) Direct infusion ESI-MS analysis of plasma and AAPH-treated plasma. Deconvoluted spectrum reports a peak at 66,443 Da, corresponding to HSA. Cysteinylated (66,566 Da) and glycated (66,607 Da) form of HSA are present in all samples. AAPH treated plasma shows an additional peak around 66,479 Da, suggesting the oxidation of HSA. ……126

Figure 2. Oxidation of plasma content using different concentrations AAPH and longer incubation times. At different concentrations AAPH and timepoints protein carbonyl content was measured using a fluorometric assay (A, values are mean ± SEM) and by western blot (B, C, values are mean ± SEM). ……..127

Figure 3. Direct infusion ESI-MS analysis of plasma and AAPH-treated plasma. Mass spectra of HSA recorded in a mass range between m/z 1400 and 1500. Native HSA shows sharp intense peaks referred to the charge ions 47+, 46+ and 45+ in untreated plasma. After incubation with increasing concentrations AAPH, the HSA peaks disappears due to the extent of modification..128

Figure 4. Spectral counting shows increased oxidation correlated over time and concentration of AAPH. Shown are the percentages of identified PSMs from the indicated modifications. ……130

Figure 5. Direct infusion ESI-MS analysis of plasma and plasma incubated with ACR or MDA. Mass spectra of HSA recorded in a mass range between m/z 1400 and 1500. Native HSA shows sharp intense peaks referred to the charge ions 47+, 46+ and 45+ in untreated plasma; the deconvoluted spectrum reports a MW 66,449 Da. After incubation with increasing concentrations of ACR or MDA, spectra lose resolution due to the formation of new peaks. The HSA peak diminishes in the deconvoluted spectra when incubated with RCS. Shown are the cysteinylated form (a) of HSA, glycated form (b) and the formation of an adduct (c) with ACR or MDA.……131
Figure 6. VC1 pull-down assay on plasma and plasma incubated with different ratios of RCS. The input fractions (IN), the unbound fractions (UNB) and eluates (E) were analyzed by SDS-PAGE followed by Coomassie staining. The gels show the same elution profile compared between plasma and plasma treated with RCS with some proteins retained by VC1 around 60 and 75 kDa, and to a less extent by the control resin. Since the elution is performed in denaturing conditions, this step removes any associated molecule from the resin, including the two VC1 glycovariants (34 and 36 kDa) and streptavidin (14 kDa). ……132
Figure 7. HSA extraction from plasma. The input fraction (IN), the flow-through fraction (F-T), the wash fraction (W) and eluate (E) were analyzed by SDS-PAGE followed by Coomassie staining……...133
Figure 8. Venn diagrams of the identified AGEs/ALEs in healthy individuals and heart failure patients, as well as if they were identified only after reduction with $NaBH_4$. Reported are the type of modification followed by the site of adduction on HSA. ……135
Figure 9. MS^2 spectrum with the b- and y-series of a peptide containing a glyoxal modification. The peak at 187.10744 represents the immonium ion of a lysine residue with a glyoxal adduct..136

Supplementary figure 1. Protein gel of plasma treated with different concentrations of AAPH and different timepoints. ……140

Chapter VII

Figure 1. Luciferase expression in R3/1 clones. A) Expression of RAGE in R3/1 Control or R3/1 RAGE (Control or NF-κB-Luc) was determined with a specific antibody against the extracellular domain of RAGE. GAPDH detection was used as normalizer. B) Cells were stimulated for 24 hours with and without IL-1α in starvation medium. Control cells (no NF-κB-Luc) show no luminescence at all, whereas the transfected cells show a clear production of luminescence, increased at higher MOI. Shown are mean ± SEM. ……..146
Figure 2. Treatment with known ligands of RAGE. Cells were treated 24 hours with indicated compounds. Results shown were corrected on protein concentration and compared to untreated

control cells. Mean ± SEM analyzed using two-way ANOVA with Holm-Sidak correction (∗∗∗∗p < 0.0001 was considered significant, CI 95%) to compare against untreated control cells or an unpaired Student's t-test (#p < 0.05, two-tailed, CI 95%) to compare between control and RAGE cells. ……..147
Figure 3. Increased NF-κB activity through different AGEs/ALEs. Cells were stimulated for 6 hours with indicated compounds, HSA and AGEs (top) or ALEs (bottom) were added at 500 µg/ml. Followed by an MTT assay (A,C) or by a luciferase luminescence measurement (B,D). Compared to untreated, mean ± SEM analyzed using ANOVA with Bonferroni correction (∗p < 0.05, ∗p < 0.01 ∗∗∗p < 0.001 and ∗∗∗∗p < 0.0001 were considered significant, CI 95%).……148
Figure 4. ALEs increase cell proliferation. A) R3/1 control cells were incubated with 500 µg/ml compounds in complete medium. Using RealTime-Glo™ MT Cell Viability Assay, luminescence was continuously monitored. Linear regression line was fitted and R square values were calculated. B) R3/1 control cells were incubated with 500 µg/ml increasing modified HSA with RCS. Linear regression line was fitted and R square values were calculated. C) Different concentrations of HSA – 1X RCS were tested for proliferation. Linear regression line was fitted and R square values were calculated. D) Cells were incubated with the same compounds at 500 µg/ml and counted manually after 70 hours. Change in cell viability compared to HSA was plotted, together with the results from the RealTime-Glo assay after 70 hours. ……..149
Figure 5. Bardoxolone increases the production of reducing enzymes. R3/1 control cells were incubated with different concentrations of bardoxolone for 24 hours, followed by the assessment of three different assays to determine cell proliferation. Compared to untreated of the relative assay, shown are mean ± SEM. ……150

Appendix I

Figure 1. Bardoxolone increases the production of reducing enzymes and rosiglitazone is able to reduce NF-κB activity. A) R3/1 control cells were incubated with different concentrations of bardoxolone for 24 hours, followed by the assessment of three different assays to determine cell proliferation. Compared to untreated of the relative assay, shown are mean ± SEM. B) R3/1 control cells were incubated for 18 hours with different concentrations of bardoxolone, followed by a 6 hour stimulation with IL-1α. Then NF-κB dependent luciferase activity was measured. Compared to control untreated, mean ± SEM are shown. Analyzed using two-way ANOVA with Bonferroni correction (compared to control IL-1α, ∗∗p < 0.01, ∗∗∗p < 0.001 and ∗∗∗∗p < 0.0001 were considered significant, CI 95%). C) R3/1 control cells were incubated with different concentrations of rosiglitazone for 24 hours, followed by the assessment of cell viability using MTT and RealTime-Glo. Compared to untreated of the relative assay, shown are mean ± SEM. D) R3/1 control cells

were incubated for 18 hours with different concentrations of rosiglitazone, followed by a 6 hour stimulation with IL-1α. Then NF-κB dependent luciferase activity was measured. Compared to control untreated, mean ± SEM are shown. Analyzed using two-way ANOVA with Bonferroni correction (compared to control untreated, #p < 0.05 and ###p < 0.001, compared to control IL-1α, ∗∗∗∗p < 0.0001 were considered significant, CI 95%).……166
Figure 2. Polyphenolic compounds are able to increase the reduction potential of R3/1 cells and decrease pro-inflammatory activity through the NF-κB pathway. A and C) R3/1 control cells were incubated with different concentrations of apple pulp extract (A) or bergamot fruit extract (C) for 24 hours, followed by the assessment of cell proliferation using MTT and RealTime-Glo. Compared to untreated of the relative assay, shown are mean ± SEM. Analyzed using two-way ANOVA with Bonferroni correction (compared to untreated RealTime-Glo, ∗∗∗∗p < 0.0001, compared to untreated MTT, #p < 0.05, ##p < 0.01 and ###p < 0.001 were considered significant, CI 95%). B and D) R3/1 control cells were incubated for 18 hours with different concentrations of apple pulp extract (B) or bergamot fruit extract (D), followed by a 6 hour stimulation with IL-1α. Then NF-κB dependent luciferase activity was measured. Compared to control untreated, mean ± SEM are shown. Analyzed using two-way ANOVA with Bonferroni correction (compared to control IL-1α, ∗p < 0.05, ∗∗∗p < 0.001 and ∗∗∗∗p < 0.0001 were considered significant, CI 95%).166

List of tables

Chapter III

Table 1. List of all enzymes involved in HNE metabolism. ……36
Table 2. Percentages of the initial radioactivity for urinary metabolites detected after 48 h. Re-elaborated data in bold, HNA lactone reported as HNL. Data taken from Gueraud et al. [43]. …39
Table 3. Percentages of the initial radioactivity after rat liver cytosolic incubation. Re-elaborated data in bold, HNA lactone reported as HNL. Data taken from Gueraud et al. [43]. …….39

Chapter IV

Table 1. Involvement of nePTMs of proteins in aging and disease [1]. …….53

Chapter V

Table 1. List of the PTMs identified on the indicated Amino acid residues in the ALEs samples obtained by in vitro incubation of HSA with RCS. ……104
Table 2. List of the PTMs identified on the indicated Amino acid residues in the ALEs-HSA samples retained by VC1. ……..104

Table S1. Known (literature based) covalent adducts induced by HNE, MDA and ACR and set as variable modifications within the PD parameters for the identification and localization of ALE-deriving adducts……..…..114
Table S2. Number of negatively charged residues found within a 5 Å radius sphere around the adducted residues. ……..115

Chapter VI

Table S1. Known (literature based) covalent adducts induced by HNE, MDA, ACR, MG, GO, ONE and sugars set as variable modifications within the PD parameters for the identification and localization of ALE-deriving adducts. ……..141
Table S2. Known (literature based) reduced covalent adducts induced by HNE, MDA, ACR, MG, GO, ONE and sugars set as variable modifications within the PD parameters for the identification and localization of ALE-deriving adducts. ……143

List of appendices

Appendix I: Anti-inflammatory activity. ……162

Chapter I: Introduction

Chapter I: Introduction

The purpose of the PhD project was to characterize pro-inflammatory advanced glycation endproducts and advanced lipoxidation endproducts and their binding mechanisms with the receptor for advanced glycation endproducts.

1.1 Oxidative stress

Oxidative stress occurs when there is an imbalance between oxidants and anti-oxidants leading to the attack of biomolecules by free radicals. They can be either produced endogenously, during cellular metabolism, or can come from exogenous sources, such as the ingestion of oxidized foodstuffs or inhalation of air pollutants. Free radicals are highly reactive species with one or more unpaired electrons, seeking other electrons to form a stable molecule. Under normal circumstances free radicals are scavenged by anti-oxidants such as tocopherols and ascorbic acid, however, increased levels of free radicals, or decreased levels of defensive mechanisms can lead to the attack of different biomolecules like proteins, lipids and DNA. Oxidation of proteins, leading to post-translational modifications (PTMs), can have multiple repercussions, such as a conformational change, aggregation and crosslinking, or establishing new interactions with other biomolecules [1]. Lipid oxidation can produce a wide variety of end products which have been described in many different pathologies. End products include long- and short-chain oxidation products and a major class of break-down products, predominantly reactive carbonyl species (RCS). RCS are highly reactive and metabolized rapidly, either by phase I and II metabolism, or by reacting with nucleophilic residues on proteins. Besides proteins and lipids, oxidative damage can occur at nuclear level, where guanine is the most susceptible base pair to oxidation and has been linked to the progression of carcinogenesis [2].

Nucleophilic targets can also be attacked by a group of sugars that is already oxidized, reducing sugars with a free aldehyde group acting as a reducing agent. Reducing sugars can also adduct proteins at Lysine residues, causing the formation of Advanced Glycation End Products (AGEs). Proteins adducted by RCS coming from the lipid peroxidation pathway are called Advanced Lipoxidation End Products. Both groups of modified proteins are explained in the following paragraphs.

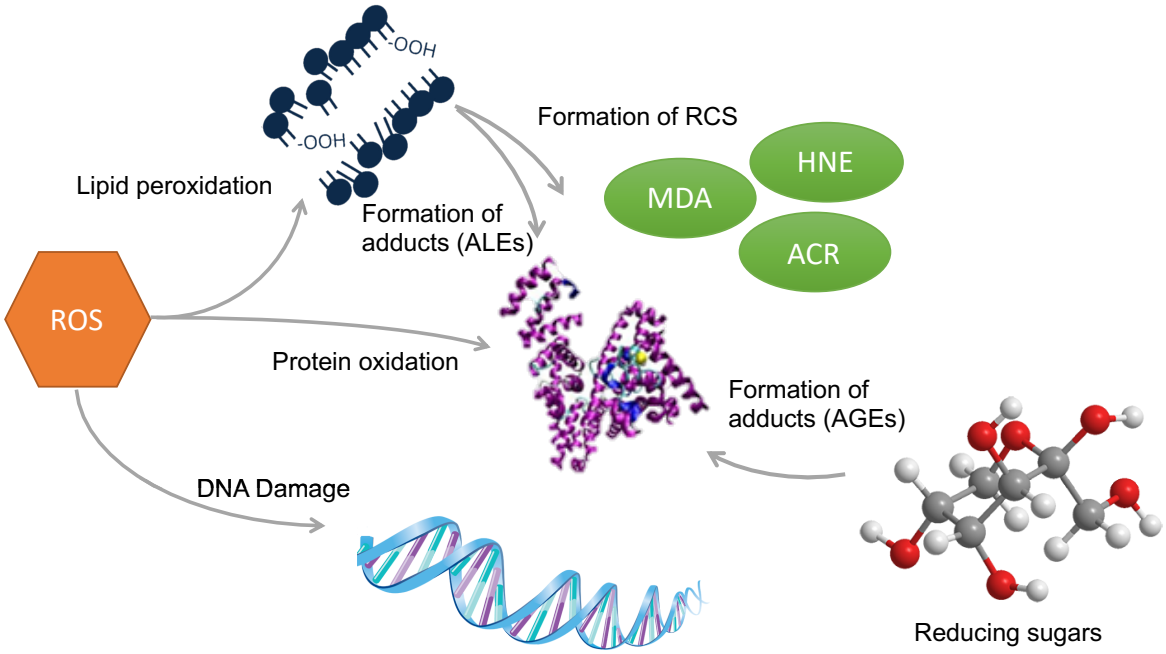

Figure 1: Overview of the different oxidation pathways of biomolecules.

1.2 Advanced Glycation End Products

Modification of amino side chains on proteins by free radicals are not the only PTMs originating from oxidative stress. Another class of compounds are advanced glycoxidation end products (AGEs), proteins covalently modified by reducing sugars or their oxidative degradation products. It is described by the Maillard reaction, which is a set of reactions starting with the condensation between the carbonyl group of a reducing sugar and a primary amino group present on amino acid side chains, for example lysine and arginine. Through dehydrations, cyclizations and Amadori rearrangements, a large variety of structures are generated, both oxidative degradation of the Amadori products and break-down products after fragmentation of ketoses producing α-dicarbonyls [3]. The first include an adduct with a reducing sugar, specifically glucose or fructose, with lysine, and further oxidize into different products such as carboxy derivatives and cross-links. The latter involves the production of α-dicarbonyls, like glyoxal and methylglyoxal, that can further react with nucleophilic amino acids.

Glyoxal is the smallest dialdehyde and is produced by sugar autoxidation pathways, lipid peroxidation pathways or via the Maillard reaction. Glyoxal can react with Arg, Lys and Cys residues to either form carboxy derivatives, imidazolone adducts, or cross-links.

Another α-dicarbonyl is methylglyoxal, which can be produced via many different pathways from mostly sugars or lipids. Heating and prolonged storage of sugars and lipids can lead to the fragmentation into methylglyoxal, but also glycolytic processes, acetone metabolism, and

metabolic pathways of threonine and glycine can lead to the production of methylglyoxal. Similar to glyoxal, methylglyoxal can react with Arg, Lys and Cys residues leading to the formation of the same set of adducts, carboxy derivatives, imidazolone adducts, or crosslinks, but also a pyrimidine adduct on Arg by adding a second methylglyoxal molecule to the imidazolone adduct.

1.3 Advanced lipoxidation end products

Advanced lipoxidation end products (ALEs) are macromolecules adducted by reactive carbonyl species (RCS), highly reactive molecules containing one or more carbonyl groups, arising from lipid peroxidation pathways or lipid metabolism. Three main classes coming from lipoxidation break-down and lipid metabolism are short chain RCS, oxidized truncated phospholipids and prostaglandin metabolites, however the main focus will be on short chain RCS. Short chain RCS can be subdivided in three groups; α,β-unsaturated aldehydes, di-aldehydes and keto-aldehydes, each of which can react with a nucleophilic target on proteins to form an ALE.

Polyunsaturated fatty acids (PUFAs) are the major source of reactive carbonyl species. Free radicals, mainly hydroxyl and peroxynitrite, attack the allylic hydrogen in PUFAs, yielding a lipid radical, which then react with oxygen to produce a lipid peroxyl radical. This radical will abstract a hydrogen from another PUFA, continuing the lipid peroxidation cycle, and form a stable lipid peroxide which can generate α,β-unsaturated aldehydes like HNE and acrolein (ACR) and dialdehydes such as malondialdehyde (MDA). Glyoxal and methylglyoxal, described before, can also be produced upon lipid peroxidation.

Defense mechanisms are in place to detoxify the production of RCS by a reaction with glutathione for example, or by reducing enzymes including alcohol dehydrogenase and aldo/keto reductase. The metabolic fate of HNE is described in chapter 3. However, when there is an excess of HNE, it can react with proteins, lipids and DNA. HNE is a lipid peroxidation break-down product of ω-6 fatty acids with three reactive groups, an aldehyde, double bond and a hydroxy group. It is able to react with nucleophilic side chains on amino acids such as Lys, His and Cys to form a Michael adduct or a Schiff base. Other adducts include unsaturated cyclic forms and cross links due to the presence of an aldehyde and an electrophilic carbon.

Acrolein shows the highest reactivity towards nucleophiles and is not only produced by lipid peroxidation, but also by metabolism of amino acids and polyamines and by exogenous sources like food. A Michael adduct on cysteine is the main site of adduction of acrolein, followed by Michael adducts on histidine and lysine. Acrolein is also able to form a Schiff base on lysine which can react with another acrolein molecule to form a cyclized adduct. Similarly, two acrolein molecules can react through a Michael addition with lysine to form another cyclized adduct.

Arginine can also be adducted by acrolein to form a propane adduct. Finally, acrolein adducts can react with other nucleophilic residues to form crosslinks.

The most abundant di-aldehyde is malondialdehyde produced upon lipid peroxidation and mainly reacts with lysine to form a propenal adduct. It can further react to produce a crosslink, or a cyclized adduct. Furthermore, it can react with arginine to form a pyrimidine adduct.

1.4 Biological significance of AGEs and ALEs

AGEs/ALEs are pathogenic factors involved in many different diseases. The formation of AGEs/ALEs can have multiple mechanisms to exert its damaging activity. One of the outcomes is a conformational change of the protein, as shown by the aggregation of α-synuclein involved in Parkinson's disease, due to the crosslinks formed by HNE [4]. Acrolein have been shown to modify the p50 subunit, a member of the NF-κB family of proteins, resulting in a differently regulated pro-inflammatory response [5]. Whereas MDA has been reported to adduct cytosine residues, mediating oxidized low-density lipoprotein-induced coronary toxicity [6]. Examples showing the direct effect of protein or DNA adduction by RCS.

Another pathology with increased levels of AGEs is diabetes mellitus, characterized by hyperglycemia. Long-term high levels of glucose increase the formation of AGEs, and many proteins have been reported to be modified during diabetes. For example glycation of human serum albumin (HSA) has been shown to play an important role during the progression of the disease and related pathologies, such as diabetic retinopathy [7]. Fibrinogen may also be glycated during diabetes, resulting in impaired fibrinolysis and vascular dysfunction [8, 9]. Collagen is another important protein affected by the high sugar levels, once glycated reports have shown that it may contribute to skeletal fragility and development of atherosclerotic plaques and fibrosis [10-12].

Adduction of RCS to proteins can also lead to circulating AGEs/ALEs, which do not show a direct effect on the protein, yet are potential modulators of numerous biological functions and have been shown to contribute in the pathogenesis of several diseases. Numerous pathologies have been shown to have an increased level of protein adducts with HNE, such as in Alzheimer's disease, systemic lupus erythematosus, diabetes and chronic pancreatitis [13-16].

Some biological functions are receptor-mediated, as in the case of galectin-3, a glycan binding protein suggested to aid in the removal of circulating AGEs and ALEs [17]. Receptors from the macrophage scavenger receptor family, like CD36 and LOX-1, have also been reported to bind AGEs. These receptors are mainly located on endothelial cells and immune cells, and their main function is the uptake and degradation of AGEs [18]. AGEs also bind the Receptor for advanced glycation end products (RAGE), activating different signalling pathways further explained in

paragraph 1.6. Whereas AGEs have been shown to have a wide variety of receptors, a specific receptor for ALEs has not been elucidated yet, despite sharing the same chemical characteristics.

1.5 Identification and characterization

AGEs/ALEs are a heterogeneous group of biomolecules, meaning, many different proteins can be adducted by a wide variety of small molecules arising from different oxidative pathways, thus many different modifications can be induced on different amino acids [3]. These AGEs/ALEs, and their involvement in many different pathologies, can be considered as biomarkers, to predict disease outcome. Likewise, diseases can be prevented if AGEs/ALEs are considered as drug targets.

However, the analysis of this group of biomolecules has proven to be quite challenging due to several reasons. As previously mentioned, it is a heterogeneous group of biomolecules, and above all, modified proteins are contained in very low amount (nanomolar range) in complex matrices compared to native proteins, implicating the need for an enrichment strategy. Several enrichment strategies are described in chapter 4, as well as the currently available analytical techniques for identification, characterization and quantification of AGEs and ALEs.

1.6 Receptor for advanced glycation end products (RAGE)

A functional-based strategy for selectively isolating pro-inflammatory modified proteins is an emerging approach, and recently a VC1 interaction assay was designed to achieve this goal [19]. The idea behind this enrichment procedure is to employ the binder of AGEs, the receptor RAGE, as a stationary phase, explained in more detail in our previous paper [19]. Whereas AGEs are known binders of RAGE, ALEs have been partially explored as ligands of the receptor.

RAGE is a type I cell surface receptor that is expressed in several cells, such as endothelial cells, smooth muscle cells, but also dendritic cells and T-lymphocytes and is predominantly located in the lungs [18]. The full-length isoform of the receptor consists of three extracellular domains, V C1 and C2, a transmembrane and a intracellular domain. RAGE has been involved in many different pathologies with a marked oxidative base, such as diabetes, atherosclerosis, neurodegenerative diseases and many different ligands of RAGE have been identified, such as amyloid β peptide, S100/calgranulin protein, HMGB1 [20]. Two different pathways can be activated upon binding to the receptor; 1) the activation of the NADPH oxidase, resulting in the production of reactive oxygen species (ROS), aiding in the formation of AGEs/ALEs and 2) the activation of the NF-κB pathway leading to a sustained pro-inflammatory and pro-fibrotic response. One of the genes activated upon NF-κB activation is the advanced glycation end products specific receptor (AGER), whose expression is therefore supported by a positive feedback loop.

RAGE has multiple isoforms having different ligands and different biological responses, such as soluble RAGE (sRAGE) and two truncated isoforms, without the intracellular domain and RAGE without the V domain. sRAGE can be produced in two different manners, pre-mRNA alternative splicing and cleaved on the membrane surface by metalloproteinases. It has sequestering activity, since it can bind the same ligands but it does not induce a biological response and has been proven to be useful as a decoy in different pathologies [21-23].

1.7 NF-κB pathway

One of the pathways activated upon RAGE binding is the NF-κB pathway. This is a signaling pathway that can be activated upon external stimuli like antigens, cytokines, reactive oxygen species etc. NF-κB is a transcription factor regulating expression of cytokines, chemokines, growth factors, apoptosis inhibitors and many more involved in cell proliferation and survival, inflammation and immune regulation. Firstly, receptors are bound by ligands able to induce the downstream pathway. Many different downstream pathways are described already, but they all have in common the release of a NF-κB subunit after the phosphorylation and degradation of the family of I-kappa-B inhibitors. After the NF-κB subunit is released, it will translocate to the nucleus where it will bind response elements (RE), unique for the protein that will be expressed subsequently. The NF-κB pathway is therefore the ideal signaling pathway to investigate the pro- or anti-inflammatory activity induced via RAGE.

References

[1] M.J. Davies, Protein oxidation and peroxidation, Biochem J 473(7) (2016) 805-25.

[2] H. Wiseman, B. Halliwell, Damage to DNA by reactive oxygen and nitrogen species: role in inflammatory disease and progression to cancer, Biochem J 313 (Pt 1) (1996) 17-29.

[3] G. Vistoli, D. De Maddis, A. Cipak, N. Zarkovic, M. Carini, G. Aldini, Advanced glycoxidation and lipoxidation end products (AGEs and ALEs): an overview of their mechanisms of formation, Free Radic Res 47 Suppl 1 (2013) 3-27.

[4] Y. Cai, C. Lendel, L. Österlund, A. Kasrayan, L. Lannfelt, M. Ingelsson, F. Nikolajeff, M. Karlsson, J. Bergström, Changes in secondary structure of α-synuclein during oligomerization induced by reactive aldehydes, Biochem Biophys Res Commun 464(1) (2015) 336-41.

[5] C. Lambert, J. McCue, M. Portas, Y. Ouyang, J. Li, T.G. Rosano, A. Lazis, B.M. Freed, Acrolein in cigarette smoke inhibits T-cell responses, J Allergy Clin Immunol 116(4) (2005) 916-22.

[6] T.C. Yang, Y.J. Chen, S.F. Chang, C.H. Chen, P.Y. Chang, S.C. Lu, Malondialdehyde mediates oxidized LDL-induced coronary toxicity through the Akt-FGF2 pathway via DNA methylation, J Biomed Sci 21 (2014) 11.
[7] V.P. Singh, A. Bali, N. Singh, A.S. Jaggi, Advanced glycation end products and diabetic complications, Korean J Physiol Pharmacol 18(1) (2014) 1-14.
[8] E.J. Dunn, H. Philippou, R.A. Ariëns, P.J. Grant, Molecular mechanisms involved in the resistance of fibrin to clot lysis by plasmin in subjects with type 2 diabetes mellitus, Diabetologia 49(5) (2006) 1071-80.
[9] S. Perween, M. Abidi, A.F. Faizy, Moinuddin, Post-translational modifications on glycated plasma fibrinogen: A physicochemical insight, Int J Biol Macromol 126 (2019) 1201-1212.
[10] X. Wang, X. Shen, X. Li, C.M. Agrawal, Age-related changes in the collagen network and toughness of bone, Bone 31(1) (2002) 1-7.
[11] A. Yuen, C. Laschinger, I. Talior, W. Lee, M. Chan, J. Birek, E.W. Young, K. Sivagurunathan, E. Won, C.A. Simmons, C.A. McCulloch, Methylglyoxal-modified collagen promotes myofibroblast differentiation, Matrix Biol 29(6) (2010) 537-48.
[12] S.F. Kemeny, D.S. Figueroa, A.M. Andrews, K.A. Barbee, A.M. Clyne, Glycated collagen alters endothelial cell actin alignment and nitric oxide release in response to fluid shear stress, J Biomech 44(10) (2011) 1927-35.
[13] M. Fukuda, F. Kanou, N. Shimada, M. Sawabe, Y. Saito, S. Murayama, M. Hashimoto, N. Maruyama, A. Ishigami, Elevated levels of 4-hydroxynonenal-histidine Michael adduct in the hippocampi of patients with Alzheimer's disease, Biomed Res 30(4) (2009) 227-33.
[14] M. Podborska, A. Sevcikova, J. Trna, P. Dite, A. Lojek, L. Kubala, Increased markers of oxidative stress in plasma of patients with chronic pancreatitis, Neuro Endocrinol Lett 30 Suppl 1 (2009) 116-20.
[15] P.A. Grimsrud, M.J. Picklo, T.J. Griffin, D.A. Bernlohr, Carbonylation of adipose proteins in obesity and insulin resistance: identification of adipocyte fatty acid-binding protein as a cellular target of 4-hydroxynonenal, Mol Cell Proteomics 6(4) (2007) 624-37.
[16] G. Wang, S.S. Pierangeli, E. Papalardo, G.A. Ansari, M.F. Khan, Markers of oxidative and nitrosative stress in systemic lupus erythematosus: correlation with disease activity, Arthritis Rheum 62(7) (2010) 2064-72.
[17] H. Vlassara, Y.M. Li, F. Imani, D. Wojciechowicz, Z. Yang, F.T. Liu, A. Cerami, Identification of galectin-3 as a high-affinity binding protein for advanced glycation end products (AGE): a new member of the AGE-receptor complex, Mol Med 1(6) (1995) 634-46.

[18] C. Ott, K. Jacobs, E. Haucke, A. Navarrete Santos, T. Grune, A. Simm, Role of advanced glycation end products in cellular signaling, Redox Biol 2 (2014) 411-29.
[19] G. Degani, A.A. Altomare, M. Colzani, C. Martino, A. Mazzolari, G. Fritz, G. Vistoli, L. Popolo, G. Aldini, A capture method based on the VC1 domain reveals new binding properties of the human receptor for advanced glycation end products (RAGE), Redox Biol 11 (2017) 275-285.
[20] I. González, J. Romero, B.L. Rodríguez, R. Pérez-Castro, A. Rojas, The immunobiology of the receptor of advanced glycation end-products: trends and challenges, Immunobiology 218(5) (2013) 790-7.
[21] C. Cheng, K. Tsuneyama, R. Kominami, H. Shinohara, S. Sakurai, H. Yonekura, T. Watanabe, Y. Takano, H. Yamamoto, Y. Yamamoto, Expression profiling of endogenous secretory receptor for advanced glycation end products in human organs, Mod Pathol 18(10) (2005) 1385-96.
[22] C. Falcone, E. Emanuele, A. D'Angelo, M.P. Buzzi, C. Belvito, M. Cuccia, D. Geroldi, Plasma levels of soluble receptor for advanced glycation end products and coronary artery disease in nondiabetic men, Arterioscler Thromb Vasc Biol 25(5) (2005) 1032-7.
[23] E. Emanuele, A. D'Angelo, C. Tomaino, G. Binetti, R. Ghidoni, P. Politi, L. Bernardi, R. Maletta, A.C. Bruni, D. Geroldi, Circulating levels of soluble receptor for advanced glycation end products in Alzheimer disease and vascular dementia, Arch Neurol 62(11) (2005) 1734-6.

Chapter II: Aim of the project

Chapter II: Aim of the project

The identification and characterization of AGEs/ALEs has proven to be crucial in the onset and development of many pathologies. Therefore, good analytical strategies need to be developed/optimized for better understanding of the exact nature of modification, to understand the role they play in disease progression. Identified AGEs/ALEs can serve as biomarker, as well as drug targets. The VC1 technique was proven to be a promising technique to accommodate the need for enrichment of AGEs for better characterization. The first aim of the project was therefore to investigate whether also ALEs are binder of RAGE, since they share the same structural properties than AGEs, and also have been shown to activate the NF-κB pathway, implicating a role for receptors, like RAGE. Furthermore, the exact molecular mechanism of protein-protein engagement with the receptor are not well understood. Using molecular modeling studies, we attempted to gain a deeper insight into the binding of ALEs with RAGE.

Since a successful enrichment strategy was developed, the second aim of this project was focused on identifying AGEs/ALEs in biological samples. The first part was focused on oxidizing healthy human plasma *in-vitro*, to elucidate which proteins are prone to undergo oxidative modification and to characterize the chemical moiety provoked by oxidative stress. AAPH was used as a radical initiator to induce oxidative conditions in plasma as well as the incubation of plasma directly with RCS, anticipating the production of AGEs/ALEs. The VC1 pull-down assay was then used to identify binders of RAGE, and to enrich AGEs/ALEs for characterization. Simultaneously, other variables during sample preparation and analysis were optimized. As explained before, AGEs/ALEs are present in very low concentrations in biological samples, hence the need for very sensitive methods and instrumentation allowing identification. Since human serum albumin (HSA) is the main protein present in plasma, around 50-60%, and has multiple nucleophilic targets, it represents the best model for characterizing AGEs/ALEs. For this reason, the focus was on extracting HSA from plasma, using the newest generation of tribrid MS for the analysis of AGEs/ALEs in plasma samples. Accordingly, plasma from heart failure patients was used as a model, since this pathology is correlated with the increase of circulating AGEs/ALEs. In addition, AGEs/ALEs could be characterized specifically increased during the disease progression.

AGEs are ligands for RAGE, meaning, they can bind and activate the receptor, inducing a signaling pathway and pro-inflammatory response. ALEs have also been shown to induce a pro-inflammatory response; however, no specific receptor has been linked to this cellular event. Therefore, we have set-up a cellular model to investigate potential RAGE ligands using a cell line with and without RAGE with a NF-κB gene reporter. Employing this cellular model, we hoped to

discriminate between RAGE binders and RAGE ligands for determining AGEs/ALEs able to induce a pro-inflammatory activity through RAGE.

Lastly, anti-inflammatory properties of natural compounds were evaluated using the cell line with NF-κB gene reporter described previously. This cell line, allowed us to perform a high-throughput screening of pure compounds or crude extracts obtained from different natural compounds, including apple and bergamot. Besides the anti-inflammatory effect, another assay was utilized that could correlate to the activation of the nrf2 pathway, activated under oxidative stress.

Chapter III: Enzymatic and non-enzymatic detoxification of 4-hydroxynonenal: Methodological aspects and biological consequences

This Chapter was integrally published as follows:

Mol, M., Regazzoni, L., Altomare, A., Degani, G., Carini, M., Vistoli, G., & Aldini, G. (2017). Enzymatic and non-enzymatic detoxification of 4-hydroxynonenal: methodological aspects and biological consequences. *Free Radical Biology and Medicine*, *111*, 328-344.

Free Radical Biology and Medicine 111 (2017) 328–344

Contents lists available at ScienceDirect

Free Radical Biology and Medicine

journal homepage: www.elsevier.com/locate/freeradbiomed

Review Article

Enzymatic and non-enzymatic detoxification of 4-hydroxynonenal: Methodological aspects and biological consequences

Marco Mol, Luca Regazzoni, Alessandra Altomare, Genny Degani, Marina Carini, Giulio Vistoli, Giancarlo Aldini*

Department of Pharmaceutical Sciences, Università degli Studi di Milano, Via Mangiagalli 25, 20133 Milan, Italy

ARTICLE INFO

Keywords:
4-Hydroxynonenal
HNE
Enzymatic
Metabolism
Adduct
Analytical

ABSTRACT

4-Hydroxynonenal (HNE), an electrophilic end-product deriving from lipid peroxidation, undergoes a heterogeneous set of biotransformations including enzymatic and non-enzymatic reactions. The former mostly involve red-ox reactions on the HNE oxygenated functions (phase I metabolism) and GSH conjugations (phase II) while the latter are due to the HNE capacity to spontaneously condense with nucleophilic sites within endogenous molecules such as proteins, nucleic acids and phospholipids. The overall metabolic fate of HNE has recently attracted great interest not only because it clearly determines the HNE disposal, but especially because the generated metabolites and adducts are not inactive molecules (as initially believed) but show biological activities even more pronounced than those of the parent compound as exemplified by potent pro-inflammatory stimulus induced by GSH conjugates. Similarly, several studies revealed that the non-enzymatic reactions, initially considered as damaging processes randomly involving all endogenous nucleophilic reactants, are in fact quite selective in terms of both reactivity of the nucleophilic sites and stability of the generated adducts. Even though many formed adducts retain the expected toxic consequences, some adducts exhibit well-defined beneficial roles as documented by the protective effects of sublethal concentrations of HNE against toxic concentrations of HNE. Clearly, future investigations are required to gain a more detailed understanding of the metabolic fate of HNE as well as to identify novel targets involved in the biological activity of the HNE metabolites. These studies are and will be permitted by the continuous progress in the analytical methods for the identification and quantitation of novel HNE metabolites as well as for proteomic analyses able to offer a comprehensive picture of the HNE-induced adducted targets. On these grounds, the present review will focus on the major enzymatic and non-enzymatic HNE biotransformations discussing both the molecular mechanisms involved and the biological effects elicited. The review will also describe the most important analytical enhancements that have permitted the here discussed advancements in our understanding of the HNE metabolic fate and which will permit in a near future an even better knowledge of this enigmatic molecule.

1. Introduction

Since its identification, 4-hydroxy-nonenal (HNE), an autoxidation product of unsaturated fats and oils, (at first erroneously described as 4-hydroxy-octenal) [1] has attracted great scientific interest, as demonstrated by the publication of more than 4200 papers since 1980 (source PubMed, setting 4-hydroxynonenal as key word, updated November 2016). Compared to other 4-hydroxyalkenals, HNE is the most extensively studied and reviewed as it was the first one discovered [1], it represents the main 4-hydroxyalkenal formed during autoxidation of unsaturated fatty acids [2], it is highly reactive [3] and numerous biological effects have been demonstrated [4]. Besides several papers dealing with its biological properties, great attention has also been paid to the metabolic fate of HNE and to the analysis of the compound as such and of the corresponding metabolites in biological matrices. Such a great interest in metabolism is explained by the fact that, due to its high reactivity, HNE undergoes a rapid disappearance and biotransformation which regulates its free content, thus making the metabolic process an important factor regulating biological activity. Moreover, HNE metabolites are not inactive species but they themselves have potent biological activities as recently found for GSH adducts [5]. Metabolism and bioanalysis are strictly connected because understanding of the metabolic pathways requires the set-up of selective and sensitive on-target and off-target methods for the identification and

Abbreviations: HNE, 4-hydroxy-*trans*-2-nonenal; ALDH, aldehyde dehydrogenase; ALDH2, aldehyde dehydrogenase 2; Alda-1, ALDH2 activator 1

* Corresponding author.
E-mail address: giancarlo.aldini@unimi.it (G. Aldini).

http://dx.doi.org/10.1016/j.freeradbiomed.2017.01.036
Received 14 December 2016; Received in revised form 26 January 2017; Accepted 26 January 2017
Available online 02 February 2017

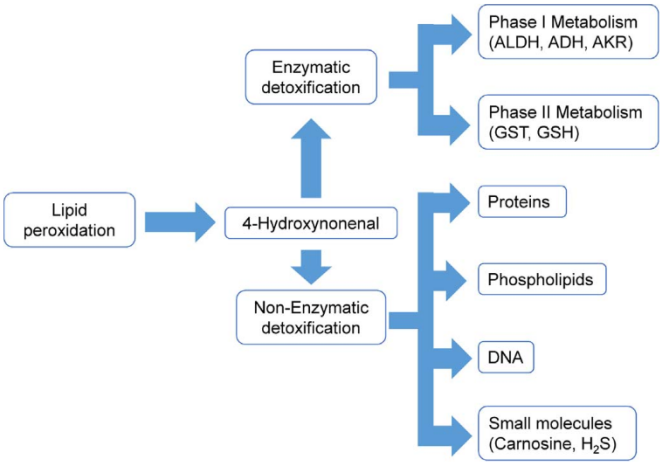

Fig. 1. Brief overview of the detoxification pathways of HNE. HNE is a toxic product of lipid peroxidation and can be detoxified enzymatically or non-enzymatically.

characterization of HNE metabolites. Hence, metabolism and bioanalysis of HNE are two fields which have in the past and will continue to attract great scientific interest.

As summarized in Fig. 1, HNE undergoes rapid enzymatic and non-enzymatic biotransformations yielding reversible and irreversible HNE derivatives. Enzymatic HNE detoxification was first described in rat hepatoma cell lines by a seminal paper in 1988 [6] and was later clarified in different cell models and animals both from a qualitative and quantitative point of view. Other 4-hydroxyalkenals, such as 4-hydroxyhexenal (HHE), have the same functional groups than HNE and are detoxified via a similar pathway. Non-enzymatic reactions also represent an important fate of HNE and are widely studied because they are responsible for several of its biological effects. From a general point of view and due to its electrophilic nature, HNE can covalently react through non-enzymatic reactions with nucleophilic substrates and in particular with peptides, proteins, nucleic acids and amino phospholipids [7]. Such extensive enzymatic and non-enzymatic HNE biotransformation regulates the content of the free HNE form which has only recently been analyzed thanks to the advent of more sensitive and selective analytical approaches.

While the enzymatic HNE biotransformation is a well-regulated process, well-explained in terms of metabolic detoxification, the role of the non-enzymatic biotransformations in modulating HNE detoxification is still debated.

The aim of the present review is to give a detailed overview of the enzymatic and non-enzymatic fate of HNE with a particular focus on understanding the biological role of non-enzymatic reactions and on the most modern analytical applications recently proposed for a qualitative and quantitative analysis of metabolites and reaction products. Such methods have in particular given a deeper insight into the non-enzymatic reactions of HNE, whose reaction products are quite difficult to identify and characterize due to their heterogeneity and low abundance. Another relevant aspect, which will be covered in the present review, regards the biological activity of the metabolites which in the past were considered as inactive detoxification products but have recently attracted more interest due to their biological activity.

2. Enzymatic detoxification

Upon lipid peroxidation of a ω-6 fatty acid HNE is generated as a toxic end product that can react with proteins, DNA and lipids to exert damaging activity. One of the systems the human body deploys to detoxify HNE is phase I metabolism using a variety of redox enzymes, and/or phase II metabolism mostly by conjugation to Glutathione (GSH) (Fig. 2).

2.1. Phase I Metabolism

2.1.1. Oxidation

HNE can be readily oxidized by different enzymes to 4-hydroxy-nonenoic acid (HNA), such as aldehyde dehydrogenases (ALDH) (Table 1) (Fig. 2). Different isoforms of ALDH have been described to oxidize the HNE carbonyl group, among which ALDH1A1, ALDH2 and ALDH3A1 are the most studied ones [8].

Many papers have been published on the role of ALDH enzymes in various different pathologies and on the protective effect they might have towards HNE cytotoxicity, thus underlying the relevance of such pathway in HNE detoxification. These protective roles were found after overexpression of these enzymes or using activator molecules. A short summary of recent papers will be outlined below.

A new model of age-related cognitive impairment to study Alzheimer's disease (AD) was proposed in ALDH2 (-/-) mice, which showed an increase of HNE adducts in the hippocampi and pathological changes that correlate with AD [9]. Other pathologies in the brain have also been associated with HNE and ALDH metabolism as exemplified by the ALDH2 *rs671* A allele, which induces higher levels of HNE and which is associated with post-stroke epilepsy susceptibility [10]. Overexpressing this enzyme was shown to partially restore activity. Furthermore, the ALDH agonist *Alda-1* successfully activated ALDH2 in a rat model of focal cerebral ischemia/reperfusion injury, decreased the accumulation of HNE and malondialdehyde (MDA), and improved brain injury [10]. ALDH2 activation could also prevent endothelial injuries induced by amyloid β peptides, which are responsible for mitochondrial dysfunction and cause cerebral degeneration [11]. Moreover, a neuroprotective effect of ALDH2 was found to be able to detoxify HNE both *in vitro* and *in vivo* [11].

HNE has also been involved in heart diseases and studies have shown protective roles of ALDH2, as confirmed by the capacity of *Alda-1* to significantly decrease aldehydic load in failing hearts [12]. The underlying mechanism of decreased mitochondrial ALDH2 activity was elucidated using murine models and an anoxia model of cardiomyocytes. Induced levels of HNE were observed after decreased ALDH2 activity that led to apoptosis of cardiomyocytes by inhibition of HSP70, phosphorylation of JNK, and activation of p53 [13]. Furthermore, the ALDH3A1 gene expression was significantly decreased in Wistar rats after administration of Doxorubicin (DOX), a chemotherapeutic agent with cardiotoxicity as a side effect mediated by oxidative stress and upregulation of HNE [14]. Another study on the effect of DOX showed a decrease in accumulation of HNE after treating mice with *Alda-1* [15].

ALDH2 activated by *Alda-1* was also successfully able to inhibit atherosclerosis and to attenuate nonalcoholic fatty liver disease (NAFLD) in mice [16]. Moreover, a high dose of ethanol leads to inhibition of ALDH2 in rats and increased levels of HNE and MDA were found in the serum [17]. Lastly, the effects of ethanol on gastric mucosa injury and the beneficial role of the antioxidant lipoic acid as activator for ALDH2 was studied [18]. Acute administration of ethanol induced injury in the gastric mucosa and increased levels of HNE, together with a reduced activity of ALDH2. When lipoic acid or *Alda-1*, used as positive control, were given before ethanol treatment, the detrimental effects of ethanol were prevented. The mechanism still needs to be elucidated. These results regarding HNE protection are truly promising especially as lipoic acid is a natural compound and can be easily given as a dietary supplement.

HNE has been implicated in many different diseases, and the effect HNE might have can be counteracted by inducing the metabolism. Numerous promising results have been described regarding ALDH enzymes and progress is being made.

HNA is not the final metabolite after oxidation of HNE, as it is able to undergo β- or ω-oxidation (Fig. 2). In the early nineties water and CO_2 were found as secondary products of HNE metabolism, and were ascribed to β-oxidation [19] as later demonstrated by Li et al. in 2013 [20]. They showed that this pathway may be inhibited in ischemic rat

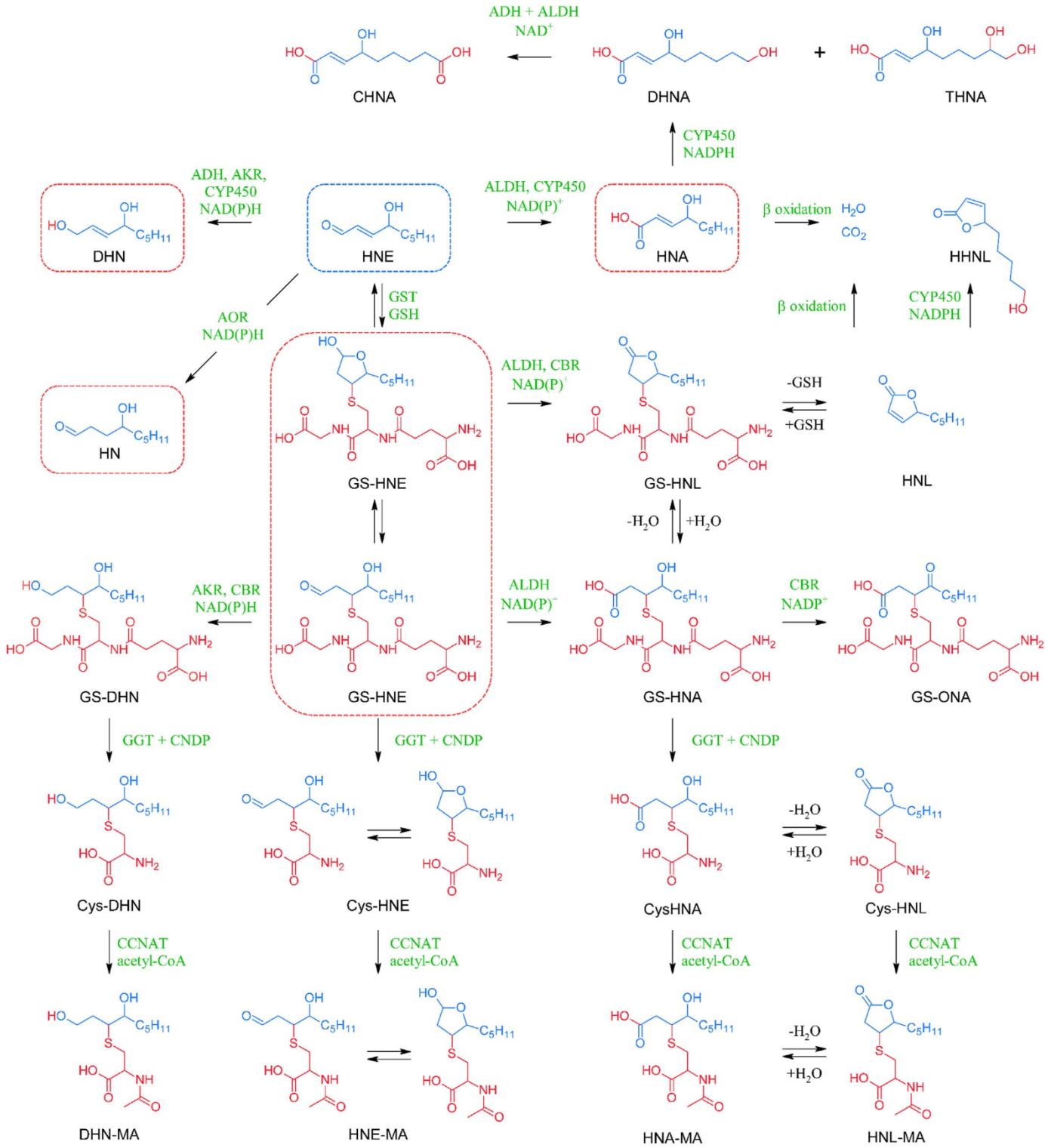

Fig. 2. Phase I and II metabolism of HNE. Any known pathway of HNE is depicted in this figure. Blue structures represent original HNE, whereas the red structures show the modifications. The enzymatic processes are shown in green.

heart and contributes to pathology since it increases the HNE concentration and the resulting protein modifications.

ω-Oxidation was first demonstrated by Alary et al. in 1998, where HNA is oxidized to 9-hydroxy-HNA, further oxidized by ADH and ALDH to 9-carboxy-HNA [21], later demonstrated in liver slices [22]. Also HNA-lactone, described further in this review, is available for microsomal ω-hydroxylation by cytochrome P450 4A enzymes [23]. More recently, it was shown that the same enzyme further catalyzes the ω-/ω-1-hydroxylation of HNA in a perfused rat liver to 4,9-dihydroxynonanoic acid and 4,8-dihydroxynonanoic acid [24] and that a ketogenic diet stimulated this process, resulting in lower HNE levels.

2.1.2. Reduction

Besides oxidation of the carbonyl group of HNE, it is also possible to be reduced to the alcohol 1,4-dihydroxynonene (DHN) via alcohol dehydrogenase (ADH) or aldo-keto reductase (AKR) enzymes (Table 1)

Table 1
List of all enzymes involved in HNE metabolism.

Name	Co-factor	Substrate	Product	Tissue site	Reference
Phase I Metabolism					
Alcohol dehydrogenases (ADH) E.C. 1.1.1.1	NADH	HNE	DHN	Hepatic Cytosol	[38]
Aldehyde dehydrogenases (ALDH) E.C. 1.2.1.3.	NAD(P)$^+$	HNE GS-HNE	HNA GS-HNA GS-HNL	Mitochondrial matrix	[38]
Aldo-keto reductases (AKR)	NADPH	HNE GS-HNE	DHN GS-DHN	Ubiquitous Gastrointestinal tract	[28]
Alkenal oxidoreductases (AOR) E.C. 1.3.1.74.	NADP$^+$/ NADPH	HNE	HN	Astrocytes	[34]
Carbonyl reductases (CBR) E.C. 1.1.1.184.	NADP$^+$/ NADPH	GS-HNE GS-HNA	GS-DHN GS-HNA GS-HNL GS-ONA	Unknown	[46,47]
Cytochrome P450 (CYP) E.C. 1.14.-.-.	NADPH	HNE	HNA DHNA DHN	Ubiquitous	[36]
Retinol dehydrogenase 12 (RDH12) E.C. 1.1.1.105.	NADPH	HNE	DHN	Photoreceptor cells	[35]
Phase II Metabolism					
Glutathione S-transferases (GST) EC 2.5.1.18.	GSH	HNE	GS-HNE	Ubiquitous	[38]
Gamma-glutamate transferase (GGT) EC 2.3.2.2.	Amino acid	GS-HNE GS-HNA GS-DHN	CysHNE-gly CysDHN-gly CysHNA-gly	Kidney Pancreas	[49]
Dehydropeptidase I (DHPI) EC 3.4.13.19. Aminopeptidase-M/N (AP-M/AP-N) EC 3.4.11.2. Cytosolic non specific dipeptidase EC 3.4.13.18.	–	CysHNE-gly CysDHN-gly CysHNA-gly	CysHNE CysDHN CysHNA	Kidney, lung	[50]
Cysteine S-conjugate N-acetyltransferase (CCNAT) EC 2.3.1.80.	Acetyl-CoA	CysHNE CysDHN CysHNA	HNE-MA DHN-MA HNA-MA	Kidney	[51,52]

(Fig. 2). ADH is a NADH dependent enzyme mainly found in the hepatic cytosol; its main function is to break down alcohols, but different isozymes have been described to show activity towards aldehydes in rats [25]. Thus far, this family of enzymes have not been extensively studied in humans and more information is needed in order to understand the metabolic relevance of these enzymes in the detoxification of HNE.

A second group of enzymes is the aldo-keto reductase superfamily, with 15 human isozymes related to pathologies and a few have been described to detoxify HNE [26,27]. Among these, AKR1B10 catalyzes the NADPH-dependent reduction of HNE to its corresponding alcohol, DHN, but also the reduction of the glutathionyl conjugate. Other isoforms, like AKR1B1, have been found to have more activity towards glutathionyl conjugates than towards free HNE [28,29]. HNE contributes to colorectal cancer (CRC) and different metabolites of HNE have been reported. AKR1B10 expression is diminished during carcinogenesis of the colon and increases the levels of HNE and acrolein contributing to the disease [30]. Controversially, another study showed that GSTA4 is activated during CRC, which aids the detoxification of HNE [31].

AKR1C1 and AKR1C2 are almost identical enzymes and both are found to be able to reduce HNE [32]. AKR1C3 has also been shown to reduce HNE in human neuroblastoma SH-SY5Y cells and to protect them from aldehyde toxicity as a model for neurodegenerative diseases [33]. Moreover, members of the AKR6 and AKR7 family have shown activity towards reactive aldehydes, like HNE.

Another enzyme described is alkenal/one oxidoreductase (AOR) which is able to reduce the C2-C3 trans double bond (Table 1) (Fig. 2) [34]. This enzyme is NAD(P)H-dependent and is also known as leukotriene B_4 12-hydroxydehydrogenase or 15-oxoprostaglandin 13-reductase. Recent studies showed a significant protective effect of cells overexpressing AO against HNE.

Furthermore, retinol dehydrogenase 12, RDH12, was shown to detoxify HNE to the corresponding alcohol in photoreceptor cells in a NADPH dependent matter (Table 1) [35].

Unlike the oxidation of HNE, the reduction has not been investigated relating to different pathologies and an effort should be made to discover protective roles of this metabolic pathway in order to offer more options against HNE cytotoxicity.

2.1.3. Oxidation and reduction

Finally, phase I metabolism includes both the reduction and oxidation of the carbonyl group on HNE yielding either DHN or HNA by the enzymes of the Cytochrome P450 (CYP) family (Table 1) (Fig. 2) [36,37]. Different human CYPs, CYP2B6, CYP3A4, CYP1A2 and CYP2J2, were found to be able to reduce the aldehyde using HPLC. It was suggested that the oxidation state of CYPs influences the product that is generated. HNE is oxidized in the presence of perferryl or ferric peroxide CYP, oxygen and NADPH, whereas it is reduced by ferrous CYP and in the presence of NADPH. To this date, no studies have described a protective role of this family of enzymes.

2.2. Phase II metabolism

2.2.1. Glutathione conjugation

To date, the only enzyme-catalyzed phase II reaction that has been characterized for HNE is its conjugation with glutathione to give 3-(*s*-glutathionyl)-4-hydroxynonanal (GS-HNE), which has been known since the nineties as a primary metabolite of HNE (Table 1) (Fig. 2) [38]. As explained in Fig. 2, since the GSH Michael addition removes the trans C2-C3 double bond, GS-HNE exists in equilibrium between the free aldehyde and its cyclic hemiacetal [7].

The enzymes catalyzing GSH conjugation belong to the alpha class glutathione S transferase family (GSTs), which play an important role in the detoxification of electrophiles. The activity of mouse liver GSTs towards HNE has been known since the nineties [39] and in the same decade an isoform with high HNE specificity (GSTA4) was characterized [40]. Mouse liver GSTA4 was also found to be inducible by HNE as demonstrated by confocal immunofluorescence microscopy experiments [41].

The role of GSTs is to catalyze the Michael addition of GSH to the electrophilic β carbon atom of HNE, making this reaction faster than the spontaneous Michael addition [40,42]. Such a reaction does not take place after HNE phase I metabolism, since both reduction and oxidation produce non-reactive primary metabolites [23]. On the other hand, secondary metabolites deriving from phase I metabolism of GS-HNE have been identified by several authors, in particular the 3-(*s*-glutathionyl)-1,4-dihydroxynonane (GS-DHN) and the 3-(*s*-glutathionyl)-4-hydroxynonanoic acid (GS-HNA), which is able to undergo an intramolecular reaction to generate the corresponding cyclic lactone (GS-HNL) (Fig. 2) [23,43,44].

Interestingly, Alary et al. demonstrated that both GS-HNE and GS-HNL undergo spontaneous retro Michael reactions, generating HNE and cis-HNA lactone (HNL), respectively. The same authors also demonstrated that HNL is more electrophilic than its open form (HNA) and therefore is able to react with GSH. They also demonstrated that GSTs are HNE selective, since purified rat liver GSTs catalyze GS-HNE retro Michael reaction but not HNL Michael addition to GSH or GS-HNL retro Michael [23].

After GSH conjugation to HNE, this intermediate is still very active and can be either reduced or oxidized (Fig. 2). Well described pathways include the NADPH dependent reduction to GS-DHN by an aldose reductase [28]. GS-HNE can also be oxidized by a NAD^+ dependent aldehyde dehydrogenase to 4-hydroxynonanoic acid–glutathione (GS-HNA) [45] or GS-HNA-lactone [23].

Additionally, a new role for the carbonyl reductase 1 (CBR1) enzyme has been described since it can catalyze both reactions of GS-HNE (Table 1) [46,47]. This enzyme is only reactive to GS-HNE, and not to HNE due to the glutathionyl moiety, as confirmed by its activity towards 3-glutathionyl-nonanal, 3-glutathionyl-hexanal and 3-glutathionyl-propanal. CBR1 is able to reduce GS-HNE in its hemiacetal form to GS-HNL in a $NADP^+$-dependent manner [46], and to oxidize the free aldehyde to GS-DHN in a NADPH-dependent manner [47]. Furthermore, CBR1 is able to convert GS-HNA to glutathionyl-4-ketononanoic acid (GS-ONA) [46]. These results have only been shown *in vitro*, and more studies are necessary to evaluate its activity *in vivo*.

However, as summarized in Fig. 2, GSH conjugates are not the final metabolites of HNE disposal. In fact, it is known that such conjugates can be further metabolized and excreted as mercapturic acids (HNE-MA, HNA-MA and DHN-MA) [48]. The pathway leading to this biotransformation is common across all GSH conjugates (GS-HNE, GS-HNA or GS-DHN). The first step is the removal of gamma-glutamate operated by gamma-glutamate transferase (GGT) [49], followed by the removal of glycine catalyzed by a heterogeneous set of dipeptidases including dehydropeptidase I, aminopeptidase M or aminopeptidase N and cytosolic non-specific dipeptidases. Nevertheless, a specific cytosolic dipeptidase for cys-gly S conjugates was described as an essential enzyme in the mercapturic route of rat liver [50]. The last step of the metabolic pathway is the N-terminus acetylation catalyzed by the enzyme cysteine S-conjugate N-acetyltransferase (CCNAT) [51,52], which only recently have been identified as the enzyme encoded by the gene NAT8 (Table 1) [53].

2.2.2. Putative phase II metabolites from uncharacterized pathways

Two glutathione-HNE 4-oxo-conjugates, namely 3-(S-glutathionyl)-4-hydroxynonanal (GS-ONE) and 3-(S-glutathionyl)-4-oxononanol (GS-ONO), were also identified as HNE metabolites of keratinocytes incubated with HNE (Fig. 3C) [54]. They possibly arise from oxidation of the 4 hydroxyl moiety of GS-HNE and GS-DHN, respectively, but the metabolic pathway of their production is still unclear.

Mercapturic acids have been found also for a set of ω-oxidized HNA derivatives (Fig. 3A) [23,55]. Alary and colleagues proposed a reaction scheme predicting the reaction of ω-oxidized HNA with GSH through a Michael reaction [23]. However, since HNA has been proven to be non-electrophilic [23] it is not clear how its ω-oxidation derivatives can react with GSH.

A more realistic pathway for the production of such metabolites could occur through the following steps:

1. ω-Oxidation of HNL to produce 4,9 dihydroxy-nonenoic acid lactone (DHNL) and 9 carboxy 4-hydroxy- nonenoic acid lactone (CHNL)
2. Formation of the glutathione conjugates GS-DHNL and GS-CHNL through a Michael reaction between GSH and either DHNL or CHNL, as already observed for HNL
3. Conversion of GS-HHNL and GS-CHNL into the corresponding mercapturic acids (HHNL-MA and CHNL-MA, respectively, Fig. 3A) following the same pathway of other GSH conjugates
4. Opening of lactones (DHNL-MA and CHNL-MA) into the corresponding acids (HHNA-MA and CHNA, respectively, Fig. 3A)

Mercapturic acids have been reported also for ω-oxidized HNE (CHNE-MA, Fig. 3B) and ω-oxidized DHN (CDHN-MA, Fig. 3B) [55]. Also in these cases, there are no hypothesis on how they can be produced.

Although GSH conjugates are the only phase II metabolites of HNE that have been fully characterized, the recent identification of two glucuronides (i.e. DHN-GCN and HNA-GCN, Fig. 3D) suggests that HNE metabolism can include other phase II reactions [55]. However, to date there are no clues relating such metabolic pathways, nor to the mechanisms leading to the production of three other metabolites assigned as 3-methylsulfanyl derivatives of 4-hydroxynonenoic acid (i.e. TM-HNA, TM-DHNA and TM-CHNA, Fig. 3E) [55].

Other metabolites identified from uncharacterized pathways are phase I metabolites [55]. Fig. 3F represents a group of metabolites in which HNE undergoes oxidation and a reduction of the C2-C3 trans double bond. It remains unclear whether 4,8,9-trihydroxy-nonanoic acid (THN) and 9-Carboxy-4-oxo-nonenoique acid (CHN) derives from the oxidation of HNA and then a reduction of the C2-C3 trans double bond, or vice versa. The proposed pathway for γ-nonalactone (NL) is a reduction of the double bond, followed by an oxidation step and lactonization [56]. The same author identified another metabolite of HNE, 4-oxononenal (ON) [57]. However, this pathway still needs to be determined.

Finally, two more putative metabolites that are oxidized, but not conjugated (Fig. 3G), have been identified [55]. To date, the pathways leading to 9-hydroxy-4-oxo-nonenoic acid (HONA) and 9-carboxy-HNE (CHNE), have not been characterized yet.

2.3. Quantitative aspects of HNE phase I and phase II metabolism

To elucidate the fate of HNE, either metabolized by phase I or II metabolism or adducted to molecules or macromolecules, many studies have been published on the quantification of HNE disposal. Experiments with tritiated HNE confirm that only a small percentage of radioactivity can be found on proteins or DNA, confirming that the vast majority of HNE disposal is due to metabolism. In particular, the percentage of HNE found on proteins was reported to be around 5% of the total HNE dose in rat liver and brain [58]. A similar amount was found in human polymorphonuclear leukocytes incubated with HNE [59] and a percentage between 2% and 8% was found in various mammalian cells and organs such as hepatocytes, intestinal enterocytes, renal tubular cells, aortic and brain endothelial cells, synovial fibroblasts, neutrophils, thymocytes, heart, tumor cells [60,61] and rat kidney cortex mitochondria [62]. Interestingly, pathologies like dia-

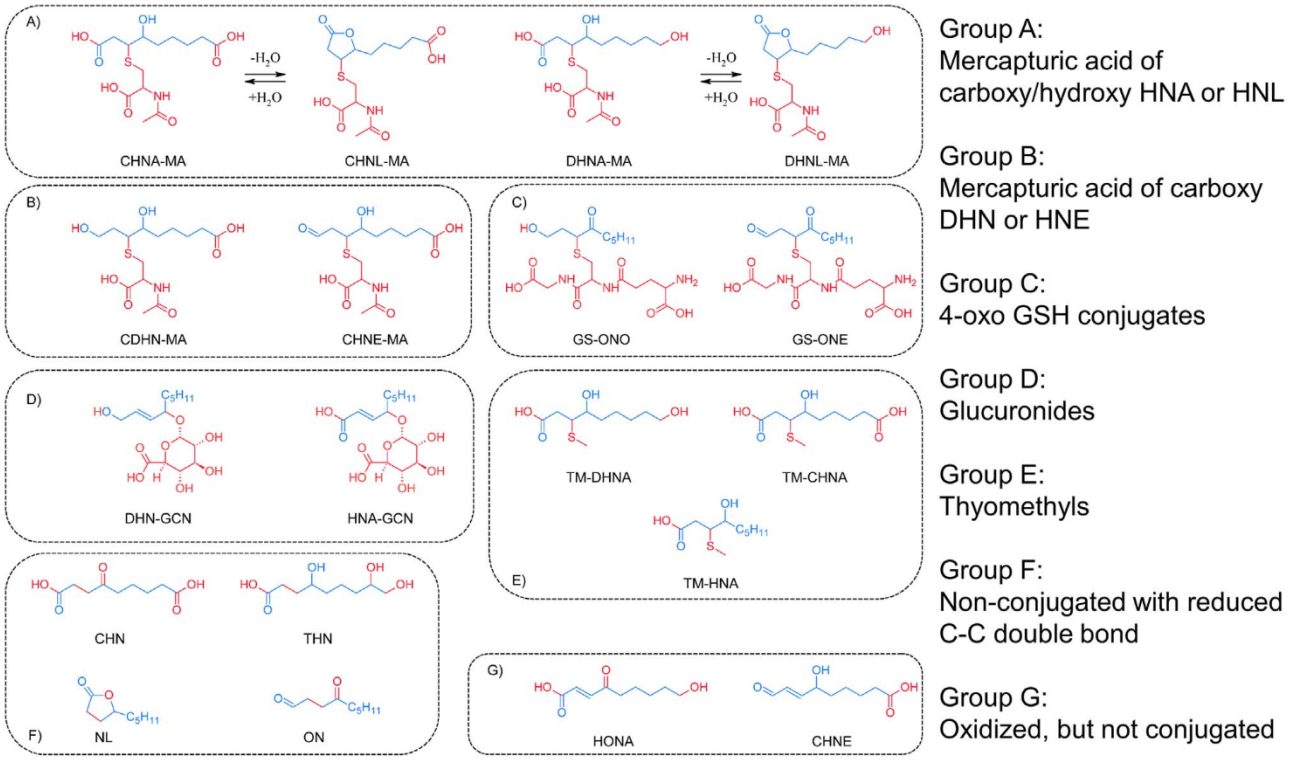

Fig. 3. Metabolites of HNE from uncharacterized pathways.

betes can negatively influence the activity of some metabolism enzymes such as GST and ALDH, while ADH activity remains unchanged [63]. Not all tissues have the same metabolic capacity and although NADH stimulated HNE metabolism reduced protein adducts in rat liver (but not in lung or brain) it seems impossible to metabolically prevent protein-HNE modification [64].

The metabolism of HNE seems to be very fast. In rat kidney cortex mitochondria, 80% of tritiated HNE is metabolized within 3 min producing DHN, HNA and GSH conjugate [62]. In hepatoma cell a dose of 25 μM HNE has a half-life of 2 min and 75% is converted into either GSH conjugates (61%) or HNA (14%), while a small percentage follows the tricarboxylic acid pathway [65]. In hepatocytes, a 100 μM HNE dose is metabolized within 3 min and accompanied by a decrease of free GSH, which is followed by its restoration in a S shaped curve up to concentrations below the initial value [61]. In serum, the physiological HNE level (about 0.1–0.2 μM) as measured by means of GC techniques was restored after 10–30 s, starting from an initial value of 1 μM HNE [61]. However, data on basal HNE level are inconsistent since antibody detection estimates a concentration of about 600–700 nM in serum of healthy subjects and diabetics [66].

Also the equilibrium between phase I and phase II metabolism seems to be influenced by the organ or cell type. For instance, many cells type are not able to convert GSH conjugates into the corresponding mercapturic acids [61].

Experiments in rat aortic smooth muscle reveals that 60% of the metabolism is linked to GSH conjugation, GS-DHN being the major metabolite [29]. Aldose reductase was the enzyme responsible for GS-HNE reduction since GS-DHN formation was prevented by the addition of a specific enzyme inhibitor. The same paper also demonstrated that 25–30% of HNE was oxidized to HNA by ALDH, since the addition of a ALDH inhibitor prevented HNA formation. Decrease of HNA was accompanied by an increase of GSH conjugation revealing that the two pathways are in competition for HNE detoxification.

Similar percentages of adducts were found in rat erythrocytes [67] but inhibitors of aldehyde or alcohol dehydrogenase (i.e. cyanamide and 4-methyl pyrazole) had no effect on the formation of HNA and GS-DHN, indicating that these enzymes are not significantly involved in the erythrocyte HNE metabolism. However, aldose reductase inhibition led to a selective decrease in the formation of GS-DHN. Nevertheless, the extent of GSH conjugation was unaffected suggesting that inhibition of GS-HNE phase I metabolism does not have a negative feedback on phase II metabolism.

After 2 min, the approximate distribution of HNE metabolites in rat hepatocytes was found to account for about 30% HNE–GSH adduct, 30% HNA, 10% DHN, while the remaining 30% of HNE followed other metabolic pathways. A key role of the β-oxidation pathway in the disposal of tritiated HNE was confirmed since water radioactivity decreased after addition of a β-oxidation inhibitor [22,60].

Leukocytes are also able to metabolize about 20% of radiolabeled HNE by β-oxidation, while mercapturic acids and proteins account for only 5% of the total radioactivity. Interestingly, HNA was found to be the main metabolite followed by DHN and GSH conjugates [59].

Unlike liver, where mercapturic pathway seems to prevail, oxidation pathways seems to be the principal responsible for HNE metabolism in the brain [58,68]. Experiments in astrocytes revealed that 90% of a 1 μM initial dose of HNE was metabolized into the expected metabolites (HNA, GS-HNE, GS-DHN) with a prevalence of oxidation products (HNA). However, an increase of the HNE initial dose decreased the percentage of HNE metabolized either as HNA or GSH conjugates [57]. A minor role of GSH conjugation in total HNE metabolism has recently been found in various rat organs [69].

2.4. Transport and excretion of HNE metabolites

Although not investigated as deeply as phase I and phase II metabolism, excretion of HNE metabolites is a relevant process to HNE disposal. Dygas et al. reported that GS-HNE conjugate can be transported by the human erythrocyte multispecific organic anion-transporting ATPase (MOAT) [70]. Interestingly, evidence of enterohepatic circulation of HNE metabolites has been obtained in rats after intravenous infusion of radiolabeled HNE [71]. The HNE metabolites GS-HNE, GS-DHN, DHN-MA and HNL-MA were detected in bile, while

urine contained only mercapturic acids (i.e. DHN-MA, HNL-MA, HNE-MA and HNA-MA). The multidrug resistance-associated protein 2 (MRP2) transporter has been identified to be GS-HNE specific in rat hepatocytes. In fact, hepatocytes from MRP2 deficient rats have a fourfold diminished ability to export GS-HNE in the extracellular media compared to hepatocytes from wild-type rats. However, the extracellular concentration of HNA (the other main HNE metabolite detected) was the same for the hepatocytes of both control and MRP2 deficient rats [72]. Also RLIP76 seems to be involved in the transport of HNE and its conjugates since excised liver tissue from RLIP76 deficient mice accumulates HNE and GS-HNE at concentrations three times higher than control [73]. Notably, since transport activity of RLIP76 mediates insulin resistance by increasing the clathrin-dependent endocytosis of insulin, one may argue that the role of this transporter in modulating the insulin resistance during oxidative stress conditions goes beyond excretion of HNE metabolites (PMID: 20007934).

2.5. Enantioselectivity of phase I and phase II reactions

Since HNE has a stereocenter (C4) and naturally occurs as a racemic mixture of (*S*)-HNE and (*R*)-HNE [74], the enantioselectivity of the enzymes involved in HNE metabolism has been studied by several authors.

For phase I metabolism, Honzatko et al. published two studies reporting enantioselectivity regarding ADH and ALDH enzymes. Both in the rat liver cytosol and guinea-pig liver cytosol (*R*)-HNE was metabolized more efficiently than the (*S*)-enantiomer [75,76]. Interestingly, in the rat liver cytosol ADH was found to be enantioselective, and ALDH showed little difference, whereas ALDH was shown to be enantioselective in guinea-pig liver cytosols. ADHs in guinea-pig liver cytosols were inactive against both HNE enantiomers. Another study, performed in rat brain mitochondria, also showed a preferential detoxification of (*R*)-HNE by ALDH using a novel method for the separation of (*R*)-HNE and (*S*)-HNE by a derivatization technique [77]. Same results were found in brain mitochondrial lysates, where rat ALDH5A showed a preference for (*R*)-HNE, however rat ALDH2 did not seem to be enantioselective [78].

GSTs enantioselectivity has been studied by several scientists who have published inconsistent results. In fact, while some authors reported that GST is not enantioselective [77] or perhaps slightly enantioselective [79–81], others have reported that GST selectively produces (*S*)-HNE [76].

In an animal experiment Gueraud et al. demonstrated that, for both HNE enantiomers, about 40% of the radioactivity originating from intravenous infusion of tritiated HNE is excreted into urine as mercapturic acids (see Table 2) [43]. (*R*)-Enantiomer was metabolized more rapidly since residual (*R*)-HNE was less than (*S*)-HNE. Moreover, urinary excretion of DHN-MA was higher for rats receiving (*R*)-HNE. This demonstrates that the enzymes catalyzing the conversion of GS-HNE into GS-DHN are enantioselective. However, the authors have not reported that the enzymes catalyzing the oxidation of the HNE glutathione conjugates are not enantioselective since the sum of the radioactivity for end-products of oxidative metabolism (HNL-MA + HNA-MA) is almost equal for both enantiomers. However, according to the data reported in Table 2, (*S*)-HNE produces more HNL-MA. This suggests that the GS-HNA/GS-HNL equilibrium reported in Fig. 2 is influenced by the configuration of the C4 carbon atom.

Table 2
Percentages of the initial radioactivity for urinary metabolites detected after 48 h. Re-elaborated data in bold, HNA lactone reported as HNL. Data taken from Gueraud et al. [43].

Metabolite	(*R*)-HNE	(*S*)-HNE
HNE-MA	0	13.3
DHN-MA	27.3	9.8
HNA-MA	9.2	6.5
HNL-MA	5.3	11.6
TOTAL MA	41.80	41.20
HNA-MA + HNL-MA	**14.50**	**18.10**
HNA-MA / HNL-MA	**1.74**	**0.56**

Table 3
Percentages of the initial radioactivity after rat liver cytosolic incubation. Re-elaborated data in bold, HNA lactone reported as HNL. Data taken from Gueraud et al. [43].

Metabolite	GS- (R)HNE	GS- (S)HNE
GS-HNE	32.6	11.4
GS-DHN	13.5	0
GS-HNL	26.8	21
HNE	2.9	15
DHN	4.3	3.9
HNA	2.2	5.1
HNL	10.5	9.8
Total	**92.80**	**66.20**
Retro Michael (HNE + DHN + HNA + HNL)	**19.90**	**33.80**

In the same paper the authors also tried to track the metabolic fate of the two enantiomers of GS-HNE incubated in rat liver cytosol, by quantitating the main products of oxidative and reductive metabolism of GS-HNE, along with GS-HNE retro Michael products. Data are reported in Table 3 and suggest that GS-(*S*)-HNE is metabolized and undergoes retro Michael reaction more than GS-(*R*)-HNE. However, the identified metabolites of GS-(*R*)-HNE accounted for more than 90% of initial radioactivity, while only 66% of the initial radioactivity was retained by the corresponding GS-(*S*)-HNE metabolites. This suggests that the higher metabolic rate observed for GS-(*S*)-HNE is due to some uncharacterized enantioselective pathways. Interestingly, by monitoring GSH adducts in various rat organs, Sadhukhan et al. found (*S*)-enantioselectivity for liver and heart, whereas brain metabolism was not enantioselective [69]. Taken together, these data demonstrate that GSTs selectivity can be organ dependent, probably due to the high GSTs polymorphism [82]. Therefore, it is not surprising that different authors can find apparently inconsistent data about GSTs enantioselectivity in experiments utilizing different animal models or different cell type/organs.

2.6. Analytical aspects of HNE metabolism tracking

Detecting HNE metabolites has proven to be quite challenging, but advancements have been made in recent years leading to the identification of metabolites and their formation. Basic analytical aspects of HNE metabolite analysis have recently been reviewed by Spickett [83]. Since the nineties, some analytical efforts have been focused on developing more sensitive methods for detecting HNE metabolites in biological specimens collected from cells, tissues or animals. Early methods were based on derivatization reactions aimed at increasing the sensitivity of UV [38], fluorometric [84] or electrochemical [85] detection of the analytes after their chromatographic separation.

Although some efforts have been made also on the development of enzyme immunoassays [86], mass spectrometry (MS) is nowadays the preferred detection technique since it is suitable for quantitation and allows the simultaneous identification even of unpredicted/new metabolites. This technique can be coupled either to gas chromatography (GC-MS) or liquid chromatography (LC-MS).

The use of GC-MS for the determination of TMS-derivatized HNE has been known since the nineties [87] and is still used for tracking HNE metabolism [88]. Concerning other modern GC based approaches, Asselin et al. described a method based on a Raney nickel reaction to convert HNE conjugates into corresponding alkanal, alkanol or acid derivatives (i.e. 4 hydroxynonanal, 1,4 dihydroxinonane, 4 hydroxynonanoic acid) followed by GC detection [89]. Moreover, an interesting method for incorporation of different number of deuterium atoms into

HNE metabolites was proposed by Li et al. [90]. The method is based on $NaBD_4$ reduction followed by TMS derivatization and GC-MS analysis. The reduction step leads to incorporation of no deuterium atom for DHN, one deuterium atom for HNE and two deuterium atoms for ONE, making the corresponding metabolites easy to distinguish by mass spectrometry.

The importance of isotope labeling for mass spectrometry detection of HNE metabolites has been discussed by Sadhukhan et al. [91] and a clear example of how to use this technique to track complex metabolic pathways has been given by Zhang et al. [92].

Importantly, also LC-MS based protocols can include isotope labeling or derivatization steps. Derivatization can be used to enhance the sensitivity of MS detection by increasing ionization efficiency of the analytes [93] or for other purposes. For instance, the use of chiral reagents has been demonstrated to be a powerful tool to chromatographically resolve enantiomers and to reveal the enantioselectivity of enzymes involved in specific metabolic pathways [77,94].

Among the applications using isotope labeling, a first application that is worthy of mention is the use of stable isotope tagged HNE. This reagent allows the detection of unpredicted metabolites by MS, fishing out signals with a peculiar isotope pattern [95].

A second application of isotope labeling that has been widely used to track HNE metabolic fate is the use of radiolabeled HNE. By using this technique, it is possible to measure the percentage of residual radioactivity in the different body or cell compartments, which is a quantitative index of the disposal of the initial dose of radiolabeled HNE. The most used reagent is tritiated HNE (^{3}H-HNE) which has been used by many authors since the nineties [21,22,29,43,71,96,97]. Notably, these two isotope labeling strategies have recently been merged to allow a comprehensive characterization of HNE metabolism after oral administration of HNE in rats [55].

Finally, sample treatment before LC-MS analyses has been a recent matter of concern. In fact, Sadhukhan et al. demonstrated that GS-HNE content can be overestimated since residual glutathione and residual HNE can react through a non-enzymatic Michael reaction. This issue was addressed by the authors who suggest spiking the samples with iodoacetic acid to quench the residual GSH activity [69].

2.7. Biological activity of phase I and II HNE metabolites

In general term, metabolism transforms lipophilic compounds into more polar, hydrophilic and readily excretable products. Phase I and II HNE metabolites fulfil this general rules since all the HNE metabolites are more hydrophilic in respect to the parent compound. Although HNE metabolites are less electrophilic in respect to HNE or not reactive at all, some of them have a biological activity which is potentiated in respect to the parent compound. In this regard, some studies have evaluated the biological activity of HNE metabolites with a particular interest on phase II metabolites. Spite et al. have found that GS-HNE is a potent proinflammatory stimulus *in vivo* and that it has also direct action on isolated human leukocytes [98]. In particular GS-HNE when injected intraperitoneally (1 μg) induced a significant infiltration of leukocytes, within the range of that stimulated by LTB4 and fMLP which was 10-fold higher than that evoked by HNE and by the reduced GSH-HNE metabolite (GS-DHN). By contrast, GS-DHN was found to induce inflammation in macrophages [99] and mitogenic signaling in smooth muscle cells [99]. A further confirm on the role of GS-HNE and GS-DHN as pro-inflammatory agents is given by the experiments in RLIP76 knockout mice in which the export of glutathione metabolites is blocked. These mice were found to be protected against inflammation and, notably, from oxidative stress–induced insulin resistance [99]. More recently a novel mechanism involving GS-HNE and GS-DHN in obesity-induced metabolic syndrome has been reported. GS-HNE and GS-DHN were found more abundant in visceral adipose tissue of ob/ob mice and diet-induced obese in respect to lean controls and able to induce the expression of inflammatory genes, including *C3*, *C4b*, *c-Fos*, *igtb2*, *Nfkb1*, and *Nos2*. These data can explain the obesity-induced decrease in the GSTA4 expression as a compensatory response, and in particular that downregulation of GSTA4 could be considered as an adaptive mechanism aimed to decrease the inflammatory cascade induced by GS-HNE and GS-DHN. The mechanism by which GS-HNE and GS-DHN transmit their message to the macrophages is yet unknown, but a cell surface receptor would seem to be most likely, such as toll-like receptors (TLRs), potentially TLR6 or TLR9, both of which show upregulated expression in response to GS-HNE and GS-DHN [5].

3. Non-enzymatic detoxification

Besides the enzymatic metabolism, HNE degradation involves a set of covalent reactions which, at least in their starting phase, occur without enzymatic processes. HNE is indeed an electrophilic compound which can spontaneously react with nucleophilic moieties within biomacromolecules such as proteins and nucleic acids as well as within small endogenous compounds such as phospholipids and peptides (Fig. 1). The marked electrophilicity of HNE is ascribable to the conjugation between the carbonyl function and the unsaturated bond which reflects in two distinct reactive centres, namely the carbonyl carbon atom and the unsaturated β-carbon atom [100]. According to hard–soft acid–base theory (HSAB), the nucleophilic reactants can be grouped depending on their preferential reactivity towards the carbonyl group (such as hydroxyl functions), the β-carbon atom (such as thiol functions) or on their capacity to condense with both electrophilic centres (such as amino groups) [101].

The condensation between the HNE carbonyl function and primary amino groups (such as that characterizing the lysine side chain) involves an initial carbinolamine intermediate followed by a dehydration reaction to give the imino adduct, which is reversible in presence of water molecules and thus is reasonably stable in physiological conditions only when surrounded by very hydrophobic environments (Fig. 4) [102]. Again, the condensation on the β-carbon atom (such as that involving the thiol function of the cysteine residue) occurs through Michael addition, the products of which also are reversible and can liberate the nucleophilic group in presence of an excess of a second nucleophilic reactant (Fig. 4) [103]. This renders the Michael adducts more stable in physiological conditions compared to the condensation products involving the carbonyl groups even though they remain reversible and such a reversibility can have relevant biological implications as detailed below.

While avoiding a systematic analysis of all proteins, the HNE-induced carbonylation has been reported in literature, the general reactivity of HNE towards biological targets and the main pathophysiological implications of the adducts will be discussed in the following sections. The reader interested in more comprehensive analyses can refer to recent extended reviews (e.g. see ref. [104]).

3.1. Protein adducts

3.1.1. HNE induced protein carbonylation: general aspects

HNE reacts with nucleophilic residues within proteins, such as the side chains of cysteine, lysine and histidine, mostly yielding the corresponding Michael adducts. As detailed above, the primary amino group of the lysine side chains can also give imino adducts which are reasonably stable when formed within hydrophobic environments (see above), while the formation of thioacetal derivatives has a negligible role in determining the reactivity of the cysteine thiol function (Fig. 4) [105]. Several studies have highlighted that HNE-induced protein carbonylation is a highly selective process since very few nucleophilic residues are carbonylated within each protein while the remaining nucleophilic sites appear to be stably unreactive. Despite the great interest attracted by the HNE-induced carbonylation, the reasons for such selectivity are still debated even though accessibility and nucleo-

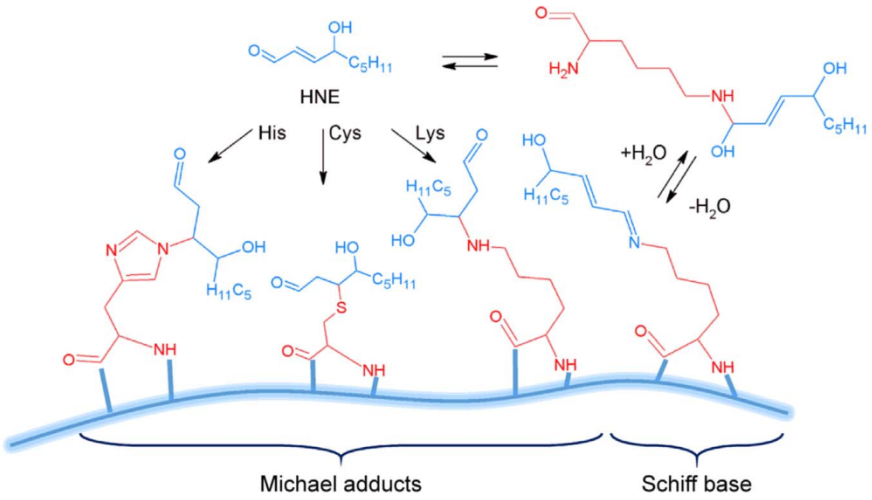

Fig. 4. HNE adduction on different protein side chains.

philicity of a given residue appear to play a pivotal role. This means that the residue reactivity is finely modulated by the protein environment and this implies that the dynamic behavior of the protein structure can largely influence the susceptibility of a given residue to carbonylation processes [106].

A meaningful example of the factors influencing the residue's reactivity is offered by human albumin, the unique free cysteine of which (Cys34) shows a remarkable reactivity towards HNE which can be rationalized by considering both the surrounding residues and its dynamic behavior. Indeed, Cys34 is contacted by three residues (namely His39, Lys41 and Tyr84) which are able to both increase Cys34 nucleophilicity and stabilize the so formed thiolate anion through a mechanism which brings to mind that seen in GST enzymes (Fig. 5) [107]. Moreover, molecular dynamics (MD) studies showed that the thiolate anion induces a set of protein conformational shifts which increases Cys34 accessibility forming a hydrophobic crevice well suited to accommodate HNE as confirmed by docking simulations [108]. As expected, accessibility and nucleophilicity play a key role

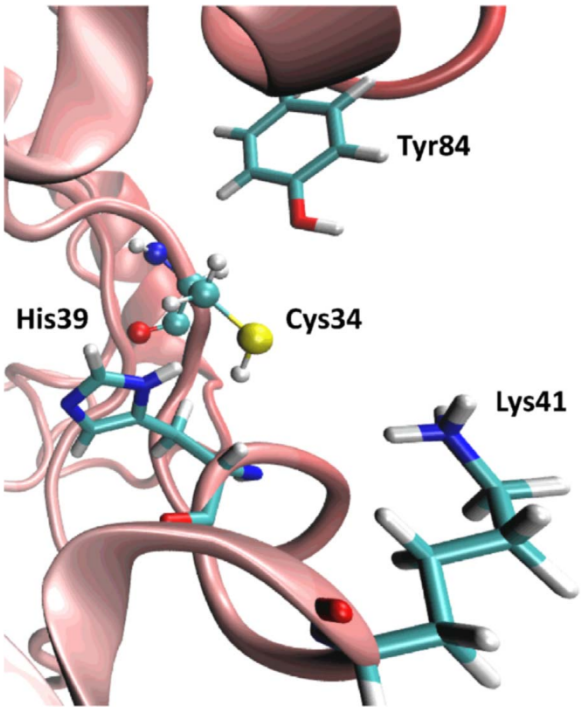

Fig. 5. Key contacts explaining the marked acidity of Cys34 in human albumin.

and appear to be markedly influenced by dynamic processes able to enhance Cys34 reactivity. This can explain the difficulty in developing provisional approaches able to discriminate between reactive and unreactive nucleophilic residues based on the protein amino acidic sequences or, at most, on the protein 3D (static) structures [109].

A third factor which can influence the residue reactivity is the so called neighboring effect, since regions rich in nucleophilic residues are found to be more susceptible in multiple protein carbonylation probably as the generation of a first protein adduct can enhance the reactivity of the neighboring nucleophilic residues. The recently reported carbonylation of the human ubiquitin provides an interesting example of such a neighboring effect since the marked reactivity towards HNE of His63 can be explained by considering the catalyzing effect exerted by adjacent Lys6 which was found to yield the imino adduct (Fig. 6) [110]. Indeed, one may suppose that there is a cross-talk between these two residues since the imino adduct on Lys6 retains the capacity to yield the Michael adduct and, more importantly, constrains the reactive electrophilic β carbon atom close to the imidazole ring of His63 in a pose stably conducive to the addition. Such a mechanism, which gained experimental confirmation in the acetylation of ubiquitin [111], highlights the major differences between the HNE-induced protein adducts since the reactions which involve a Michael addition switch off the HNE reactivity forming adducts which are reversible but no longer electrophilic, while the imino condensation exerts only a sort of physical trapping of HNE giving reversible and still electrophilic adducts. Their reactivity and lability suggests that the imino adducts can also act as intermediates to promote the condensation with neighboring histidine or cysteine residues through a mechanism which resembles that observed for carnosine (see below).

3.1.2. *Biological effects of HNE protein modification*

3.1.2.1. Damaging effects. Protein carbonylation is usually seen as an undesired effect which exerts clear toxicological consequences by profoundly altering the biological functions of the adducted proteins (Fig. 7) [112]. Its overall cellular effect depends on the role played by the adducted proteins and can induce apoptosis when affecting signaling cascades involved in cell growth and differentiation [113]. In detail, the toxic effects exerted by HNE protein adducts can occur through two major mechanisms. Firstly, the adducts can alter the protein conformation inducing misfolding events with clear toxic outcomes especially when affecting structural proteins such as those involved in the cytoskeleton [114]. A clear example is provided by α-synuclein, which reacts with HNE forming protein adducts which are able to seed the α-synuclein amyloidogenesis by inducing conformation changes which are different from those seen in amyloid fibrils based on

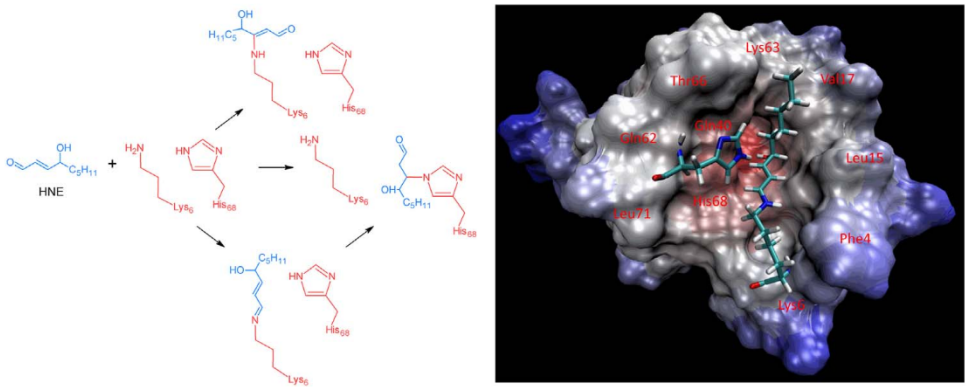

Fig. 6. Reaction mechanism for the cross-talk between Lys6 and His68 of ubiquitin. Right figure depicts proximity between Lys6 and His68. Reproduced from ref. [110] with the permission of Elsevier.

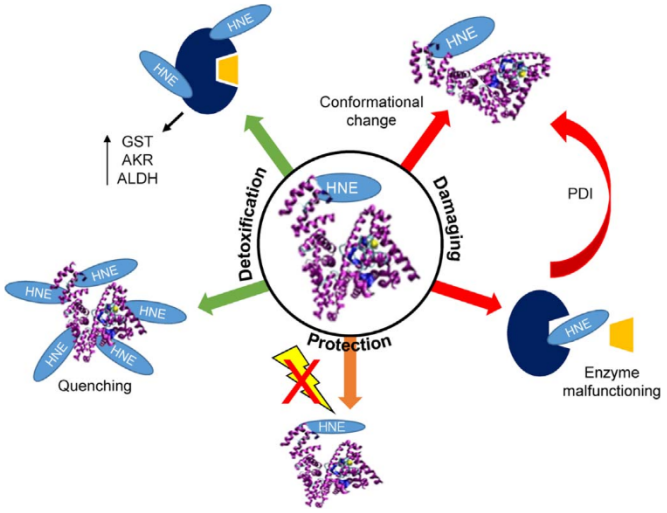

Fig. 7. Multifaceted biological effects exerted by HNE carbonylation.

β–sheet stabilization [115]. A second mechanism affects enzymes and receptors and induces their substantial inactivation by masking nucleophilic residues which play key roles in the protein function. Among the numerous enzymes which are found to be affected by HNE carbonylation, two enzymatic classes are worthy of mention. The first group includes enzymes (such as Serine/Threonine-Protein Kinase AKT2) which are variously involved in the cellular response to oxidative stress and the carbonylation of which induces a vicious circle which progressively exacerbates the stress condition [116,117]. The second class involves enzymes which assist the folding of other proteins, such as Protein Disulfide Isomerase (PDI) [118], which are consequently unable to correctly fold, thus indirectly propagating the structural alterations exerted by HNE. With regard to receptor carbonylation, HNE usually induces an aberrant signaling of the adducted proteins by inhibiting or even endlessly stimulating them. An interesting example is provided by a very recent study revealing that the aberrant TRPV1-dependent regulation of coronary blood flow (CBF) observed in diabetic patients is ascribable to the formation of a covalent adduct between HNE and Cys621 of TRPV1 which is located on the pore and the modification of which inhibits TRPV1 currents thus contributing to the microvascular dysfunctions as seen in diabetic patients [119].

3.1.2.2. Protein HNE adduction as a protective and modulatory detoxifying mechanism. Even though the carbonylation of these proteins is usually seen as a toxic consequence induced by the HNE accumulation under stress conditions, it can also have protective and modulatory effects (Fig. 7). A first protective mechanism can be rationalized by considering the general reversibility of these adducts which suggests that they can have a role similar to that of cysteinylation by protecting critical residues during severe stress conditions. Indeed, highly oxidative conditions can irreversibly oxidize the thiol functions into sulphinic and sulphonic acids by which the protein function is irremediably lost [120], while HNE-induced covalent modifications of the thiol group can protect them from irreversible modifications allowing their restoration when the oxidative stress disappears. Clearly, such a protective mechanism would occur at the expense of temporarily inactivating the proteins. The possible protective roles of HNE are further substantiated by a recent study which revealed that a vast majority of HNE adducts shows a dynamic behavior and rapidly disappear in intact cells. In contrast, few protein adducts were found to be highly stable during the time thus suggesting that, along with the already mentioned selectivity of the residue's reactivity, there is also a selectivity in the adduct stability which is modulated by factors present only in intact and metabolically active cells and cannot be restricted to sole chemical factors [121].

A second protective mechanism is seen in those proteins which possess extremely reactive residues and are richly carbonylated by HNE. When their concentration is largely higher than that of HNE, one may figure out that these reactive proteins have a sacrificial role since they are able to trap HNE almost completely with a minimal impact on its overall function even assuming that the adducted proteins lose their biological activities. Some abundant extracellular and cellular proteins such as albumin and actin have been identified as sacrificial substrates of HNE. The high reactivity of such protein is not only due to their abundance but also due to the presence of reactive and accessible cysteine residues. Albumin rapidly reacts with HNE (rate constant of 50.61 ± 1.89 M-1 s-1) and is the main reagent responsible for the rapid disappearance of HNE in serum. By considering a second-order reaction and a mean plasma concentration of 600 nmol/mL, the half-life of 10 nmol/mL of HNE in human plasma would be less than 17 s, which was then confirmed experimentally [108]. The high reactivity of HNE towards HSA is due to the presence of several accessible nucleophilic residues, among which Cys34 was found to be the most reactive [122]. The rate constant of Cys34 was found to be almost 1 order of magnitude higher than that of GSH, and such a different reactivity was explained by molecular modelling studies showing a markedly higher acidity of the thiol group of Cys34 in respect to that of GSH as above reported. Actin is another abundant protein which was found to be highly reactive towards HNE and also for this cellular protein the high reactivity is due to a cysteine residue, Cys374, which is characterized by a significant accessible surface and a substantial thiol acidity due to the particular surrounding microenvironment [123].

The high reactivity and efficient quenching of some abundant proteins such as actin and albumin open a question regarding their potential role as non-enzymatic detoxifying agents of HNE and more in

general of lipid electrophilic break-down products. This view is reinforced by the fact that, at least for actin, the biological activity is not hampered by covalent binding with HNE [124]. Moreover, the covalent binding to cysteine residues is reversible and the free form could be restored by a transfer with GSH as below reported. Hence the accessible cysteine residues of albumin (Cys34) and actin (Cys374) which are not involved in disulfide bridge as well in the biological function of the proteins, seem to have the biological role of scavenging HNE before it can impact some nucleophilic sites of the protein whose adduction could compromise the protein function [125].

Furthermore, pathways activated upon HNE-induced carbonylation do not necessarily lead to aberrant signaling events as mentioned above but it can also play modulatory roles as exemplified by those reported for glutamate–cysteine ligase. This enzyme which catalyzes the rate-limiting step in GSH biosynthesis was found to be significantly activated by the HNE carbonylation which affects a cysteine residue of its modulatory subunit (Cys35). Such a post-translational regulation can clearly influence the GSH homeostasis increasing the GSH level (and the consequent detoxification effects) during oxidative stress [126].

Finally, HNE has been found to form cysteine adducts on the protein Keap-1 (Kelch-like ECH-associated protein 1), which alters its conformation inducing the release of Nuclear factor (erythroid-derived 2)-like 2 (Nrf2), which is subsequently exported to the nucleus [127]. This transcription factor induces antioxidant response element-dependent genes and upregulates several detoxifying enzymes, like GSTs, AKR and ALDH. Given this protective pathway activated by HNE, studies have been focusing on the protective role the aldehyde might have. Cardiomyocytes incubated with a sublethal concentration of HNE showed resistance against toxic concentrations of HNE due to GSH biosynthesis after Nrf2 translocation [128]. The same cardioprotective effect was found in mice after intravenous administration of HNE. In human colon cancer cells, KEAP-1 was silenced in order to elevate Nrf2 levels. Levels of different AKR enzymes were subsequently increased and these cells were more resistant to HNE than the control [129]. Recently, a slightly different mechanism was described to induce GSTA4 expression, where oncogenic transcription factor AP-1 containing the components c-Jun and Nrf2 was activated upon HNE exposure in a model for colorectal carcinogenesis [31]. Contrarily, another study showed that HNE exposure led to a reduced GSH concentration in epithelial cells [130]. After treatment with N-acetylcysteine (NAC), enzymes involved in GSH biosynthesis were upregulated by Nrf2, protecting the cells from HNE-induced apoptosis. These studies show that, at a balanced concentration, HNE can exhibit protective effects via the Nrf2 transcription pathway.

3.1.3. Proteomic study for identifying HNE protein targets

The advent of high resolution MS and its application in proteomics has greatly furthered our knowledge of the non-enzymatic fate of HNE and, in particular, of the reactions of HNE with nucleophilic macromolecules such as proteins and DNA. From an analytical point of view, identifying HNE-adducts is quite challenging due to the fact that such analytes are heterogeneous and present in a negligible amount, thus requiring a suitable sample preparation coupled to a highly sensitive and specific MS method. A great advancement in this field has been reached by using novel sample preparation strategies aimed at selectively isolating HNE modified proteins or peptides. Such strategies can be divided into two groups, the first based on modified HNE and the second on unmodified HNE. Methods belonging to the first group use modified HNE such as HNE containing a terminal alkyne group which, once HNE reacts with proteins, is tagged by click chemistry with biotin (Fig. 8). The adducted proteins are then separated by using an avidin based resin and identified by bottom-up MS [131]. Such analytical strategies work well and are quite selective and sensitive when identifying the biological targets of HNE but are clearly limited to *in vitro* systems such as cell cultures or tissue preparations and cannot be applied to *ex-vivo* conditions. So far, some *in vitro* studies have been reported and based on the identified protein targets, the biological effect of HNE has been explained. As an example, Chacko et al. studied the molecular mechanisms through which HNE induces a significant decrease in the oxidative burst response and phagocytosis of neutrophils [132]. Mass spectrometric analysis of alkyne-HNE treated neutrophils followed by click chemistry detected modification of approximately 100 cytoskeletal, metabolic, redox and signaling proteins that are critical for the oxidative burst mediated by NADPH oxidase. A similar approach has recently been applied to the identification of the HNE modified platelet proteins [133].

Another approach widely used to identify HNE adducted proteins is that based on the use of tagged derivatizing agents which once bound with the Michael adducts between HNE and proteins/peptides, are then fished out by using a suitable affinity stationary phase (Fig. 9). Enrichment can be carried out at protein or peptide level. Biotin hydrazide is an example of tagged derivatizing agent; it reacts with the carbonyl group of HNE forming the corresponding hydrazone derivative which, after a reducing step carried out to prevent hydrolytic cleavage, is enriched by using a streptavidin based stationary phase. Aldehyde/keto reactive group (ARP) is also used as tagged derivatizing agent; by reacting with the carbonyl group of HNE it forms the corresponding aldoxime derivative which does not require the reducing step being a stable reaction product. The approach based on tagged derivatizing agents has the advantage that can be applied to *ex vivo* samples but the disadvantage is that it can only identify Michael adducts but not reaction products lacking the carbonyl moiety (Schiff base and cross links). Several proteomic papers based on such a strategy have been reported using both *in vitro* and *ex-vivo* samples. Tzeng and Maier applied the strategy to identify the adducted proteins in liver mitochondrial proteome. Pathway analysis indicated that proteins associated with metabolic processes, including amino acid, fatty acid, and glyoxylate and dicarboxylate metabolism, bile acid synthesis and TCA cycle, showed enhanced reactivity to HNE adduction. In contrast, proteins associated with oxidative phosphorylation displayed retardation toward HNE adduction. Galligan et al. identified HNE liver protein targets in a 6-week murine model for alcoholic liver disease (ALD) [134].

The two above mentioned approaches have identified in *in vitro* (cells, tissue) and *ex vivo* conditions a list of proteins targeted by HNE. Such information, beside permitting a better explanation of the biological activity of HNE also underlies the concept that HNE does not randomly bind the whole proteome but selectively binds proteins characterized by a certain reactivity. This important aspect has been further addressed by quantitative and semi-quantitative chemo proteomic studies as well as by molecular modelling studies as above described. By using a semi-quantitative chemoproteomic method named competitive activity-based profiling method, Wang et al. have measured the reactivity of HNE against more than a thousand cysteines in parallel in the human proteome [135]. A set of proteins reactive towards HNE characterized by the presence of discrete sites of hypersensitivity or “hot spots” was identified among which Cys22 of ZAK was found to be highly reactive. ZAK is a kinase, activating JNK, ERK, and p38 MAPK pathways in both cancer and inflammation. HNE binding inhibits ZAK activity thus limiting the extent of JNK activation caused by oxidative stress, which could help certain cell types, such as tumor and immune cells, to survive in the presence of high levels of reactive oxygen species.

3.1.4. HNE Protein adduct stability and metabolic turnover

Proteins modified by HNE show increased proteolytic susceptibility for removal by the proteasome. When the HNE modification is increased, involving extensive cross-links, HNE modified proteins become poor substrates for proteasomal degradation, leading to an accumulation of non-degradable compounds. A more extensive HNE adduction inhibits the proteasome, and further impairs cellular protein

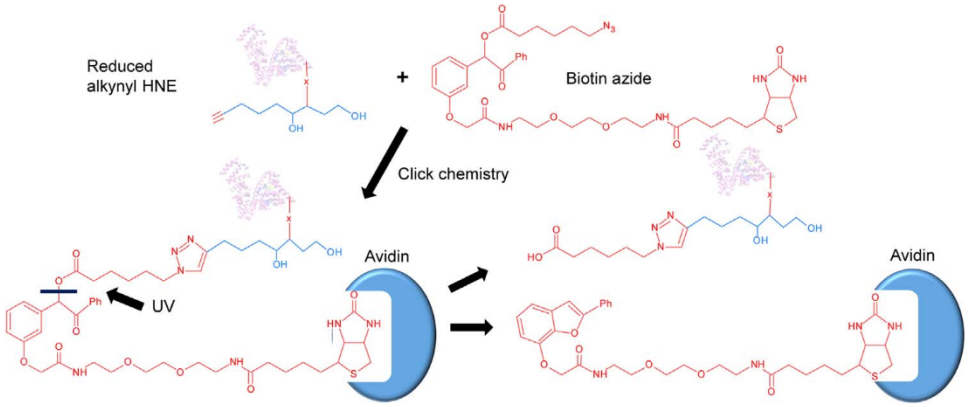

Fig. 8. Reaction scheme between protein adduct involving HNE containing an alkynyl tail and biotin azide using click chemistry. So adducted proteins can then be separated using avidin.

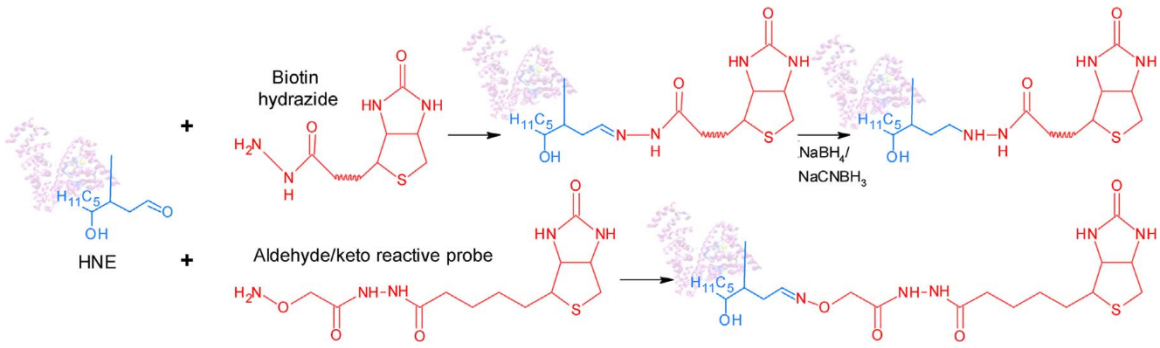

Fig. 9. Derivatizing agents to identify HNE adducts based on biotin hydrazide and aldehyde/keto reactive probe.

turnover [136]. By using novel chemoproteomic approaches able to measure the semi-quantitative amount of the adducted protein, it has been demonstrated that HNE-protein adducts undergo a rapid metabolic turnover which also involves a pathway independent of the proteosomal system and which requires an intact cellular environment. In this regard Yang et al. recently developed a quantitative and sensitive strategy capable of depicting sub-proteome susceptibility to HNE injury in the hepatic mitochondrion [121]. By incubating HNE with RKO cells, they found that about 87% of quantifiable HNE-adducted proteins showed at least a 2-fold decrease over the course of 4 h. Such a turnover was attributed to some unknown repair or reversion processes, rather than to an overall protein degradation, as confirmed by the fact that the turnover of HNE-protein adducts in cells was not affected by co-incubation with the proteasome inhibitor MG132. Nevertheless, some HNE adducts were found stable over the 4 h of incubation. As an example, of four cysteine residues modified by HNE on FAM120A, Cys919, Cys1088, and Cys1103 showed dramatic decreases in S-alkylation after 1–4 h recovery periods, whereas S-alkylation on Cys531 remained almost unchanged. It was also found that the rapid turnover requires an intact cellular environment since protein alkylation did not change significantly in cell lysates. The authors concluded that HNE-induced protein carbonylation is highly dynamic in intact cells and that adduct turnover rates vary in a site-specific manner. Accordingly, Just et al. found that the HNE adduct with the α7 subunit of the 20 S proteasome is quite unstable in neonatal foreskin fibroblast by significantly reducing within 6 h and that the rapid turnover was not affected by inhibition of either the proteasomal system or lysosomal autophagy and was found to constitute a spontaneously unstable linkage of HNE to the proteasomal subunit [137].

Taken together these studies well indicate that HNE-protein adducts are quite unstable and undergo a rapid biotransformation although some protein adducts remain stable. Such rapid turnover can be partially explained by considering the degradation catalyzed by the proteosomal system although an independent pathway should be considered. One possible mechanism of the rapid HNE-protein degradation adducts is that mediated by GSH which removes the HNE adduct from the protein due to the reversibility of the Michael adduct which involves all nucleophilic residues and is added to the well-known lability of imino adducts involving only lysine residues. Several papers have described, using direct and indirect evidences, the ability of GSH to remove HNE from proteins. HNE was reported to inhibit glutathione peroxidase in a concentration-dependent manner, an effect which was almost completely (89%) prevented by 1 mM glutathione added to the incubation mixture 30 min after HNE spiking [138]. Direct evidence of the ability of GSH to remove HNE from the covalent adduct has been reported by Carbone et al. who found that 4 mM GSH removed HNE from the PDI protein adducts [139]. Korotchkina et al. demonstrated the reversibility of HNE induced protein inactivation in cells [140]. When HepG2 cells were treated with 1 mM HNE, the α-keto acid dehydrogenase complex activities were found to be significantly reduced and then partially restored by treating cells with 3 mM for 30 min. The enzymatic activities further increased by prolonging the incubation to 120 min thus indicating that HNE-induced inactivation of α-keto acid dehydrogenase complexes could be reversed in a time-dependent manner by cysteine.

The fate of HNE protein adducts is still under investigation and represents a quite interesting field of research.

3.2. Adducts with nucleic acids

Due to its electrophilicity, HNE can also condense with the four ring bases in nucleic acids showing a reactivity which parallels their nucleophilicity [141]. In fact, the major detected adduct involves the guanine ring which condenses with HNE to give the four possible diastereomers of the exocyclic 1,N2-propano-dG adducts (HNE-dG) through a Michael addition. When epoxidized to 2,3-epoxy-4-hydroxynonanal (EHN), it can also condense with adenine to yield two major adducts, namely 1,N6-ethenodA (edA) and 7-(1′,2′-dihydroxyheptyl)-l,

N6-etheno-dA (DHHedA) [142]. With a reactivity which is largely influenced by stereochemistry, the DHHedA adduct can then open and liberate the free aldehyde which can cyclize to give the corresponding hemiacetal ring or can condense with the opposite guanine base to form the carbinolamine intermediate which then dehydrates to yield cross-link adducts stabilized by an imino function or by a tetrahydrofuran ring. The capacity to accommodate bulky moieties as in the case of hemiacetals or to arrange the reactive aldehyde close to the opposite base ring can clearly rationalize the observed stereospecific formation of such adducts. When unable to cross-link with adjacent bases, the reactive aldehyde can condense with amino groups from peptides or proteins forming mixed HNE-DNA-protein adducts [143].

With regard the biological implications of the HNE-DNA adducts, several studies showed that they are genotoxic and mutagenic by inducing the G·C to T·A transversions, while nucleotide excision repair (NER) was found to be the major pathway involved in repairing 4-HNE-DNA adducts [144]. Notably, kinetic studies revealed competitive effects in the repairing of DNA adducts by HNE and acrolein since the former are repaired markedly more rapidly than the latter the repairing of which appears to be inhibited by HNE-dG adducts. This can explain why the level of the HNE-DNA adducts was found to be almost unaltered even in tissues with elevated oxidative stress (e.g. brain tissue from AD patients), while the acrolein-DNA adducts show increased levels [145]. Even though the above described cross-link adducts are reversible and appear to be present at low levels *in vivo*, they can induce severe genotoxic implications especially because of their difficult reparation which requires the cooperation of multiple enzymes belonging to different pathways. The EHN-DNA adducts are even more mutagenic than those which come from HNE and were detected in rodent and human cancer tissues [146].

3.3. Adducts with endogenous peptides

Besides the already mentioned adducts with GSH, HNE can condense with other peptides among which the histidine containing peptides play a major role [147]. Carnosine, which represents the prototype of these small molecules, is able to stably quench HNE through a concerted mechanism which resembles that already described for ubiquitin and involves firstly the amino terminal group to give the imino intermediate and then the imidazole ring which reacts with the β carbon atom to yield the corresponding Michael adduct [148]. The already mentioned reversibility of the imino derivative can explain the selectivity of carnosine towards α,β unsaturated carbonyls which is also ascribable to the fact that the imidazole alone is unable to give the Michael addition [149]. The histidine containing peptides also include a set of carnosine analogues which differ in the length of the amino terminal residue (e.g. homocarnosine, [150]), in the methylation of the imidazole ring (e.g. anserine) or in the modifications in the carboxyl group (e.g. carnosinamide). HNE quenching capacity is also shown by several dipeptides in which β alanine is replaced by proteinogenic residues [151]. All these dipeptides show the same quenching mechanism already described for carnosine with a reactivity towards HNE which can be related to their nucleophilicity, flexibility and lipophilicity as evidenced by a recent comparative study [152]. As a rule, all these analogues show a quenching activity lower than carnosine, even though some of them retain a notable reactivity (as shown by anserine and carnosinamide). The beneficial effects exerted by carnosine in several animal models have attracted huge interest in the last few years even though carnosine has a restricted medicinal role in humans since it is rapidly hydrolyzed in human plasma by a specific dipeptidase [153]. This means that carnosine can elicit its protective effect only in those tissues which express the carnosine synthase enzyme such as skeletal muscle, brain and heart [154]. This prompted the development of several synthetic carnosine analogues which maintain quenching activity and selectivity while showing favorable pharmacokinetic profiles and the analysis of which goes beyond the scope of this review [155]. Another endogenous peptide which showed a HNE quenching capacity is the tripeptide Gly-His-Lys (GHK) even though it possesses a lower reactivity which is explainable by considering unfavorable conformational properties of GHK [156].

Again, insulin and angiotensin II are two (longer) peptides which yield stable adducts with HNE endowed with impaired physiological functions. In detail, adducted insulin reveals a markedly reduced hypoglycemic effect thus suggesting that these covalent modifications might be involved in the pathogenesis of insulin resistance [157], while modified angiotensin II might be unable to interact with its receptor or might inhibit aminopeptidase A, which converts Ang II into Ang III [158].

3.4. HNE and small endogenous molecules

3.4.1. Reactions with cofactors and vitamins

Along with the above-mentioned dipeptides, other small endogenous molecules are able to stably condense with HNE. In detail, some cofactors and vitamins (thiamine, pyridoxamine and lipoic acid) are found to react with HNE yielding covalent adducts which contribute to their overall physiological functions [159]. Among them, pyridoxamine has attracted great interest in the last few years for its therapeutic applications and indeed it reached clinical phase III for diabetic nephropathy by NephroGenex Inc [160]. The potential reactivity of ascorbic acid is still questioned and, even though a possible Michael addition between HNE and activated C-H groups of ascorbic acid was reported, its protective effect against HNE can be ascribed to its modulating effects on multidrug resistant protein (MRP)-mediated transport of GSH-HNE conjugate metabolites [161].

3.4.2. Reaction with hydrogen sulphide (H_2S)

Recently, a detoxification mechanism of HNE driven by hydrogen sulphide, an endogenous vascular gasotransmitter and neuromodulator, was proposed by observing that NaHS, a H_2S generator, dose-dependently inhibited HNE induced cell toxicity. Moreover, hydrogen sulphide was found to inhibit HNE protein modification both in in vitro and cells experiments. Although no reaction products were identified and characterized, a reaction mechanism was proposed involving the formation of 3-mercapto-4-hydroxy-nonanal as an initial product which can react with a second HNE molecule [162]. The scavenging effect of hydrogen sulphide was finally underlined by considering its lipophilic nature and the fact that HNE is formed and preferentially distributes in biomembranes.

3.4.3. Reaction with aminophospholipids

In 90's, Guichardant et al. firstly reported, in *in vitro* conditions, the covalent reaction between HNE and phospholipids containing amino groups and particularly phosphatidylethanolamine (PE). The reaction products were then identified and characterized by LC-MS as the Michael adduct plus a minor Schiff base adduct, which was partly cyclized as a pyrrole derivative via a loss of water. By contrast, phosphatidylserine was found to poorly react with HNE, producing only a small amount of Michael adduct while the Schiff-base was non-detectable [163]. The Schiff base as the main reaction product between HNE and PE was then confirmed after oxidation (UV irradiation and Fe^{2+}/ascorbate) of cerebral cortex homogenates [164]. The first study reporting the formation of Michael adducts between HNE and PE in biological matrices was published by Bacot et al. who reported the formation of HNE-PE Michael adducts in human blood platelets in response to oxidative stress and in retinas of streptozotocin-induced diabetic rats [165]. Adducts were identified by using a sensitive GC-MS negative ion chemical ionization (NICI) method after cleavage of the phosphodiester bonds and derivatization of the ethanolamine-alkenal moiety. HNE-PE Michael adduct was then found to be formed, together with other PE lipid aldehydes adducts, in high-density lipoproteins exposed to myeloperoxidase and to induce monocyte adhesion to

cultured endothelial cells [166]. The effects of such covalent modification on membrane function was then investigated by O. Jovanovic et al. who demonstrated that HNE driven modification of membrane induces changes of the biophysical properties of the membrane such as membrane order parameter, boundary potential and membrane curvature [167]. Taken together these data well demonstrate that HNE react with PE forming both Michael adduct and Schiff base and that this last is a favorable product due to the anhydrous environment. Some results also indicate that such reaction have a damaging effect by inducing an inflammatory response and changing the biological properties of the membrane. More studies are needed to establish whether this reaction occurs in *in vivo* conditions where other nucleophilic substrates such as proteins can compete with PE. However, it should be noted that the HNE reaction with PE in the cell membrane could be favoured due to several factors: 1) the absence of the GSH detoxifying system, 2) the lipophilic milieu which stabilizes the Schiff base reaction product and 3) the PE membrane localization which is closed to the site of HNE formation [168].

4. Conclusion and future perspectives

Following the first paper on HNE metabolism in hepatoma cell lines published at the end of the 1980s and although the routes of some phase I and phase II metabolites still need to be elucidated, the main enzymatic detoxification reactions of HNE have been clarified in *in vitro* and animal models. Our knowledge of metabolic detoxification has grown in parallel with the advent of novel analytical instruments such as LC-MS and GC-MS and sample preparation procedures which have permitted the identification, characterization and quantification of both phase I and II metabolites in biological matrices. In particular, phase II metabolites involving GSH and mercapturic adduction can now be easily detected and fully characterized by LC-ESI-MS while HNE and phase I metabolites are measured by GC-MS after a suitable derivatization reaction. Untargeted analytical methods have also permitted the identification of unpredicted metabolites and in particular adducts with small molecules such as peptides (carnosine and histidine containing peptides) and phospholipids. Thanks to such recent analytical approaches and by using radioactive and stable isotopes of HNE, as recently published by the group of Gueraud, the HNE metabolism of rodents has been quite well addressed, also from a quantitative point of view. By contrast more studies are needed for a better clarification of the HNE metabolism of humans in different physio-pathological conditions and to trace the HNE sources (endogenous and dietary pathways).

In recent years some studies on the biological effects of HNE metabolites have been carried out, demonstrating that they are not inactive and devoid of biological effects but in some cases have a potentiated effect in respect to HNE, as in the case of the pro-inflammatory action of GS-HNE adducts. These studies are of great interest especially considering that GS-HNE adducts and in particular the urinary mercapturic derivatives are well dosed in humans [169], are increased by some conditions and habits such as smoking [170] and can be modulated by supplements such as vitamin C intake [161].

Although the main metabolic fate of HNE is enzymatically driven, great interest is focused on the non-enzymatic reactions involving biomolecules such as proteins and phospholipids. Interest in this type of metabolic fate has grown in parallel with the advent of highly sensitive and specific MS methods which have permitted the identification of unknown covalent adducts and in particular proteomic techniques for the identification of HNE protein adducts. Another aspect stimulating the interest in a non-enzymatic fate of HNE is due to the biological effects of the protein adducts and that protein adduction is not a random process but is quite selective, targeting proteins with some specific features. We still need to better understand the biological effects of protein HNE adduction which depend on the identity of the target proteins. Some proteins, such as actin and albumin can act as detoxifying molecules. Others, such as α-synuclein [171] and lipid phosphatase PTEN [172], induce a damaging effect while others, glutamate-cysteine ligase [126] and transcription factor Nrf2 [128], modulate a protective effect and in particular an increased antioxidant response. Hence, at least in some cases, protein adduction is not a random process involving the HNE fraction escaping the enzymatic metabolism but more likely an endogenous pathway required for HNE detoxification or cell signaling. In other words, HNE stimulates cells for an antioxidant defence, induces the elimination of damaged cellular components or even serves to protect of the organism by inducing apoptosis in severely injured cells.

Clearly we should also consider a fraction of HNE, targeting sensitive proteins and acting as a damaging mediator, whose scavenging by a boosted enzymatic or non-enzymatic detoxification, this last mediated by covalent sequestering agents, could represent a promising therapeutic approach [105].

Another important aspect requiring future investigations deals with the molecular and presumably enzymatic mechanisms regulating the fast disappearance of HNE adducted proteins, a process whose elucidation will permit a better understanding of the biological activity of HNE and the identification of novel targets to modulate their activity.

Taken together these studies well indicate that the non-enzymatic protein adduction of HNE is a quite complex mechanism which depends on several factors such as i) the reactivity of the nucleophilic sites which regulate which proteins of the whole proteome are preferentially modified, ii) the absolute amount of the proteins, iii) the stability of the adducts. Several questions arise and in particular whether the covalent adduction by some abundant and reactive proteins such as albumin and actin is an endogenous non-enzymatic detoxification process or an unwanted protein modification.

Acknowledgements

This work has been funded by the European Union's Horizon 2020 research and innovation programme under the Marie Sklowdowska-Curie grant agreement number 675132 (http://cordis.europa.eu/project/rcn/198275_en.html).

References

[1] E. Schauenstein, J. Zangger, M. Ratzenhofer, On the effect of hydroxyoctenal on ehrlich ascites tumor cells, Z. Nat. B 19 (1964) 923–929.
[2] H. Esterbauer, K.H. Cheeseman, M.U. Dianzani, G. Poli, T.F. Slater, Separation and characterization of the aldehydic products of lipid peroxidation stimulated by ADP-Fe2+ in rat liver microsomes, Biochem. J. 208 (1) (1982) 129–140.
[3] K.S. Fritz, D.R. Petersen, An overview of the chemistry and biology of reactive aldehydes, Free Radic. Biol. Med. 59 (2013) 85–91.
[4] K. Zarkovic, A. Jakovcevic, N. Zarkovic, Contribution of the HNE-immunohistochemistry to modern pathological concepts of major human diseases, Free Radic. Biol. Med. (2016).
[5] B.I. Frohnert, D.A. Bernlohr, Glutathionylated products of lipid peroxidation: a novel mechanism of adipocyte to macrophage signaling, Adipocyte 3 (3) (2014) 224–229.
[6] M. Ferro, U.M. Marinari, G. Poli, M.U. Dianzani, G. Fauler, H. Zollner, H. Esterbauer, Metabolism of 4-hydroxynonenal by the rat hepatoma cell line MH1C1, Cell Biochem. Funct. 6 (4) (1988) 245–250.
[7] R.J. Schaur, Basic aspects of the biochemical reactivity of 4-hydroxynonenal, Mol. Asp. Med. 24 (4–5) (2003) 149–159.
[8] B. Yoval-Sánchez, J.S. Rodríguez-Zavala, Differences in susceptibility to inactivation of human aldehyde dehydrogenases by lipid peroxidation byproducts, Chem. Res. Toxicol. 25 (3) (2012) 722–729.
[9] Y. D'Souza, A. Elharram, R. Soon-Shiong, R.D. Andrew, B.M. Bennett, Characterization of Aldh2 (-/-) mice as an age-related model of cognitive impairment and Alzheimer's disease, Mol. Brain 8 (2015) 27.
[10] H. Yang, Z. Song, G.P. Yang, B.K. Zhang, M. Chen, T. Wu, R. Guo, The ALDH2 rs671 polymorphism affects post-stroke epilepsy susceptibility and plasma 4-HNE levels, PLoS One 9 (10) (2014) e109634.
[11] J.M. Guo, A.J. Liu, P. Zang, W.Z. Dong, L. Ying, W. Wang, P. Xu, X.R. Song, J. Cai, S.Q. Zhang, J.L. Duan, J.L. Mehta, D.F. Su, ALDH2 protects against stroke by clearing 4-HNE, Cell Res. 23 (7) (2013) 915–930.
[12] K.M. Gomes, J.C. Campos, L.R. Bechara, B. Queliconi, V.M. Lima, M.H. Disatnik, P. Magno, C.H. Chen, P.C. Brum, A.J. Kowaltowski, D. Mochly-Rosen, J.C. Ferreira, Aldehyde dehydrogenase 2 activation in heart failure restores mitochondrial function and improves ventricular function and remodelling, Cardiovasc. Res. 103 (4) (2014) 498–508.
[13] A. Sun, Y. Zou, P. Wang, D. Xu, H. Gong, S. Wang, Y. Qin, P. Zhang, Y. Chen,

M. Harada, T. Isse, T. Kawamoto, H. Fan, P. Yang, H. Akazawa, T. Nagai, H. Takano, P. Ping, I. Komuro, J. Ge, Mitochondrial aldehyde dehydrogenase 2 plays protective roles in heart failure after myocardial infarction via suppression of the cytosolic JNK/p53 pathway in mice, J. Am. Heart Assoc. 3 (5) (2014) e000779.
[14] M. Hlaváčová, J. Gumulec, T. Stračina, M. Fojtů, M. Raudenská, M. Masařík, M. Nováková, H. Paulová, Different doxorubicin formulations affect plasma 4-hydroxy-2-nonenal and gene expression of aldehyde dehydrogenase 3A1 and thioredoxin reductase 2 in rat, Physiol. Res. 64 (Suppl 5) (2015) S653–S660.
[15] J. Deng, D. Coy, W. Zhang, M. Sunkara, A.J. Morris, C. Wang, L. Chaiswing, D. Clair StM. Vore, P. Jungsuwadee, Elevated glutathione is not sufficient to protect against doxorubicin-induced nuclear damage in heart in multidrug resistance-associated protein 1 (Mrp1/Abcc1) null mice, J. Pharm. Exp. Ther. 355 (2) (2015) 272–279.
[16] A. Stachowicz, R. Olszanecki, M. Suski, A. Wiśniewska, J. Totoń-Żurańska, J. Madej, J. Jawień, M. Białas, K. Okoń, M. Gajda, K. Głombik, A. Basta-Kaim, R. Korbut, Mitochondrial aldehyde dehydrogenase activation by Alda-1 inhibits atherosclerosis and attenuates hepatic steatosis in apolipoprotein E-knockout mice, J. Am. Heart Assoc. 3 (6) (2014) e001329.
[17] W. Wang, L.L. Lin, J.M. Guo, Y.Q. Cheng, J. Qian, J.L. Mehta, D.F. Su, P. Luan, A.J. Liu, Heavy ethanol consumption aggravates the ischemic cerebral injury by inhibiting ALDH2, Int. J. Stroke 10 (8) (2015) 1261–1269.
[18] J.H. Li, G.X. Ju, J.L. Jiang, N.S. Li, J. Peng, X.J. Luo, Lipoic acid protects gastric mucosa from ethanol-induced injury in rat through a mechanism involving aldehyde dehydrogenase 2 activation, Alcohol 56 (2016) 21–28.
[19] T. Grune, W.G. Siems, T. Petras, Identification of metabolic pathways of the lipid peroxidation product 4-hydroxynonenal in in situ perfused rat kidney, J. Lipid Res. 38 (8) (1997) 1660–1665.
[20] Q. Li, S. Sadhukhan, J.M. Berthiaume, R.A. Ibarra, H. Tang, S. Deng, E. Hamilton, L.E. Nagy, G.P. Tochtrop, G.F. Zhang, 4-Hydroxy-2(E)-nonenal (HNE) catabolism and formation of HNE adducts are modulated by β oxidation of fatty acids in the isolated rat heart, Free Radic. Biol. Med. 58 (2013) 35–44.
[21] J. Alary, L. Debrauwer, Y. Fernandez, A. Paris, J.P. Cravedi, L. Dolo, D. Rao, G. Bories, Identification of novel urinary metabolites of the lipid peroxidation product 4-hydroxy-2-nonenal in rats, Chem. Res. Toxicol. 11 (11) (1998) 1368–1376.
[22] A. Laurent, E. Perdu-Durand, J. Alary, L. Debrauwer, J.P. Cravedi, Metabolism of 4-hydroxynonenal, a cytotoxic product of lipid peroxidation, in rat precision-cut liver slices, Toxicol. Lett. 114 (1–3) (2000) 203–214.
[23] J. Alary, Y. Fernandez, L. Debrauwer, E. Perdu, F. Gueraud, Identification of intermediate pathways of 4-hydroxynonenal metabolism in the rat, Chem. Res. Toxicol. 16 (3) (2003) 320–327.
[24] Z. Jin, J.M. Berthiaume, Q. Li, F. Henry, Z. Huang, S. Sadhukhan, P. Gao, G.P. Tochtrop, M.A. Puchowicz, G.F. Zhang, Catabolism of (2E)-4-hydroxy-2-nonenal via omega- and omega-1-oxidation stimulated by ketogenic diet, J. Biol. Chem. 289 (46) (2014) 32327–32338.
[25] M.D. Boleda, N. Saubi, J. Farrés, X. Parés, Physiological substrates for rat alcohol dehydrogenase classes: aldehydes of lipid peroxidation, omega-hydroxyfatty acids, and retinoids, Arch. Biochem. Biophys. 307 (1) (1993) 85–90.
[26] M. Singh, A. Kapoor, A. Bhatnagar, Oxidative and reductive metabolism of lipid-peroxidation derived carbonyls, Chem. Biol. Interact. 234 (2015) 261–273.
[27] T.M. Penning, The aldo-keto reductases (AKRs): overview, Chem. Biol. Interact. 234 (2015) 236–246.
[28] S. Srivastava, A. Chandra, A. Bhatnagar, S.K. Srivastava, N.H. Ansari, Lipid peroxidation product, 4-hydroxynonenal and its conjugate with GSH are excellent substrates of bovine lens aldose reductase, Biochem. Biophys. Res. Commun. 217 (3) (1995) 741–746.
[29] S. Srivastava, D.J. Conklin, S.Q. Liu, N. Prakash, P.J. Boor, S.K. Srivastava, A. Bhatnagar, Identification of biochemical pathways for the metabolism of oxidized low-density lipoprotein derived aldehyde-4-hydroxy trans-2-nonenal in vascular smooth muscle cells, Atherosclerosis 158 (2) (2001) 339–350.
[30] X. Zu, R. Yan, J. Pan, L. Zhong, Y. Cao, J. Ma, C. Cai, D. Huang, J. Liu, F.L. Chung, D.F. Liao, D. Cao, Aldo-keto reductase 1B10 protects human colon cells from DNA damage induced by electrophilic carbonyl compounds, Mol. Carcinog. (2016).
[31] Y. Yang, M.M. Huycke, T.S. Herman, X. Wang, Glutathione S-transferase alpha 4 induction by activator protein 1 in colorectal cancer, Oncogene (2016).
[32] M.E. Burczynski, G.R. Sridhar, N.T. Palackal, T.M. Penning, The reactive oxygen species–and Michael acceptor-inducible human aldo-keto reductase AKR1C1 reduces the alpha,beta-unsaturated aldehyde 4-hydroxy-2-nonenal to 1,4-dihydroxy-2-nonene, J. Biol. Chem. 276 (4) (2001) 2890–2897.
[33] R.C. Lyon, D. Li, G. McGarvie, E.M. Ellis, Aldo-keto reductases mediate constitutive and inducible protection against aldehyde toxicity in human neuroblastoma SH-SY5Y cells, Neurochem. Int. 62 (1) (2013) 113–121.
[34] R.A. Dick, M.K. Kwak, T.R. Sutter, T.W. Kensler, Antioxidative function and substrate specificity of NAD(P)H-dependent alkenal/one oxidoreductase. A new role for leukotriene B4 12-hydroxydehydrogenase/15-oxoprostaglandin 13-reductase, J. Biol. Chem. 276 (44) (2001) 40803–40810.
[35] L.D. Marchette, D.A. Thompson, M. Kravtsova, T.N. Ngansop, M.N. Mandal, A. Kasus-Jacobi, Retinol dehydrogenase 12 detoxifies 4-hydroxynonenal in photoreceptor cells, Free Radic. Biol. Med. 48 (1) (2010) 16–25.
[36] I. Amunom, L.J. Stephens, V. Tamasi, J. Cai, W.M. Pierce Jr.D.J. Conklin, A. Bhatnagar, S. Srivastava, M.V. Martin, F.P. Guengerich, R.A. Prough, Cytochromes P450 catalyze oxidation of alpha,beta-unsaturated aldehydes, Arch. Biochem. Biophys. 464 (2) (2007) 187–196.
[37] I. Amunom, L.J. Dieter, V. Tamasi, J. Cai, D.J. Conklin, S. Srivastava, M.V. Martin, F.P. Guengerich, R.A. Prough, Cytochromes P450 catalyze the reduction of alpha,beta-unsaturated aldehydes, Chem. Res. Toxicol. 24 (8) (2011) 1223–1230.
[38] D.P. Hartley, J.A. Ruth, D.R. Petersen, The hepatocellular metabolism of 4-hydroxynonenal by alcohol dehydrogenase, aldehyde dehydrogenase, and glutathione S-transferase, Arch. Biochem. Biophys. 316 (1) (1995) 197–205.
[39] D. Goon, M. Saxena, Y.C. Awasthi, D. Ross, Activity of mouse liver glutathione S-transferases toward trans,trans-muconaldehyde and trans-4-hydroxy-2-nonenal, Toxicol. Appl. Pharmacol. 119 (2) (1993) 175–180.
[40] I. Hubatsch, M. Ridderstrom, B. Mannervik, Human glutathione transferase A4-4: an alpha class enzyme with high catalytic efficiency in the conjugation of 4-hydroxynonenal and other genotoxic products of lipid peroxidation, Biochem. J. 330 (Pt 1) (1998) 175–179.
[41] H. Raza, M.A. Robin, J.K. Fang, N.G. Avadhani, Multiple isoforms of mitochondrial glutathione S-transferases and their differential induction under oxidative stress, Biochem. J. 366 (Pt 1) (2002) 45–55.
[42] D.R. Petersen, J.A. Doorn, Reactions of 4-hydroxynonenal with proteins and cellular targets, Free Radic. Biol. Med. 37 (7) (2004) 937–945.
[43] F. Gueraud, F. Crouzet, J. Alary, D. Rao, L. Debrauwer, F. Laurent, J.P. Cravedi, Enantioselective metabolism of (R)- and (S)-4-hydroxy-2-nonenal in rat, Biofactors 24 (1–4) (2005) 97–104.
[44] J. Alary, F. Gueraud, J.P. Cravedi, Fate of 4-hydroxynonenal in vivo: disposition and metabolic pathways, Mol. Asp. Med. 24 (4–5) (2003) 177–187.
[45] W. Black, Y. Chen, A. Matsumoto, D.C. Thompson, N. Lassen, A. Pappa, V. Vasiliou, Molecular mechanisms of ALDH3A1-mediated cellular protection against 4-hydroxy-2-nonenal, Free Radic. Biol. Med. 52 (9) (2012) 1937–1944.
[46] R. Moschini, E. Peroni, R. Rotondo, G. Renzone, D. Melck, M. Cappiello, M. Srebot, E. Napolitano, A. Motta, A. Scaloni, U. Mura, A. Del-Corso, NADP(+)-dependent dehydrogenase activity of carbonyl reductase on glutathionylhydroxynonanal as a new pathway for hydroxynonenal detoxification, Free Radic. Biol. Med. 83 (2015) 66–76.
[47] R. Rotondo, R. Moschini, G. Renzone, T. Tuccinardi, F. Balestri, M. Cappiello, A. Scaloni, U. Mura, A. Del-Corso, Human carbonyl reductase 1 as efficient catalyst for the reduction of glutathionylated aldehydes derived from lipid peroxidation, Free Radic. Biol. Med. 99 (2016) 323–332.
[48] T. Petras, W.G. Siems, T. Grune, 4-hydroxynonenal is degraded to mercapturic acid conjugate in rat kidney, Free Radic. Biol. Med. 19 (5) (1995) 685–688.
[49] M. Enoiu, R. Herber, R. Wennig, C. Marson, H. Bodaud, P. Leroy, N. Mitrea, G. Siest, M. Wellman, gamma-Glutamyltranspeptidase-dependent metabolism of 4-hydroxynonenal-glutathione conjugate, Arch. Biochem. Biophys. 397 (1) (2002) 18–27.
[50] C. Josch, H. Sies, T.P. Akerboom, Hepatic mercapturic acid formation: involvement of cytosolic cysteinylglycine S-conjugate dipeptidase activity, Biochem. Pharmacol. 56 (6) (1998) 763–771.
[51] C.A. Hinchman, N. Ballatori, Glutathione conjugation and conversion to mercapturic acids can occur as an intrahepatic process, J. Toxicol. Environ. Health 41 (4) (1994) 387–409.
[52] M.W. Duffel, W.B. Jakoby, Cysteine S-conjugate N-acetyltransferase from rat kidney microsomes, Mol. Pharmacol. 21 (2) (1982) 444–448.
[53] M. Veiga-da-Cunha, D. Tyteca, V. Stroobant, P.J. Courtoy, F.R. Opperdoes, E. Van Schaftingen, Molecular identification of NAT8 as the enzyme that acetylates cysteine S-conjugates to mercapturic acids, J. Biol. Chem. 285 (24) (2010) 18888–18898.
[54] G. Aldini, P. Granata, M. Orioli, E. Santaniello, M. Carini, Detoxification of 4-hydroxynonenal (HNE) in keratinocytes: characterization of conjugated metabolites by liquid chromatography/electrospray ionization tandem mass spectrometry, J. Mass Spectrom. 38 (11) (2003) 1160–1168.
[55] J. Keller, M. Baradat, I. Jouanin, L. Debrauwer, F. Gueraud, "Twin peaks": searching for 4-hydroxynonenal urinary metabolites after oral administration in rats, Redox Biol. 4 (2015) 136–148.
[56] A. Kubatova, A. Honzatko, J. Brichac, E. Long, M.J. Picklo, Analysis of HNE metabolism in CNS models, Redox Rep. 12 (1) (2007) 16–19.
[57] A. Kubatova, T.C. Murphy, C. Combs, M.J. Picklo Sr., Astrocytic biotransformation of trans-4-hydroxy-2-nonenal is dose-dependent, Chem. Res. Toxicol. 19 (6) (2006) 844–851.
[58] K.R. Sidell, K.S. Montine, M.J. Picklo Sr.S.J. Olsen, V. Amarnath, T.J. Montine, Mercapturate metabolism of 4-hydroxy-2-nonenal in rat and human cerebrum, J. Neuropathol. Exp. Neurol. 62 (2) (2003) 146–153.
[59] W. Siems, C. Crifo, E. Capuozzo, K. Uchida, T. Grune, C. Salerno, Metabolism of 4-hydroxy-2-nonenal in human polymorphonuclear leukocytes, Arch. Biochem. Biophys. 503 (2) (2010) 248–252.
[60] W.G. Siems, H. Zollner, T. Grune, H. Esterbauer, Metabolic fate of 4-hydroxynonenal in hepatocytes: 1,4-dihydroxynonene is not the main product, J. Lipid Res. 38 (3) (1997) 612–622.
[61] W. Siems, T. Grune, Intracellular metabolism of 4-hydroxynonenal, Mol. Asp. Med. 24 (4–5) (2003) 167–175.
[62] O. Ullrich, T. Grune, W. Henke, H. Esterbauer, W.G. Siems, Identification of metabolic pathways of the lipid peroxidation product 4-hydroxynonenal by mitochondria isolated from rat kidney cortex, FEBS Lett. 352 (1) (1994) 84–86.
[63] N. Traverso, S. Menini, P. Odetti, M.A. Pronzato, D. Cottalasso, U.M. Marinari, Diabetes impairs the enzymatic disposal of 4-hydroxynonenal in rat liver, Free Radic. Biol. Med. 32 (4) (2002) 350–359.
[64] R. Zheng, A.C. Dragomir, V. Mishin, J.R. Richardson, D.E. Heck, D.L. Laskin, J.D. Laskin, Differential metabolism of 4-hydroxynonenal in liver, lung and brain of mice and rats, Toxicol. Appl. Pharmacol. 279 (1) (2014) 43–52.
[65] R.B. Tjalkens, L.W. Cook, D.R. Petersen, Formation and export of the glutathione conjugate of 4-hydroxy-2, 3-E-nonenal (4-HNE) in hepatoma cells, Arch. Biochem. Biophys. 361 (1) (1999) 113–119.
[66] S. Toyokuni, S. Yamada, M. Kashima, Y. Ihara, Y. Yamada, T. Tanaka, H. Hiai, Y. Seino, K. Uchida, Serum 4-hydroxy-2-nonenal-modified albumin is elevated in patients with type 2 diabetes mellitus, Antioxid. Redox Signal. 2 (4) (2000) 681–685.
[67] S. Srivastava, B.L. Dixit, J. Cai, S. Sharma, H.E. Hurst, A. Bhatnagar, S.K. Srivastava, Metabolism of lipid peroxidation product, 4-hydroxynonenal (HNE) in rat erythrocytes: role of aldose reductase, Free Radic. Biol. Med. 29 (7) (2000) 642–651.
[68] T. Murphy, V. Amarnath, M.J. Picklo, Oxidation of 4-hydroxynonenal in rat brain slices, Chem. Biol. Interact. 143–144 (2003) 101–105.

[69] S. Sadhukhan, Y. Han, Z. Jin, G.P. Tochtrop, G.F. Zhang, Glutathionylated 4-hydroxy-2-(E)-alkenal enantiomers in rat organs and their contributions toward the disposal of 4-hydroxy-2-(E)-nonenal in rat liver, Free Radic. Biol. Med. 70 (2014) 78–85.
[70] A. Dygas, P. Makowski, S. Pikula, Is the glutathione conjugate of trans-4-hydroxy-2-nonenal transported by the multispecific organic anion transporting-ATPase of human erythrocytes? Acta Biochim. Pol. 45 (1) (1998) 59–65.
[71] A. Laurent, J. Alary, L. Debrauwer, J.P. Cravedi, Analysis in the rat of 4-hydroxynonenal metabolites excreted in bile: evidence of enterohepatic circulation of these byproducts of lipid peroxidation, Chem. Res. Toxicol. 12 (10) (1999) 887–894.
[72] J.F. Reichard, J.A. Doorn, F. Simon, M.S. Taylor, D.R. Petersen, Characterization of multidrug resistance-associated protein 2 in the hepatocellular disposition of 4-hydroxynonenal, Arch. Biochem. Biophys. 411 (2) (2003) 243–250.
[73] S.S. Singhal, S. Yadav, C. Roth, J. Singhal, RLIP76: a novel glutathione-conjugate and multi-drug transporter, Biochem. Pharmcol. 77 (5) (2009) 761–769.
[74] C. Schneider, K.A. Tallman, N.A. Porter, A.R. Brash, Two distinct pathways of formation of 4-hydroxynonenal. Mechanisms of nonenzymatic transformation of the 9- and 13-hydroperoxides of linoleic acid to 4-hydroxyalkenals, J. Biol. Chem. 276 (24) (2001) 20831–20838.
[75] A. Hiratsuka, K. Hirose, H. Saito, T. Watabe, 4-Hydroxy-2(E)-nonenal enantiomers: (S)-selective inactivation of glyceraldehyde-3-phosphate dehydrogenase and detoxification by rat glutathione S-transferase A4-4, Biochem. J. 349 (Pt 3) (2000) 729–735.
[76] A. Hiratsuka, K. Tobita, H. Saito, Y. Sakamoto, H. Nakano, K. Ogura, T. Nishiyama, T. Watabe, (S)-preferential detoxification of 4-hydroxy-2(E)-nonenal enantiomers by hepatic glutathione S-transferase isoforms in guinea-pigs and rats, Biochem. J. 355 (Pt 1) (2001) 237–244.
[77] A. Honzatko, J. Brichac, T.C. Murphy, A. Reberg, A. Kubatova, I.P. Smoliakova, M.J. Picklo Sr., Enantioselective metabolism of trans-4-hydroxy-2-nonenal by brain mitochondria, Free Radic. Biol. Med 39 (7) (2005) 913–924.
[78] J. Brichac, K.K. Ho, A. Honzatko, R. Wang, X. Lu, H. Weiner, M.J. Picklo Sr., Enantioselective oxidation of trans-4-hydroxy-2-nonenal is aldehyde dehydrogenase isozyme and Mg2+ dependent, Chem. Res. Toxicol. 20 (6) (2007) 887–895.
[79] L.M. Balogh, A.G. Roberts, L.M. Shireman, R.J. Greene, W.M. Atkins, The stereochemical course of 4-hydroxy-2-nonenal metabolism by glutathione S-transferases, J. Biol. Chem. 283 (24) (2008) 16702–16710.
[80] L.M. Balogh, I. Le Trong, K.A. Kripps, L.M. Shireman, R.E. Stenkamp, W. Zhang, B. Mannervik, W.M. Atkins, Substrate specificity combined with stereopromiscuity in glutathione transferase A4-4-dependent metabolism of 4-hydroxynonenal, Biochemistry 49 (7) (2010) 1541–1548.
[81] L.M. Balogh, W.M. Atkins, Interactions of glutathione transferases with 4-hydroxynonenal, Drug Metab. Rev. 43 (2) (2011) 165–178.
[82] J.D. Hayes, J.U. Flanagan, I.R. Jowsey, Glutathione transferases, Annu Rev. Pharmacol. Toxicol. 45 (2005) 51–88.
[83] C.M. Spickett, The lipid peroxidation product 4-hydroxy-2-nonenal: advances in chemistry and analysis, Redox Biol. 1 (2013) 145–152.
[84] Y.M. Liu, H. Jinno, M. Kurihara, N. Miyata, T. Toyo'oka, Determination of 4-hydroxy-2-nonenal in primary rat hepatocyte cultures by liquid chromatography with laser induced fluorescence detection, Biomed. Chromatogr. 13 (1) (1999) 75–80.
[85] C. Goldring, A.F. Casini, E. Maellaro, B. Del Bello, M. Comporti, Determination of 4-hydroxynonenal by high-performance liquid chromatography with electrochemical detection, Lipids 28 (2) (1993) 141–145.
[86] F. Gueraud, G. Peiro, H. Bernard, J. Alary, C. Creminon, L. Debrauwer, E. Rathahao, M.F. Drumare, C. Canlet, J.M. Wal, G. Bories, Enzyme immunoassay for a urinary metabolite of 4-hydroxynonenal as a marker of lipid peroxidation, Free Radic. Biol. Med. 40 (1) (2006) 54–62.
[87] X.P. Luo, M. Yazdanpanah, N. Bhooi, D.C. Lehotay, Determination of aldehydes and other lipid peroxidation products in biological samples by gas chromatography-mass spectrometry, Anal. Biochem. 228 (2) (1995) 294–298.
[88] M. Guichardant, M. Lagarde, Analysis of biomarkers from lipid peroxidation: a comparative study, Eur. J. Lipid Sci. Technol. 111 (1) (2009) 75–82.
[89] C. Asselin, B. Bouchard, J.C. Tardif, C. Des Rosiers, Circulating 4-hydroxynonenal-protein thioether adducts assessed by gas chromatography-mass spectrometry are increased with disease progression and aging in spontaneously hypertensive rats, Free Radic. Biol. Med. 41 (1) (2006) 97–105.
[90] Q. Li, K. Tomcik, S. Zhang, M.A. Puchowicz, G.F. Zhang, Dietary regulation of catabolic disposal of 4-hydroxynonenal analogs in rat liver, Free Radic. Biol. Med. 52 (6) (2012) 1043–1053.
[91] S. Sadhukhan, Y. Han, G.F. Zhang, H. Brunengraber, G.P. Tochtrop, Using isotopic tools to dissect and quantitate parallel metabolic pathways, J. Am. Chem. Soc. 132 (18) (2010) 6309–6311.
[92] G.F. Zhang, R.S. Kombu, T. Kasumov, Y. Han, S. Sadhukhan, J. Zhang, L.M. Sayre, D. Ray, K.M. Gibson, V.A. Anderson, G.P. Tochtrop, H. Brunengraber, Catabolism of 4-hydroxyacids and 4-hydroxynonenal via 4-hydroxy-4-phosphoacyl-CoAs, J. Biol. Chem. 284 (48) (2009) 33521–33534.
[93] T.I. Williams, M.A. Lovell, B.C. Lynn, Analysis of derivatized biogenic aldehydes by LC tandem mass spectrometry, Anal. Chem. 77 (10) (2005) 3383–3389.
[94] A. Honzatko, J. Brichac, M.J. Picklo, Quantification of trans-4-hydroxy-2-nonenal enantiomers and metabolites by LC-ESI-MS/MS, J. Chromatogr. B Anal. Technol. Biomed. Life Sci. 857 (1) (2007) 115–122.
[95] I. Jouanin, M. Baradat, M. Gieules, S. Tache, F.H. Pierre, F. Gueraud, L. Debrauwer, Liquid chromatography/electrospray ionisation mass spectrometric tracking of 4-hydroxy-2(E)-nonenal biotransformations by mouse colon epithelial cells using [1,2-13C2]-4-hydroxy-2(*E*)-nonenal as stable isotope tracer, Rapid Commun. Mass Spectrom. 25 (19) (2011) 2675–2681.
[96] J. Alary, F. Bravais, J.P. Cravedi, L. Debrauwer, D. Rao, G. Bories, Mercapturic acid conjugates as urinary end metabolites of the lipid peroxidation product 4-hydroxy-2-nonenal in the rat, Chem. Res. Toxicol. 8 (1) (1995) 34–39.
[97] P.J. Boon, H.S. Marinho, R. Oosting, G.J. Mulder, Glutathione conjugation of 4-hydroxy-trans-2,3-nonenal in the rat in vivo, the isolated perfused liver and erythrocytes, Toxicol. Appl. Pharmacol. 159 (3) (1999) 214–223.
[98] M. Spite, L. Summers, T.F. Porter, S. Srivastava, A. Bhatnagar, C.N. Serhan, Resolvin D1 controls inflammation initiated by glutathione-lipid conjugates formed during oxidative stress, Br. J. Pharmacol. 158 (4) (2009) 1062–1073.
[99] B.I. Frohnert, E.K. Long, W.S. Hahn, D.A. Bernlohr, Glutathionylated lipid aldehydes are products of adipocyte oxidative stress and activators of macrophage inflammation, Diabetes 63 (1) (2014) 89–100.
[100] R.M. LoPachin, T. Gavin, D.R. Petersen, D.S. Barber, Molecular mechanisms of 4-hydroxy-2-nonenal and acrolein toxicity: nucleophilic targets and adduct formation, Chem. Res. Toxicol. 22 (9) (2009) 1499–1508.
[101] R.M. Lopachin, A.P. Decaprio, Protein adduct formation as a molecular mechanism in neurotoxicity, Toxicol. Sci. 86 (2) (2005) 214–225.
[102] Y.Q. Ding, Y.Z. Cui, T.D. Li, New views on the reaction of primary amine and aldehyde from DFT study, J. Phys. Chem. A 119 (18) (2015) 4252–4260.
[103] M.R. Weissman, K.T. Winger, S. Ghiassian, P. Gobbo, M.S. Workentin, Insights on the application of the retro Michael-type addition on Maleimide-functionalized gold nanoparticles in biology and nanomedicine, Bioconjug Chem. 27 (3) (2016) 586–593.
[104] R.J. Schaur, W. Siems, N. Bresgen, P.M. Eckl, 4-Hydroxy-nonenal-A bioactive lipid peroxidation product, Biomolecules 5 (4) (2015) 2247–2337.
[105] G. Aldini, M. Carini, K.J. Yeum, G. Vistoli, Novel molecular approaches for improving enzymatic and nonenzymatic detoxification of 4-hydroxynonenal: toward the discovery of a novel class of bioactive compounds, Free Radic. Biol. Med. 69 (2014) 145–156.
[106] E. Maisonneuve, A. Ducret, P. Khoueiry, S. Lignon, S. Longhi, E. Talla, S. Dukan, Rules governing selective protein carbonylation, PLoS One 4 (10) (2009) e7269.
[107] B. Testa, S.D. Krämer, The biochemistry of drug metabolism–an introduction: part 4. reactions of conjugation and their enzymes, Chem. Biodivers. 5 (11) (2008) 2171–2336.
[108] G. Aldini, G. Vistoli, L. Regazzoni, L. Gamberoni, R.M. Facino, S. Yamaguchi, K. Uchida, M. Carini, Albumin is the main nucleophilic target of human plasma: a protective role against pro-atherogenic electrophilic reactive carbonyl species? Chem. Res. Toxicol. 21 (4) (2008) 824–835.
[109] Y. Xu, K.C. Chou, Recent progress in predicting posttranslational modification sites in proteins, Curr. Top. Med. Chem. 16 (6) (2016) 591–603.
[110] L. Bertoletti, L. Regazzoni, A. Altomare, R. Colombo, M. Colzani, G. Vistoli, L. Marchese, M. Carini, E. De Lorenzi, G. Aldini, Advanced glycation end products of beta2-microglobulin in uremic patients as determined by high resolution mass spectrometry, J. Pharm. Biomed. Anal. 91 (2014) 193–201.
[111] J.M. Macdonald, A.L. Haas, R.E. London, Novel mechanism of surface catalysis of protein adduct formation. NMR studies of the acetylation of ubiquitin, J. Biol. Chem. 275 (41) (2000) 31908–31913.
[112] A.K. Hauck, D.A. Bernlohr, Oxidative stress and lipotoxicity, J. Lipid Res. 57 (11) (2016) 1976–1986.
[113] M. Csala, T. Kardon, B. Legeza, B. Lizák, J. Mandl, É. Margittai, F. Puskás, P. Száraz, P. Szelényi, G. Bánhegyi, On the role of 4-hydroxynonenal in health and disease, Biochim. Biophys. Acta 1852 (5) (2015) 826–838.
[114] J.A. Hardin, N. Cobelli, L. Santambrogio, Consequences of metabolic and oxidative modifications of cartilage tissue, Nat. Rev. Rheumatol. 11 (9) (2015) 521–529.
[115] Y. Cai, C. Lendel, L. Österlund, A. Kasrayan, L. Lannfelt, M. Ingelsson, F. Nikolajeff, M. Karlsson, J. Bergström, Changes in secondary structure of α-synuclein during oligomerization induced by reactive aldehydes, Biochem. Biophys. Res. Commun. 464 (1) (2015) 336–341.
[116] G. Leonarduzzi, F. Robbesyn, G. Poli, Signaling kinases modulated by 4-hydroxynonenal, Free Radic. Biol. Med. 37 (11) (2004) 1694–1702.
[117] S. Dalleau, M. Baradat, F. Guéraud, L. Huc, Cell death and diseases related to oxidative stress: 4-hydroxynonenal (HNE) in the balance, Cell Death Differ. 20 (12) (2013) 1615–1630.
[118] C. Muller, J. Bandemer, C. Vindis, C. Camaré, E. Mucher, F. Guéraud, P. Larroque-Cardoso, C. Bernis, N. Auge, R. Salvayre, A. Negre-Salvayre, Protein disulfide isomerase modification and inhibition contribute to ER stress and apoptosis induced by oxidized low density lipoproteins, Antioxid. Redox Signal. 18 (7) (2013) 731–742.
[119] D.J. DelloStritto, P. Sinharoy, P.J. Connell, J.N. Fahmy, H.C. Cappelli, C.K. Thodeti, W.J. Geldenhuys, D.S. Damron, I.N. Bratz, 4-Hydroxynonenal dependent alteration of TRPV1-mediated coronary microvascular signaling, Free Radic. Biol. Med. 101 (2016) 10–19.
[120] J. Yang, V. Gupta, K.A. Tallman, N.A. Porter, K.S. Carroll, D.C. Liebler, Global, in situ, site-specific analysis of protein S-sulfenylation, Nat. Protoc. 10 (7) (2015) 1022–1037.
[121] J. Yang, K.A. Tallman, N.A. Porter, D.C. Liebler, Quantitative chemoproteomics for site-specific analysis of protein alkylation by 4-hydroxy-2-nonenal in cells, Anal. Chem. 87 (5) (2015) 2535–2541.
[122] G. Aldini, L. Gamberoni, M. Orioli, G. Beretta, L. Regazzoni, R. Maffei Facino, M. Carini, Mass spectrometric characterization of covalent modification of human serum albumin by 4-hydroxy-trans-2-nonenal, J. Mass Spectrom. 41 (9) (2006) 1149–1161.
[123] G. Aldini, I. Dalle-Donne, G. Vistoli, R. Maffei Facino, M. Carini, Covalent modification of actin by 4-hydroxy-trans-2-nonenal (HNE): LC-ESI-MS/MS evidence for Cys374 Michael adduction, J. Mass Spectrom. 40 (7) (2005) 946–954.
[124] I. Dalle-Donne, M. Carini, G. Vistoli, L. Gamberoni, D. Giustarini, R. Colombo, R. Maffei Facino, R. Rossi, A. Milzani, G. Aldini, Actin Cys374 as a nucleophilic target of alpha,beta-unsaturated aldehydes, Free Radic. Biol. Med. 42 (5) (2007) 583–598.
[125] G. Aldini, M. Orioli, M. Carini, Alpha,beta-unsaturated aldehydes adducts to actin and albumin as potential biomarkers of carbonylation damage, Redox Rep. 12 (1) (2007) 20–25.
[126] D.S. Backos, K.S. Fritz, J.R. Roede, D.R. Petersen, C.C. Franklin, Posttranslational modification and regulation of glutamate-cysteine ligase by the α,β-unsaturated

aldehyde 4-hydroxy-2-nonenal, Free Radic. Biol. Med. 50 (1) (2011) 14–26.
[127] A.L. Levonen, A. Landar, A. Ramachandran, E.K. Ceaser, D.A. Dickinson, G. Zanoni, J.D. Morrow, V.M. Darley-Usmar, Cellular mechanisms of redox cell signalling: role of cysteine modification in controlling antioxidant defences in response to electrophilic lipid oxidation products, Biochem. J. 378 (Pt 2) (2004) 373–382.
[128] Y. Zhang, M. Sano, K. Shinmura, K. Tamaki, Y. Katsumata, T. Matsuhashi, S. Morizane, H. Ito, T. Hishiki, J. Endo, H. Zhou, S. Yuasa, R. Kaneda, M. Suematsu, K. Fukuda, 4-hydroxy-2-nonenal protects against cardiac ischemia-reperfusion injury via the Nrf2-dependent pathway, J. Mol. Cell Cardiol. 49 (4) (2010) 576–586.
[129] K.A. Jung, M.K. Kwak, Enhanced 4-hydroxynonenal resistance in KEAP1 silenced human colon cancer cells, Oxid. Med. Cell Longev. 2013 (2013) 423965.
[130] Y. Ji, Z. Dai, G. Wu, Z. Wu, 4-Hydroxy-2-nonenal induces apoptosis by activating ERK1/2 signaling and depleting intracellular glutathione in intestinal epithelial cells, Sci. Rep. 6 (2016) 32929.
[131] A. Vila, K.A. Tallman, A.T. Jacobs, D.C. Liebler, N.A. Porter, L.J. Marnett, Identification of protein targets of 4-hydroxynonenal using click chemistry for ex vivo biotinylation of azido and alkynyl derivatives, Chem. Res. Toxicol. 21 (2) (2008) 432–444.
[132] B.K. Chacko, S.B. Wall, P.A. Kramer, S. Ravi, T. Mitchell, M.S. Johnson, L. Wilson, S. Barnes, A. Landar, V.M. Darley-Usmar, Pleiotropic effects of 4-hydroxynonenal on oxidative burst and phagocytosis in neutrophils, Redox Biol. 9 (2016) 57–66.
[133] S. Ravi, M.S. Johnson, B.K. Chacko, P.A. Kramer, H. Sawada, M.L. Locy, L.S. Wilson, S. Barnes, M.B. Marques, V.M. Darley-Usmar, Modification of platelet proteins by 4-hydroxynonenal: potential Mechanisms for inhibition of aggregation and metabolism, Free Radic. Biol. Med. 91 (2016) 143–153.
[134] J.J. Galligan, R.L. Smathers, K.S. Fritz, L.E. Epperson, L.E. Hunter, D.R. Petersen, Protein carbonylation in a murine model for early alcoholic liver disease, Chem. Res. Toxicol. 25 (5) (2012) 1012–1021.
[135] C. Wang, E. Weerapana, M.M. Blewett, B.F. Cravatt, A chemoproteomic platform to quantitatively map targets of lipid-derived electrophiles, Nat. Methods 11 (1) (2014) 79–85.
[136] T. Grune, K.J. Davies, The proteasomal system and HNE-modified proteins, Mol. Asp. Med. 24 (4–5) (2003) 195–204.
[137] J. Just, T. Jung, N.A. Friis, S. Lykkemark, K. Drasbek, G. Siboska, T. Grune, P. Kristensen, Identification of an unstable 4-hydroxynoneal modification on the 20S proteasome subunit α7 by recombinant antibody technology, Free Radic. Biol. Med. 89 (2015) 786–792.
[138] F. Bosch-Morell, L. Flohé, N. Marín, F.J. Romero, 4-Hydroxynonenal inhibits glutathione peroxidase: protection by glutathione, Free Radic. Biol. Med. 26 (11–12) (1999) 1383–1387.
[139] D.L. Carbone, J.A. Doorn, Z. Kiebler, D.R. Petersen, Cysteine modification by lipid peroxidation products inhibits protein disulfide isomerase, Chem. Res. Toxicol. 18 (8) (2005) 1324–1331.
[140] L.G. Korotchkina, H. Yang, O. Tirosh, L. Packer, M.S. Patel, Protection by thiols of the mitochondrial complexes from 4-hydroxy-2-nonenal, Free Radic. Biol. Med. 30 (9) (2001) 992–999.
[141] D. Gillingham, S. Geigle, O. Anatole von Lilienfeld, Properties and reactivity of nucleic acids relevant to epigenomics, transcriptomics, and therapeutics, Chem. Soc. Rev. 45 (9) (2016) 2637–2655.
[142] X. Wei, H. Yin, Covalent modification of DNA by α, β-unsaturated aldehydes derived from lipid peroxidation: recent progress and challenges, Free Radic. Res. 49 (7) (2015) 905–917.
[143] I.G. Minko, I.D. Kozekov, T.M. Harris, C.J. Rizzo, R.S. Lloyd, M.P. Stone, Chemistry and biology of DNA containing 1,N(2)-deoxyguanosine adducts of the alpha,beta-unsaturated aldehydes acrolein, crotonaldehyde, and 4-hydroxynonenal, Chem. Res. Toxicol. 22 (5) (2009) 759–778.
[144] Z. Feng, W. Hu, S. Amin, M.S. Tang, Mutational spectrum and genotoxicity of the major lipid peroxidation product, trans-4-hydroxy-2-nonenal, induced DNA adducts in nucleotide excision repair-proficient and -deficient human cells, Biochemistry 42 (25) (2003) 7848–7854.
[145] S. Choudhury, M. Dyba, J. Pan, R. Roy, F.L. Chung, Repair kinetics of acrolein- and (E)-4-hydroxy-2-nonenal-derived DNA adducts in human colon cell extracts, Mutat. Res. 751–752 (2013) 15–23.
[146] Y. Fu, R.G. Nath, M. Dyba, I.M. Cruz, S.R. Pondicherry, A. Fernandez, C.L. Schultz, P. Yang, J. Pan, D. Desai, J. Krzeminski, S. Amin, P.P. Christov, Y. Hara, F.L. Chung, In vivo detection of a novel endogenous etheno-DNA adduct derived from arachidonic acid and the effects of antioxidants on its formation, Free Radic. Biol. Med. 73 (2014) 12–20.
[147] B.C. Song, N.S. Joo, G. Aldini, K.J. Yeum, Biological functions of histidine-dipeptides and metabolic syndrome, Nutr. Res. Pract. 8 (1) (2014) 3–10.
[148] A.A. Boldyrev, G. Aldini, W. Derave, Physiology and pathophysiology of carnosine, Physiol. Rev. 93 (4) (2013) 1803–1845.
[149] S. Zhou, E.A. Decker, Ability of carnosine and other skeletal muscle components to quench unsaturated aldehydic lipid oxidation products, J. Agric. Food Chem. 47 (1) (1999) 51–55.
[150] K. Bauer, Carnosine and homocarnosine, the forgotten, enigmatic peptides of the brain, Neurochem. Res. 30 (10) (2005) 1339–1345.
[151] G. Vistoli, D. De Maddis, V. Straniero, A. Pedretti, M. Pallavicini, E. Valoti, M. Carini, B. Testa, G. Aldini, Exploring the space of histidine containing dipeptides in search of novel efficient RCS sequestering agents, Eur. J. Med. Chem. 66 (2013) 153–160.
[152] G. Vistoli, M. Colzani, A. Mazzolari, D.D. Maddis, G. Grazioso, A. Pedretti, M. Carini, G. Aldini, Computational approaches in the rational design of improved carbonyl quenchers: focus on histidine containing dipeptides, Future Med. Chem. 8 (14) (2016) 1721–1737.
[153] F. Bellia, G. Vecchio, E. Rizzarelli, Carnosinases, their substrates and diseases, Molecules 19 (2) (2014) 2299–2329.
[154] J. Drozak, M. Veiga-da-Cunha, D. Vertommen, V. Stroobant, E. Van Schaftingen, Molecular identification of carnosine synthase as ATP-grasp domain-containing protein 1 (ATPGD1), J. Biol. Chem. 285 (13) (2010) 9346–9356.
[155] G. Vistoli, M. Carini, G. Aldini, Transforming dietary peptides in promising lead compounds: the case of bioavailable carnosine analogs, Amino Acids 43 (1) (2012) 111–126.
[156] G. Beretta, R. Artali, L. Regazzoni, M. Panigati, R.M. Facino, Glycyl-histidyl-lysine (GHK) is a quencher of alpha,beta-4-hydroxy-trans-2-nonenal: a comparison with carnosine. insights into the mechanism of reaction by electrospray ionization mass spectrometry, 1H NMR, and computational techniques, Chem. Res. Toxicol. 20 (9) (2007) 1309–1314.
[157] W. Aoi, Y. Naito, T. Yoshikawa, Role of oxidative stress in impaired insulin signaling associated with exercise-induced muscle damage, Free Radic. Biol. Med. 65 (2013) 1265–1272.
[158] R. Takahashi, T. Goto, T. Oe, S.H. Lee, Angiotensin II modification by decomposition products of linoleic acid-derived lipid hydroperoxide, Chem. Biol. Interact. 239 (2015) 87–99.
[159] G. Aldini, G. Vistoli, M. Stefek, N. Chondrogianni, T. Grune, J. Sereikaite, I. Sadowska-Bartosz, G. Bartosz, Molecular strategies to prevent, inhibit, and degrade advanced glycoxidation and advanced lipoxidation end products, Free Radic. Res. 47 (Suppl 1) (2013) 93–137.
[160] J.P. Dwyer, B.A. Greco, K. Umanath, D. Packham, J.W. Fox, R. Peterson, B.R. Broome, L.E. Greene, M. Sika, J.B. Lewis, Pyridoxamine dihydrochloride in diabetic nephropathy (PIONEER-CSG-17): lessons learned from a pilot study, Nephron 129 (1) (2015) 22–28.
[161] H.C. Kuiper, R.S. Bruno, M.G. Traber, J.F. Stevens, Vitamin C supplementation lowers urinary levels of 4-hydroperoxy-2-nonenal metabolites in humans, Free Radic. Biol. Med. 50 (7) (2011) 848–853.
[162] S.M. Schreier, M.K. Muellner, H. Steinkellner, M. Hermann, H. Esterbauer, M. Exner, B.M. Gmeiner, S. Kapiotis, H. Laggner, Hydrogen sulfide scavenges the cytotoxic lipid oxidation product 4-HNE, Neurotox. Res. 17 (3) (2010) 249–256.
[163] M. Guichardant, P. Taibi-Tronche, L.B. Fay, M. Lagarde, Covalent modifications of aminophospholipids by 4-hydroxynonenal, Free Radic. Biol. Med. 25 (9) (1998) 1049–1056.
[164] S. Stadelmann-Ingrand, R. Pontcharraud, B. Fauconneau, Evidence for the reactivity of fatty aldehydes released from oxidized plasmalogens with phosphatidylethanolamine to form Schiff base adducts in rat brain homogenates, Chem. Phys. Lipids 131 (1) (2004) 93–105.
[165] S. Bacot, N. Bernoud-Hubac, N. Baddas, B. Chantegrel, C. Deshayes, A. Doutheau, M. Lagarde, M. Guichardant, Covalent binding of hydroxy-alkenals 4-HDDE, 4-HHE, and 4-HNE to ethanolamine phospholipid subclasses, J. Lipid Res. 44 (5) (2003) 917–926.
[166] L. Guo, Z. Chen, V. Amarnath, S.S. Davies, Identification of novel bioactive aldehyde-modified phosphatidylethanolamines formed by lipid peroxidation, Free Radic. Biol. Med. 53 (6) (2012) 1226–1238.
[167] O. Jovanovic, A.A. Pashkovskaya, A. Annibal, M. Vazdar, N. Burchardt, A. Sansone, L. Gille, M. Fedorova, C. Ferreri, E.E. Pohl, The molecular mechanism behind reactive aldehyde action on transmembrane translocations of proton and potassium ions, Free Radic. Biol. Med. 89 (2015) 1067–1076.
[168] S. Bacot, N. Bernoud-Hubac, B. Chantegrel, C. Deshayes, A. Doutheau, G. Ponsin, M. Lagarde, M. Guichardant, Evidence for in situ ethanolamine phospholipid adducts with hydroxy-alkenals, J. Lipid Res. 48 (4) (2007) 816–825.
[169] H.C. Kuiper, C.L. Miranda, J.D. Sowell, J.F. Stevens, Mercapturic acid conjugates of 4-hydroxy-2-nonenal and 4-oxo-2-nonenal metabolites are in vivo markers of oxidative stress, J. Biol. Chem. 283 (25) (2008) 17131–17138.
[170] H.C. Kuiper, B.L. Langsdorf, C.L. Miranda, J. Joss, C. Jubert, J.E. Mata, J.F. Stevens, Quantitation of mercapturic acid conjugates of 4-hydroxy-2-nonenal and 4-oxo-2-nonenal metabolites in a smoking cessation study, Free Radic. Biol. Med. 48 (1) (2010) 65–72.
[171] W. Xiang, J.C. Schlachetzki, S. Helling, J.C. Bussmann, M. Berlinghof, T.E. Schäffer, K. Marcus, J. Winkler, J. Klucken, C.M. Becker, Oxidative stress-induced posttranslational modifications of alpha-synuclein: specific modification of alpha-synuclein by 4-hydroxy-2-nonenal increases dopaminergic toxicity, Mol. Cell Neurosci. 54 (2013) 71–83.
[172] C.T. Shearn, R.L. Smathers, D.S. Backos, P. Reigan, D.J. Orlicky, D.R. Petersen, Increased carbonylation of the lipid phosphatase PTEN contributes to Akt2 activation in a murine model of early alcohol-induced steatosis, Free Radic. Biol. Med. 65 (2013) 680–692.

Chapter IV: Methods for detection and quantification of non-enzymatic protein modifications

This Chapter is submitted as a book chapter in Sadowska-Bartosz, I. (ed.) *Non-Enzymatic Protein Modifications in Health, Disease and Ageing.* Elsevier.

Chapter IV: Methods for detection and quantification of non-enzymatic protein modifications

[1]Genny Degani, [2]Giovanna Baron, [2]Marco Mol, [2]Marina Carini, [2]Giancarlo Aldini, [2]Alessandra Altomare

[1] University of Milan, Department of Biosciences, Milano, Italy.

[2] University of Milan, Department of Pharmaceutical Sciences, Milano, Italy.

Abstract

It has been clearly demonstrated that non-enzymatic protein post-translational modifications (nePTMs) induced by chemically reactive compounds occur progressively and are amplified in various oxidative-based diseases, making nePTM-derived products not also as interesting biomarkers but also as drug target when involved in pathogenetic mechanisms. The analytical aspects of nePTMs (identification, characterization and quantification) represents a scientific challenge due to the fact that are heterogeneous, contained in a negligible amount in respect to native proteins and quite chemically and metabolically unstable. Several analytical techniques have so far been reported to fully profile nePTMs and to this regards, mass spectrometry is one of the most promising techniques since it offers many analytical alternatives for the development of accurate assays for the detection of the modification itself, for the mapping of the modification sites and for the precise quantification of the modified peptide in different biological conditions. This chapter is focused on taking an inventory of the most updated analytical methods available for the measurement of nePTM – derived products in biological fluids, focusing on colorimetric assays, fluorescence measurements, immunological, chromatographic and mass spectrometry methods. In the last section a comprehensive description of the quantification using mass spectrometry is described.

Key Words

Non-Enzymatic Post-Translational Modifications; nePTMs; analytical methods; mass spectrometry; MS; Top-down MS Approach; Bottom-Up MS Approach; Quantitative MS;

4.1 Introduction

In biological systems proteins undergo a wide array of modifications (post-translational modifications – PTMs) that alter their function and their structure. Many post-translational modifications (PTMs) of proteins have already been described, and have been found to determine protein activity, stability, specificity, transportability and lifespan [1].

It is possible to distinguish two types of protein modification, one initiated / catalyzed in the presence of specific enzymes (enzymatic modifications) and the other which occurs in the presence of chemically reactive compounds (e.g. reactive oxygen- and nitrogen-species); the latter type of modification is known as non-enzymatic (nePTM) and usually occurs stochastically [2]. While such modifications are essential for the protein functionality, depending on the ternary structure they can be physiologically damaging. Such nePTMs which alter the structural and biological properties of proteins in living organisms include oxidation, racemization, isomerization, deamidation, nitration, carbonylation, carbamylation and glycation (or glycoxidation) [2, 3].

These cumulative modifications, which affect all proteins over their lifespan, are generally characterized by the binding of small metabolites to free reactive groups of proteins, followed by subsequent molecular rearrangements. Diverse reactive species are responsible for the formation of a range of oxidative products, while different amino-acid side chains can undergo modification contributing to an additional variety of final derivatives. Some of these end-products are unstable, present in very low quantities and decompose quickly, in which case the physiological response of an organism to nePTM proteins can be to repair and/or to degrade [3]. Other modified proteins acquire stability by further structural adjustments, which may end with misfolding, with, for instance, an increased chance of self-aggregation into insoluble fibrillar structures, which accumulate in cells and tissues [3]. One of the most prevalent covalent modifications is protein glycation, usually followed by a sequence of further reactions and rearrangements producing the so-called advanced glycosylation end products (AGEs). Glycated proteins are more prone to form cross-links with other proteins, leading to structural and functional alterations [3].

By virtue of scientific progress, it has been more clearly demonstrated in recent years, that non-enzymatic post-translational modifications (nePTMs) occur progressively and are amplified in various diseases such as diabetes mellitus, chronic renal failure or atherosclerosis (Table 1.) [4]. Accordingly, nePTM –derived products are considered promising and useful biomarkers for these diseases.

Table 1. Involvement of nePTMs of proteins in aging and disease [1].

Disease	Reaction Involved
Aging	Oxidation
	Glycation / Glycoxidation
	Carbonylation
	Amino Acid Modifications
Atherosclerosis	Glycation / Glycoxidation
	Carbonylation
	Carbamylation
	Oxidation / Nitration
Chronic renal failure	Carbamylation
	Glycation / Glycoxidation
	Carbonylation
	Oxidation
Diabetes Mellitus	Glycation / Glycoxidation
	Carbonylation
Neurodegenerative Diseases	Glycation / Glycoxidation
	Carbonylation
	Oxidation / Nitration
Osteoporosis	Glycation / Glycoxidation
Retinopathy	Glycation / Glycoxidation
	Carbonylation
	Carbamylation

Another important aspect requires an understanding of the biochemistry and metabolism of modified proteins. The nature, site and extent of nePTM give rise to a population of that specific protein with alterations in structure and function ranging from being fully active to totally inactive molecules. Since there is an extremely low probability that any two molecules will be modified/damaged in exactly the same way and to the same extent, an increase in molecular heterogeneity is inevitable [5]. Therefore, accurate identification, detection and quantification of nePTM has gained increased attention in the last two decades since they are essential for establishing connection between specific protein structure and specific biological role [3].

Analysis of nePTM covers two distinct features: (i) determination of the modification itself (i.e. chemical group or small entity), such as the number of carbonyl groups, disulfide bonds, etc. and their specific location in the protein sequence and (ii) determination of the quantity of the specifically-modified protein, such as AGE-albumin or hemoglobin, in relation to the non-modified form and/or between two distinct conditions, e.g. healthy and diseased [3].

However, the complexity of proteins makes analysis, detection and quantification of non-enzymatic post-translational modification a very difficult challenge.
This chapter is focused on taking an inventory of the analytical methods available for the measurement of nePTM – derived products.

4.2 Analytical methods for qualitative identification of nePTMs

The connection of the molecular aging of protein with the development of long term complication of several diseases has been well established, making nePTM-derived products interesting biomarkers. Unfortunately, thus far they are not currently used in routine clinical laboratory practice, except for glycated hemoglobin.
In this context three major problems have been encountered:

- The huge variability of the structure of these compounds: from a chemical point of view nePTM–derived products are quite heterogeneous and some of them are probably still unknown;
- The chemical and metabolic instability of nePTM–derived products:
- The lack of specific and highly sensitive methods suited to the low basal rate of most of the nePTMs involved in the molecular damaging of proteins [4]. nePTM–derived products are usually contained in a negligible amount (nanomolar range concentration, or less) in respect to the native protein.

The methods used for the detection of nePTMs should be characterized by high specificity and sensitivity, but also robustness and reproducibility [4]. In fact the methods used range from simple techniques such as the colorimetric or immunoassay methods, easily implementable in every research or clinical laboratory but which are generally poorly specific, to more specific methods, such as mass spectrometry, which however requires specific sophisticated instrumentations and specific skills [4].
The recent implementation in clinical chemistry laboratories of mass spectrometry–based methods that provide higher specificity and sensitivity has facilitated the measurement of nePTM –derived products [4]. Mass spectrometry (MS) is certainly one of the most promising techniques since it offers many advantages and analytical alternatives for the development of fast and accurate assays to study modified proteins [6].
In detail, mass spectrometry can identify and separately quantitate multiple analytes (including macromolecules – i.e. proteins) in one single scan. Identification is performed by the analyzer, which allows the determination of the molecular weight through the measurement of the mass to charge ratio of a molecule's gas phase ions. The ions are then separately counted by the detector,

which produces a signal that is proportional to their concentration therefore allowing quantitation [6].

The evolution of instrument technology has led to the development of commercial analyzers able to detect analytes at trace levels (sensitivity), reducing, therefore, the sample amount required for the analysis [6]. Instrument selectivity (the ability to distinguish molecules with similar molecular weight) has also been improved over the years. In this field one of the most important discoveries has been the so-called high-resolution mass analyzers (HR-MS), which are capable of separating molecules with very similar molecular weight but different elemental composition. This innovation is accompanied by a continuous updating of the analyzers capable of multistage mass spectrometry experiments (i.e. tandem mass spectrometry). This technology is still the basis for the development of many MS-based methods since it enables the collection of tandem mass spectra, which can be considered as molecule fingerprints usually allowing their unambiguous identification [6].

Importantly, MS does not require the analytes to be labelled before detection, although there is a panel of labelling procedures uniquely designed for mass spectrometry with the scope of expanding the use of this technique.

Thus, MS appears to be the ultimate tool that should be used for the detection and the accurate mapping of modification sites in the primary structure of a protein. It can also be used to quantify the abundance of the peptide carrying the modified residue compared to that of the unmodified peptide or such abundance in different biological conditions [3].

The unique feature of MS is that it can be used to analyze any protein modification without *a priori* assumptions about the type of modification (untargeted approach). nePTM can be analyzed by MS in **"top-down"** experiments that analyze intact proteins, or in **"bottom up"** experiments that rely on sample proteolysis prior to mass spectrometric detection. The top down experiments provide more information about individual proteins, including full characterization of each present protein form and its modifications (Figure 1).

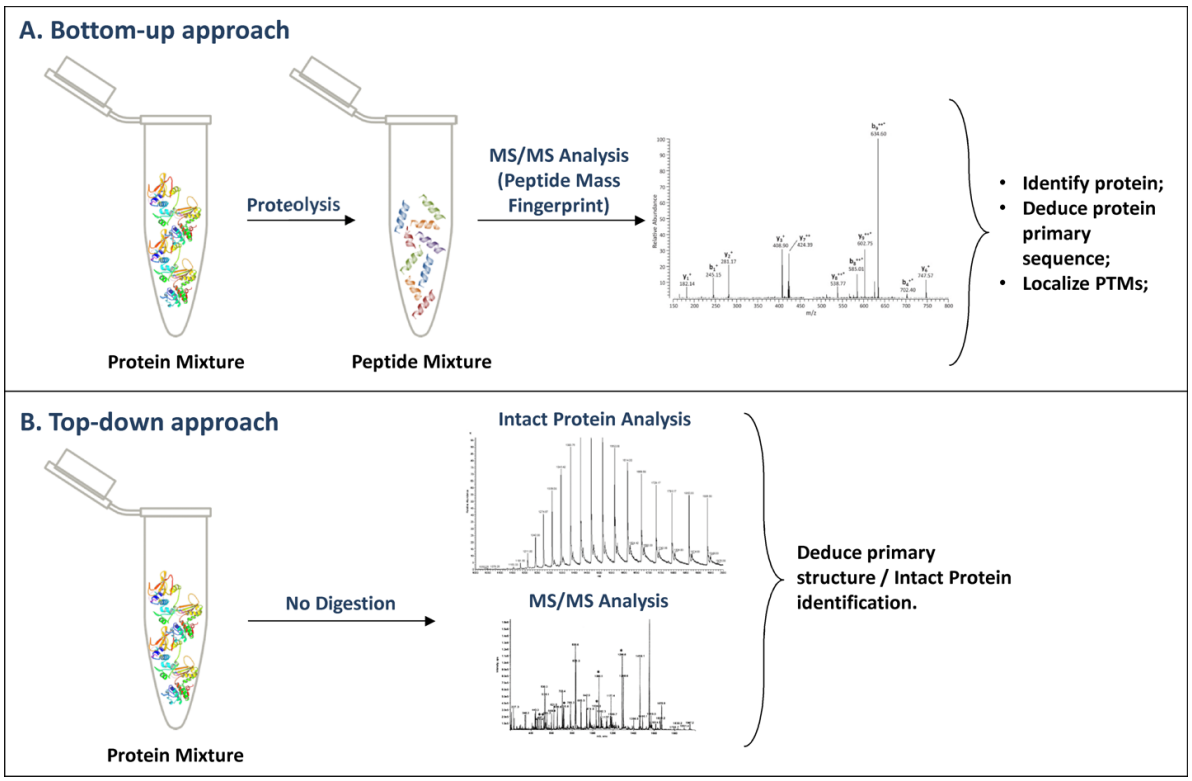

Figure 1. Schematic of bottom-up vs. top-down approaches in proteomics.

Using the mass difference between the genome deduced protein sequence and peptide masses observed experimentally it is possible to identify any protein modification [7]. For example, oxidation of a Met residue (131 Da) increases its mass to 147 Da by the addition of a single oxygen atom (16 Da). Through observation of the discrete mass difference of the intact protein (top-down approach) it is possible to assign the respective modification. However, top-down proteomics is a relatively immature field compared to bottom-up proteomics, and still suffers from serious limitations [3]. Mass spectrometry based sequencing allows for site-specific assignment of modifications at the resolution of individual amino-acids (bottom-up approach) [3, 7].

4.2.1 MS top down

Given the importance of PTMs in the regulation of intracellular signalling and the link between the aberrant or altered PTM of a number of proteins and certain human diseases, the top-down MS approach holds significant promise for the elucidation of nePTM-associated disease mechanisms by providing a powerful method for the identification, characterization, and quantification of nePTM, which can subsequently be correlated with disease etiology [8]. This top-down technology is beginning to capture the interest of biologists and mass spectrometrists, whose main goal is the elucidation of the interaction networks operative in cellular pathways [9].

Top-down mass spectrometry is a technology which strives to preserve the post-translationally modified forms of proteins present *in vivo* by measuring them intact, rather than measuring peptides produced from them by proteolysis. Intact protein analysis results in reduced sample complexity (in terms of the number of individual species present in the sample) in comparison to the protein digests analyzed using the bottom-up approach [8].

Intact protein ions are introduced into the gas phase by ESI and all intact protein forms in a sample are analysed by MS. In this way a specific protein form of interest can be directly isolated and, subsequently, fragmented in the mass spectrometer by MS/MS strategies to map both amino acid variations (arising from alternative splicing events and poly-morphisms/mutations) and PTMs. If a sufficient number of informative fragment ions are observed, this analysis can provide a complete description of the primary sequence of the protein and reveal all of its modifications, as well as any correlations that exist between these modifications. Although the molecular masses of intact proteins have been successfully measured by MALDI– and ESI–mass spectrometry for some time [10], it has proved difficult to produce extensive gas-phase fragmentation of intact protein ions, especially from large proteins.

The establishment of electron-based MS/MS techniques, namely, electron capture dissociation (ECD) and electron transfer dissociation (ETD), represents a significant advance for top-down MS by providing reliable methods for the localization and characterization of labile PTMs, such as phosphorylation and glycosylation [8]. Top-down MS with ECD/ETD has unique advantages for the dissection of molecular complexity via the quantification of protein forms, unambiguous localization of PTMs and polymorphisms/mutations, discovery of unexpected PTMs and sequence variations, identification and quantification of positional isomers, and the interrogation of PTM interdependence [8]. Recently, a number of top-down proteomics studies have linked protein form alterations to disease phenotypes, highlighting the potential for top-down proteomics in the elucidation of nePTM-associated disease mechanisms [8]. However, the top-down approach is still facing challenges associated with protein solubility, separation, and the detection of large intact proteins, as well as the complexity of the human proteome. Due to the high dynamic range of protein expression and extreme complexity of the proteome, its fractionation/separation is a critical step prior to MS analysis. While bottom-up proteomics boasts mature and reliable separation methods, which include gel- and LC-based separation methodologies, effective separation strategies that are high-throughput, rapid, and compatible with top-down MS analysis are still scarce [8]. Moreover, top-down analysis of proteins larger than approximately 70 kDa remains challenging due to the difficulty associated with detecting and fragmenting these

molecular behemoths. Thus, new technological developments are urgently needed to advance the field of top-down proteomics [8].

4.2.2 MS Bottom UP

In contrast to the top-down approach, the bottom-up approach is significantly more sensitive and, in fact, has been successful in identifying proteins and determining details of their sequence and PTMs [11].

The bottom-up approach involves proteolysis of proteins into short peptides (8–30 amino acids) prior to LC-MS/MS analysis. Protein digestion into short peptides facilitates both LC separation and high-resolution MS detection. Different proteolytic enzymes can be used, but trypsin is the protease of choice for its efficiency and specificity of cleavage. The resulting “tryptic peptides” are then analyzed by electrospray ionization (ESI) or matrix-assisted laser desorption/ionization (MALDI). These mass spectrometry techniques allow peptide and protein molecular ions to be put into the gas phase without fragmentation [10]. The ESI– or MALDI–mass spectrometry analyses take place in two stages. First, the masses of the intact tryptic peptides are determined; these peptide ions are then fragmented in the gas phase to reveal their sequence and modifications. The bottom-up approach is especially useful in protein identification, since tryptic peptides are readily solubilized and separated, tasks that are considerably more difficult for the parent proteins. In addition, many tryptic peptides can be readily analyzed by mass spectrometry analysis, providing useful fragmentation ladders [10] that often yield sufficient information to identify the parent protein. Due to the availability of human and other species genomic databases, irrespective of the MS platform used, raw MS data can be compared to protein databases using searching tools such as MASCOT and SEQUEST [12].

Unfortunately, only a small amount of the tryptic peptides are normally detected, and only a fraction of these yield useful fragmentation ladders. It is similar to a jigsaw puzzle, where many of the pieces are missing. But even if we had all the pieces, the picture would still be incomplete, because to produce a sufficient number of tryptic peptide ions to allow for their detection by mass spectrometry it is currently necessary to examine the pieces of a billion or more copies of the protein of interest. So really we have a billion puzzles, some of which are the same, but many of which are slightly different, because they correspond to copies of the protein containing different modifications. Additionally, mass spectrometry relies on ionization of the peptides that are measured. In positive-ion operating mode, ionization of peptides largely depends on the presence of basic sites like N-terminal amine and the side groups of Lys, Arg and His residues. Generation of some modifications, e.g. carbonyl products of Arg and Lys (to give glutamic and 2-amino-adipic semialdehydes) is associated with the loss of the guanidine and ammonia groups, typically

carrying a positive charge. This leads to decreased ionization efficiency and reduces the chance of detecting those peptides using positive-ion mode MS, making analysis of oxidized proteins exceptionally challenging [3].

The complexity of investigating PTMs within protein proteolytic peptides is due to: (i) the frequent existence of isobaric peptides, (ii) the uncertain positioning of PTMs on neighbouring modifiable residues and (iii) the difficulty of distinguishing between several isobaric PTM combinations [13]. Finally, the above aspects not only complicate identification of the correct sequence and of the PTM sites, they also make it very difficult to quantify the relative abundance of positional isomers that often co-elute, at least partially.

Comprehensive interpretation of MS data obtained from nePTM focused experiments is an additional analytical challenge. The complexity of the data and the limitations of the existing tools for bioinformatics very often lead to misinterpretation of the results. For example, modification of Lys and Arg residues frequently makes them inaccessible for trypsin proteolysis leading to a large number of missed cleavages. The resulting peptides require large numbers of missed cleavages to be included in data analysis algorithms increasing the chance of false positive identifications. Another difficulty stems from the many different modifications that need to be included. Searching algorithms (e.g. MASCOT, SEQUEST) often cannot search with an unlimited number of modifications, necessitating several searches of the same data. This increases data processing time and the risk of false positive identifications. New types of modification can only be found if manual data analysis is carried out, but this approach is labour intensive, time consuming and cannot be used effectively with complex protein mixtures. Identification of oxidized peptides with a search algorithm poses several other technical problems [3]. In spite of the difficulties in identifying nePTM sites, the combination of labelling and enrichment methods could lead to the identification of several hundred modification sites in specific proteins [3].

4.2.3 Chemical derivatization and enrichment methods

Although modern mass spectrometry instruments are characterized by an exceptional sensitivity that permits the detection of peptides at sub-femtomole levels, the investigation of protein nePTM is still an analytical challenge [14]. This is mainly because, as stated above, modified proteins occur in negligible amounts with respect to the native protein. Therefore, modification of a given site is often present in only a small fraction of the protein molecules of a given type [3].

The technical challenges related to the identification of nePTM proteins led scientists to develop specific strategies that allow the analysis to be focused on a particular type of protein modification. In particular, due to their low abundance, modified proteins need to be selectively isolated from native proteins; a possible strategy to reverse this dynamic range in favour of the protein adducts

is the specific enrichment and/or chemical derivatization methods that target a certain class of modifications (Figure 2.). This creates a “handle” by which modified peptides/proteins can be pulled out from the complex mixture, which of course includes the non-modified peptides/proteins [3].

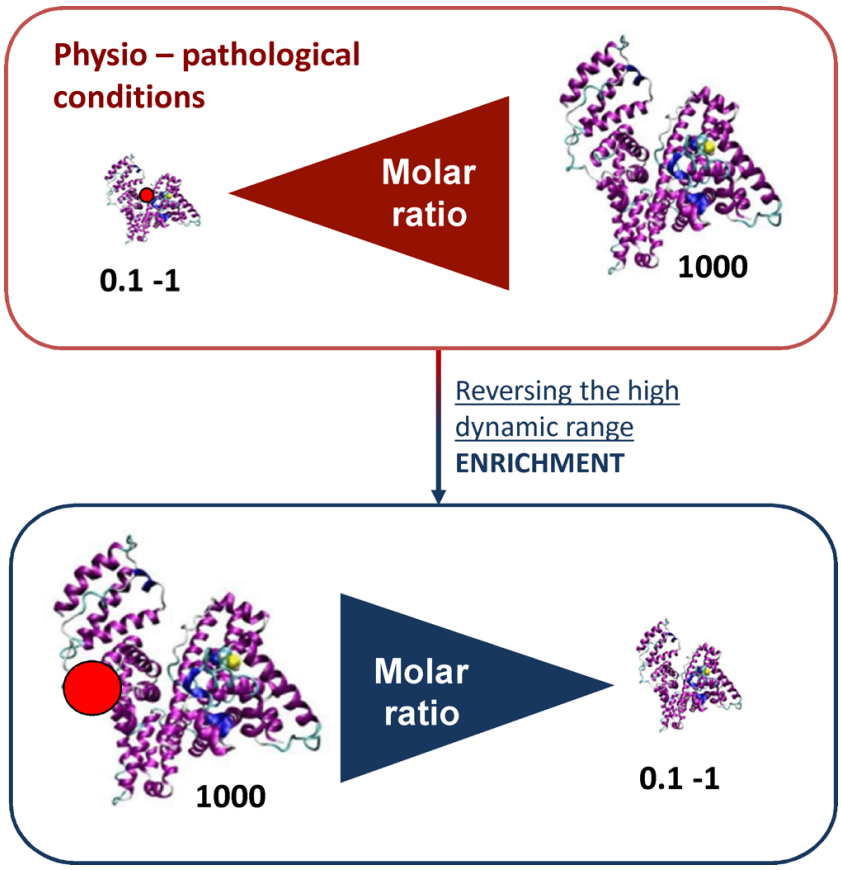

Figure 2. Enrichment strategy to reverse this dynamic range in favour of the protein adducts.

Different analytical strategies have been developed for the enrichment of specific nePMTs, and they can be grouped into two major approaches: gel-based and non-gel-based methods. In the gel-based methods, modified proteins extracted from biological tissues are separated using one/two-dimensional gel electrophoresis separation, whereby proteins migrate into a polyacrylamide gel according to their relative mobilities. Separated proteins can be transferred onto a Western blot membrane and specific antibodies used to visualize target spots. Antibodies are selected based on the type of the modification (nePTM) to be studied (e.g., protein carbonyls, 4-HNE, 3-NT, and glutathionylation).

Spots of interest are excised from the gel and modified proteins identified using a bottom-up MS approach [15-18]. Gel-based methods are advantageous because they target a specific subset of

the proteome and numerous gels can be run and aligned, using sophisticated software tools. Alternative approaches, which do not involve gels but rather liquid chromatography separations, and MS and tandem MS (MS/MS), have also been applied in this context. Non-gel proteomic methods include derivatization and/or enrichment procedures of modified proteins, in-solution proteolytic digestion, followed by the nanoflow LC separation of peptides and automated MS and MS/MS data acquisition [19].

4.3 Overview of the analytical methods for the measurements of specific nePTM

In the following section we report an overview of the analytical methods for the measurements of specific nePTM in biological fluids, focusing in particular on colorimetric assays, fluorescence measurements, immunological, chromatographic and mass spectrometry methods. In the last section a comprehensive description of the quantification using mass spectrometry will be described.

4.3.1 Carbonylation

Carbonylation is one of the most commonly occurring oxidative nePTMs and its measurement is considered a good indicator of the extent of oxidative damage of proteins associated with various conditions of oxidative stress, aging, and physiological disorders [20]. Thus, the number of carbonyl groups observed within a protein usually correlates with protein damage caused by oxidative stress.

Protein carbonyl groups are generated by direct oxidation of several amino acid side chains (i.e., Lys, Arg, Pro, Thr, His, and others), backbone fragmentation, hydrogen atom abstraction from alpha carbons and Michael addition reactions of His, Lys, and Cys residues with products of lipid peroxidation causing inactivation, crosslinking, or breakdown of proteins. The most abundant carbonyls in aged cells are 2-amino-adipic semialdehyde (AAS) and gamma-glutamyl semialdehyde (GGS). Protein carbonyls are also produced by glycation/ glycoxidation of Lys amino groups, forming AGEs [20, 21], and Michael adducts of a,b-unsaturated aldehydes produced by lipid peroxidation (Figure 3.) [22].

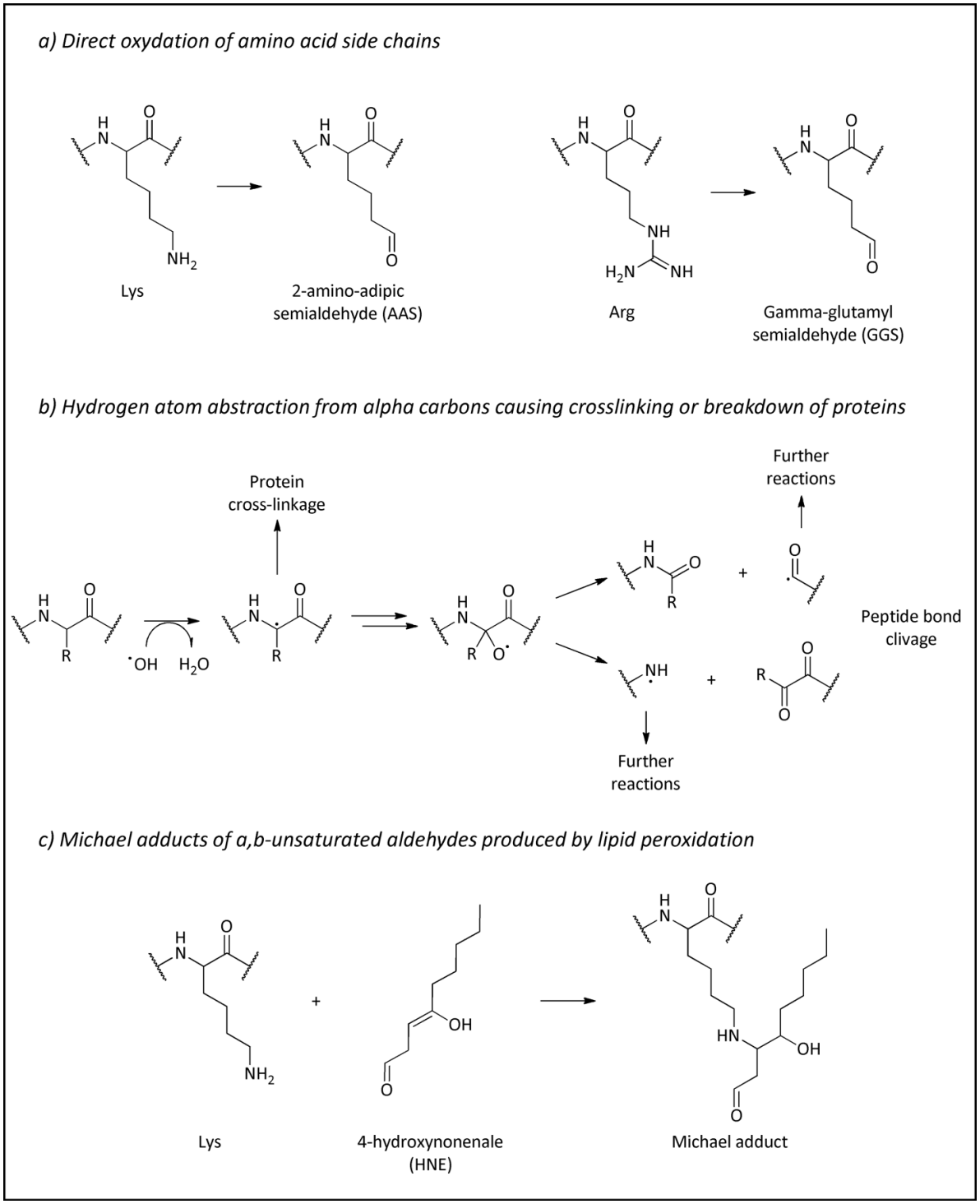

Figure 3. Primary and secondary protein carbonyls generated by direct oxidation of amino acid side chains (i.e., Lys, Arg, Pro, Thr, His, and others) – Panel A; hydrogen atom abstraction from alpha carbons causing crosslinking or breakdown of proteins – Panel B; and Michael addition reactions of His, Lys, and Cys residues with products of lipid peroxidation – Panel C.

For the derivatization of carbonyls the Oxyblot gel-based technique was developed. In this procedure, carbonyls react with 2,4-dinitrophenylhydrazine (DNPH) to form 2,4-dinitrophenylhydrazone (DNP-hydrazone) characterized by an absorbance at 370 nm (Figure 4. – panel A). After treatment, protein samples can be resolved by gel electrophoresis (mono- or two-dimensional), transferred onto a nitrocellulose or PVDF membrane (Western Blot) (Figure 4. – panel A), and recognized by specific antibodies against DNP [2]. As stated above, spots of interest are excised from the gel and modified proteins identified using a bottom-up approach. This strategy permits the detection of protein carbolnyls (PCO) on low abundant proteins. Despite the extensive usage of DNPH for derivatizing PCO it should be noted that DNPH is not exclusive to carbonyl groups, since it could also react with sulfenic acids—oxidized thiol groups—under acidic catalysis conditions [23]. Biotin-hydrazide may be used to selectively label carbonyl groups with fluorescein or peroxidase linked avidin [24, 25].

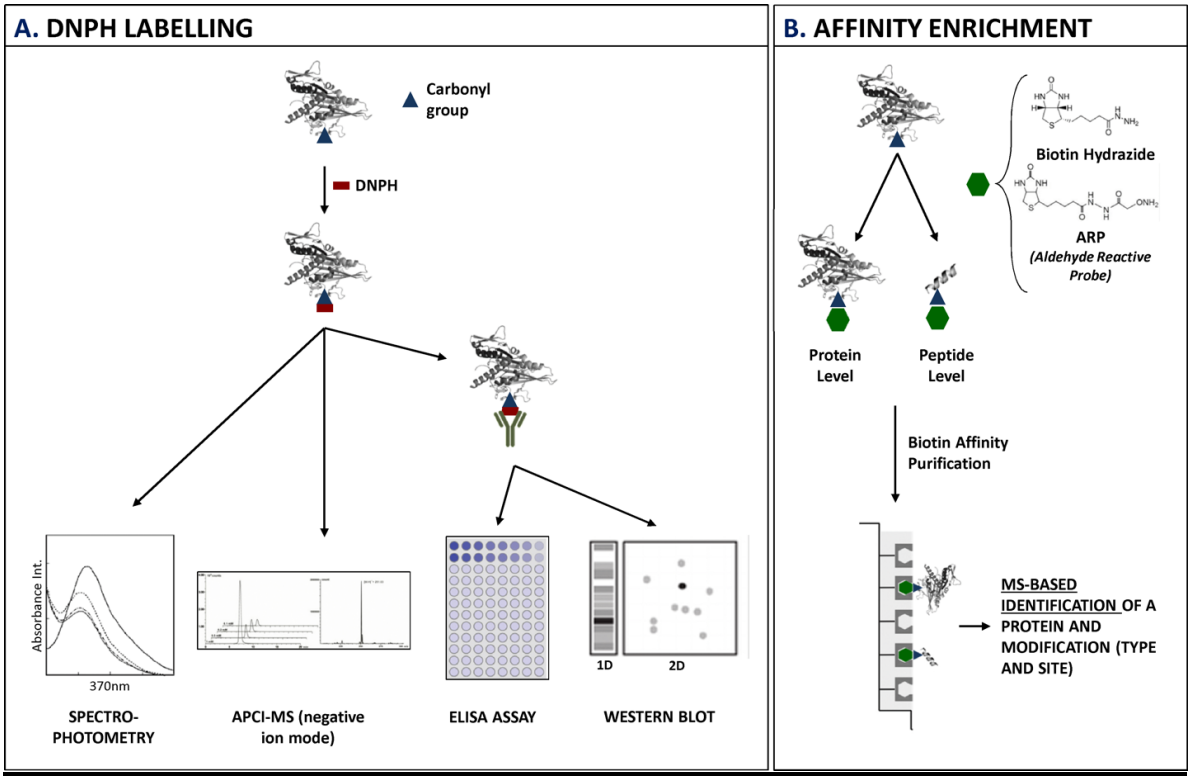

Figure 4. Summary of the selected protein-carbonylation detection methods. Depending on the sample type, experimental aims and instrumentation available analysis of protein-carbonylation may be carried out via DNPH labelling (Spectrophotometric, ELISA, Western blot, APCI-MS) – Panel A; or by using Affinity chromatography to enrich the protein-carbonyl adducts, subsequently analyzed by MS – Panel B. Depending on the depth of the analysis, the techniques might be used individually or in combination.

With the DNPH derivatization of PCO groups, the number of modification sites identified is limited when using ESI-MS. This could be attributed to the low ESI efficiency of DNPH-derivatized peptide ionization in positive mode. The two nitro groups present on the benzene ring of DNPH have a strong electron withdrawing effect which may diminish the stability of the protonated peptide. Detection of the nanomolar range of aldehyde-DNPH derivatives can be achieved in negative mode by using the atmospheric pressure chemical ionization source (APCI) (Figure 4. – panel A) [26]. More favourable ionization behaviours of DNPH-labelled carbonylated peptides arise in negative ion mode ESI which has the advantage that the DNPH moiety is useful for the easy identification of the PCO site [27].

Non-gel proteomics approaches have been widely applied in the study of protein carbonylation; a key step in these approaches is the incorporation of enrichment procedures for PCO which is necessary since the average abundance of carbonylated proteins has been reported as ~0.2% in human plasma. Through the elimination of the majority of unmodified proteins the chemical interference in the LC and MS dimensions can be minimized increasing the identification of PCO modified proteins. One of the most common methods uses avidin-affinity chromatography to enrich biotin-hydrazide derivatized carbonylated peptides and proteins (Figure 4. – panel B). Derivatization with biotin hydrazide also results in the formation of a Schiff base which can be reduced to a more stable C-N bond. Mirzaei and co-workers have successfully applied biotin/avidin affinity chromatography proteomics to study PCOs in *in vitro* metal-catalyzed oxidation models: yeast, rat and human plasma tissues, and diabetic rats [28-30]. A similar tag uses a biotin-based hydrazide instead of DNPH, the N-(Aminooxyacetyl)-N'-biotinylhydrazine, also called Aldehyde reactive probe (ARP) [31-33]. The biotin-derivatized protein can be visualized by standard detection methods such as Western blot using horseradish peroxidase-conjugated streptavidin (HRP-streptavidin) or enriched using streptavidin or avidin-affinity chromatography. This ARP however undergoes substantial fragmentation in MS/MS experiments, decreasing peptide confidence after database searching due to the complexity of the spectra. The development of an algorithm which incorporates ARP fragment ions and neutral loss into the database searching has enhanced PCO identification with ARPs.

In addition to biotin/avidin-based approaches, other enrichment reagents such as Girard's P and Oxidation-specific Element-Coded Affinity Tags for PCO have been reported in literature [30]. Some reagents are able to directly increase the ionization efficiency of PCO prior to MS analysis. An example is the dansylhydrazide which enhances efficiency of ionization due to its secondary nitrogens. Dansylhydrazide generates reproducible fragmentation patterns which allow MS^3 scans to be employed for localization of PCO sites in proteins [34].

4.3.2 Glycation (Early and Advanced Glycation end Products)

Glycation is a spontaneous nePTM of proteins that involves the non-enzymatic covalent attachment of a reducing sugar or sugar derivative to a protein. Glycation adducts are classified into two groups: early-stage glycation adducts and advanced glycation end products (AGEs) [35]. Carbonyl groups of sugars react with the free amino groups of amino acids (mostly occuring at lysine residue side chains) to form a Schiff base that rapidly undergoes molecular rearrangement to form a stable ketoamine called an Amadori product (Figure 5.). The Amadori products, like fructosamines, are typical early-stage glycation adducts [4, 35].

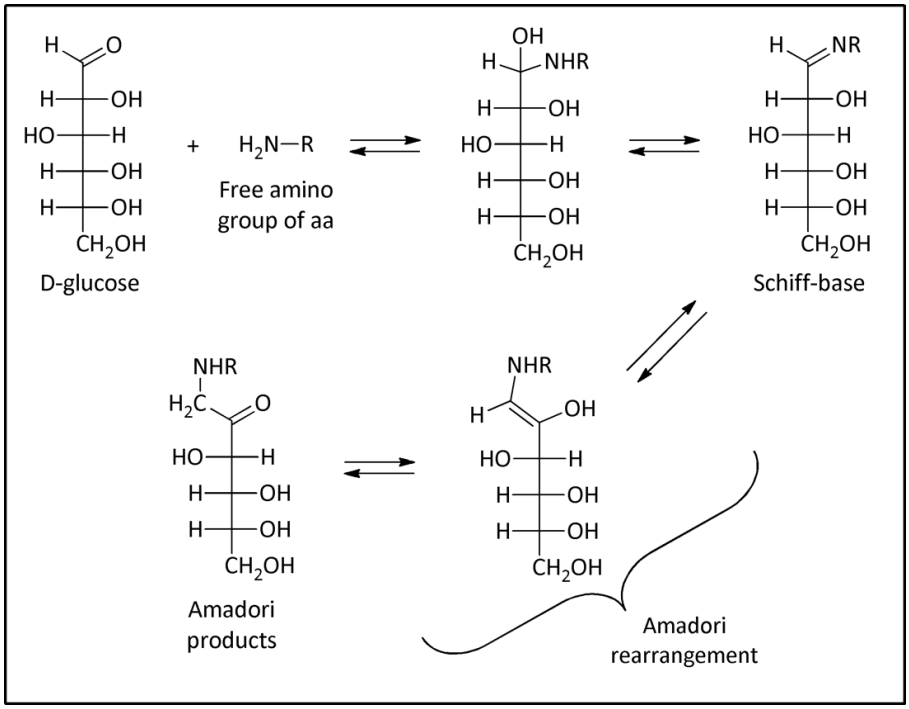

Figure 5. Early-stage glycation adducts and advanced glycation end products (AGEs) mainly derived from the glycation pathway. Carbonyl groups of sugars react with the free amino groups of amino acids (mostly occuring at lysine residue side chains) to form a Schiff base that rapidly undergoes molecular rearrangement to form a stable ketoamine called an Amadori product.

For the measurement of fructosamines in serum samples, a colorimetric technique has been reported. It exploits the ability of ketoamines, such as fructosamines, to reduce, under alkaline conditions, the nitro-blue tetrazolium chloride (NBT) salt. The colour developed is assayed at absorbance of 520 nm and is directly proportional to the serum fructosamine concentration [36, 37]. Another technique consisting of the HPLC measurement of furosine, which results from the degradation of fructosamines during the acid hydrolysis of proteins, can also provide valuable information [2, 4].

The identification of the first glycated form of Hemoglobin (Hb) dates to the late 1950s and to this day glycated hemoglobin evaluation is used in routine practice in monitoring diabetic patients and provides a retrospective indication of the quality of glycemic level [4, 35, 38, 39]. Hb A1c is the most abundant glycated species of hemoglobin in human blood and corresponds to the binding of glucose on the N-terminal valine residue of the hemoglobin β chain. Hb A1c may be specifically evaluated by ion exchange chromatography (minicolumns, low-pressure liquid chromatography, HPLC) or by immunological assays [4, 39]. Electrophoretic and isoelectrofocusing methods have been described, but have not provided enough sensitivity or resolution for clinical purposes [40]. Other methods have been proposed to evaluate total glycated hemoglobin, by affinity-based chromatography on boronic acid, using minicolumns or HPLC [41]. In the absence of any internationally agreed reference method for the quantification of glucose adducts on hemoglobin chains, in 2002 the International Federation of Clinical Chemistry and Laboratory Medicine (IFCC) Working Group reported a reference method for Hb A1c measurement [42]. Using this method, Hb is cleaved into peptides by enzymatic digestion with endoproteinase Glu-C. Then the obtained glycated and non-glycated N-terminal hexapeptides of the β chain are separated and quantified by HPLC coupled to ESI mass spectrometry. Alternatively a two-dimensional approach consisting of HPLC and capillary electrophoresis with UV-detection could be used. Hb A1c is measured as the ratio between the glycated and non-glycated hexapeptides [4, 42].

In later stage reactions of glycation, Schiff base and fructosamine adducts are further processed by an irreversible set of reactions including dehydratation, cyclization, fragmentation and oxidation to generate many stable end-stage adducts named AGEs [4, 35, 36]. The terminology used to classify end products is sometimes unsuitable, since the reactions that involve glycation, oxidation and carbonylation are often intertwined [4].

It is known that some AGEs are fluorescent compounds, therefore total AGEs can be determined measuring AGE-fluorescence. Three different ranges of AGE-fluorescence were established (excitation/emission: 330/395, 365/440, 485/530 nm) [37, 43]. However, not all AGEs are fluorescent molecules, for example carboxy-methyl lysine (CML), a member of the group, does not fluoresce [43]. Moreover the sensitivity is low and it is not possible to detect specific modifications. Nevertheless, a device called AGE Reader was recently developed by DiagnOptics B.V. (Groningen, The Netherlands). The AGE Reader uses ultra-violet light to excite auto fluorescence of AGEs in human skin tissue. This method for the quantitation of AGEs actually finds an increasing propagation in the diagnosis and assessment of complications in diseases since it is fast and non-invasive [43].

Common analytical methods for the quantitative determination of AGEs are based on ELISA or Western blot, however the existence of commercially available antibodies is limited for example to total AGEs or to specific adducts such as CML or carboxy ethyl lysine (CEL) [36, 43]. Detected protein adducts using the canonical immuno-techniques could be easily identified by the above described MS protein sequencing (bottom-up) approach. Proteomics studies provide a powerful approach to the identification of proteins susceptible to glycation in complex protein mixtures and also the identification of the lysine and arginine residues within proteins particularly susceptible to glycation.

With a view to the enrichment of AGEs, all the hitherto mentioned techniques have some limitations. In fact, even though the keto/aldehydic groups are characteristic of some AGEs, not all AGEs contain free carbonyl groups. Thus, the derivatization/enrichment strategy allows the identification of only a small fraction of AGEs. Moreover carbonyl groups are characterized by instability since they could readily undergo Schiff base formation with proximate lysine residues, even when stored at -80°C [18].

Based on such premises, recently a novel function based enrichment strategy that enables the capture of the modified proteins on the basis of their biological interactions rather than their structure has been developed. For the development of this strategy use has been made of the interaction of AGEs with the receptor for advanced glycation end products (RAGE). In addition to the damaging effects that AGEs induce, they also activate RAGE resulting in the induction of pro-inflammatory and pro-fibrotic responses. RAGE is a transmembrane glycoprotein and its extracellular portion contains one V-type (V) and two consecutive C-type Ig-like domains (C1-C2). The V and C1 domains are involved in ligand binding and form a single integrated unit connected to the C2 domain through a flexible linker. RAGE has a short cytoplasmic tail that is devoid of any enzymatic activity but is essential for the intracellular signal transduction activated by the binding with the ligands. The enrichment strategy we set up is based on RAGE affinity chromatography. A recombinant form of the RAGE domain involved in ligand binding (VC1) was expressed and purified from the yeast *Pichia pastoris*, a suitable host for the production of soluble and stable forms of human RAGE (Figure 6. – panel A) [59]. The recombinant protein was designed with a C-terminal tandem tag: one tag to facilitate the purification procedure, the other for the immobilization of the recombinant protein on an insoluble matrix. The method (pull-down) consisted of (i) attaching the VC1 domain to magnetic beads exploiting the C-terminal tag (Figure 6. – panel B), (ii) isolating proteins that are retained by their specific binding to VC1 (Figure 6. – panel C), (iii) protease digestion of the retained polypeptides, (iv) analysis by LC-MS/MS in order to identify the protein and the type and site of AGEs modification (Figure 6. – panel D). The method

was firstly validated by using RCS modified human serum albumin (HSA). The adducts isolated by pull-down experiments were fully elucidated by LC-ESI-MS. Selectivity was tested by spiking AGEs-HSA in sera. Moreover, this method also led to the isolation of Advanced Lipoxidation end Products (ALEs) [60].

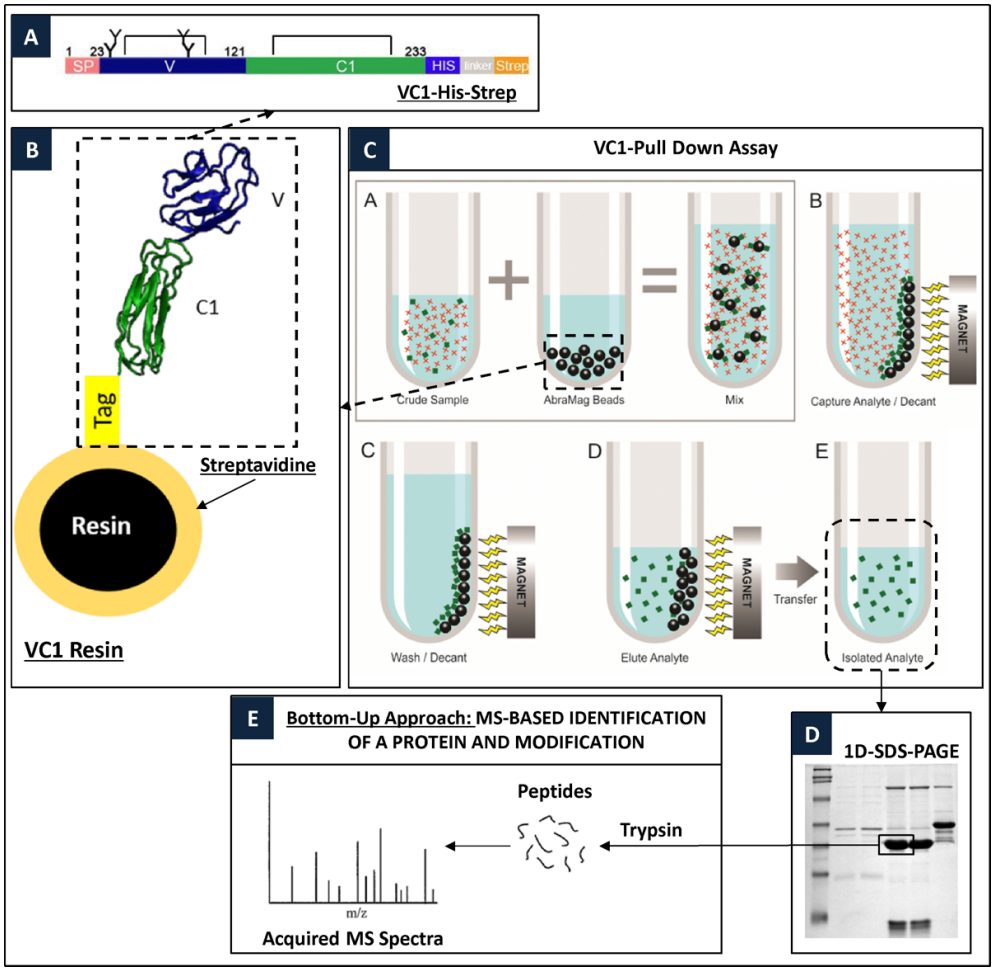

Figure 6. Schematic representation of the pull-down assay strategy.

4.3.3 Deamidation, isomerization or racemization

Proteins and peptides are susceptible, both *in vivo* and *in vitro* (e.g. during storage of proteins), to a variety of chemical modifications that can affect their structure and biological functions, and one of the most frequent modifications is the deamidation of asparagine residues , a spontaneous non-enzymatic reaction [44]. Usually this reaction is associated with protein degradation [45-48], but recently deamidation has been linked to triggering apoptosis in cancer cells [49-51] as well as other regulatory functions [52-55].

The rates of deamidation depend on pH, temperature and protein structure. Therefore, it is difficult to distinguish natural protein deamidation from artefactual deamidation occurring during sample preparation [4, 56, 57]. Under physiological conditions, deamidation proceeds through formation of a five-membered succinimide ring intermediate by the condensation of the side-chain amide group of asparagine with the carbonyl group of the following amino acid. A similar nucleophilic attack on the Asp side chain leads to the dehydration of the aspartic acid (Figure 7.).

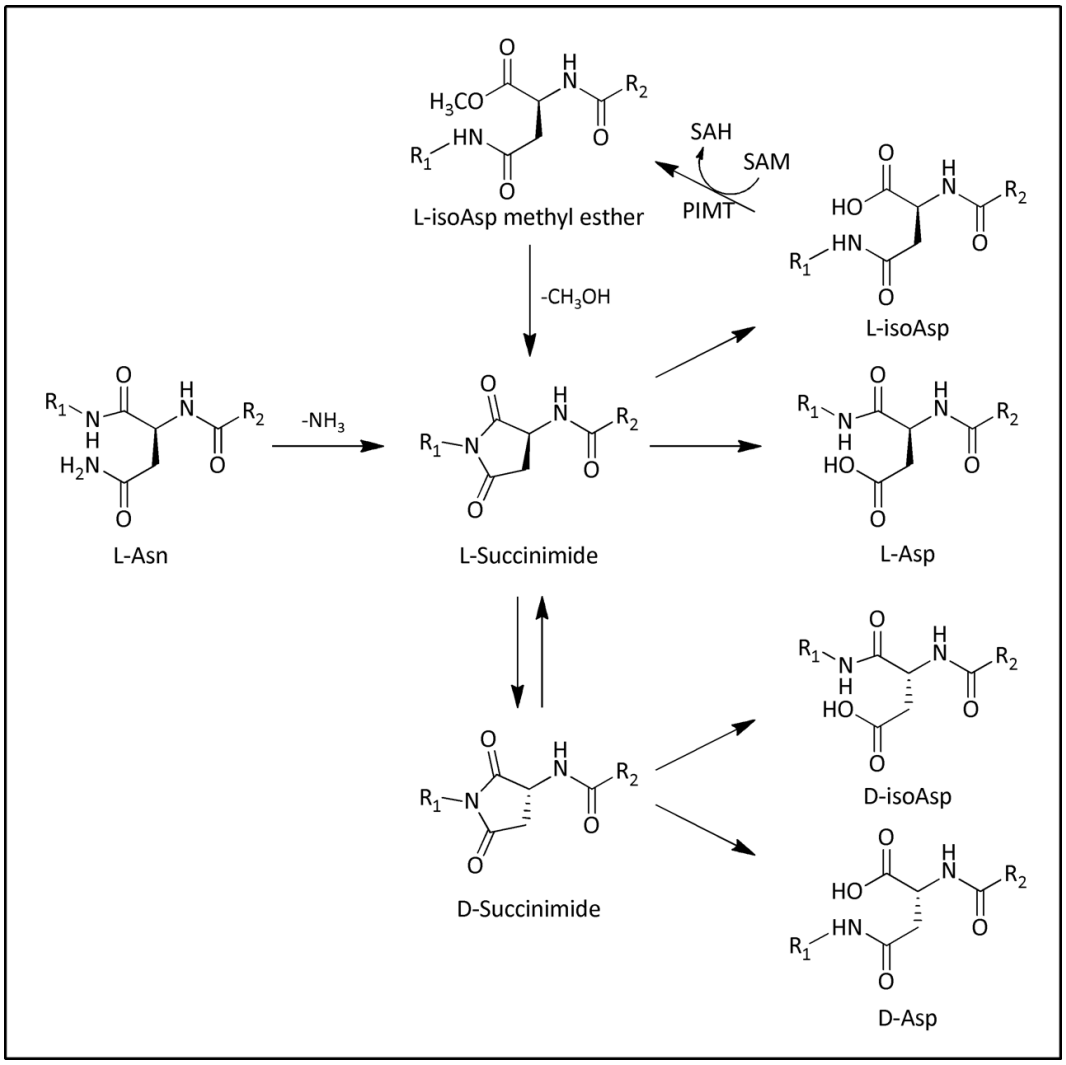

Figure 7. Deamidation proceeds through the formation of a five-membered succinimide ring intermediate by the condensation of the side-chain amide group of asparagine with the carbonyl group of the following amino acid. The L-succinimidyl intermediate then undergoes a relatively rapid hydrolysis at either the α- or β-carbonyl group to generate L-isoaspartate (L-iso-Asp) and normal L-aspartate (L-Asp). The free α-carbonyl group of L-iso-Asp can be methylated by the enzyme L-isoaspartyl O-methyltransferase (PIMT) with S-adenosylmethionine (SAM) as the methyl donor

which is transformed to S-adenosylhomocysteine (SAH). Enzymatic methylation is usually followed by spontaneous ester hydrolysis leads to reformation of the L-succinimide intermediate. The formation of L-succinimide can also be accompanied by enhanced racemization at the α-carbon to generate a mixture of D-succinimidyl, D-aspartyl, and D-isoaspartyl compounds.

The L-succinimidyl intermediate then undergoes a relatively rapid hydrolysis at either the α- or β-carbonyl group to generate L-isoaspartate (L-iso-Asp) and normal L-aspartate (L-Asp) in a ratio of approximately 3 : 1 [44, 58]. The formation of L-succinimide can also be accompanied by enhanced racemization at the α-carbon to generate a mixture of D-succinimidyl, D-aspartyl, and D-isoaspartyl compounds (Figure 7.). The final products of asparagine deamidation are a mixture of these acidic isomers of aspartic acid and isoaspartic acid, with the same mass shift.

Among the products of non-enzymatic reaction, L-iso-Asp is typically the predominant form, and leads to a significant change in the backbone structure of the protein, which is often accompanied by a loss of biological activity [59].

The free α-carbonyl group of L-iso-Asp can be methylated by the enzyme L-isoaspartyl O-methyltransferase (PIMT) with S-adenosylmethionine (SAM) as the methyl donor which is transformed to S-adenosylhomocysteine (SAH). Enzymatic methylation followed by spontaneous ester hydrolysis leads to reformation of the L-succinimide intermediate, which is again hydrolyzed to a mixture of L-Asp and L-iso-Asp. The overall result of this “repair” process is that a certain percentage (15%–25%) of the original L-iso-Asp population is converted back to L-Asp. D-Asp residues undergo similar enzymatic repair.

Just as asparagine deamidates under acidic conditions so too does glutamine, proceeding via a glutarimide intermediate at neutral or alkaline conditions. The deamidation rate of glutamine is slower in comparison with asparagine. The final products of glutamine deamidation are α- and γ-glutamic acid.

In general, deamidation introduces an additional negative charge to the protein and can be detected by charge-sensitive separation methods such as isoelettrofocusing, 2D electrophoresis or ion-exchange chromatography, possibly in combination with mass spectrometry [59-61].

The use of specific antibodies against iso-Asp and D-Asp have only recently been reported [62-65] and have not as yet been commercialized. Global analysis of iso-Asp residue content in the protein sample is usually performed by the ISOQUANT detection kit (Promega, Madison, WI) as follows. The enzyme Protein Isoaspartyl Methyltransferase (PIMT) is used to specifically detect the presence of isoaspartic acid residues in a target protein. PIMT catalyzes the transfer of a methyl group from S-adenosyl-L-methionine (SAM) to isoaspartic acid at the a-carboxyl position,

generating S-adenosyl homocysteine (SAH) which can be detected by reversed phase HPLC and its quantity estimated by comparing the chromatographic peak area with a standard curve [66-68]. ISOQUANT and similar global approaches require at least picomolar quantities of the target, cannot identify proteins where this process occurs and do not reveal the protein site of the deamidation/isomerization. Therefore, there is a growing interest in the use of **mass spectrometry**, which is a much more sensitive technique (femtomoles to attomoles) that produces site- and molecule-specific information.

The general procedure starts from the separation on a SDS-PAGE or 2D gel of the crude protein; the band or spot density in the stained gel serves as a semi-quantitative measure of the relative abundances of different isoforms. Electrophoresis-separated isoforms are then subjected to enzymatic digestion, typically with trypsin. The tryptic mixture is either directly analyzed with MALDI TOF mass spectrometry, or additionally separated by reverse-phase HPLC and ionized by on-line electrospray ionization (ESI).

Mass spectrometric identification of deamidated peptides is relatively straightforward, as deamidation adds to the mass of intact molecule +0.984 Da (the mass difference between –OH and –NH2 groups).

Deamidation at the identified sites was found to be slow for the intact, folded protein, and accelerated for partially unfolded molecules at degradation conditions. Deamidation was also enhanced after reduction, alkylation, and tryptic digestion, i.e. the typical sample preparation procedures used in proteomics, which raises the risk of overestimating the quantification of deamidation at proteome level. Recently the use of a short, modified digestion protocol that does not induce measureable deamidation *in vivo* has been suggested [69]. Alternatively, *in vitro* and *in vivo* occurring deamidation processes can be distinguished by using $H_2{}^{18}O$ instead of ordinary water for protein digestion and sample storage [70]. Deamidation that occurs during protein digestion and storage will then give peptides 2Da heavier than those undergoing *in vivo* deamidation.

Protein digestion and associated *in vitro* deamidation can be avoided altogether if the top-down approach is applied, involving tandem mass spectrometry of individual protein molecules having the same or similar mass. Because of technical and other limitations, the top-down approach works best for molecules below 20–25 kDa, and thus, remains relatively low-throughput and is limited in terms of protein molecular mass and sample amount.

Unlike Asn deamidation, Asp isomerization analysis presents a significant challenge for mass spectrometry, as isomerization by definition does not change the elemental composition and thus is “silent” in the mass spectrometric sense. Fortunately, structural changes induced by

isomerization usually change the retention time of the peptide in reversed-phase liquid chromatography, which thus permits isomer separation; the Asp isoforms were assigned based on the known order of peptide elution at given HPLC conditions (iso-Asp, L-Asp, D-Asp and succinimide).

However, in high-throughput proteomics experiments the presence of a peak at a certain mass is not specific enough for reliable iso-Asp identification because of the noise present in MS/MS spectra as well as the probability of accidental match with unrelated ionic species. Identification of the iso-Asp sites by mass spectrometry requires MS/MS method specific to iso-Asp. Lehmann et al. [71] have noticed that replacement of L-Asp by L-iso-Asp resulted in shifts in the b/y intensity ratio of complementary b and y ions generated by cleavages N- and C-terminal to the iso-Asp, with the Asp immonium ion abundance at m/z 88 also decreased. However, these authors conceded that the b/y ion intensity ratio and the immonium ion intensity vary considerably depending on the peptide sequence and instrumental settings. Thus the abundance changes are difficult to use in practice for detection of iso-Asp.

A set of iso-Asp specific fragments in electron capture dissociation (ECD) of synthetic peptides were found to be a more reliable criterion [72]. Besides the conventional N-Cα bond cleavage in ECD that leads to complementary c and z fragments, a research group detected a diagnostic cleavage giving c_n. + 58.0054 ($C_2H_2O_2$) and z_{l-n} − 56.9976 (C_2HO_2), where n is the position of the isoaspartyl residue and l is the peptide length. These diagnostic fragments are usually less abundant than the adjacent conventional c_n and z_{l-n} species. The same fragments are observed with the electron transfer dissociation (ETD [73]) technique which is similar to ECD but employs radical anions instead of free electrons. Elsewhere, it was found that higher-energy collisional dissociation (HCD [74]) of both positive as well as negative ions also fails in this task. This means that ECD/ETD are the only MS/MS technologies applied to electrospray-produced ions that provide reliable diagnostic ions for iso-Asp detection.

The above approach to iso-Asp analysis provides high throughput in respect to peptide candidate detection but requires time-consuming validation of the detected iso-Asp candidates. Another limitation of the current approach is the relatively low speed and sensitivity of ECD/ETD when high-resolution mass analyzers are used [75].

4.3.4 Methionine and cysteine oxidation

Oxidation is involved not only in the formation of AGEs, but also in protein aging where proteins are directly altered by reactive oxygen species (ROS). Among ROS modifications methionine and cysteine oxidation are the most studied.

Methionine (Met) has a sulphur-containing side chain that is susceptible to oxidation; methionine is usually oxidized yielding to methionine sulfoxide and methionine sulfone. Under physiological conditions, sulfoxide formation can be enzymatically reversed by the action of specific reductases including methionine sulfoxide reductase (MSRA) [76]. The Met oxidation-reduction process has been found to play a key role in the activation-deactivation cycle of several crucial signalling proteins and the maintenance of homeostatic balance in physiological systems [77, 78]. Apart from its regulation effect, Met oxidation in proteins plays a prominent role in aging and age-related degenerative diseases [20, 21, 79, 80] resulting in the loss of protein function [59, 81, 82].

Despite its significance in cellular functions and implications for various pathological conditions, Met oxidation has been largely overlooked in protein structural characterization. This is partly due to the fact that Met oxidation can be artefactually introduced during sample preparation, purification and analysis [83-85], presenting another degree of complexity in characterization of Met oxidation in proteins.

For the detection of methionine oxidative products, anti-methionine sulfoxide antibodies against an oxidized methionine-rich zein protein (MetO-DZS18) have been obtained, but their specificity is questionable [86].

Several mass spectrometry (MS)-based methods have recently been introduced to characterize Met(O) in proteins and peptides, overcoming the limitations of the conventional protein analysis methods, such as Edman degradation, gel electrophoresis and amino acid analysis, where methionine sulfoxide residues are reduced, and detected as methionines [87-89].

An advanced peptide-based method to map *in vivo* oxidized methionines and quantify their degree of oxidation has been described and is based on combined fractional diagonal chromatography (COFRADIC). With COFRADIC it is possible to isolate a specific set of peptides by altering a peptide functional group or the side-chain of targeted amino acids in between consecutive and identical reverse phase-HPLC. According to this method it is possible to separate the methionine sulfoxide containing peptides taking advantage of the hydrophobic shift introduced in the peptides due to enzymatic reduction of methionine sulfoxides with methionine sulfoxide reductase. The shifted peptides are collected for further LC-MS/MS analysis [59].

Among the MS-based techniques, tandem MS (MS/MS) [90] is particularly attractive; the peptide sequence and the position of Met(O) can be directly determined through the gas-phase fragmentation [14], usually through collision-induced dissociation (CID) (a popular technique currently implemented on most commercial MS/MS instruments). A distinct fragmentation pathway in CID of Met(O)-containing peptides is the neutral loss of 64 Da from the precursor and/or product ions [83, 84]. The characteristic neutral loss of 64 Da corresponds to the ejection of

methanesulfenic acid (CH_3SOH, 64 Da) from the side chain of Met(O). The loss of 64 Da is unique, in proteins and peptides, to Met(O), and is particularly useful to differentiate between Met(O) and phenylalanine (both residues have the same nominal mass of 147 Da) in MS/MS peptide sequencing (Figure 8.). However, this low-energy pathway can further inhibit the backbone sequence fragmentation by CID, especially for larger polypeptides. In fact, the complete MS/MS characterization of Met(O) using CID has so far been limited to small peptides, such as those from enzymatic digestion [83, 84].

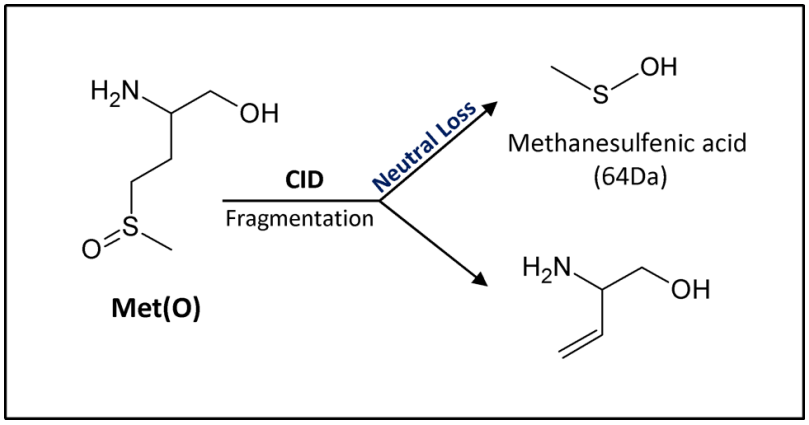

Figure 8. The neutral loss of 64 Da, due to the ejection of methanesulfenic acid (CH_3SOH, 64 Da) from the side chain of Met(O), is unique and particularly useful to differentiate between Met(O) and phenylalanine (same nominal mass of 147 Da) in peptide mass fingerprint analysis.

Electron capture dissociation (ECD) [91-93] has recently emerged as a powerful alternative in MS/MS of multiply charged proteins and peptides generated by electrospray ionization (ESI) [94] using Fourier transform ion cyclotron resonance (FTICR) mass spectrometry. ECD, a technique based on partial neutralization of multiply-protonated ions with electrons, typically renders extensive inter-residue backbone cleavage to yield *c* and *z* fragment ions, in contrast to the *b* and *y* fragment ions produced from the amide bond cleavage by conventional energetic fragmentation methods, including CID. Furthermore, ECD is a nonergodic fragmentation technique, i.e., a feature exemplified by the ability of ECD to preserve the labile side chain modification groups on the peptide backbone fragments [95-98], in contrast to CID and other conventional fragmentation techniques which typically eject the labile modifications first, resulting in the case of Met(O) in the loss of CH_3SOH.

ECD and CAD are complementary fragmentation techniques that provide “easy-to-interpret” spectra for rapid identification and localization of the Met(O) residues in peptides. The characteristic elimination of CH_3SOH (64 Da) in CID serves as a signature tag for the presence of Met(O) in peptides. ECD then offers extensive backbone fragmentation without detaching the

labile side chain, to allow for the direct localization of the Met(O) residues. The accurate mass measurement of FTICR/MS can also assist in the unequivocal determination of Phe and Met(O), as these two residues share the same nominal mass (147 Da) but differ in exact mass by 0.033 Da (Phe, 147.0684; Met(O), 147.0354).

Cysteine residues have become the subject of intensifying research interest in redox-proteomics because of their redox-reactive thiol side chain. Certain reactive cysteine residues can function as redox-switches, which sense changes in the local redox-environment by flipping between the reduced and oxidized states, in response to fluctuations in the various ROS. Protein cysteine residues exist not only as free thiols or disulfides, that help maintain the 3D structure of proteins, but depending on their local concentration, Cys can react with ROS to form one of several reversible (S-glutathionylation, sulfenic acid, inter- and intramolecular disulfide bonds and S-sulfhydration) or irreversible (sulfininc or sulfonic acid) modifications (Figure 9.) [99, 100]. Due to the variety, and in some cases, unstable nature of the different Cys modifications, several techniques have been developed for their investigation.

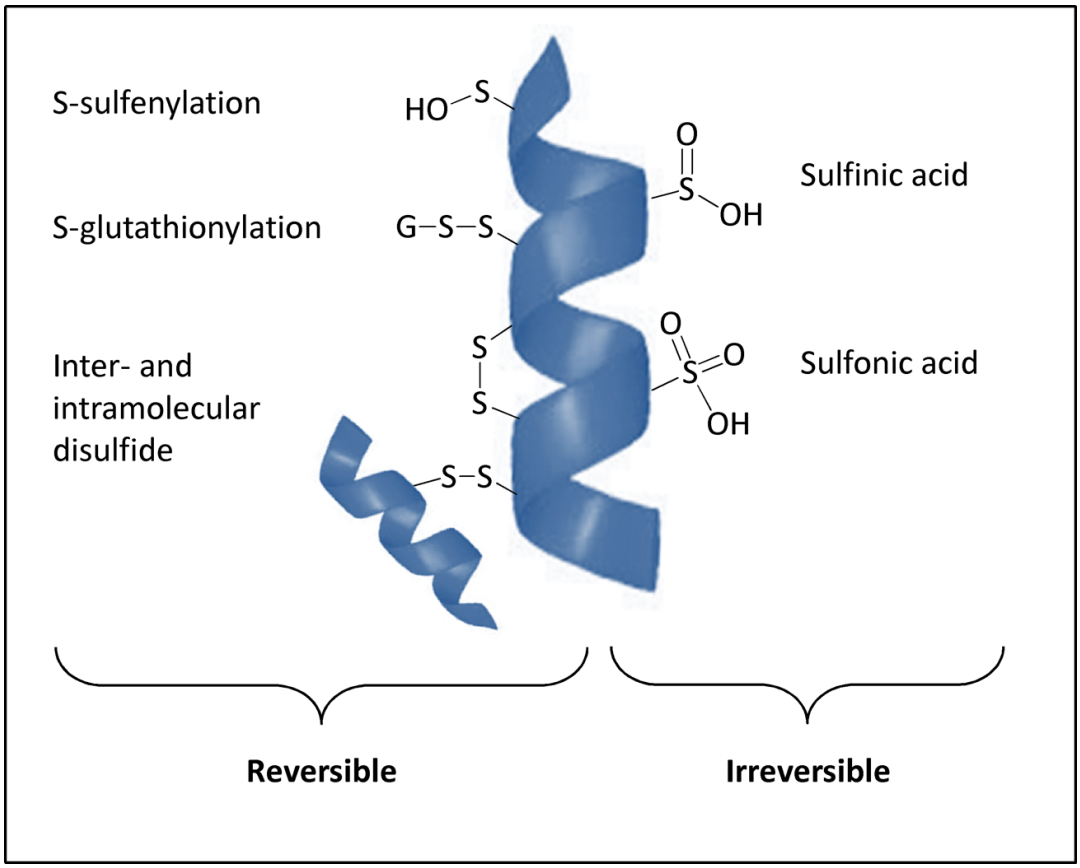

Figure 9. Common oxidative cysteine modifications: physiologically reversible and irreversible oxidative post-translational modifications that can occur to the thiol side chain of a Cys.

The formation of sulphenic acid may be reversed, for example by glutathione (GSH), while the formation of the sulphinic or sulphonic acids is usually irreversible [59]. The easiest method available for the detection of disulfide bonds is electrophoretic separation under first non-reducing and then reducing conditions. Some cysteine modifications can also be detected using specific antibodies against S-glutathionylated proteins, sulfenic or sulfonic acid modifications. However, their use has been limited to targeting and assaying the modification status of single proteins [59]. Another approach for the detection of oxidized cysteine residues takes advantage of the fact that the reversibly oxidized thiols can be labelled. First the unmodified cysteine residues are blocked using thiol-specific reagents such as maleimides, iodoacetic acid or iodoacetamide, then oxidized thiols are reduced using specific agents for the modification of interest. The newly exposed thiols are labelled with fluorescent dyes such as Cy3 and Cy5, which have a maleimide group that forms a thioether bond with the free thiols of cysteines. Comparison of gels stained with these dyes and a total protein staining (for example by using Sypro Ruby) provides information about cysteine modifications [101]. Alternatively, reduced cysteine residues can be labelled with a thiol-reactive biotin. This method could be used for both detection and/or enrichment using anti-biotin immunoblotting and/or streptavidin affinity chromatography.

The identification of individual modified Cys residues and of the specific redox-modification have been achieved using proteomics techniques, often by coupling enrichment strategies (biotin-streptavidin enrichment-based methods) with high throughput mass spectrometry (MS) analysis [102].

S-Sulfenylation - Sulfenylation, also known as sulfenic acid modifications, are reversible, labile moieties that have been challenging to study with traditional techniques. Sulfenic acid is the first oxidative form generated by hydrogen peroxide oxidation of a thiolate forming an R-SOH group [103]. Proteomics analysis of sulfenyl has been performed using a few different methodologies.

A biotin switch style assay which used m-arsenite in place of ascorbate in order to specifically reduce sulfenic acids has been developed [104]. The method validation demonstrated the progressive loss of sulfenated signal with increased peroxide treatment, indicating that m-arsenite is specific to sulfenic acid and not the further oxidative forms [105].

More commonly, sulfenic acid modifications have been targeted using dimedone chemistry. Dimedone-based probes, conjugated with biotin or azide, have been reported to stably and specifically label sulfenylated thiols [106, 107]. This reaction has been shown to directly target SOH groups and does not require the blocking step or specific reducing agent necessary for biotin switch style approaches. Once labelled, the biotin group or, in the case of azide conjugated probes, a ‘click’ chemistry addition of a biotin moiety, can be used for enrichment and detection.

Recently, the sulfenic acid ligation reaction using aryl-nitroso compounds has been reported; the approach reacts rapidly in aqueous conditions and is highly selective for sulfenic acid modifications, including being orthogonal to free cysteine-thiols. The 2-nitrosobenzoic ester derivative they examined is more stable and specific at neutral pH than the aryl diazonium salts [108]. With further development, this chemistry has great promise for the detection of sulfenic acid modifications in complex biological systems.

Disulfide bonds - Cys can also be modified through reaction with another available Cys forming a protein disulfide bond. The introduction of new disulfide interactions has the potential to significantly alter protein conformation or association, affecting function. Analysis of these modifications presents a particular problem: the relatively large number of static disulfides can make isolation/detection of the smaller pool of dynamic bonds difficult. Several strategies have been utilized to detect and identify regulatory disulfides.

One of the longest standing and most successful techniques for examining intermolecular disulfide bonds is the direct identification of disulfide bonded peptides by MS. This is challenging but it offers the most conclusive evidence of a disulfide interaction. In the majority of MS studies, Cys are reduced and alkylated prior to analysis removing any possibility of disulfide observation. Disulfide linked or looped peptides can be difficult to ionize and have been found to be more resistant to fragmentation in collision induced dissociation (CID) [109, 110]. Recently, two approaches have been presented which attempt to improve this situation. Electrospray ionization (ESI) coupled with CID can produce an asymmetric cleavage of the disulfide bond resulting in Cys with a disulfohydral and dehydroalanine residue across the cleavage site; representing signature masses which can be used for unambiguous identification of the residues involved [111]. In an alternative approach, disulfide bonds are cleaved electrolytically immediately prior to analysis [112]. The disulfide bonded peptides can be recognized by the loss of ionization energy when compared to a control sample. Unfortunately, neither of these approaches is currently suitable for complex samples or high throughput analysis; however, software is being developed that will aid in this endeavour [112].

It is important to note that in dealing with disulfide bonds or other thiol-modifications, many MS protocols perform trypsin digestion in ammonium bicarbonate at pH 8.5. This may be above the pKa of many Cys causing their conversion to more reactive thiolates which can lead to disulfide rearrangement during sample processing. When dealing with cysteine sensitive samples the use of a lower pH buffer, such as ammonium acetate (pH 6.5), is recommend to achieve better disulfide bond fidelity [113].

Sulfinic and Sulfonic Acid - Unlike the previously discussed thiol-modifications, those involving sulfinic and sulfonic acids are biologically irreversible and have generally been regarded as oxidative damage rather than signalling modifications [114]. These modifications arise from the additional oxidation of a sulfenic (RS-OH) to form a sulfinic ($RS-O_2H$) and subsequently a sulfonic group ($RS-O_3H$) [115]. Due to their relative stability compared to the reversible thiol modifications they do not require a replacement strategy and can be detected directly by mass spectrometry; however, this presents its own complications.

Sulfonic acid modified residues can be captured using a polyarginine resin. This technique is based on the coordination between the positive amine groups of the arginine and negatively charged sulfo-groups resulting in a sensitive and specific capture of sulfonated peptides.

Unfortunately, there is currently no specific enrichment chemistry for sulfinic acid modified thiols. In some cases antibodies have been raised against the specific sulfinic and sulfonic acid modified forms of individual proteins such as GAPDH, DJ-1 and Prx [116].

Once these irreversible modifications have been enriched, detecting them by either MALDI or ESI MS can be difficult. The high negative charge associated with the sulfo-group can inhibit ionization by MALDI. To improve detection, groups have included diammonium hydrogencitrate in the matrix which have been found to improve ionization [117]. Additionally, sulfinic and sulfonic acid fragmentation can be difficult to distinguish from the fragmentation patterns of other post-translational modifications necessitating high resolution MS instruments to differentiate them. Both sulfinic acid and hydropersulfide modifications result in a 32 Da mass shift while sulfonic acid and phophorylation can experience an 80 Da neutral loss by CID [118]. The loss of the sulfo-group can make determination of the specific Cys difficult. Electron transfer dissociation (ETD) is preferable to electron capture dissociation (ECD) for sulfonic acid-containing peptide fragmentation since it prevents the neutral loss of the moiety. Also, it has been reported that sodium adducts can stabilize the SO_3 groups, further helping to prevent loss and improving site assignment [119].

S-Glutathionylation - In addition to the reactive oxygen species, there are other potential thiol-reactive agents such as glutathione (GSH) which can result in oxidative post-translational modifications. GSH is a cysteine-containing tripeptide (glutamate-cysteine-glycine) which can be an electron donor for oxidative species and form stable but reversible mixed disulfide bonds with available Cys [120]. The selective addition of a glutathione group to a protein has been found to regulate protein function. Cellular levels of S-glutathionylation increase during oxidative stress and it has been proposed that S-glutathionylation functions as a temporary thiol ‘cap’, protecting critical Cys from potentially damaging irreversible oxidative modifications [121].

S-glutathionlyation modifications have been enriched and identified using a protocol similar to the biotin switch assay previously outlined. For this application, glutaredoxin (Grx), which specifically targets GSH modifications, is used as the specific reducing agent [122-124]. After reduction, newly exposed thiols can be labelled and detected using any of the various thiol-reactive tags discussed above for MS analysis. Compared with other oxidative PTMs, S-glutathionlyation is a relatively stable modification with a unique mass and therefore direct analysis is also possible. S-glutathionylation can be specifically targeted through the use of a biotin-labelled glutathione ester [125-127]. This cell permeable reagent can be loaded into cells and when harvested the proteins and individual Cys that received the biotinylated glutathione can be easily captured with avidin and identified by MS. Another potential option is the use of antibodies to detect and enrich S-glutathionylated proteins. As mentioned above, this modification is sufficiently stable and antibodies raised against a GSH epitope can be used for detection in immuno-based assays (e.g. ELISA, immunohistochemistry, Western blots).

4.3.5 Protein nitration

Reactive nitrogen species (RNS), together with ROS, could act to damage proteins, causing cellular stress [4]. Among RNS-induced modifications, tyrosine and tryptophan nitration and cysteine nitrosylation are the most studied (Figure 10).

Reactive nitrogen species are generated *in vivo* during an inflammatory reaction. As other nePTM-derived products, nitration products could be considered general biomarkers of disease progression.

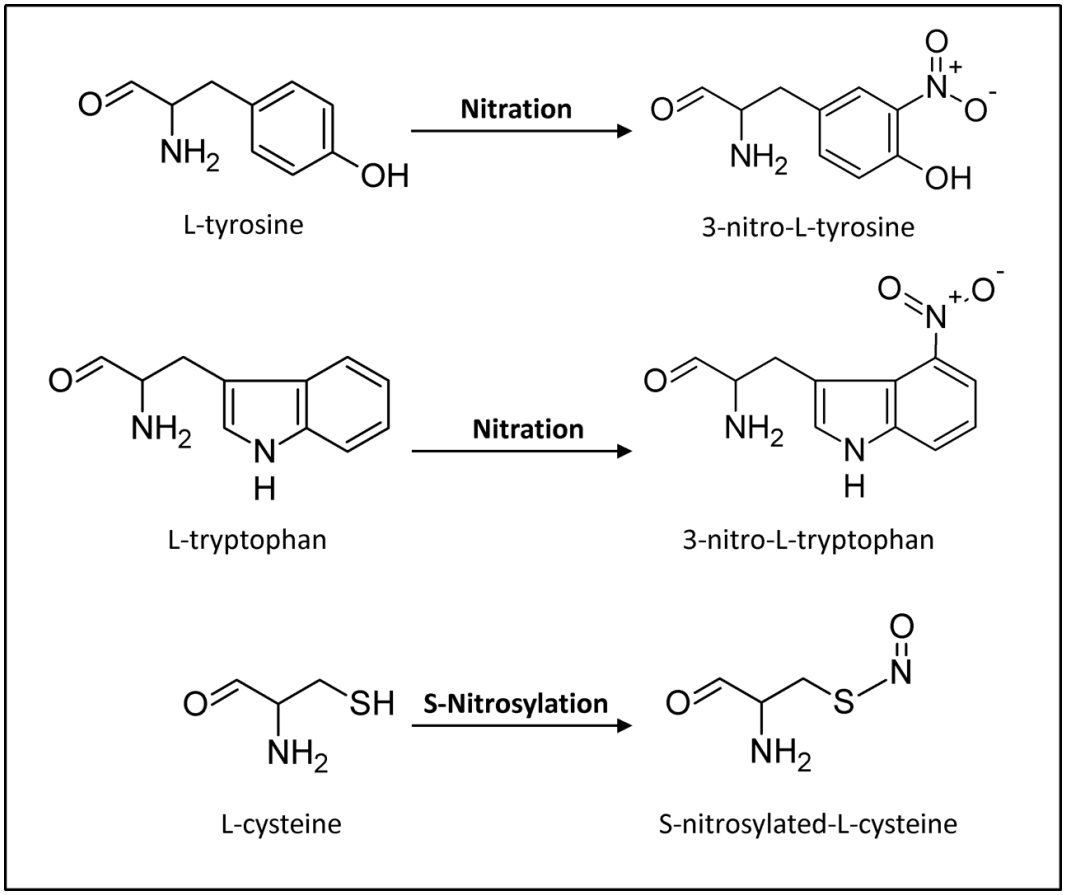

Figure 10. The most studied RNS-induced modifications: tyrosine and tryptophan nitration, and cysteine S-nitrosylation (also known as S-nitrosation).

Tyrosine and Tryptophan nitration - The most common products resulting from protein nitration are nitrotyrosine and nitrotryptophan. Nitrotyrosine is derived from the reaction between tyrosine and peroxynitrite, a strong nitrating agent [59, 60]. Nitrotyrosine has an absorption peak at 280 nm as does tyrosine, but nitrotyrosine in acidic solutions presents an additional peak at 357 nm and in basic solutions at 430 nm. Thus, nitrotyrosine can be traced by UV–Vis photometry, but only in samples characterized by low complexity [128]. Regarding nitrotryptophan, since tryptophan exhibits the strongest fluorescence with an excitation maximum at 280 nm and an emission maximum between 305 nm and 355 nm, nitrotryptophan formation can be detected by fluorescence quenching. Both nitrotyrosine and nitrotryptophan are relatively stable modifications, thus they can be suitably analyzed by immunochemical detection with specific antibodies [34], followed by a peptide mass fingerprinting (PMF) MS analysis [129]. Moreover, exploiting the fact that nitration changes the chemical properties of tyrosine, it is possible to selectively derivatize/enrich the modified proteins. The Biotin/avidin-based method is widely used to enrich

nitrotyrosine (3-NT) – modified proteins or peptides [130]. To label with biotin tags, primary amino groups of nitrated peptides have to be blocked, prior to 3-NT reduction to 3-aminotyrosine. Amine-reactive biotin tags are then incubated with 3-NT reduced peptides and enriched through avidin chromatography. This general strategy can employ different blocking reagents and biotin-based tags, making it a flexible method of protein nitration identification [130].

S-Nitrosylation – S-nitrosylation (SNO), also known as S-nitrosation, results from the covalent addition of a nitrosonium ion (NO+) equivalent to a Cys-thiol. Since SNO-modifications are very labile, they are challenging to study using traditional biochemical techniques.

Typically, two steps are needed to analyze the thiol proteome (S-nitrosylated proteins - PSNO), avoiding the gel-separation step: blocking free thiols and reducing reversibly oxidized thiols [131]. For instance, free thiol groups (SH) can be blocked with a reagent that does not react with nitrosothiols, which are then reduced to thiols with ascorbate and the SH goups thus produced are derivatized with a biotinylated thiol reagent so that derivatized proteins can then be identified by immunoblotting and/or immunoaffinity. Anti-SNO antibodies have recently been developed and can be used in proteomics approaches. On the other hand, once the modified sites are labelled with the stable biotin group, they can be easily detected or enriched by streptavidin affinity chromatography.

Another derivatization method aimed at purifying reversibly oxidized proteins (PROP) uses N-ethylmaleimide (NEM) to block unmodified thiol groups and reduce oxidized thiols to generate new free thiols. Commercially available thiol reactive beads which contain a 2- pyridyl disulfide group can be used to react with newly formed thiols and isolate oxidized proteins. After isolation, the bead-SS- protein disulfide bond can be reduced by dithiothreitol which can be labelled with iodoacetamide. Different blocking reagents can be differentiated by MS, so unmodified and oxidized cysteines can be identified simultaneously. Selecting the best label for an experiment depends on two factors: (i) the need for a permanent mass tag in the MS analysis and (ii) the amenability to relative quantification.

4.4 MS Quantification

Modern protein mass spectrometry techniques are used both to detect nePTMs and to quantify their amounts. This can be done either as a relative measurement defining the difference between two conditions, e.g. diseased versus control sample or as an absolute measurement. Combined measurements of modified and unmodified forms of a particular peptide allow the percentage site occupancy to be defined, i.e. the number of modified molecules in relation to the number of unmodified molecules [3].

In fact, relative quantitation is the most commonly used quantitative strategy in proteomics. This can be achieved using several different techniques, for example the stable isotope labelling by amino acids in cell culture (SILAC) approach [136, 137], various chemical labelling procedures, e.g. trypsin-catalyzed ^{18}O labelling [138], dimethyl labelling [139, 140] or by isobaric labelling, i.e. Isobaric tag for relative and absolute quantitation (iTRAQ) and Tandem mass tag (TMT) (Figure 11. – panel A).

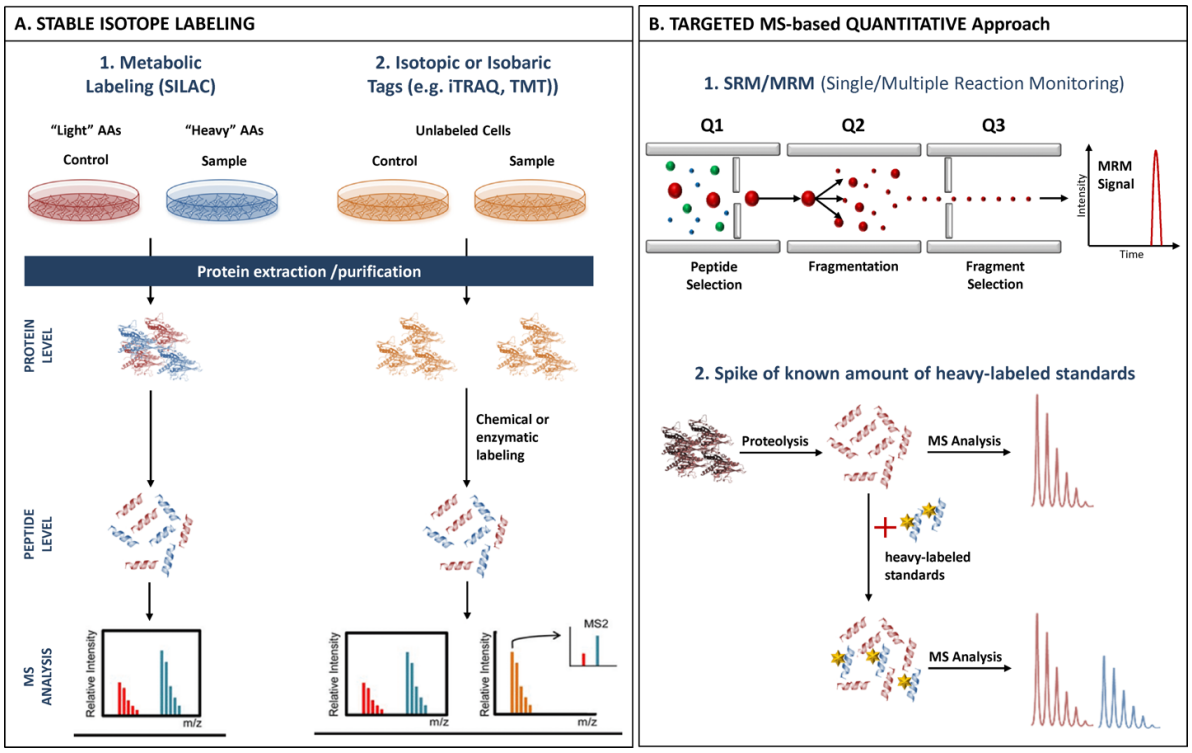

Figure 11. Summary of the main quantitative MS methods. Panel-A. Stable isotope labelling by amino acids in cell culture (SILAC) approach (Panel-A1) or chemical (isotopic or isobaric) labelling procedures, e.g. trypsin-catalyzed 18O labelling, iTRAQ, TMT (Panel-A2); Panel-B. Absolute quantitation of peptides and proteins by B1. Multiple reactions monitoring (MRM) or Single / selected reaction monitoring (SRM) (Panel-B1), or by spiking known amounts of heavy-labelled standards into the sample prior to LC–MS/MS analysis and subsequently comparing the intensities of such standards with the analyte (Panel-B2).

Absolute quantitation of peptides and proteins is used to determine exact amounts of the analyzed samples [3]. Multiple reactions monitoring (MRM) or single or selected reaction monitoring (SRM) is a targeted MS based quantitative approach (Figure 11. – panel B). This technique allows measurement of the quantity of specific peptides of interest, selected according to their m/z and fragment ions generated upon MS–MS fragmentation. The resulting fragment ions confirm the

identity of the precursor and their intensity is proportional to its abundance. This technique is often described as large scale quantitative analysis since it allows for simultaneous quantification of up to 100 proteins in one LC MS-SRM experiment [3].

Alternatively, the absolute quantitation of peptides and proteins is achieved by spiking known amounts of heavy-labelled standards into the sample prior to LC–MS/MS analysis and subsequently comparing the intensities of such standards with the analyte (Figure 11. – panel B) [3]. Unfortunately, most oxidative modifications are not available through commercial sources of synthetic peptides. Nevertheless, SRM using heavy-labelled internal standards has the potential to be a powerful technique for monitoring oxidative modifications [141].

Methods for quantification of simple and small analytes are relatively easily and reliably standardized; it is a much harder task to standardize methods for quantification of complex and large analytes, such as proteins, in physiological fluids or cell/tissue samples. There are many requirements for the standardization of a quantitative method and its quality control, some specific ones for PTMs are listed below:

- Reliable identification of nePTM which are directly correlated to the specific modifying reaction or reactive species which causes it.
- High specificity of intra-molecular nePTM recognition (as little as possible cross-recognition with similar nePTM within the same protein).
- High specificity of inter-molecular nePTM recognition (as little as possible cross-recognition of the same nePTM in different proteins).
- High sensitivity of nePTM recognition (detection of minor modification).
- “Acceptable justification” concerning determination of specific nePTM in relation to the specific (patho)physiological disturbance.
- “High-throughput” method and the equipment to support it.

The implementation of new technologies based on proteomics (mass spectrometry) in clinical laboratories constitutes a decisive step in the development of their use, even though methodological problems, such as the lack of standardization, have to be resolved [4].

Since there are two aspects of PTM protein quantification, each standardization needs to be handled separately. If the idea is to quantify certain PTMs which may be present on many proteins, a common standard possessing the particular PTM may be used. If the idea is to quantify a certain PTM on a specific protein, the standard can be that same protein modified to express that particular PTM. Alternatively, for the second purpose, the specific protein may be isolated and then measured against a common protein standard which has the appropriate PTM. In both cases, the first step is to define suitable standard(s) [3].

It is reasonable to choose a standard from among already existing commercial products rather than of creating new one(s), as manufacturers have probably already solved practical problems concerning continuous production of PTM proteins, their stabilization and storage. Several producers of PTM proteins and also a number of products have been found there way onto the market [3]. Nowadays it is also possible to synthesize peptides with specific PTM commercially. This approach is widely used in the field of phosphoproteomics, but other modifications can also be synthesized. Unfortunately, this does not work very well with protein oxidation for many reasons, e.g. stability and cross reactivity of the products. In the case of carbonyls some pseudo-aldehydes can be used.

Obviously, there is a need for reliable standards, produced and tested under strict conditions and precisely characterized in respect to the type of PTM, the quantity and, if possible, the position within the relevant protein molecule.

The most difficult analytical task dependent on the quality of standardization is detection and accurate quantification of minor proteins in complex (physiological) specimens. Since one specific nePTM protein is most often a minor fraction of the entire population of that protein, the detection range of the nePTM molecule is several fold lower than for the entire protein. As no official standardization in the field of PTM proteins exists except for HbA1c, it is reasonable to start with standardization and quality control in the quantification of specific nePTMs present on all (or many) proteins in a chosen sample, as this is an easier task [3].

Since no method is perfect and no standard will suit all methods equally, some consensus decisions have to be made. The most important concern the assessment of the inaccuracy and uncertainty measurement. If the test is standardized to have very high sensitivity, it may record false negative results. If the test is standardized to have relatively low specificity, it may give false positive results.

Standardization and quality control are instruments to achieve comparability of nePTM protein quantification results over time and space, enabling definition of decision-making criteria that can be used in the assessment of health in relation to ageing and diseases [3].

It is very difficult to obtain inter-laboratory standardization in the analysis of modified proteins. This is due to the existence of a wide variety of instrumental and experimental setups. Over recent years scientists have become aware of this drawback and now acknowledge the necessity of standardization and unification. International initiatives have been undertaken during the last few years. The most prominent is The Human Proteome Organization (HUPO) Proteomics Standard Initiative (PSI). Its major focus is standardization of large scale proteomics experiments to facilitate data validation, accessibility and experimental transparency [142]. As an example of such work it

has become a quality standard to use phosphoRS or similar algorithms to evaluate the probabilities associated with the precise localization of phosphorylation sites in peptide sequences [143].

In summary, the range of mass spectrometry based tools for characterization of protein nePTMs is broad. All of these tools have strong points and limitations. To take full advantage of MS technology experimental aims and all instrumentation at hand should be carefully considered.

References

1. Schreiber, G. and A.E. Keating, *Protein binding specificity versus promiscuity.* Curr Opin Struct Biol, 2011. **21**(1): p. 50-61.
2. Soskić, V., K. Groebe, and A. Schrattenholz, *Nonenzymatic posttranslational protein modifications in ageing.* Exp Gerontol, 2008. **43**(4): p. 247-57.
3. Nedić, O., A. Rogowska-Wrzesinska, and S.I. Rattan, *Standardization and quality control in quantifying non-enzymatic oxidative protein modifications in relation to ageing and disease: Why is it important and why is it hard?* Redox Biol, 2015. **5**: p. 91-100.
4. Jaisson, S. and P. Gillery, *Evaluation of nonenzymatic posttranslational modification-derived products as biomarkers of molecular aging of proteins.* Clin Chem, 2010. **56**(9): p. 1401-12.
5. Rattan, S.I., *Increased molecular damage and heterogeneity as the basis of aging.* Biol Chem, 2008. **389**(3): p. 267-72.
6. Riccardi Sirtori, F., et al., *MS methods to study macromolecule-ligand interaction: Applications in drug discovery.* Methods, 2018. **144**: p. 152-174.
7. Larsen, M.R., et al., *Analysis of posttranslational modifications of proteins by tandem mass spectrometry.* Biotechniques, 2006. **40**(6): p. 790-8.
8. Gregorich, Z.R. and Y. Ge, *Top-down proteomics in health and disease: challenges and opportunities.* Proteomics, 2014. **14**(10): p. 1195-210.
9. Siuti, N. and N.L. Kelleher, *Decoding protein modifications using top-down mass spectrometry.* Nat Methods, 2007. **4**(10): p. 817-21.
10. Chait, B.T. and S.B. Kent, *Weighing naked proteins: practical, high-accuracy mass measurement of peptides and proteins.* Science, 1992. **257**(5078): p. 1885-94.
11. Aebersold, R. and M. Mann, *Mass spectrometry-based proteomics.* Nature, 2003. **422**(6928): p. 198-207.
12. Perkins, D.N., et al., *Probability-based protein identification by searching sequence databases using mass spectrometry data.* Electrophoresis, 1999. **20**(18): p. 3551-67.

13. El Kennani, S., et al., *Proteomic Analysis of Histone Variants and Their PTMs: Strategies and Pitfalls.* Proteomes, 2018. **6**(3).
14. Zhao, Y. and O.N. Jensen, *Modification-specific proteomics: strategies for characterization of post-translational modifications using enrichment techniques.* Proteomics, 2009. **9**(20): p. 4632-41.
15. Wittmann-Liebold, B., H.R. Graack, and T. Pohl, *Two-dimensional gel electrophoresis as tool for proteomics studies in combination with protein identification by mass spectrometry.* Proteomics, 2006. **6**(17): p. 4688-703.
16. Sultana, R., et al., *Detection of carbonylated proteins in two-dimensional sodium dodecyl sulfate polyacrylamide gel electrophoresis separations.* Methods Mol Biol, 2008. **476**: p. 153-63.
17. Butterfield, D.A., T. Reed, and R. Sultana, *Roles of 3-nitrotyrosine- and 4-hydroxynonenal-modified brain proteins in the progression and pathogenesis of Alzheimer's disease.* Free Radic Res, 2011. **45**(1): p. 59-72.
18. Sheehan, D., B. McDonagh, and J.A. Bárcena, *Redox proteomics.* Expert Rev Proteomics, 2010. **7**(1): p. 1-4.
19. Butterfield, D.A., et al., *Mass spectrometry and redox proteomics: applications in disease.* Mass Spectrom Rev, 2014. **33**(4): p. 277-301.
20. Berlett, B.S. and E.R. Stadtman, *Protein oxidation in aging, disease, and oxidative stress.* J Biol Chem, 1997. **272**(33): p. 20313-6.
21. Stadtman, E.R. and B.S. Berlett, *Reactive oxygen-mediated protein oxidation in aging and disease.* Chem Res Toxicol, 1997. **10**(5): p. 485-94.
22. Sultana, F., et al., *Age-related changes in cardio-respiratory responses and muscular performance following an Olympic triathlon in well-trained triathletes.* Eur J Appl Physiol, 2012. **112**(4): p. 1549-56.
23. Dalle-Donne, I., et al., *Protein carbonylation: 2,4-dinitrophenylhydrazine reacts with both aldehydes/ketones and sulfenic acids.* Free Radic Biol Med, 2009. **46**(10): p. 1411-9.
24. Oh-Ishi, M., T. Ueno, and T. Maeda, *Proteomic method detects oxidatively induced protein carbonyls in muscles of a diabetes model Otsuka Long-Evans Tokushima Fatty (OLETF) rat.* Free Radic Biol Med, 2003. **34**(1): p. 11-22.
25. Yoo, B.S. and F.E. Regnier, *Proteomic analysis of carbonylated proteins in two-dimensional gel electrophoresis using avidin-fluorescein affinity staining.* Electrophoresis, 2004. **25**(9): p. 1334-41.

26. Korchazhkina, O., C. Exley, and S. Andrew Spencer, *Measurement by reversed-phase high-performance liquid chromatography of malondialdehyde in normal human urine following derivatisation with 2,4-dinitrophenylhydrazine.* J Chromatogr B Analyt Technol Biomed Life Sci, 2003. **794**(2): p. 353-62.
27. Bollineni, R.C.h., M. Fedorova, and R. Hoffmann, *Identification of carbonylated peptides by tandem mass spectrometry using a precursor ion-like scan in negative ion mode.* J Proteomics, 2011. **74**(11): p. 2351-9.
28. Mirzaei, H. and F. Regnier, *Affinity chromatographic selection of carbonylated proteins followed by identification of oxidation sites using tandem mass spectrometry.* Anal Chem, 2005. **77**(8): p. 2386-92.
29. Madian, A.G. and F.E. Regnier, *Profiling carbonylated proteins in human plasma.* J Proteome Res, 2010. **9**(3): p. 1330-43.
30. Madian, A.G. and F.E. Regnier, *Proteomic identification of carbonylated proteins and their oxidation sites.* J Proteome Res, 2010. **9**(8): p. 3766-80.
31. Slade, P.G., et al., *Proteins modified by the lipid peroxidation aldehyde 9,12-dioxo-10(E)-dodecenoic acid in MCF7 breast cancer cells.* Chem Res Toxicol, 2010. **23**(3): p. 557-67.
32. Chavez, J., et al., *New role for an old probe: affinity labeling of oxylipid protein conjugates by N'-aminooxymethylcarbonylhydrazino d-biotin.* Anal Chem, 2006. **78**(19): p. 6847-54.
33. Chavez, J.D., W.H. Bisson, and C.S. Maier, *A targeted mass spectrometry-based approach for the identification and characterization of proteins containing α-aminoadipic and γ-glutamic semialdehyde residues.* Anal Bioanal Chem, 2010. **398**(7-8): p. 2905-14.
34. Palmese, A., et al., *Dansyl labeling and bidimensional mass spectrometry to investigate protein carbonylation.* Rapid Commun Mass Spectrom, 2011. **25**(1): p. 223-31.
35. Rabbani, N., A. Ashour, and P.J. Thornalley, *Mass spectrometric determination of early and advanced glycation in biology.* Glycoconj J, 2016. **33**(4): p. 553-68.
36. Aldini, G., et al., *Molecular strategies to prevent, inhibit, and degrade advanced glycoxidation and advanced lipoxidation end products.* Free Radic Res, 2013. **47 Suppl 1**: p. 93-137.
37. Schmitt, A., et al., *Characterization of advanced glycation end products for biochemical studies: side chain modifications and fluorescence characteristics.* Anal Biochem, 2005. **338**(2): p. 201-15.

38. Wang, S.H., et al., *In-depth comparative characterization of hemoglobin glycation in normal and diabetic bloods by LC-MSMS.* J Am Soc Mass Spectrom, 2014. **25**(5): p. 758-66.
39. Gillery, P., G. Dumont, and A. Vassault, *Evaluation of GHb assays in France by national quality control surveys.* Diabetes Care, 1998. **21**(2): p. 265-70.
40. Pellati, F. and S. Benvenuti, *Chromatographic and electrophoretic methods for the analysis of phenethylamine [corrected] alkaloids in Citrus aurantium.* J Chromatogr A, 2007. **1161**(1-2): p. 71-88.
41. Flückiger, R., T. Woodtli, and W. Berger, *Quantitation of glycosylated hemoglobin by boronate affinity chromatography.* Diabetes, 1984. **33**(1): p. 73-6.
42. Jeppsson, J.O., et al., *Approved IFCC reference method for the measurement of HbA1c in human blood.* Clin Chem Lab Med, 2002. **40**(1): p. 78-89.
43. Vanhooren, V., et al., *Protein modification and maintenance systems as biomarkers of ageing.* Mech Ageing Dev, 2015. **151**: p. 71-84.
44. Geiger, T. and S. Clarke, *Deamidation, isomerization, and racemization at asparaginyl and aspartyl residues in peptides. Succinimide-linked reactions that contribute to protein degradation.* J Biol Chem, 1987. **262**(2): p. 785-94.
45. Harris, R.J., et al., *Identification of multiple sources of charge heterogeneity in a recombinant antibody.* J Chromatogr B Biomed Sci Appl, 2001. **752**(2): p. 233-45.
46. Zhang, W. and M.J. Czupryn, *Analysis of isoaspartate in a recombinant monoclonal antibody and its charge isoforms.* J Pharm Biomed Anal, 2003. **30**(5): p. 1479-90.
47. Liu, H., G. Gaza-Bulseco, and J. Sun, *Characterization of the stability of a fully human monoclonal IgG after prolonged incubation at elevated temperature.* J Chromatogr B Analyt Technol Biomed Life Sci, 2006. **837**(1-2): p. 35-43.
48. Vlasak, J., et al., *Identification and characterization of asparagine deamidation in the light chain CDR1 of a humanized IgG1 antibody.* Anal Biochem, 2009. **392**(2): p. 145-54.
49. Kutuk, O. and A. Letai, *Regulation of Bcl-2 family proteins by posttranslational modifications.* Curr Mol Med, 2008. **8**(2): p. 102-18.
50. Zhao, R., F.T. Yang, and D.R. Alexander, *An oncogenic tyrosine kinase inhibits DNA repair and DNA-damage-induced Bcl-xL deamidation in T cell transformation.* Cancer Cell, 2004. **5**(1): p. 37-49.
51. Deverman, B.E., et al., *Bcl-xL deamidation is a critical switch in the regulation of the response to DNA damage.* Cell, 2002. **111**(1): p. 51-62.

52. Eggleton, P., R. Haigh, and P.G. Winyard, *Consequence of neo-antigenicity of the 'altered self'.* Rheumatology (Oxford), 2008. **47**(5): p. 567-71.
53. Takata, T., et al., *Deamidation destabilizes and triggers aggregation of a lens protein, betaA3-crystallin.* Protein Sci, 2008. **17**(9): p. 1565-75.
54. Weintraub, S.J. and B.E. Deverman, *Chronoregulation by asparagine deamidation.* Sci STKE, 2007. **2007**(409): p. re7.
55. Kosugi, S., et al., *Suppression of protein l-isoaspartyl (d-aspartyl) methyltransferase results in hyperactivation of EGF-stimulated MEK-ERK signaling in cultured mammalian cells.* Biochem Biophys Res Commun, 2008. **371**(1): p. 22-7.
56. McCudden, C.R. and V.B. Kraus, *Biochemistry of amino acid racemization and clinical application to musculoskeletal disease.* Clin Biochem, 2006. **39**(12): p. 1112-30.
57. Hao, P., et al., *Detection, evaluation and minimization of nonenzymatic deamidation in proteomic sample preparation.* Mol Cell Proteomics, 2011. **10**(10): p. O111.009381.
58. Johnson, B.A., et al., *Formation of isoaspartate at two distinct sites during in vitro aging of human growth hormone.* J Biol Chem, 1989. **264**(24): p. 14262-71.
59. Černý, M., et al., *Advances in purification and separation of posttranslationally modified proteins.* J Proteomics, 2013. **92**: p. 2-27.
60. Bischoff, R. and H. Schlüter, *Amino acids: chemistry, functionality and selected non-enzymatic post-translational modifications.* J Proteomics, 2012. **75**(8): p. 2275-96.
61. Bae, N., et al., *An electrophoretic approach to screen for glutamine deamidation.* Anal Biochem, 2012. **428**(1): p. 1-3.
62. Motoie, R., et al., *Localization of D-β-aspartyl residue-containing proteins in various tissues.* Int J Mol Sci, 2009. **10**(5): p. 1999-2009.
63. Fujii, N., et al., *Localization of biologically uncommon D-beta-aspartate-containing alphaA-crystallin in human eye lens.* Mol Vis, 2000. **6**: p. 1-5.
64. Miura, Y., et al., *Immunohistochemical study of chronological and photo-induced aging skins using the antibody raised against D-aspartyl residue-containing peptide.* J Cutan Pathol, 2004. **31**(1): p. 51-6.
65. Shin, Y., et al., *Abeta species, including IsoAsp23 Abeta, in Iowa-type familial cerebral amyloid angiopathy.* Acta Neuropathol, 2003. **105**(3): p. 252-8.
66. Johnson, B.A. and D.W. Aswad, *Optimal conditions for the use of protein L-isoaspartyl methyltransferase in assessing the isoaspartate content of peptides and proteins.* Anal Biochem, 1991. **192**(2): p. 384-91.

67. Kharbanda, K.K., et al., *Accumulation of proteins bearing atypical isoaspartyl residues in livers of alcohol-fed rats is prevented by betaine administration: effects on protein-L-isoaspartyl methyltransferase activity.* J Hepatol, 2007. **46**(6): p. 1119-25.
68. Schurter, B.T. and D.W. Aswad, *Analysis of isoaspartate in peptides and proteins without the use of radioisotopes.* Anal Biochem, 2000. **282**(2): p. 227-31.
69. Ren, D., et al., *An improved trypsin digestion method minimizes digestion-induced modifications on proteins.* Anal Biochem, 2009. **392**(1): p. 12-21.
70. Li, X., et al., *Use of 18O labels to monitor deamidation during protein and peptide sample processing.* J Am Soc Mass Spectrom, 2008. **19**(6): p. 855-64.
71. Lehmann, W.D., et al., *Analysis of isoaspartate in peptides by electrospray tandem mass spectrometry.* Protein Sci, 2000. **9**(11): p. 2260-8.
72. Cournoyer, J.J., et al., *Deamidation: Differentiation of aspartyl from isoaspartyl products in peptides by electron capture dissociation.* Protein Sci, 2005. **14**(2): p. 452-63.
73. Syka, J.E., et al., *Peptide and protein sequence analysis by electron transfer dissociation mass spectrometry.* Proc Natl Acad Sci U S A, 2004. **101**(26): p. 9528-33.
74. Olsen, J.V., et al., *Higher-energy C-trap dissociation for peptide modification analysis.* Nat Methods, 2007. **4**(9): p. 709-12.
75. Yang, H. and R.A. Zubarev, *Mass spectrometric analysis of asparagine deamidation and aspartate isomerization in polypeptides.* Electrophoresis, 2010. **31**(11): p. 1764-72.
76. Guan, Z., N.A. Yates, and R. Bakhtiar, *Detection and characterization of methionine oxidation in peptides by collision-induced dissociation and electron capture dissociation.* J Am Soc Mass Spectrom, 2003. **14**(6): p. 605-13.
77. Hoshi, T. and S. Heinemann, *Regulation of cell function by methionine oxidation and reduction.* J Physiol, 2001. **531**(Pt 1): p. 1-11.
78. Stadtman, E.R., et al., *Cyclic oxidation and reduction of protein methionine residues is an important antioxidant mechanism.* Mol Cell Biochem, 2002. **234-235**(1-2): p. 3-9.
79. Stadtman, E.R. and R.L. Levine, *Protein oxidation.* Ann N Y Acad Sci, 2000. **899**: p. 191-208.
80. Vogt, W., *Oxidation of methionyl residues in proteins: tools, targets, and reversal.* Free Radic Biol Med, 1995. **18**(1): p. 93-105.
81. Hardin, S.C., et al., *Coupling oxidative signals to protein phosphorylation via methionine oxidation in Arabidopsis.* Biochem J, 2009. **422**(2): p. 305-12.
82. Levine, R.L., et al., *Methionine residues may protect proteins from critical oxidative damage.* Mech Ageing Dev, 1999. **107**(3): p. 323-32.

83. Schey, K.L. and E.L. Finley, *Identification of peptide oxidation by tandem mass spectrometry.* Acc Chem Res, 2000. **33**(5): p. 299-306.
84. Lagerwerf, F.M., et al., *Identification of oxidized methionine in peptides.* Rapid Commun Mass Spectrom, 1996. **10**(15): p. 1905-10.
85. Steen, H. and M. Mann, *Similarity between condensed phase and gas phase chemistry: fragmentation of peptides containing oxidized cysteine residues and its implications for proteomics.* J Am Soc Mass Spectrom, 2001. **12**(2): p. 228-32.
86. Wehr, N.B. and R.L. Levine, *Wanted and wanting: antibody against methionine sulfoxide.* Free Radic Biol Med, 2012. **53**(6): p. 1222-5.
87. Kotiaho, T., et al., *Electrospray mass and tandem mass spectrometry identification of ozone oxidation products of amino acids and small peptides.* J Am Soc Mass Spectrom, 2000. **11**(6): p. 526-35.
88. Zhu, H., et al., *Residue-specific mass signatures for the efficient detection of protein modifications by mass spectrometry.* Anal Chem, 2002. **74**(7): p. 1687-94.
89. Hollemeyer, K., E. Heinzle, and A. Tholey, *Identification of oxidized methionine residues in peptides containing two methionine residues by derivatization and matrix-assisted laser desorption/ionization mass spectrometry.* Proteomics, 2002. **2**(11): p. 1524-31.
90. Hunt, D.F., et al., *Protein sequencing by tandem mass spectrometry.* Proc Natl Acad Sci U S A, 1986. **83**(17): p. 6233-7.
91. McLafferty, F.W., et al., *Electron capture dissociation of gaseous multiply charged ions by Fourier-transform ion cyclotron resonance.* J Am Soc Mass Spectrom, 2001. **12**(3): p. 245-9.
92. Ge, Y., et al., *Top down characterization of larger proteins (45 kDa) by electron capture dissociation mass spectrometry.* J Am Chem Soc, 2002. **124**(4): p. 672-8.
93. Sze, S.K., et al., *Top-down mass spectrometry of a 29-kDa protein for characterization of any posttranslational modification to within one residue.* Proc Natl Acad Sci U S A, 2002. **99**(4): p. 1774-9.
94. Fenn, J.B., et al., *Electrospray ionization for mass spectrometry of large biomolecules.* Science, 1989. **246**(4926): p. 64-71.
95. Kelleher, N.L., et al., *Localization of labile posttranslational modifications by electron capture dissociation: the case of gamma-carboxyglutamic acid.* Anal Chem, 1999. **71**(19): p. 4250-3.
96. Shi, S.D., et al., *Phosphopeptide/phosphoprotein mapping by electron capture dissociation mass spectrometry.* Anal Chem, 2001. **73**(1): p. 19-22.

97. Mirgorodskaya, E., P. Roepstorff, and R.A. Zubarev, *Localization of O-glycosylation sites in peptides by electron capture dissociation in a Fourier transform mass spectrometer.* Anal Chem, 1999. **71**(20): p. 4431-6.
98. Håkansson, K., et al., *Electron capture dissociation and infrared multiphoton dissociation MS/MS of an N-glycosylated tryptic peptic to yield complementary sequence information.* Anal Chem, 2001. **73**(18): p. 4530-6.
99. Forman, H.J., J.M. Fukuto, and M. Torres, *Redox signaling: thiol chemistry defines which reactive oxygen and nitrogen species can act as second messengers.* Am J Physiol Cell Physiol, 2004. **287**(2): p. C246-56.
100. Forrester, M.T. and J.S. Stamler, *A classification scheme for redox-based modifications of proteins.* Am J Respir Cell Mol Biol, 2007. **36**(2): p. 135-7.
101. Izquierdo-Álvarez, A., et al., *Differential redox proteomics allows identification of proteins reversibly oxidized at cysteine residues in endothelial cells in response to acute hypoxia.* J Proteomics, 2012. **75**(17): p. 5449-62.
102. Chouchani, E.T., et al., *Proteomic approaches to the characterization of protein thiol modification.* Curr Opin Chem Biol, 2011. **15**(1): p. 120-8.
103. Kettenhofen, N.J. and M.J. Wood, *Formation, reactivity, and detection of protein sulfenic acids.* Chem Res Toxicol, 2010. **23**(11): p. 1633-46.
104. Burgoyne, J.R. and P. Eaton, *A rapid approach for the detection, quantification, and discovery of novel sulfenic acid or S-nitrosothiol modified proteins using a biotin-switch method.* Methods Enzymol, 2010. **473**: p. 281-303.
105. Saurin, A.T., et al., *Widespread sulfenic acid formation in tissues in response to hydrogen peroxide.* Proc Natl Acad Sci U S A, 2004. **101**(52): p. 17982-7.
106. Charles, R.L., et al., *Protein sulfenation as a redox sensor: proteomics studies using a novel biotinylated dimedone analogue.* Mol Cell Proteomics, 2007. **6**(9): p. 1473-84.
107. Leonard, S.E., K.G. Reddie, and K.S. Carroll, *Mining the thiol proteome for sulfenic acid modifications reveals new targets for oxidation in cells.* ACS Chem Biol, 2009. **4**(9): p. 783-99.
108. Lo Conte, M. and K.S. Carroll, *Chemoselective ligation of sulfinic acids with aryl-nitroso compounds.* Angew Chem Int Ed Engl, 2012. **51**(26): p. 6502-5.
109. Hung, C.W., et al., *Collision-induced reporter fragmentations for identification of covalently modified peptides.* Anal Bioanal Chem, 2007. **389**(4): p. 1003-16.
110. Lioe, H. and R.A. O'Hair, *Comparison of collision-induced dissociation and electron-induced dissociation of singly protonated aromatic amino acids, cystine and related*

simple peptides using a hybrid linear ion trap-FT-ICR mass spectrometer. Anal Bioanal Chem, 2007. **389**(5): p. 1429-37.

111. Mormann, M., et al., *Fragmentation of intra-peptide and inter-peptide disulfide bonds of proteolytic peptides by nanoESI collision-induced dissociation.* Anal Bioanal Chem, 2008. **392**(5): p. 831-8.
112. Zhang, Y., H.D. Dewald, and H. Chen, *Online mass spectrometric analysis of proteins/peptides following electrolytic cleavage of disulfide bonds.* J Proteome Res, 2011. **10**(3): p. 1293-304.
113. Saito, K., et al., *Verification of protein disulfide bond arrangement by in-gel tryptic digestion under entirely neutral pH conditions.* Proteomics, 2010. **10**(7): p. 1505-9.
114. Paulsen, C.E. and K.S. Carroll, *Orchestrating redox signaling networks through regulatory cysteine switches.* ACS Chem Biol, 2010. **5**(1): p. 47-62.
115. Reddie, K.G. and K.S. Carroll, *Expanding the functional diversity of proteins through cysteine oxidation.* Curr Opin Chem Biol, 2008. **12**(6): p. 746-54.
116. Woo, H.A., et al., *Reversible oxidation of the active site cysteine of peroxiredoxins to cysteine sulfinic acid. Immunoblot detection with antibodies specific for the hyperoxidized cysteine-containing sequence.* J Biol Chem, 2003. **278**(48): p. 47361-4.
117. Kinumi, T., et al., *Effective detection of peptides containing cysteine sulfonic acid using matrix-assisted laser desorption/ionization and laser desorption/ionization on porous silicon mass spectrometry.* J Mass Spectrom, 2006. **41**(1): p. 103-12.
118. Medzihradszky, K.F., et al., *O-sulfonation of serine and threonine: mass spectrometric detection and characterization of a new posttranslational modification in diverse proteins throughout the eukaryotes.* Mol Cell Proteomics, 2004. **3**(5): p. 429-40.
119. Medzihradszky, K.F., et al., *Sulfopeptide fragmentation in electron-capture and electron-transfer dissociation.* J Am Soc Mass Spectrom, 2007. **18**(9): p. 1617-24.
120. Giustarini, D., et al., *S-glutathionylation: from redox regulation of protein functions to human diseases.* J Cell Mol Med, 2004. **8**(2): p. 201-12.
121. Hill, B.G. and A. Bhatnagar, *Protein S-glutathiolation: redox-sensitive regulation of protein function.* J Mol Cell Cardiol, 2012. **52**(3): p. 559-67.
122. Reynaert, N.L., et al., *In situ detection of S-glutathionylated proteins following glutaredoxin-1 catalyzed cysteine derivatization.* Biochim Biophys Acta, 2006. **1760**(3): p. 380-7.
123. Aesif, S.W., et al., *In situ analysis of protein S-glutathionylation in lung tissue using glutaredoxin-1-catalyzed cysteine derivatization.* Am J Pathol, 2009. **175**(1): p. 36-45.

124. Gravina, S.A. and J.J. Mieyal, *Thioltransferase is a specific glutathionyl mixed disulfide oxidoreductase.* Biochemistry, 1993. **32**(13): p. 3368-76.
125. Brennan, J.P., et al., *The utility of N,N-biotinyl glutathione disulfide in the study of protein S-glutathiolation.* Mol Cell Proteomics, 2006. **5**(2): p. 215-25.
126. Sullivan, D.M., R.L. Levine, and T. Finkel, *Detection and affinity purification of oxidant-sensitive proteins using biotinylated glutathione ethyl ester.* Methods Enzymol, 2002. **353**: p. 101-13.
127. Sullivan, D.M., et al., *Identification of oxidant-sensitive proteins: TNF-alpha induces protein glutathiolation.* Biochemistry, 2000. **39**(36): p. 11121-8.
128. Yang, H., Y. Zhang, and U. Pöschl, *Quantification of nitrotyrosine in nitrated proteins.* Anal Bioanal Chem, 2010. **397**(2): p. 879-86.
129. Ikeda, K., et al., *Detection of 6-nitrotryptophan in proteins by Western blot analysis and its application for peroxynitrite-treated PC12 cells.* Nitric Oxide, 2007. **16**(1): p. 18-28.
130. Abello, N., et al., *Chemical labeling and enrichment of nitrotyrosine-containing peptides.* Talanta, 2010. **80**(4): p. 1503-12.
131. Hu, W., et al., *Selection of thiol- and disulfide-containing proteins of Escherichia coli on activated thiol-Sepharose.* Anal Biochem, 2010. **398**(2): p. 245-53.
132. Sultana, R., M. Perluigi, and D.A. Butterfield, *Proteomics identification of oxidatively modified proteins in brain.* Methods Mol Biol, 2009. **564**: p. 291-301.
133. Roe, M.R., et al., *Proteomic mapping of 4-hydroxynonenal protein modification sites by solid-phase hydrazide chemistry and mass spectrometry.* Anal Chem, 2007. **79**(10): p. 3747-56.
134. Rauniyar, N., K. Prokai-Tatrai, and L. Prokai, *Identification of carbonylation sites in apomyoglobin after exposure to 4-hydroxy-2-nonenal by solid-phase enrichment and liquid chromatography-electrospray ionization tandem mass spectrometry.* J Mass Spectrom, 2010. **45**(4): p. 398-410.
135. Rauniyar, N. and L. Prokai, *Isotope-coded dimethyl tagging for differential quantification of posttranslational protein carbonylation by 4-hydroxy-2-nonenal, an end-product of lipid peroxidation.* J Mass Spectrom, 2011. **46**(10): p. 976-85.
136. Mann, M., *Functional and quantitative proteomics using SILAC.* Nat Rev Mol Cell Biol, 2006. **7**(12): p. 952-8.
137. Ong, S.E., et al., *Stable isotope labeling by amino acids in cell culture, SILAC, as a simple and accurate approach to expression proteomics.* Mol Cell Proteomics, 2002. **1**(5): p. 376-86.

138. Mirgorodskaya, O.A., et al., *Quantitation of peptides and proteins by matrix-assisted laser desorption/ionization mass spectrometry using (18)O-labeled internal standards.* Rapid Commun Mass Spectrom, 2000. **14**(14): p. 1226-32.
139. Hsu, J.L., et al., *Stable-isotope dimethyl labeling for quantitative proteomics.* Anal Chem, 2003. **75**(24): p. 6843-52.
140. Boersema, P.J., et al., *Multiplex peptide stable isotope dimethyl labeling for quantitative proteomics.* Nat Protoc, 2009. **4**(4): p. 484-94.
141. Madian, A.G., et al., *Differential carbonylation of proteins as a function of in vivo oxidative stress.* J Proteome Res, 2011. **10**(9): p. 3959-72.
142. Hermjakob, H., *The HUPO proteomics standards initiative--overcoming the fragmentation of proteomics data.* Proteomics, 2006. **6 Suppl 2**: p. 34-8.
143. Taus, T., et al., *Universal and confident phosphorylation site localization using phosphoRS.* J Proteome Res, 2011. **10**(12): p. 5354-62.

Chapter V: Advanced lipoxidation end products (ALEs) as RAGE binders: Mass spectrometric and computational studies to explain the reasons why

This Chapter was integrally published as follows:

M. Mol, G. Degani, C. Coppa, G. Baron, L. Popolo, M. Carini, G. Aldini, G. Vistoli, A. Altomare, Advanced lipoxidation end products (ALEs) as RAGE binders: mass spectrometric and computational studies to explain the reasons why, Redox Biol. (2018) 101083.

Redox Biology xxx (xxxx) xxxx

Contents lists available at ScienceDirect

Redox Biology

journal homepage: www.elsevier.com/locate/redox

Research paper

Advanced lipoxidation end products (ALEs) as RAGE binders: Mass spectrometric and computational studies to explain the reasons why

Marco Mol[a,1], Genny Degani[b,1], Crescenzo Coppa[a], Giovanna Baron[a], Laura Popolo[b], Marina Carini[a], Giancarlo Aldini[a,*], Giulio Vistoli[a], Alessandra Altomare[a]

[a] Department of Pharmaceutical Sciences, Via Mangiagalli 25, Università degli Studi di Milano, 20133 Milano, Italy
[b] Department of Biosciences, Via Celoria 26, Università degli Studi di Milano, 20133 Milano, Italy

ARTICLE INFO

Keywords:
Advanced lipoxidation end products (ALEs)
Human serum albumin (HSA)
RAGE
Pull-down assay
VC1 domain
Reactive Carbonyl Species (RCS)
4-hydroxy-*trans*− 2-nonenal (HNE)
Acrolein (ACR) and malondialdehyde (MDA)

ABSTRACT

Advanced Lipoxidation End-products (ALEs) are modified proteins that can act as pathogenic factors in several chronic diseases. Several molecular mechanisms have so far been considered to explain the damaging action of ALEs and among these a pathway involving the receptor for advanced glycation end products (RAGE) should be considered. The aim of the present work is to understand if ALEs formed from lipid peroxidation derived reactive carbonyl species (RCS) are able to act as RAGE binders and also to gain a deeper insight into the molecular mechanisms involved in the protein-protein engagement. ALEs were produced in vitro, by incubating human serum albumin (HSA) with 4-hydroxy-*trans*− 2-nonenal (HNE), acrolein (ACR) and malondialdehyde (MDA). The identification of ALEs was performed by MS. ALEs were then subjected to the VC1 Pull-Down assay (VC1 is the ligand binding domain of RAGE) and the enrichment factor (the difference between the relative abundance in the enriched sample minus the amount in the untreated one) as an index of affinity, was determined. Computation studies were then carried out to explain the factors governing the affinity of the adducted moieties and the site of interaction on adducted HSA for VC1-binding. The in silico analyses revealed the key role played by those adducts which strongly reduce the basicity of the modified residues and thus occur at their neutral state at physiological conditions (e.g. the MDA adducts, dihydropyridine-Lysine (DHPK) and N-2-pyrimidyl-ornithine (NPO), and acrolein derivatives, N-(3-formyl-3,4-dehydro-piperidinyl) lysine, FDPK). These neutral adducts become unable to stabilize ion-pairs with the surrounding negative residues which thus can contact the RAGE positive residues.

In conclusion, ALEs derived from lipid peroxidation-RCS are binders of RAGE and this affinity depends on the effect of the adduct moiety to reduce the basicity of the target amino acid and on the acid moieties surrounding the aminoacidic target.

1. Introduction

The oxidative degradation of lipids (lipid peroxidation) results in the formation of a wide variety of break-down products including small molecules containing a carbonyl moiety and characterized by chemical reactivity and for this reason called reactive carbonyl species (RCS) [1]. Lipid-derived reactive carbonyl species (RCS) are quite heterogeneous, belonging to different chemical classes including α,β-unsaturated aldehydes [4-hydroxynonenal (HNE), acrolein (ACR)], keto-aldehydes [methylglyoxal (MGO), 4-oxo-nonenal (ONE)] and di-aldehydes [malondialdehyde (MDA) and glyoxal (GO)] [2]. RCS react with different nucleophilic substrates and in particular with the nucleophilic amino acids of protein (arginine, lysine, cysteine and histidine) through a reaction called protein lipoxidation and involving the carbonyl moiety and the electrophilic center (e.g. the C3 of an α,β-unsaturated moiety). The reaction products between proteins and RCS, advanced lipoxidation products (ALEs), are now recognized not only as biomarker of RCS formation but also as bioactive/damaging biomolecules [3,4]. Moreover, RCS are currently recognized as being involved in the onset and progression of several diseases including diabetic retinopathy [5], atherosclerosis [6], renal disease [7] and metabolic disorders [8]. Based on their pathogenetic role, ALEs are now considered as promising drug target and molecules effective in preventing ALE formation have been reported to have beneficial effects in some animal models [9,10].

* Corresponding author.
E-mail address: giancarlo.aldini@unimi.it (G. Aldini).
[1] Equally contributed.

https://doi.org/10.1016/j.redox.2018.101083
Received 6 November 2018; Received in revised form 6 December 2018; Accepted 15 December 2018

However, it should be considered that the effect of protein lipoxidation and of RCS can be double-sided, because besides a damaging mechanism as above mentioned, in some conditions and depending on their levels, they can exert protective effects associated with the induction of antioxidant defense mechanisms [11].

Several molecular mechanisms have so far been considered to explain the damaging action of ALEs, which can include one of the following mechanisms, depending on the damaging process and the target protein itself: protein dysfunction, protein oligomerization, signal transduction and immune response [3,6]. Moreover, adduction of RCS to proteins can also lead to the formation of ALEs acting as binders and activators of some receptors as in the case of galectin-3, a glycan binding protein which has been suggested to aid in the removal of circulating AGEs and ALEs [12].

ALEs which are formed from RCS deriving either from lipid and reducing sugar oxidation, such as glyoxal and methylglyoxal, (in this paper called AGEs/ALEs) are known to act as binders and activators of the receptor RAGE [13,14]. RAGE is a type I cell surface receptor that is expressed in several cells, such as endothelial cells, smooth muscle cells, but also dendritic cells and T-lymphocytes and is predominantly located in the lungs [15]. RAGE has been involved in many different pathologies with a marked oxidative base, such as diabetes, atherosclerosis, neurodegenerative diseases and many different ligands of RAGE have been identified, such as amyloid β peptide, S100/calgranulin protein, HMGB1 [16]. Two different pathways can be activated upon binding to the receptor: 1) the activation of the NADPH oxidase, resulting in the production of reactive oxygen species (ROS), which are detrimental to the cells and 2) the activation of the NF-κB pathway leading to a sustained pro-inflammatory and pro-fibrotic response [17].

However, there are some ALEs (in this paper called as ALEs-lipox), widely detected in several oxidative based and inflammatory diseases [6,18], which are formed by RCS only deriving from a lipid peroxidation process, such as MDA, HNE and ACR. For these ALEs-lipox very few data are available on their RAGE interaction. Shanmugam et al. [19] reported that synthetic ALE (malondialdehyde-lysine [MDA-Lys]) induces oxidative stress and also activates the transcriptional factor nuclear factor-kB (NF-kB) in THP-1 monocytes partly via the receptor for AGEs (RAGE).

The aim of the present paper is to understand whether ALEs-lipox are able to act as RAGE binders as do AGEs and AGEs/ALEs and also to gain a deeper insight into the molecular mechanisms involved in the protein-protein engagement. Our starting hypothesis, the involvement of ALEs-lipox in RAGE activation, is supported by several facts such as that ALEs/AGEs and ALEs-lipox share some structural properties such as the covalent modifications by aldehydes of nucleophilic residues and that ALEs-lipox are pro-inflammatory and pro-fibrotic compounds activating the NF-kB pathway, a mechanism which could be addressed to a RAGE activation pathway. Fig. 1 shows the work flow of the study.

To test this hypothesis, a set of ALEs was firstly prepared and fully characterized by MS. ALEs were formed using the well-known lipid peroxidation derived RCS and in particular HNE, ACR and MDA. Since ALEs are quite heterogeneous also when formed by a single attacking RCS, for each tested RCS the different ALEs were fully identified by a bottom-up MS approach in terms of adducted moiety and modification site. The RAGE binding ability of each identified ALE was then determined using the VC1 assay as previously reported [20]. For each identified ALE the VC1 binding ability was then related to the variation in the ionization state of the adducted residues as well as to the abundance of surrounding negative residues that, after the ALE generation, become available for RAGE binding. Computation studies were then carried out to explain the factors governing the affinity of the adducted moieties and the site of interaction on adducted HSA for VC1-binding.

The overall data permit the elucidation of the structural requirements for ALEs to become RAGE binders together with the molecular mechanisms involved in the protein-protein engagement.

2. Materials and methods

2.1. Reagents

Formic acid (FA), trifluoroacetic acid (TFA) and acetonitrile (ACN) were LC-MS grade; sodium dodecyl sulfate (SDS), ammonium bicarbonate, malondialdehyde tetrabutylammonium salt (MDA-TS), acrolein (ACR), HEPES, NaCl, sodium dihydrophosphate, disodium phosphate and all other chemicals were analytical grade and purchased from Sigma-Aldrich (Milan, Italy). 4-Hydroxy-2-*trans*-nonenal dimethylacetal (HNE-DMA, catalog Number H9538) was purchased from Sigma-Aldrich (Milan, Italy) and recombinant HSA expressed in *P. pastoris* were purchased from Sigma Aldrich (Milan, Italy). Streptavidin-coated magnetic beads (Streptavidin Mag Sepharose™) were purchased from GE Healthcare (Milan, Italy)

Ultrapure water was prepared by a Milli-Q purification system (Millipore, Bedford, MA, USA).

Any KD ™ Mini Protean® TGX ™ precast gel, Standard Precision Plus prestained protein standards, Laemmli sample buffer (2 ×/ 4 ×), Running buffer and Bio-Safe Coomassie, together with the threo-1,4-Dimercapto-2,3-butanediol (DTT) and iodoacetamide (IAA) were supplied by Bio-Rad Laboratories, Inc. Trypsin and Chymotrypsin sequencing grade were purchased from Roche Diagnostics SpA (Monza, Italy).

Digestion buffer was 50 mM ammonium bicarbonate; destaining solution was prepared mixing acetonitrile with digestion buffer (1:1 v/v); reducing solution was 10 mM DTT in digestion buffer; alkylating solution was 55 mM iodoacetamide in digestion buffer; extraction solution was prepared as follows: 3% TFA/30% ACN in H_2O MilliQ.

2.2. In vitro generation of ALEs-HSA

4-hydroxy-*trans*− 2-nonenal (HNE) was prepared as previously described [21]. HSA modified with MDA was prepared dissolving HSA in 10 mM phosphate buffer pH 7.4 at a concentration equal to 100 μM (6.7 mg ml^{-1}). HSA was incubated, as previously described [20] in the dark at 37 °C and 400 rpm and using the following molar ratios between protein and MDA: 1:6.3, 1:63, 1:630, 1:6300, 1: 12600. HSA modified with ACR or HNE was prepared dissolving HSA in 10 mM phosphate buffer pH 7.4 at a concentration equal to 75 μM (5 mg ml^{-1}). HSA was incubated in the dark at 37 °C and at 400 rpm in molar ratios protein: ACR equal to 1:10, 1:100, 1:1000, 1:2500 and 1:5000 and in molar ration protein: HNE equal to 1:10, 1:100, 1:200, 1:1000 and 1:2000. HSA incubated without RCS was used as a control untreated sample. The reactions were stopped after 24, 48 or 72 h removing the excess of RCS by ultrafiltration using Amicon Ultra filter units 0.5 ml, cut-off 10 kDa (Millipore).

2.3. Intact protein analysis by MS

ALEs obtained by incubating HSA with RCSs were analyzed by direct infusion on a triple-quadrupole (TQ) mass spectrometer (Finnigan TSQ Quantum Ultra, ThermoQuest, Milan, Italy) equipped with an Electrospray Finnigan Ion Max source. For MS analyses, samples were desalted by using Amicon Ultra filter units 0.5 ml, cut-off 10 kDa (Millipore) and washed three times with water. Samples were then diluted to 1 $mgml^{-1}$ with a final composition of CH_3CN–H_2O–HCOOH (30:70:0.1, v/v/v). Aliquots of 50 μl were injected into the mass spectrometer at a flow rate of 25 μl min^{-1} by using a ThermoQuest autosampler. Each sample was analyzed for 5 min under the following instrumental conditions: positive-ion mode; ESI voltage 3.5 kV, capillary temperature 350 °C, Q3 scan range 1200–1500 *m/z*, Q3 power 0.4 amu, scan time 1 s, Q2 gas pressure 1.5 Torr, skimmer offset 10 V, microscan set to 3. Full instrument control and ESI mass spectra acquisitions were carried out by Xcalibur software (version 2.0.7, Thermo Fisher Scientific, Rodano, MI, Italy). Mass spectra deconvolution was performed using MagTran software (version 1.02) [22].

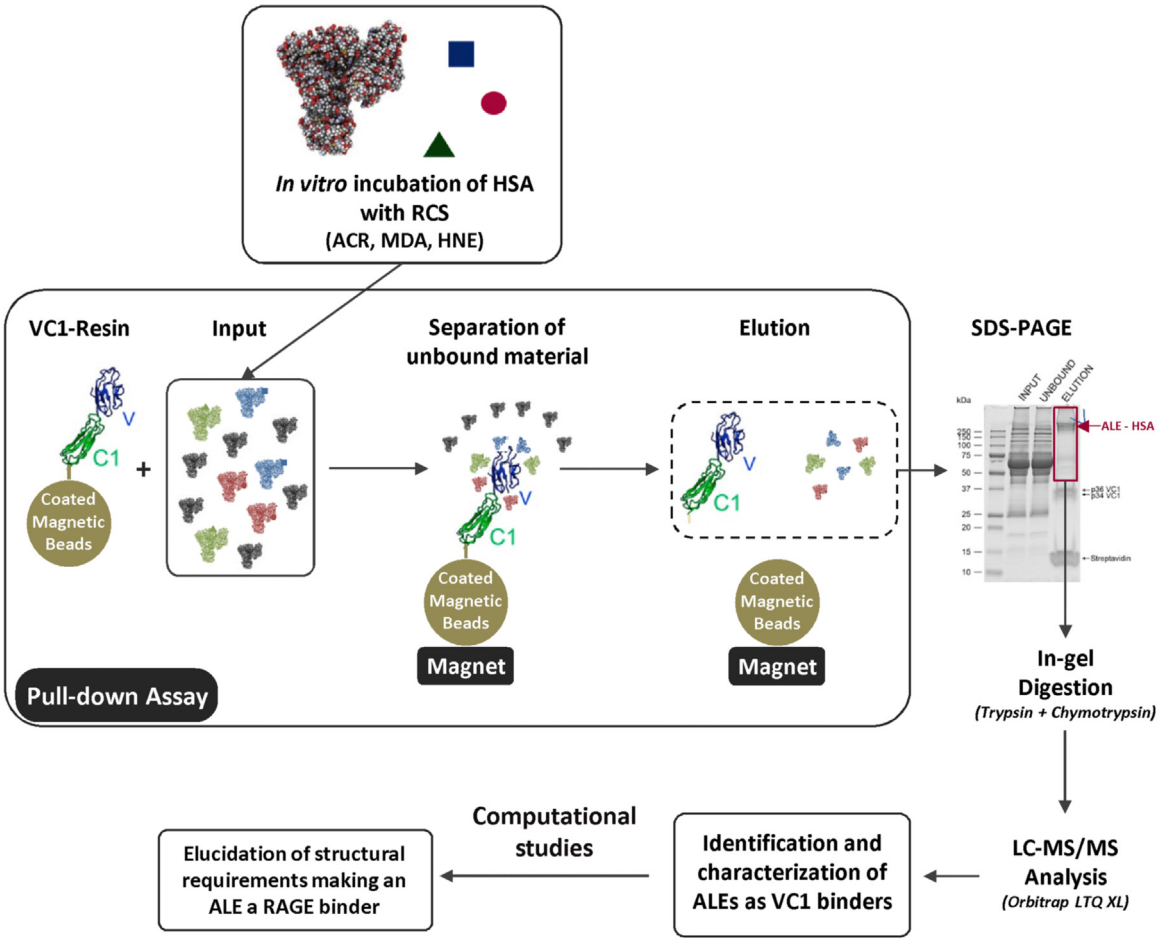

Fig. 1. Work flow of the study. ALEs-lipox were firstly prepared by incubating HSA with lipid peroxidation derived RCS (HNE, ACR and MDA) and then fully characterized by MS. The RAGE binding ability of each identified ALE was then determined by using the VC1 assay as previously reported [20]. Computation studies were then carried out to explain the factors governing the affinity of the adducted moieties and the site of interaction on adducted HSA for VC1-binding.

2.4. VC1 pull-down assay

VC1-His-Strep was expressed and purified from *Pichia pastoris* culture supernatant as previously described [23]. The recombinant protein was immobilized on streptavidin-coated magnetic beads by exploiting the affinity of the Strep tag towards streptavidin. In order to obtain the VC1-resin, 50 µg of purified VC1-His-Strep in 170 µl of 20 mM HEPES pH 7.1, 100 mM NaCl were added to 5 µl of packed streptavidin coated-beads, previously equilibrated with the same buffer. A volume of 170 µl of 20 mM HEPES pH 7.1, 100 mM NaCl were added to the same amount of beads in a different tube in order to obtained the Control-resin. After 1 h of incubation at 4 °C on a rotary mixer, the unbound material was carefully removed and the magnetic beads were washed with 500 µl of buffer (20 mM HEPES pH 7.1, 100 mM NaCl). The VC1- and Control-resin were incubated for 1 h at 4 °C with 160 µl of ALE-HSA or untreated HSA at the concentration of 125 µg ml^{-1} in 20 mM HEPES pH 7.1, 100 mM NaCl. The unbound material was carefully removed and the beads were washed twice with 500 µl of Buffer (20 mM HEPES pH 7.1, 100 mM NaCl). The elution was performed by boiling the beads for 5 min in 15 µl of Laemmli Sample Buffer 4x mixed with 400 mM DTT, then with other 15 µl of buffer (20 mM HEPES pH 7.1, 100 mM NaCl). The two eluates were pooled.

2.5. Electrophoretic procedures

The fractions obtained from pull-down experiments were analyzed by SDS PAGE. To 20 µl of input and unbound fractions, 7 µl of Laemmli Sample Buffer 4x mixed with 400 mM DTT were added. The samples were denatured incubating for 5 min at 95 °C. Input, unbound and elution samples were separated by SDS-PAGE on Any KD ™ Mini Protean® TGX ™ precast gels and stained with Bio-Safe Coomassie blue (Bio-Rad). Images were acquired using the calibrated densitometer GS-800 and analyzed by the software Quantity one (Bio-Rad).

2.6. ALE-HSA in-gel digestion

Proteins bands corresponding to ALEs-HSA and obtained by incubating HSA with HNE, ACR and MDA (input), and those cut from the fraction retained by VC1, were excised from gels using a scalpel, finely chopped, transferred to a new eppendorf and washed with 200 µl of digestion buffer. An aliquot of 200 µl of destaining solution was added to each gel portion and heated at 37 °C for 10 min in the thermomixer (1400 rpm); the destaining solution was then discarded and this step was repeated until destaining was completed. Afterwards, gel pieces were incubated with 150 µl of reducing solution at 56 °C for 1 h and then with 150 µl of alkylating solution at room temperature for 45 min in the dark. In-gel digestion of ALE-HSA adducts was performed by overnight-incubation at 37 °C with 1 µg of sequencing-grade trypsin (Roche) dissolved in digestion buffer. ALE-HSA samples were also subjected to a second digestion by a sequencing-grade chymotrypsin (1 µg) for 7 h at 25 °C in the presence of calcium chloride (10 mM). The peptide mixtures were acidified with formic acid up to a final concentration of 1%.

To guarantee better protein detection, peptide mixtures were

extracted by a 10 min-incubation with extraction solution and by an additional 10 min-incubation with pure acetonitrile. The two extracts were combined and dried in a vacuum concentrator (Martin Christ.). Digested peptide mixtures were then dissolved in an appropriate volume (20 µl) of 0.1% formic acid for mass spectrometry (MS) analysis.

2.7. Mass spectrometry analyses

Peptides from the in-gel digestion were separated by reversed-phase (RP) nanoscale capillary liquid chromatography (nanoLC) and analyzed by electrospray tandem mass spectrometry (ESI-MS/MS). For each analysis 5 µl of solubilized peptides were injected onto a C18HALO PicoFrit column (75 mM x 10 cm, 2.7 mM particles, pores 100 Å, New Objective, USA) by means of an autosampler. Samples were loaded onto the fused silica column at 400 nl/min of mobile phase consisting of 99% of phase A and 1% of phase B (0.1% HCOOH in CH3CN) for 15 min. Peptide separation was performed with a 55 min linear gradient of phase B (1–35%). The separative gradient was followed by 5 min at 80% of phase B to rinse the column, and 15 min of 99% of phase A and 1% of phase B served to re-equilibrate the column to the initial conditions. The nano-chromatographic system, an UltiMate 3000 RSLCnano System (Dionex), was connected to an LTQ-Orbitrap XL mass spectrometer (Thermo Scientific Inc., Milan, Italy) equipped with a nanospray ion source (dynamic nanospray probe, Thermo Scientific Inc., Milan, Italy) set as follows: positive ion mode, spray voltage 1.8 Kv; capillary temperature 220 °C, capillary voltage 35 V; tube lens offset 120 V. The LTQ-Orbitrap XL mass spectrometer was operated in data-dependent acquisition mode (DDA) to acquire both the full MS spectra and the MS/MS spectra. Full MS spectra were acquired in "profile" mode, by the Orbitrap (FT) analyzer, in a scanning range between 300 and 1500 *m/z*, using a capillary temperature of 220 °C, AGC target $= 5 \times 10^5$ and resolving power 60,000 (FWHM at 400 *m/z*). Tandem mass spectra MS/MS were acquired by the Linear Ion Trap (LTQ) in CID mode, automatically set to fragment the nine most intense ions in each full MS spectrum (exceeding 1×10^4 counts) under the following conditions: centroid mode, isolation width of the precursor ion of 2.5 *m/z*, AGC target 1×10^4 and normalized collision energy of 35 eV. Dynamic exclusion was enabled (exclusion dynamics for 45 s for those ions observed 3 times in 30 s). Charge state screening and monoisotopic precursor selection were enabled, singly and unassigned charged ions were not fragmented. Xcalibur software (version 2.0.7, Thermo Scientific Inc., Milan, Italy) was used to control the mass spectrometer.

2.8. Identification and localization of protein adducts

The software Proteome Discoverer (version 1.3.0.339, Thermo Scientific, USA), implemented with the algorithm SEQUEST, was used to compare the experimental full and tandem mass spectra with the theoretical ones obtained by the *in silico* digestion of the HSA sequence (Uniprot P02768). Trypsin and chymotrypsin were selected as the cleaving proteases, allowing a maximum of 2 missed cleavages. Peptide and fragment ion tolerances were set to 5 ppm and 10 mmu, respectively. Cysteine carbamidomethylation was set as fix modification (+57.02147); methionine oxidation was allowed as a variable modification in addition to the known HNE-, ACR- or MDA-derived modifications as listed in Table S1.

As a quality filter, only peptide with an Xcore value grater then 2.2 for doubly-charged peptides, 2.5 for triply-charged, 2.75 for quadruply-charged peptide ions, and 3 for charge states quintuple or higher were considered as genuine peptide identifications. To ensure the lowest number of false positives, the mass values experimentally recorded were further processed through a combined search with the Database Decoy, where the protein sequences are inverted and randomized. This operation allows the calculation of the false discovery rate (FDR) for each match, so that all the proteins out of range of FDR between to 0.01 (strict) and 0.05 (relaxed) were rejected.

For the localization of ALE-deriving modifications, the MS/MS spectra of modified peptides were manually inspected; for the confident mapping of the modification sites, spectra were requested to match the expected ions (*b* and/or *y*) neighboring the modified amino acid residue both at the N- and C-termini.

2.9. Semi-quantitative analysis of ALE-HSA adducts

The relative extent of each protein modification has been calculated by determining the amount of the modified peptide in respect to the native one, by assuming that the ionization efficiency of the native and the modified peptides are equal. In particular, the single ion traces (SIC) of the native and modified peptides were firstly reconstituted by setting as filter ion the *m/z* values of the corresponding precursor protonated peptides. The peak areas were then automatically calculated by the Qual Browser tool of the Xcalibur data system (version 2.0.7, Thermo Scientific Inc., Milan, Italy) and then the relative abundance calculated by using the Eq. (1).

$$\text{Relative Abundance\%} = \frac{\text{Modified Peptide Peak Area}}{(\text{Modified Peptide Peak Area} + \text{Native Peptide Peak Area})} * 100 \quad (1)$$

The relative abundance of each modified peptide was determined in both the input and enriched samples. The retention efficiency of each identified ALEs towards VC1 was then determined by the *Enrichment Factor* value, calculated as the differences between the relative abundance in the enriched sample minus the amount in the untreated one (Enrichment factor = %VC1-%NoVC1).

2.10. Computational studies

The prediction of the pK values of the simulated adducts was performed by PM7-based semi-empirical calculations using MOPAC [24]. The simulations involved simplified model compounds by focusing on the adducted side chains and neglecting the backbone atoms. Specifically, the predictions involved the FDPK, mono and double N-propenal MA adducts of lysine. Indeed and as experimentally known, 2-amino pyrimidine and dihydropyridine (i.e., NPO and DHPK adducts) are neutral at physiological pH, while cyclic guanidines (see HTP0) retain the strong basicity of the guanidine group. With regard to HSA protein, the retrieved resolved structure (PDB Id 1A06) was used, after a preliminary optimization, to calculate the negative residues within a 5 Å radius sphere around each adducted residues and to generate the corresponding adducts as induced by MDA e ACR. As discussed in the Results section, two adducted HSA structures were manually generated using the VEGA suite of program [25]: the first carrying all the ACR-based adducts and the second structure with all the MDA-based adducts. The analysis was focused on Arg and Lys adducts only because they are numerous enough to derive a sort of structure-affinity relationships (SAR). Similarly, these analyses do not consider the HNE-induced modifications because they are too limited to develop clear relationships. In order to allow a suitable reorganization of the environments around all inserted adducts, the minimized adducted HSA structures underwent 1 ns of MD simulations by Namd [26] keeping the backbone atoms constrained to avoid excessive distortions of the resolved folding. With regard to RAGE structure, the NMR-derived V structure (PDB Id: 2mov) was prepared and utilized as done in previous studies. Protein-protein docking was performed using GRAMM [27] with the default parameters and generating 1000 complexes for each adducted HSA structure.

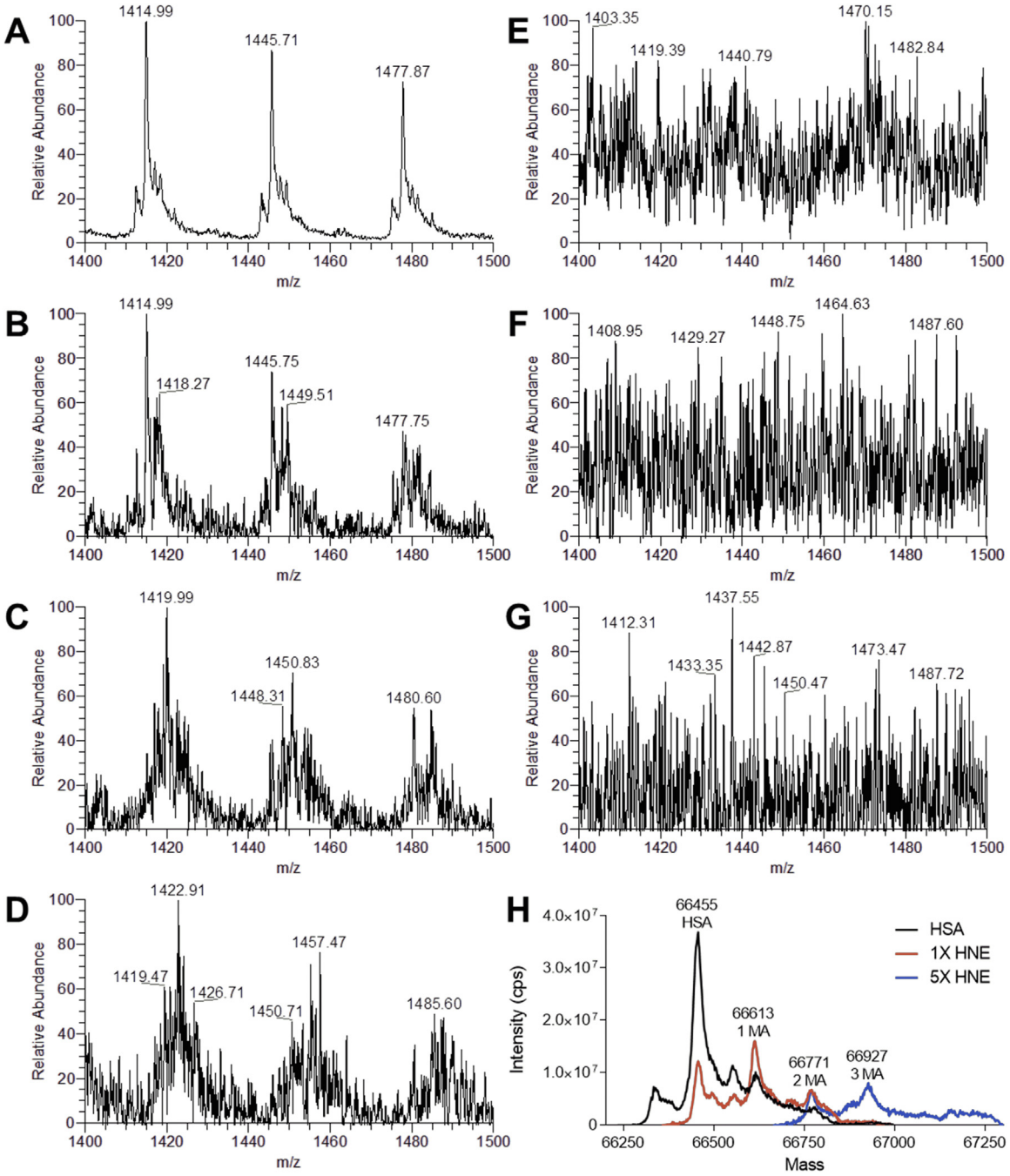

Fig. 2. Direct infusion ESI-MS analysis of native and HNE-modified HSA. Mass spectra of HSA recorded in a mass range between *m/z* 1400 and 1500. A) Native HSA shows sharp intense peaks referred to the charge ions 47 + , 46 + and 45 + ; the deconvoluted spectrum reports a MW 66,455 Da (H). When HSA is reacted with HNE at increasing molar ratios 1:1 (B), 1:5 (C), 1:10 (D), additional peaks relative to HNE adducts appear. At higher molar ratios 1:100 (E), 1:200 (F) and 1:1000 (G) the MS spectra lose resolution and become flat due to the presence of multiple adducts. H) Deconvoluted spectra showing the MS of HSA and protein adducts. MS spectra relative to HSA incubated with HNE at 1:100 M ratio and higher cannot be deconvoluted due to the extent of modification.

3. Results

3.1. Intact protein analysis of HSA and ALEs-HSA by MS

In order to investigate the interaction between RAGE and ALEs-lipox, different ALEs-lipox were produced in-vitro by incubating HSA with different concentrations of the well-known lipid derived RCS and in particular: acrolein (ACR), malondialdehyde (MDA) and 4-hydroxy-*trans*− 2-nonenal (HNE). After 24, 48 and 72 h, aliquots of the incubation mixtures were withdrawn, and the reaction was stopped by removing the excess of RCS by ultrafiltration. Intact protein analysis by direct infusion MS was used to evaluate the extent of HSA modifications. Fig. 2 shows the spectra of native HSA (panel A) and HSA incubated with increasing molar ratios of HNE [1:1 (B), 1:5 (C), 1:10 (D), 1:100 (E), 1:200 (F) and 1:1000 (G)]. Panel A) shows the MS-spectrum (mass range between *m/z* 1400 and 1500) of native and non-modified HSA, characterized by three sharp multicharged ions at *m/z* 1414.99, 1445.71 and 1477.87 relative to the three multicharged ions at 47 + , 46 + and 45 + . When HSA was incubated with HNE in a 1:1 M ratio, besides the three peaks relative to native HSA, a new set of peaks at *m/z* 1418.43, 1449.15, and 1481.40 is detectable and relative to the HNE Michael adduct of native HSA (MW shifted by 156 Da), as confirmed in

the deconvoluted spectrum (panel H). The number of adducted HNE moieties per molecule of HSA increases proportionally with the increase of molar ratios reaching 3 and 5 HNE moles per mole of HSA at 1:5 and 1:10 HSA: HNE molar ratios, as also confirmed by the deconvoluted spectra (panel H shows the deconvoluted spectra HSA incubated in the presence of HNE at a 1:5 M ratio). At higher HNE molar ratios (1:100, 1:200 and 1:1000, panels E, F and G, respectively) the MS spectra do not show any detectable peaks due the formation of such a large number of adducts and consequently of so many ions which cover the *m/z* scan range thus eliminating the detection of sharp ions.

Intact protein analysis was also performed on ALEs-lipox formed by incubating HSA with ACR and MDA, showing the same stepwise increase of modifications with the higher amount of RCS incubated with HSA (Supplementary Figs. 1 and 2).

Intact protein analysis well indicates that by using a wide range of molar ratios and different time-points a quite wide array of ALEs for each tested RCS was generated.

3.2. Pull-down assay with modified albumins

In order to characterize ALE-lipox modifications selectively enriched by RAGE, we performed a VC1 pull-down assay as previously described [20]. HSA and HSA treated with MDA, ACR or HNE were assayed for binding to VC1-resins and to control resin. As expected, unmodified HSA was not retained by the VC1-resin (Fig. 3, panel A). HSA modified by MDA and ACR are characterized by a different migration pattern on a SDS-PAGE analysis, with the appearance of oligomeric bands proportional to the increase of the HSA-RCS molar ratio (Fig. 3, panel B: HSA-MDA at 72 h, panel D: HSA-ACR 72 h, panel F: HSA-HNE 72 h). At increasing molar ratios and incubation time, higher amounts of albumin modified with MDA or ACR were eluted from the VC1 resin, with a predominance of the high molecular weight (HMW) species. The modified albumins were retained by the VC1-resin, but not by the control resin, as shown in Fig. 3 (panel C: HSA-MDA molar ratio 1:12,600, 72 h; panel: E HSA-ACR molar ratio 1:5000, 72 h, panel: G HSA-HNE molar ratio 1:2000, 72 h). The time course analysis and the pull-down experiments with HSA-MDA have previously been published [20]. The time course analysis and the pull-down experiments with HSA-ACR and HSA-HNE are reported in Supplementary Fig. 3 and Supplementary Fig. 4 respectively.

3.3. Identification and localization of protein adducts by mass spectrometry

ALEs-lipox in the reaction mixtures and those enriched by VC1 were analyzed by bottom-up MS in order to identify the PTMs and to localize the amino acid residues involved in the protein adduct formation.

Tables 1 and 2 summarize the identified ALEs before and after VC1 enrichment, respectively. It should be noted that the tables summarize the overall PTMs identified at different molar ratios and incubation times. The ALEs not retained (identified only in the input samples), retained (identified after VC1 enrichment) and present in both input and elution samples are reported in the Venn diagrams of Fig. 4.

With regard to MDA (Table 2), only di-hydropyridine adducts on lysines (DHPK), and N-2-pyrimidyl-ornithine adducts on arginines (NPO) were retained by VC1-domain. The n-propenal modifications of lysine (NPK), largely identified before enrichment, were not identified after the enrichment.

ACR induced a set of modifications which were identified only after VC1 enrichment and in particular the N-(3-formyl-3,4-dehydro-piperidinyl) lysine (FDPK) modifications, the Michael adduct on cysteines, the double Michael adduct of lysines, the Michael adduct of histidine, the N-2-(4 hydroxy-tetrahydro-pyrimidyl) ornitine (propane-arginine, HTPO) and the Nε-(3-methylpyridinium)-lysine (MP-lysine) (Table 2).

Most of the ALEs generated by HNE were found both before or after enrichment, with the exception of few Michael adducts which were selectively retained by VC1 (not detected before enrichment) (Table 2). Interestingly, a novel + 138 Da adduct was detected on Arg209 and Arg485 with HNE (novel cyclic aduct, HNE-CY, Table 2). In agreement with the adducts which arginine yields with other RCS (as seen for ACR and MDA) and by considering the well-known reactivity of the guanidine function [see for example [28]) this adduct can be supposed to include a 2-amino pyrimidine scaffold even though its precise structural characterization would require additional studies.

3.4. Semi-quantitative analysis of ALE-HSA adducts

A semiquantitative analysis reporting the relative abundance of each modified peptide in respect of the native peptide was then carried out for each identified modification in both the input (% No VC1) and enriched samples (%VC1). The values were then used to calculate the enrichment factor (EF) calculated as reported in the method section. The values of the EF range between − 100 and + 100, where − 100 means that the modification has not been retained at all by the VC1 domain (it is only present in the input but not in the enriched sample), + 100 means that the modification has been identified because it is enriched by the VC1 (the modification is not detected in the input due to low abundance) and 0 means that they are equally distributed. Values between 0 and + 100 indicate that the modification is retained by VC1 and that the retention efficiency increases as the value increases above 0.

In Fig. 5, panels A, B and C show the EF for ALEs-lipox obtained by using MDA, ACR and HNE, respectively. Regarding MDA, an overview analysis indicates that most of the N-Propenal-Lys and NPO adducts are not retained, with a few exception, while DHPK modifications significantly increase the affinity of ALEs. As better described in the computational analysis paragraph the data indicate that for MDA, VC1 affinity is determined by the nature of the adduct.

In the case of ACR, with some exceptions explained in the following paragraph, the FDPK adduct is more effective in respect to the mono and bis Michael adducts in increasing the binding towards VC1. In the case of HNE, most of the identified adducts were not found to be effective in increasing the retention affinity with the exception of few residues.

3.5. Computational results

With a view to rationalizing the key factors influencing the RAGE binding of the monitored adducts, *in silico* studies were performed. They were focused on the adducts on arginine and lysine residues as formed by ACR and MDA since they are numerous, with a very broad range of affinity, thus allowing the development of clear structure-affinity relationships.

As a preamble it should be remembered that the RAGE-ligand interacting regions (i.e. the VC1 domain) are characterized by a rich set of positively charged residues especially in the V portion: the resulting positive RAGE surface shows an understandable non-specific affinity for acidic proteins which can bind RAGE by stabilizing extended sets of salt bridges. On these grounds, one may figure out that a given covalent adduct can induce RAGE binding via two major mechanisms: it can introduce acid moieties which directly contact the RAGE residues (as seen for example with CML and CEL adducts) or it can reduce the basicity of the adducted residues. In this second indirect mechanism, the adducts can elicit RAGE binding mostly because they are able to destabilize ionic clusters on the protein surface and to liberate negatively charged residues which enhance their accessibility and they become available to stabilize ion-pairs with the positive RAGE residues.

The here monitored covalent adducts do not introduce negative functions and thus they should induce RAGE binding by the second indirect mechanism. Such a hypothesis implies that the monitored RAGE binding might be explained by considering two major factors: the basicity of the formed adducts and the number of the surrounding negatively charged residues. Indeed, when the generated adduct retains a

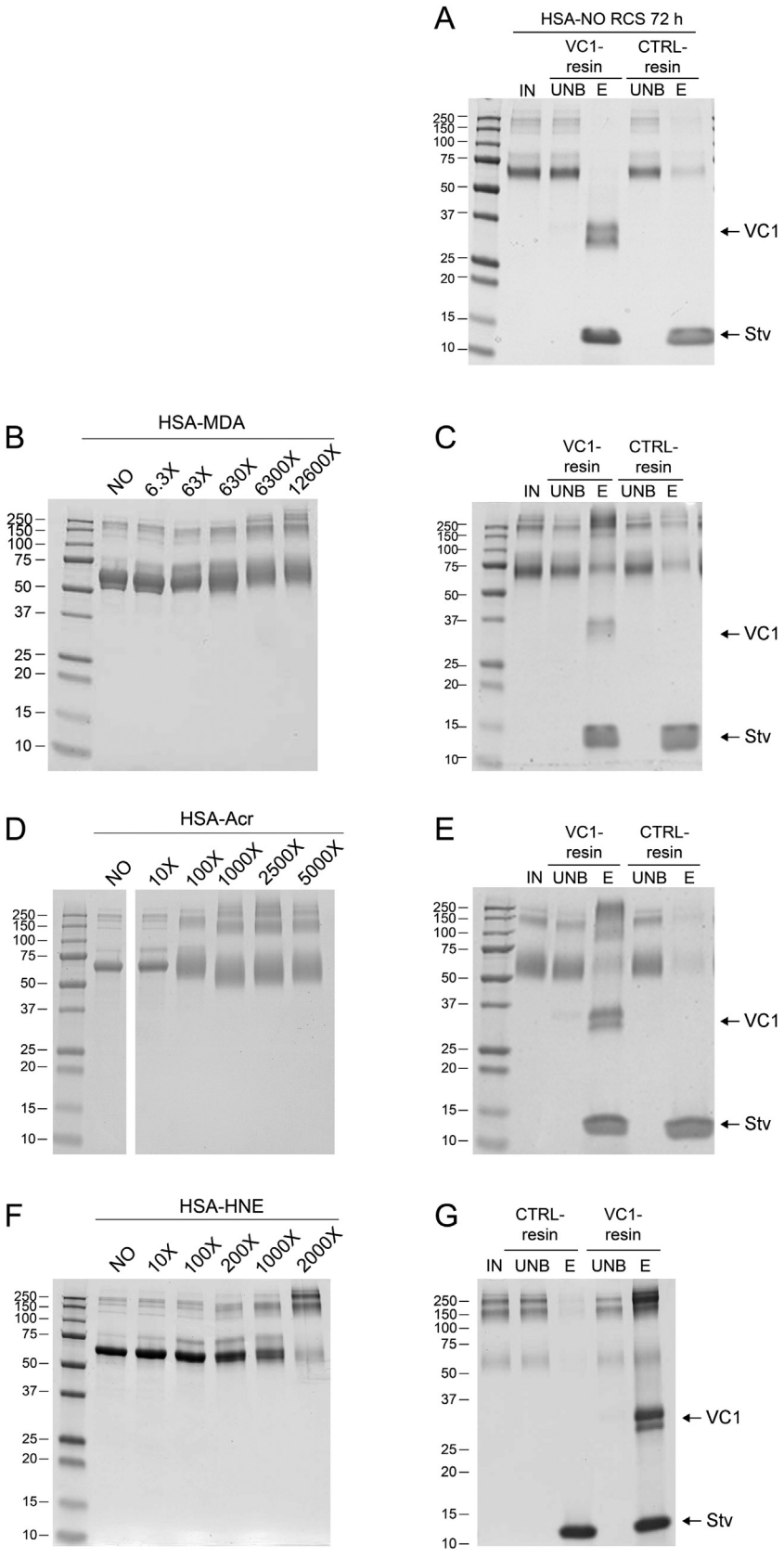

Fig. 3. Modified albumin obtained by incubation of recombinant HSA in the presence of different molar ratio of RCS and VC1 pull-down assay. A) VC1 pull-down assay with untreated HSA. SDS PAGE analysis followed by Coomassie staining of the modified HSA obtained by 72 h incubation with the indicated molar ratio of RCS (panel B: MDA; panel D: ACR; panel F: HNE). The highest molar ratio of HSA-MDA (1:12,600), HSA-ACR (1:5000) or HSA-HNE (1:2000) were used as input (IN) in the pull-down assays with the VC1 and control (CTRL)-resins. The IN fractions, the unbound fractions (UNB) and eluates (E) were analyzed by SDS-PAGE followed by Coomassie staining. The gels show that untreated HSA does not bind VC1 (panel A), whereas high MW species of HSA-MDA (panel C), HSA-ACR (panel E) and HSA-HNE (panel G) are retained by the VC1-resin, but not by the CTRL-resin. Since the elution is performed in denaturing conditions, this step removes any associated molecule from the resin, including the two VC1 glycovariants (34 and 36 kDa) and streptavidin (Stv, 14 kDa), indicated by arrows.

marked basicity which renders the protonated form still predominant at physiological pH, the surrounding negative residues would remain shielded around it and unavailable to contact the RAGE residues. On the other hand, an adduct devoid of surrounding negative residues would be unable to induce strong ionic contacts with RAGE regardless of its basicity. On these grounds the here reported *in silico* analyses can be subdivided into three steps: in the first, the basicity of the considered adducts was predicted by semi-empirical calculations; in the second,

Table 1
List of the PTMs identified on the indicated Amino acid residues in the ALEs samples obtained by in vitro incubation of HSA with RCS.

	PTMs	Amino Acid residue
MDA	*N-propenal-Lysine* **(NPK)**	Lys12, Lys20, Lys41, Lys162, Lys174, Lys212, Lys225, Lys233, Lys140, Lys262, Lys274, Lys281, Lys323, Lys359, Lys351, Lys372, Lys378, Lys389, Lys402, Lys414, Lys466, Lys475, Lys500, Lys525, Lys545, Lys564, Lys573, Lys574
	dihydropyridine-lysine **(DHPK)**	Lys41, Lys174, Lys225, Lys233, Lys274, Lys276, Lys313, Lys323, Lys359, Lys378, Lys389, Lys402, Lys466, Lys500, Lys519, Lys545, Lys573
	*N-2-pyrimidyl-ornithine (***NPO)**	Arg209, Arg218, Arg144, Arg145, Arg257, Arg337, Arg484
ACR	*Michael Adduct (N-propanal derivative)* **(ACR-MA)**	His39, Cys75, His128, Cys169, His338, Cys392, His510
	N-2-(4 hydroxy-tetrahydro-pyrimidyl) ornitine (propane-arginine, ***HTPO)***	Arg209, Arg257, Arg337
	N,N-bispropenal-Lysine **(2ACR-K-MA)**	Lys41, Lys73, Lys174
	N-(3-formyl-3,4-dehydro-piperidinyl) lysine **(FDPK)**	Lys174, Lys225, Lys233, Lys274, Lys323, Lys372, Lys378, Lys389, Lys500
HNE	*Michael adduct* (**HNE-MA**)	His105, Lys106, His242, His288, His338, Arg428
	Schiff Base (**HNE-SB**)	Lys106
	Novel cyclic adduct ***(HNE-CY)***	Arg209
	2-pentyl-pyrrole (**PP**)	Lys106
	2,3 dihydro-pentyl-furan (**DHPF**)	Cys53, His105, Cys448, Cys487

the number of surrounding negative residues was calculated by using the refined HSA structure and by considering the number of aspartates and glutamates in a 5 Å radius sphere around each adducted residue. Finally, protein-protein docking simulations were performed by considering the V-domain of RAGE and the adducted HSA structures. For simplicity, the docking simulations involved the HSA structure including simultaneously all found adducts. Such a strategy clearly reduces the computational time and allows synergistic effects between adjacent adducts to be revealed.

Fig. 6 shows the ALEs structures and for some of them reports the predicted basicity for the considered adducts and reveals that they can be subdivided into two main groups depending on whether they retain part of the basicity of the unmodified residues or become non-ionizable derivatives at physiological conditions. When focusing attention on arginine adducts, N-2-pyrimidyl-ornithine (NPO, from MDA) is completely neutral at physiological pH, while HTPO retains a large part of the arginines strong basicity. Similarly, and with regard to lysine adducts, the DHPK adduct (from MDA) is a neutral adduct, the single Michael adduct (N-Propenal lysine, from MDA) is slightly less basic than lysine ($\Delta = -0.6$), while the double Michael adduct and the FDPK derivative (from ACR) show a similarly reduced basicity ($\Delta = -2.0$) compared to the unmodified residue. In other words, and at physiological conditions, one may assume that (a) RP and DHPK adducts are always neutral, (b) HTPR and NP-lysine are still protonated, (c) double MA and FDPK are in equilibrium between the two forms and the neutral state can play a significant role.

This simple observation can explain: (a) why NPO is the only arginine adduct (considering both MDA and ACR) which shows some affinitive residues; (b) why the DHPK adducts show a retention efficiency markedly higher than N-propenal-lysines (among the MDA-induced lysine adducts) and (c) why double MA and FDPK show a comparable retention efficiency (among the ACR-induced lysine adducts). In general, one may conclude that the ionization properties of the monitored adducts play a pivotal role in determining their overall affinity towards RAGE, while the binding of each single adduct might be rationalized by considering its specific environment as discussed below.

Table S2 (supplementary material) compiles the number of negative residues included within a 5 Å radius sphere around each adducted residue and allows for some insightful considerations. With regard to neutral arginine adducts (NPO), Table S2 (supplementary materials) clearly evidences that the two highly affinitive adducts are surrounded by a markedly higher number of negative residues (5 for Arg10 and 4 for Arg472). Interestingly the other three NPO adducts showing a positive EF value (Arg117, Arg337 and Arg428) show 2 surrounding negative residues while all adducts with negative EF value show at most 1 residue.

The compiled results for lysine adducts appear to be less clear even though one may observe that almost all affinitive adducts possess more than 2 surrounding residues. The more difficult interpretability of the data concerning the lysine adducts can be explained by considering that (a) they include different adducts with different ionization properties and (b) some adducts (e.g. DHPK) can be directly involved in RAGE binding, thus requiring less surrounding negative residues. Moreover and due to the very high number of adducted lysines one may figure out synergistic effects between adjacent lysine adducts which may generate very extended ionic networks not conveniently described by considering 5 Å radius spheres.

Taken together, the obtained results seem to confirm that the MDA

Table 2
List of the PTMs identified on the indicated Amino acid residues in the ALEs-HSA samples retained by VC1.

	PTMs	Amino Acid residue
MDA	*dihydropyridine-lysine* **(DHPK)**	Lys41, Lys51, Lys195, Lys205, Lys233, Lys274, Lys276, Lys313, Lys359, Lys378, Lys389, Lys414, Lys432, Lys436, Lys466, Lys500, Lys541, Lys545, Lys560, Lys564, Lys574
	*N − 2-pyrimidyl-ornithine (***NPO)**	Arg10, Arg117, Arg144, Arg257, Arg337, Arg428, Arg472
ACR	*Michael Adduct (N-propanal derivative)* **(ACR-MA)**	Cys200, His338, His510
	N − 2-(4 hydroxy-tetrahydro-pyrimidyl) ornitine (propano-arginine, ***HTPO)***	Arg337
	N,N-bispropenal-Lysine **(2ACR-K-MA)**	Lys41
	N-(3-formyl − 3,4-dehydro-piperidinyl) lysine **(FDPK)**	Lys225, Lys233, Lys262, Lys274, Lys323, Lys372, Lys378, Lys389, Lys500, Lys545
	N-(3-Methylpyridinium)-lysine ***(MPK)***	Lys 233
HNE	*Michael adduct* (**HNE-MA**)	His105, Lys106, His242, Cys289, His288, His338, Arg428
	Schiff Base (**HNE-SB**)	Lys106
	Novel cyclic adduct ***(HNE-CY)***	Arg485
	2-pentyl-pyrrole (**PP**)	Lys106
	2,3 dihydro-pentyl-furan (**DHPF**)	His105, Cys476, Cys477, Cys487

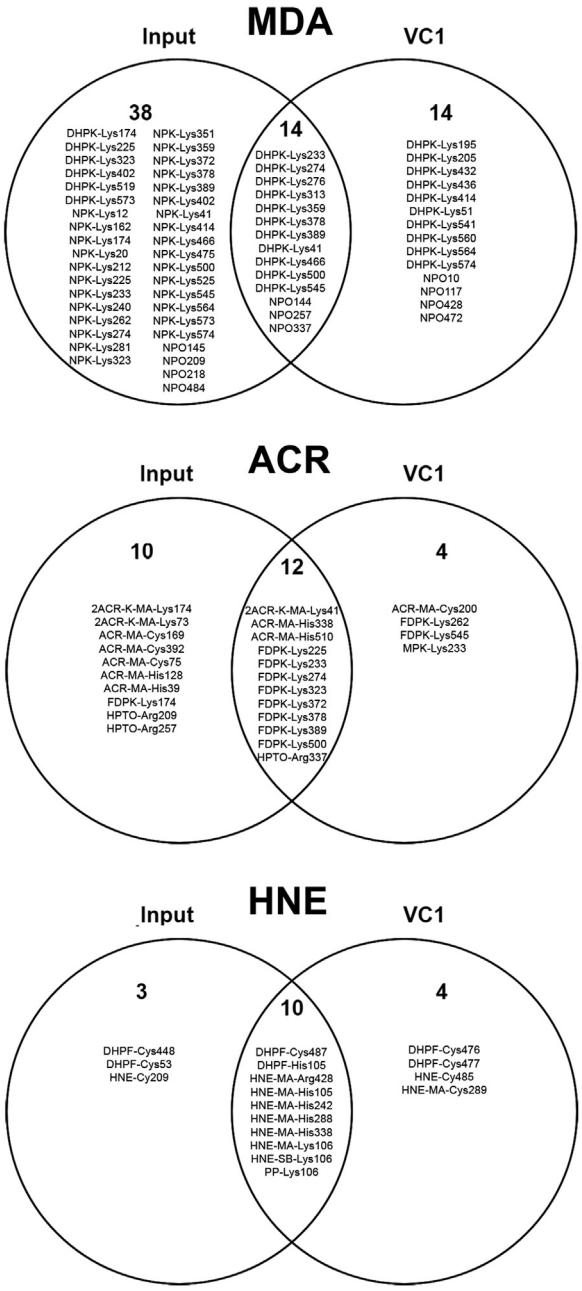

Fig. 4. Venn diagrams of the identified ALEs as reported in Table 1 and 2. ALEs are reported as the modified amino acid residues. The upper diagram refers to ALEs obtained by treating HSA with MDA, the middle with ACR and the lower with HNE. The input reports ALEs not retained by VC1 and present only in the input samples; VC1 are the ALEs identified only after VC1-enrichment; the intersections report the ALEs found both in the input and VC1-enriched samples.

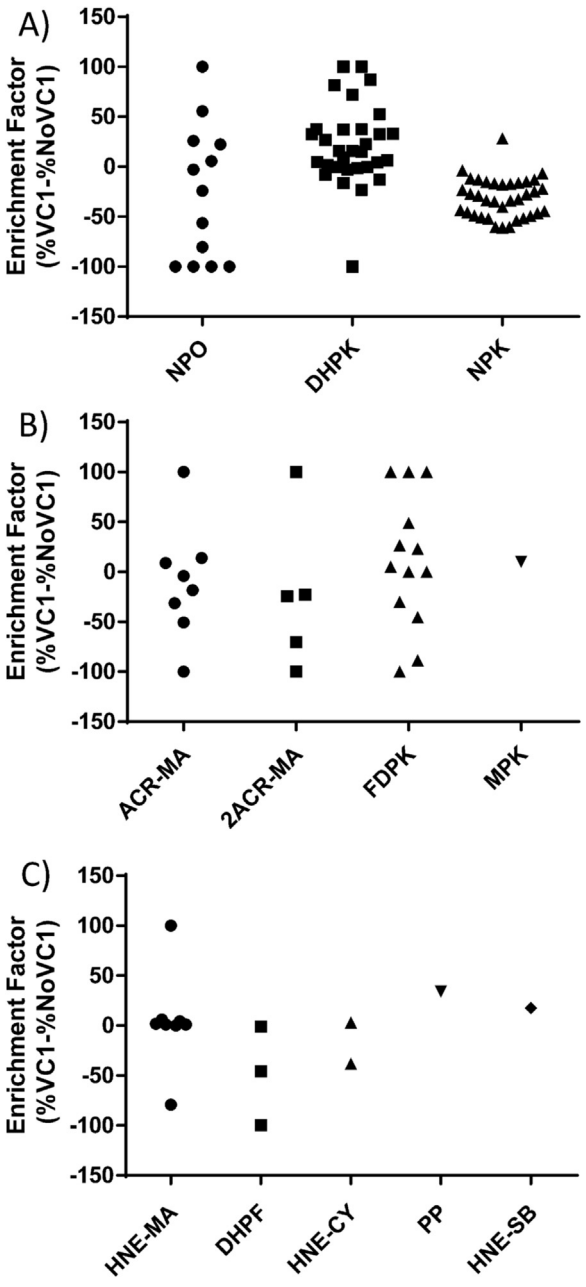

Fig. 5. Enrichment Factor (EF) graphical distribution. Enrichment Factor (EF) graphical distribution by means of vertical scatter plot overviewing the affinity of each identified ALEs towards VC1; all EF values spotted have been calculated as the differences between the relative abundance in the enriched sample minus the amount in the untreated one (Enrichment factor = %VC1-%NoVC1), and graphically grouped as: MDA-adducts (panel A), ACR-adducts (panel B) and HNE-adducts (panel C).

and ACR-induced adducts act as RAGE binders mostly when they occur in their neutral state at physiological pH and thus they are able to destabilize ionic clusters on protein surface and to liberate negatively charged residues which are no longer shielded and expose their carboxylate groups with a sort of "*flowering effect*" which promotes ion-pairing between adducted HSA and RAGE. With a view to confirming the supposed binding mechanism, the last part of these *in silico* studies involved protein-protein docking simulations which were performed to generate the corresponding RAGE-adducted HSA complexes. While avoiding a systematic analysis of all simulated HSA adducts, some representative putative complexes will be presented in order to further corroborate the proposed mechanism and to gain deeper insights on the involved interactions.

Fig. 7 (panel A) shows the putative complex as computed for the most affinitive NPO adduct (Arg472, from MDA) and reveals that the several negative residues surrounding the adduct are involved in an extended network of ion-pairs with the RAGE residues. In detail, Asp494 and Glu495 approach Arg70 of RAGE while Glu492 contacts RAGE-Lys90. Interestingly and although the RAGE surface is rich in positive residues, the complex also shows a salt bridge in which the positive residue comes from the HSA surface as seen in the salt bridge between RAGE-Glu88 and Arg410. It should be noted that also the simulated NPO adduct is found to elicit a charge transfer interaction with

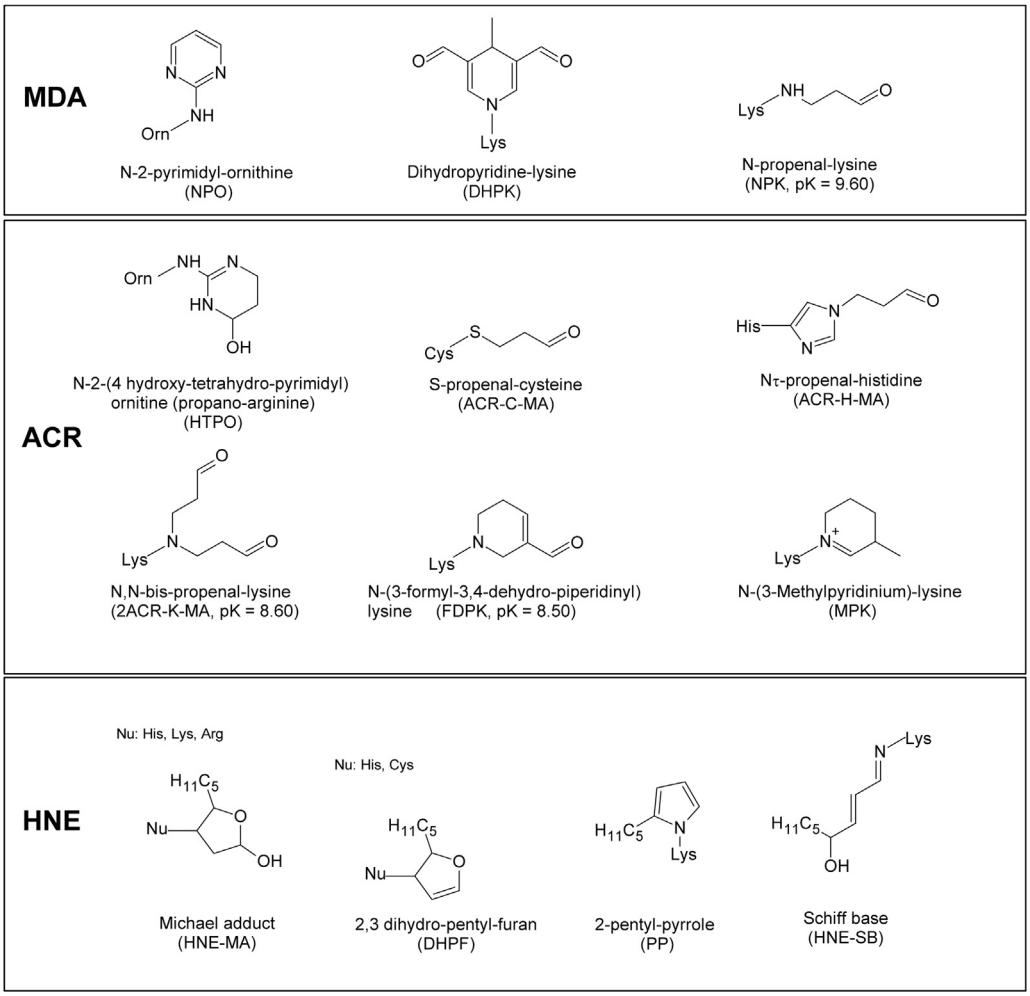

Fig. 6. Chemical structures of ALEs-lipox formed by incubating HSA with MDA, ACR and HNE and identified by MS. For some ALEs the pK values are reported in brackets.

RAGE-Arg78. In this way, the interaction surface between HSA and RAGE is stabilized by a rich set of ionic interactions which are clearly promoted by the neutralization of Arg472 and which can explain the observed RAGE binding.

Fig. 7 (panel B) shows the computed complex for a very affinitive DHPK adduct (Lys436, from MDA) and highlights the potential synergistic role between adjacent adducts as supposed above. Indeed, the complex reveals that Lys433 is closely surrounded by several other MDA-based adducts (i.e., DHPK432 and DHPK519 plus NPO-Arg117 and NPO-Arg428) which contribute to the overall binding by directly interacting with the RAGE residues (see for example the reinforced H-bonds that DHPK436 elicits with Arg78 and Arg94), and through the surrounding negative residues (not reported in Fig. 7 for clarity). The found ion-pairs include Arg78-Glu400, Arg94-Asp183, Lys80-Glu188 and Lys32-Glu396. Notably, all the reported adducts show a positive EF value apart from DHPK519, whose poor results can be ascribed to the shielding effect played by the close Arg186 residue and which further confirms the key role of the ionizable surrounding residues.

Finally, Fig. 7 panel C reports the putative complex for a highly affinitive FPDK adduct (on Lys262, from ACR) and emphasizes the key role played by the three negative residues surrounding it and which are involved in clear ionic interactions with the positive RAGE residues. Interestingly and despite such a favorable environment Lys262 does not give affinitive adducts with MDA. This finding can be explained by considering that Lys262 generates only the ionized N-propenal adduct with MDA. Such a result suggests that the ionization properties play a largely dominant role which cannot be counteracted by the surrounding negative residues. Remarkably, the figure describing the entire RAGE-HSA complex shows that the ionic contacts are not limited to the region surrounding the FPD adduct but additional salt bridges are present in the entire contact surface. This suggests that the RAGE-HSA binding is initially promoted by the focused set of ionic contacts which can be stabilized around the adduct and then is reinforced by a more extended set of additional ion-pairs which characterize the entire contact surface. Notably, these additional contacts which do not involve adducted residues are per se unable to promote the RAGE-HSA binding but they play a clearly beneficial role in that the initial binding is triggered by the contacts stabilized by the residues surrounding the adduct with a sort of hierarchical mechanism which brings to mind that described for protein folding.

Although the affinity of the HNE-based adducts was not analyzed in silico, the observed EF values of the peptides including Lys106 are in clear agreement with the basicity of the detected adducts. Indeed, the retention efficiency is found to be quite high for those adducts which abrogate the lysine basicity (i.e. Schiff base and 2-pentylpyrrole) to markedly decrease when the adduct only slightly reduces the basicity as in the Michael adduct.

Even though HSA is not the ideal protein target to study in-depth the RAGE binding on cysteines since most HSA cysteines are involved in disulfide bridges, the general incapacity of the cysteine adducts to bind RAGE can be clearly rationalized in terms of the proposed flowering effect. Carbonylation of cysteines does not result in neutralization of

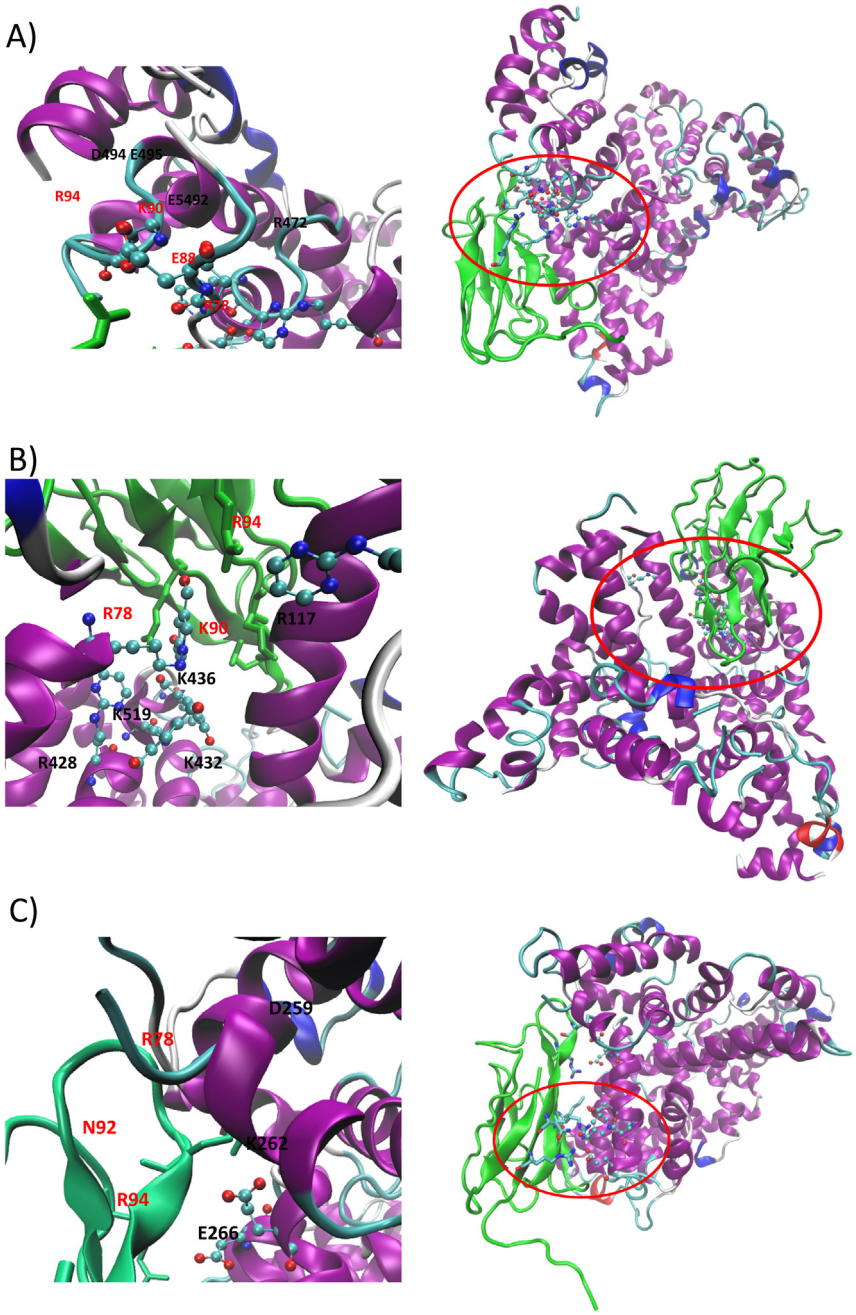

Fig. 7. Putative RAGE-HSA complex as computed by protein-protein docking and induced by RP-Arg472 (6 A), DHPK-Lys436 (6B) and FDP-Lys262 (6 C). For each simulated adduct, the right panel shows the entire RAGE-HSA complex while the left panel focuses on key interactions stabilized by the adduct and its surrounding residues.

positively charged residues but conversely it can neutralize particularly acid cysteines with an opposite and unfavorable electron-deficient effect on the protein surface

4. Discussion

Much evidence indicates that the pro-inflammatory and pro-fibrotic effects of AGEs and AGEs/ALEs are due, among other mechanisms, to RAGE binding and activation [18,29–31]. The engagement mechanisms between AGEs and RAGE are still not fully elucidated and great scientific interest is now focused on understanding which are the structural moieties of AGEs that turn a protein to a RAGE binder and hence to a pro-inflammatory mediator. The study is further complicated by the fact that AGEs and AGEs/ALEs are characterized by a wide heterogeneity not only due to the variability of the adducted moieties which differ on the basis of the attacking RCS but also due to the variable target protein and sites of modification.

A rich set of positively charged residues represents a structural feature of RAGE which could explain its binding properties with ligands [32]. In particular such positive charges result in a positive RAGE surface, which drives the engagement with ligands characterized by acidic or in general negatively charge residues, able to stabilize the protein-protein interaction by an extended set of salt bridges [33]. While considering that the RAGE binding is clearly promoted by those AGEs/ALEs, which are characterized by the presence of carboxylic moieties such as CML and CEL [13], the mechanisms, by which a local and structurally limited modification, such as that induced by a AGE/ALE adduct, can trigger the RAGE affinity in large biomacromolecules,

are still not precisely understood. This lack of understanding is even more pronounced when considering that many AGEs and almost all ALEs (see below) do not introduce acid functions but at most they modulate the basicity of the adducted residues.

While on one hand several studies have reported on the engagement between AGEs and AGEs/ALEs on VC1 and RAGE, on the other, little is known about the effect of ALEs from RCS formed only by lipid peroxidation such as HNE, MDA and ACR. These ALEs, here called ALEs-lipox, are formed abundantly in several oxidative based conditions and their damaging property has been widely reported. Several molecular mechanisms have been suggested to explain the ALEs-lipox damaging effect and among these are protein dysfunction, protein oligomerization, signal transduction and immune response [19]. Moreover, by considering a pro-inflammatory and pro-fibrotic response induced by ALEs-lipox, a RAGE dependent mechanism could also be considered.

In the present report we have evaluated the binding property of a wide set of ALEs-lipox formed by incubating HSA with the three most abundant lipid peroxidation RCS, namely HNE, ACR and MDA. The wide set of modifications were achieved by incubating the target protein with RCS at different molar ratios and time points as confirmed by MS intact protein analysis.

The high concentrations of the aldehydes and in particular their content in high molar excess in respect to the substrate, very far from biological conditions, were used in order to obtain the maximum number of adducts which can be generated from the reaction of RCS with the protein substrate. Although the resulting ALEs are not characterized by acid moieties, as reported in the literature and here confirmed by bottom-up analyses, we found using a VC1 pull-down assay that some of the generated ALEs bind to the VC1. This is a quite novel finding since to our knowledge no study has so far reported the ability of ALEs from lipid peroxidation RCS to interact with VC1. The VC1 binding assay coupled to a high resolution MS approach has also permitted the identification of which ALEs moieties are responsible for the VC1 binding and the sites of modification. The wide set of data and in particular the chemical diversity of the structures identified as binder and non binder, have also permitted a SAR study leading to the molecular explanation of why only some ALEs bind to VC1. As shown in Fig. 8, besides the well known VC1 engagement based on the acid residues of the protein ligand, we here found another potential mechanism which may involve adducts that do not introduce acid groups but only reduce the basicity of the modified residues. The mechanism, called *the flowering effect,* is based on a two-step process and involves exposed basic residues (mainly Lys and Arg) which in the non-adducted protein form a set of ionic bridges with the carboxylic groups of surrounding aspartate and glutamate residues. In the first step, the RCS form a covalent adduct with the positively charged residues, abolishing or greatly reducing their basicity. Consequently, the adducted residues are present in their neutral form at physiological conditions and such a change in their ionization state destabilizes the ionic bridges and renders the surrounding anionic residues more accessible and available to stabilize ion-pairs with the positive RAGE residues. Such a mechanism explains why only one set of the identified ALEs acts as RAGE binder. In other words we found the basic features that make an ALE a RAGE binder and which strictly depend on the type of the adduct and on the site of modification. In particular we found that only some of the several adducts formed by lipid peroxidation RCS abolish or greatly reduce the basicity of the target amino acids and among these RP (from MDA) and DHPK adducts are always neutral while HTPR, MA-Arg and NP-lysine do not affect the basic character. The second requirement is the presence of a cluster of negative side chains surrounding the target residue, which then becomes available to RAGE positive charges once the amino acid is modified, thus stabilizing the protein-protein complex.

We currently do not know whether ALEs-VC1 binding elicits RAGE activation and hence if they lead a RAGE-dependent biological response. Some studies such as that by Shanmugam et al. [34] reporting that ALEs from MDA can induce a RAGE dependent biological response, would suggest this. We are now working on this aspect by using cell models and ALEs enriched by the VC1 assay as potential RAGE activators.

5. Conclusions

In summary by using an integrated MS (intact protein and bottom-up approach) and computational approach we have found that some ALEs generated from lipid peroxidation RCS are RAGE binders. We have also found the basic features that ALEs from HNE, MDA and ACR must have to be a RAGE binder: 1) the covalent adducts should greatly reduce or abolish the basicity of the target amino acid, 2) the basic amino acid should be at the center of a set of carboxylic acids which, once the residue is modified, become available to freely contact the RAGE positive residues. Interestingly, the here proposed *flowering effect* can also be involved in the RAGE binding of the adducts which insert an acid function. Indeed and besides the direct contacts stabilized by the adduct, one may suppose that introduced anionic function exerts a similar effect on the surrounding negative residues thus promoting their ionic interactions with the positive residues on RAGE surface. Stated differently, the *flowering effect* might be a common mechanism triggering the affinity of adducted proteins towards RAGE even though it significantly increases its relevance for the adducts that do not add

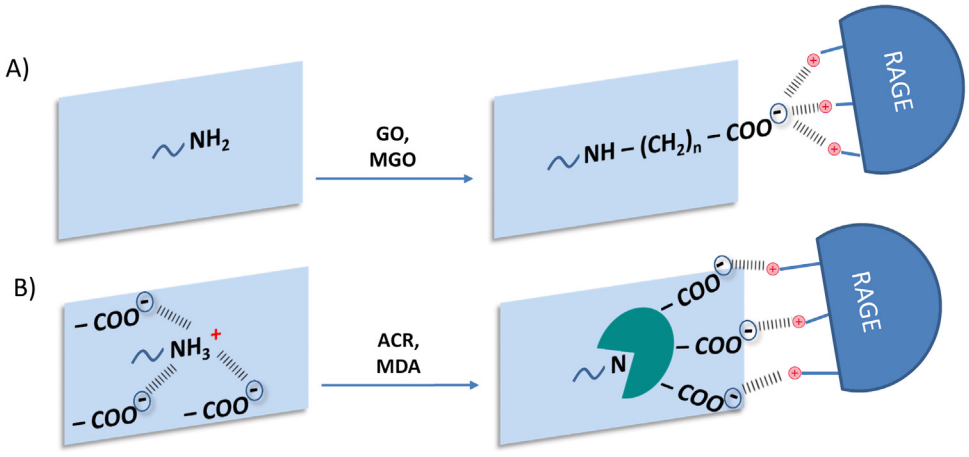

Fig. 8. Mechanism explaining AGEs/ALEs and ALEs-lipox binding to VC1. A) VC1 engagement based on the acid residues of the protein ligand. Such a mechanism occurs when RCS, such as GO and MGO react with the basic residue forming a carboxylated adduct (CML and CEL) which directly contacts the RAGE residues. B) Panel B summarizes the mechanism described in the present paper for explaining the binding of ALEs-lipox to VC1 and called the "*flowering effect*". It is based on a two-step process and involves exposed basic residues (mainly Lys and Arg) which in the non-adducted protein form a set of ionic bridges with the carboxylic groups of surrounding aspartate and glutamate residues. Lipid peroxidation derived RCS react with the basic residue and abolish or greatly reduce their basicity. Consequently, the adducted residues shift in a neutral form and such a change in the ionization state destabilizes the ionic bridges and renders the surrounding anionic residues more accessible and available to stabilize ion-pairs with the positive RAGE residues.

carboxylic functions such as those as seen here.

Moreover, one may expect that such a mechanism can modulate the affinity of carbonylated proteins towards a variety of target proteins not necessarily limited to RAGE. More generally and since a similar mechanism was proposed to explain the protein-protein interactions triggered by the acetylation of lysines, one may hypothesize that the ionic perturbation of the protein surface, that shifts from a polyzwitterionic situation to a polyanionic or polycationic condition, can be a general mechanism, by which post translational modifications involving ionizable side chains modulate the interacting capacity of the modified proteins.

Acknowledgements

This work has been funded by the European Union's Horizon 2020 research and innovation programme under the Marie Sklowdowska-Curie grant agreement number 675132 (http://cordis.europa.eu/project/rcn/198275_en.html).

Conflict of interest

GD, LP and GA are co-authors of a patent application (WO2016IB52391 20160427) entitled “Improved system for the expression of the receptor for the advanced glycation end products (AGEs) and the advanced lipid glycation end products (ALEs) and applications thereof”.

Appendix A. Supplementary material

Supplementary data associated with this article can be found in the online version at doi:10.1016/j.redox.2018.101083.

References

[1] F. Gueraud, M. Atalay, N. Bresgen, A. Cipak, P.M. Eckl, L. Huc, I. Jouanin, W. Siems, K. Uchida, Chemistry and biochemistry of lipid peroxidation products, Free Radic. Res. 44 (10) (2010) 1098–1124.

[2] G. Vistoli, D. De Maddis, A. Cipak, N. Zarkovic, M. Carini, G. Aldini, Advanced glycoxidation and lipoxidation end products (AGEs and ALEs): an overview of their mechanisms of formation, Free Radic. Res. 47 (Suppl 1) (2013) 3–27.

[3] G. Aldini, G. Vistoli, M. Stefek, N. Chondrogianni, T. Grune, J. Sereikaite, I. Sadowska-Bartosz, G. Bartosz, Molecular strategies to prevent, inhibit, and degrade advanced glycoxidation and advanced lipoxidation end products, Free Radic. Res 47 (Suppl 1) (2013) 93–137.

[4] M. Mol, L. Regazzoni, A. Altomare, G. Degani, M. Carini, G. Vistoli, G. Aldini, Enzymatic and non-enzymatic detoxification of 4-hydroxynonenal: methodological aspects and biological consequences, Free Radic. Biol. Med 111 (2017) 328–344.

[5] T. Curtis, The role lipid aldehydes and ALEs in the pathogenesis of diabetic retinopathy, Free Radic. Biol. Med 75 (Suppl 1) (2014) S8.

[6] A. Negre-Salvayre, C. Coatrieux, C. Ingueneau, R. Salvayre, Advanced lipid peroxidation end products in oxidative damage to proteins. Potential role in diseases and therapeutic prospects for the inhibitors, Br. J. Pharmacol. 153 (1) (2008) 6–20.

[7] C. Iacobini, S. Menini, C. Ricci, A. Scipioni, V. Sansoni, G. Mazzitelli, S. Cordone, C. Pesce, F. Pugliese, F. Pricci, G. Pugliese, Advanced lipoxidation end-products mediate lipid-induced glomerular injury: role of receptor-mediated mechanisms, J. Pathol. 218 (3) (2009) 360–369.

[8] S. Sasson, Nutrient overload, lipid peroxidation and pancreatic beta cell function, Free Radic. Biol. Med 111 (2017) 102–109.

[9] E.J. Anderson, G. Vistoli, L.A. Katunga, K. Funai, L. Regazzoni, T.B. Monroe, E. Gilardoni, L. Cannizzaro, M. Colzani, D. De Maddis, G. Rossoni, R. Canevotti, S. Gagliardi, M. Carini, G. Aldini, A carnosine analog mitigates metabolic disorders of obesity by reducing carbonyl stress, J. Clin. Invest (2018).

[10] C. Iacobini, S. Menini, C. Blasetti Fantauzzi, C.M. Pesce, A. Giaccari, E. Salomone, A. Lapolla, M. Orioli, G. Aldini, G. Pugliese, FL-926-16, a novel bioavailable carnosinase-resistant carnosine derivative, prevents onset and stops progression of diabetic nephropathy in db/db mice, Br. J. Pharmacol. 175 (1) (2018) 53–66.

[11] W. Łuczaj, A. Gęgotek, E. Skrzydlewska, Antioxidants and HNE in redox homeostasis, Free Radic. Biol. Med 111 (2017) 87–101.

[12] H. Vlassara, Y.M. Li, F. Imani, D. Wojciechowicz, Z. Yang, F.T. Liu, A. Cerami, Identification of galectin−3 as a high-affinity binding protein for advanced glycation end products (age): a new member of the age-receptor complex, Mol. Med 1 (6) (1995) 634–646.

[13] J. Xue, V. Rai, D. Singer, S. Chabierski, J. Xie, S. Reverdatto, D.S. Burz, A.M. Schmidt, R. Hoffmann, A. Shekhtman, Advanced glycation end product recognition by the receptor for ages, Structure 19 (5) (2011) 722–732.

[14] N. Grossin, M.P. Wautier, J. Picot, D.M. Stern, J.L. Wautier, Differential effect of plasma or erythrocyte AGE-ligands of RAGE on expression of transcripts for receptor isoforms, Diabetes Metab. 35 (5) (2009) 410–417.

[15] C. Ott, K. Jacobs, E. Haucke, A. Navarrete Santos, T. Grune, A. Simm, Role of advanced glycation end products in cellular signaling, Redox Biol. 2 (2014) 411–429.

[16] I. González, J. Romero, B.L. Rodríguez, R. Pérez-Castro, A. Rojas, The immunobiology of the receptor of advanced glycation end-products: trends and challenges, Immunobiology 218 (5) (2013) 790–797.

[17] K. Kierdorf, G. Fritz, RAGE regulation and signaling in inflammation and beyond, J. Leukoc. Biol. 94 (1) (2013) 55–68.

[18] J.W. Baynes, Chemical modification of proteins by lipids in diabetes, Clin. Chem. Lab. Med. 41 (9) (2003) 1159–1165.

[19] G. Aldini, I. Dalle-Donne, R.M. Facino, A. Milzani, M. Carini, Intervention strategies to inhibit protein carbonylation by lipoxidation-derived reactive carbonyls, Med. Res. Rev. 27 (6) (2007) 817–868.

[20] G. Degani, A.A. Altomare, M. Colzani, C. Martino, A. Mazzolari, G. Fritz, G. Vistoli, L. Popolo, G. Aldini, A capture method based on the VC1 domain reveals new binding properties of the human receptor for advanced glycation end products (RAGE), Redox Biol. 11 (2017) 275–285.

[21] M. Colzani, A. Criscuolo, G. Casali, M. Carini, G. Aldini, A method to produce fully characterized ubiquitin covalently modified by 4-hydroxy-nonenal, glyoxal, methylglyoxal, and malondialdehyde, Free Radic. Res 50 (3) (2016) 328–336.

[22] Z. Zhang, A.G. Marshall, A universal algorithm for fast and automated charge state deconvolution of electrospray mass-to-charge ratio spectra, J. Am. Soc. Mass Spectrom. 9 (3) (1998) 225–233.

[23] G. Degani, M. Colzani, A. Tettamanzi, L. Sorrentino, A. Aliverti, G. Fritz, G. Aldini, L. Popolo, An improved expression system for the VC1 ligand binding domain of the receptor for advanced glycation end products in Pichia pastoris, Protein Expr. Purif. 114 (2015) 48–57.

[24] J.J. Stewart, Optimization of parameters for semiempirical methods VI: more modifications to the NDDO approximations and re-optimization of parameters, J. Mol. Model 19 (1) (2013) 1–32.

[25] A. Pedretti, L. Villa, G. Vistoli, VEGA: a versatile program to convert, handle and visualize molecular structure on windows-based PCs, J. Mol. Graph. Model. 21 (1) (2002) 47–49.

[26] J.C. Phillips, R. Braun, W. Wang, J. Gumbart, E. Tajkhorshid, E. Villa, C. Chipot, R.D. Skeel, L. Kalé, K. Schulten, Scalable molecular dynamics with NAMD, J. Comput. Chem. 26 (16) (2005) 1781–1802.

[27] E. Katchalski-Katzir, I. Shariv, M. Eisenstein, A.A. Friesem, C. Aflalo, I.A. Vakser, Molecular surface recognition: determination of geometric fit between proteins and their ligands by correlation techniques, Proc. Natl. Acad. Sci. USA 89 (6) (1992) 2195–2199.

[28] W. Guo, Base mediated direct C–H amination for pyrimidines synthesis from amidines and cinnamaldehydes using oxygen as green oxidants, Chin. Chem. Lett. 27 (1) (2016) 4.

[29] S. Del Turco, G. Basta, An update on advanced glycation endproducts and atherosclerosis, Biofactors 38 (4) (2012) 266–274.

[30] R. Ramasamy, S.J. Vannucci, S.S.D. Yan, K. Herold, S.F. Yan, A.M. Schmidt, Advanced glycation end products and RAGE: a common thread in aging, diabetes, neurodegeneration, and inflammation, Glycobiology 15 (7) (2005) 16R–28R.

[31] M. Takeuchi, J. Takino, S. Yamagishi, Involvement of the Toxic AGEs (TAGE)-RAGE System in the Pathogenesis of Diabetic Vascular Complications: a Novel Therapeutic Strategy, Curr. Drug Targets 11 (11) (2010) 1468–1482.

[32] H. Park, F.G. Adsit, J.C. Boyington, The 1.5 Å crystal structure of human receptor for advanced glycation endproducts (RAGE) ectodomains reveals unique features determining ligand binding, J. Biol. Chem. 285 (52) (2010) 40762–40770.

[33] M. Koch, S. Chitayat, B.M. Dattilo, A. Schiefner, J. Diez, W.J. Chazin, G. Fritz, Structural basis for ligand recognition and activation of RAGE, Structure 18 (10) (2010) 1342–1352.

[34] N. Shanmugam, J.L. Figarola, Y. Li, P.M. Swiderski, S. Rahbar, R. Natarajan, Proinflammatory effects of advanced lipoxidation end products in monocytes, Diabetes 57 (4) (2008) 879–888.

Appendix A

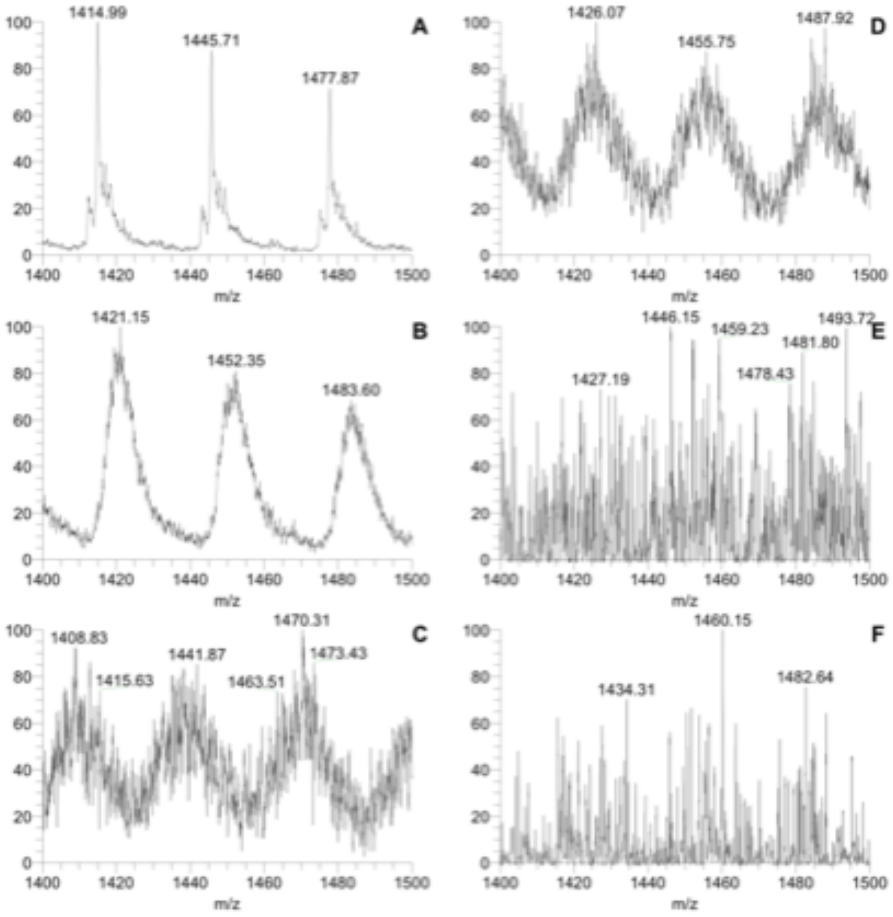

Supplementary Figure 1. Direct infusion ESI-MS analysis of native and ACR-modified HSA. Spectra of HSA with charge 47 + , 46 + and 45 + are shown. A) Native HSA shows a sharp intense peak with multiple low abundant peaks. When HSA is reacted with increasing concentrations of ACR, 1: 10 (B), 1: 100 (C), 1: 1000 (D), 1: 2500 (E) and 1: 5000 (F), the sharp peak diminishes and new peaks appear, confirming that HSA has been modified with different adducts of ACR.

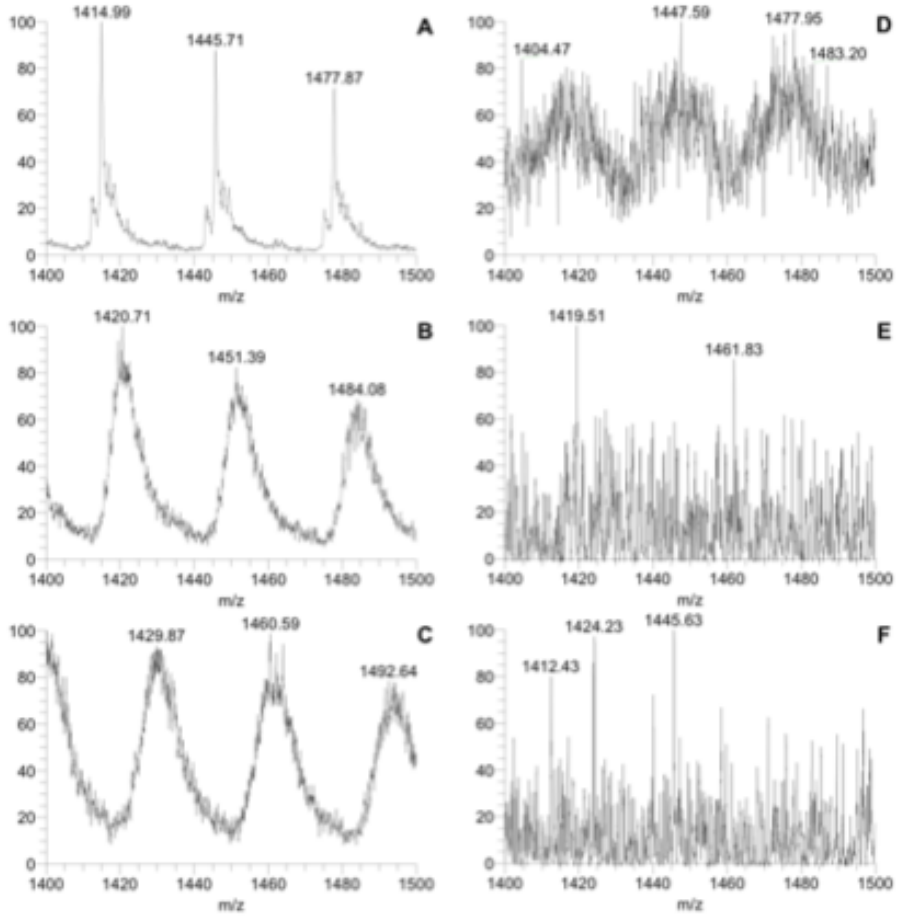

Supplementary Figure 2. Direct infusion ESI-MS analysis of native and MDA-modified HSA. Spectra of HSA with charge 47 + , 46 + and 45 + are shown. A) Native HSA shows a sharp intense peak with multiple low abundant peaks. When HSA is reacted with increasing concentrations of MDA, 1: 6.3 (B), 1: 63 (C), 1: 630 (D), 1: 6.300 (E) and 1: 12.600 (F), the sharp peak diminishes and new peaks appear, confirming that HSA has been modified with different adducts of MDA.

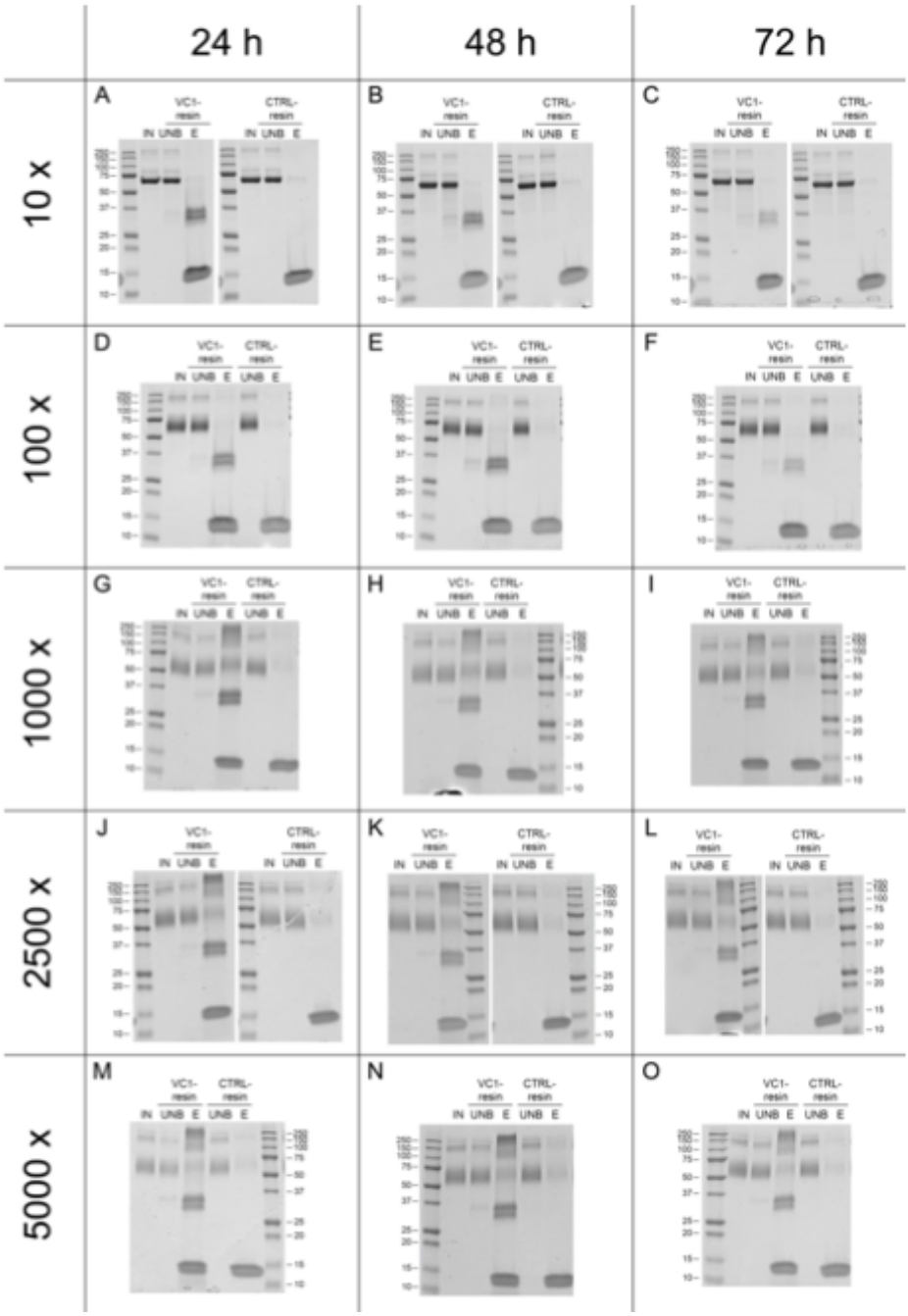

Supplementary Figure 3: Time course analysis of the dose-dependent modification of HSA by ACR. Recombinant HSA was incubated with increasing concentrations of ACR (molar ration HSA-ACR from 1:10–1:5000) as reported in Materials and methods. At 24, 48 and 72 h of incubation, aliquots were withdrawn and after removal of free acrolein, pull-down assays with the VC1-resin or control (CTRL)-resin were performed. A specific binding of both the monomer of modified HSA and of the HMW-species to the VC1-resin was detected at increasing concentrations, starting from the molar ratio 1:1000.

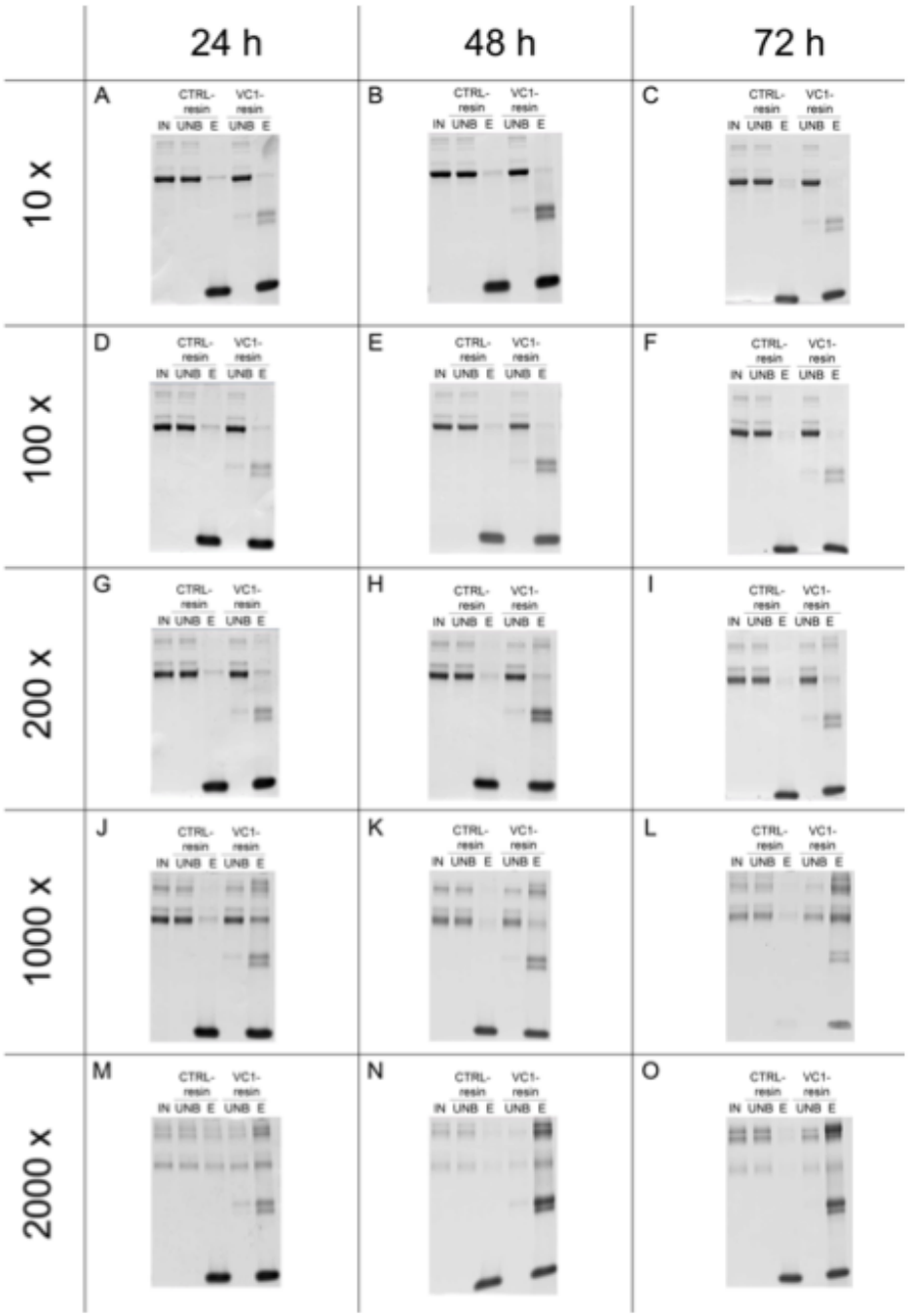

Supplementary Figure 4: Analysis of the dose-dependent modification of HSA by HNE. Recombinant HSA was incubated with increasing concentrations of HNE (molar ration HSA-HNE from 1:10–1:2000) as reported in Materials and methods. At 24, 48 and 72 h of incubation, aliquots were withdrawn and after removal of free HNE, pull-down assays with the VC1-resin or control (CTRL)-resin were performed. A specific binding of modified HSA to the VC1-resin was detected at increasing concentrations, starting from the molar ratio 1:200. At 1:1000 is evident the interaction with VC1 of both the monomer of modified HSA and the HMW-species.

Table S1. Known (literature based) covalent adducts induced by HNE, MDA and ACR and set as variable modifications within the PD parameters for the identification and localization of ALE-deriving adducts.

HNE

PTM	AA Res. Involved	ΔM
Michael adduct (**HNE-MA**)	Cys His Lys Arg	+ 156.110502 Da
Schiff Base (**HNE-SB**)	Lys Arg	+ 138.01446 Da
2-pentilpyrrole (**PP**)	Lys Arg	+ 120.0939 Da
Dehydropentylfuran (**DHPF**)	Cys His Lys Arg	+ 138.10446 Da

MDA

PTM	AA Res. Involved	ΔM
N-propenal-Lysine **(NPK)**	Lys	+ 54.01056 Da
Di-dihydropyridine-lysine **(DHPK)**	Lys	+ 134.03678 Da
*Malondialdehyde argpyrimidine***(MDA-RP)**	Arg	+ 36.0000 Da

ACR

PTM	AA Res. Involved	ΔM
Michael Adduct (propanal derivative) **(ACR-MA)**	Cys Lys His	+ 56.02621 Da
Hydroxy-tetra-hydropyrimidine (Propane-arginine) (HTPR) (**HTPR)**	Arg	+ 56.02621 Da
Double Michael Adduct **(2ACR-KMA)**	Lys	+ 112.05243 Da
Schiff Base (**ACR-SB**)	Lys	+ 38.01565 Da
Formyl-dehydro-piperidyl-lysine **(FDPK)**	Lys	+ 94.04186 Da
Methylpyridine-lysine **(MPK)**	Lys	+ 77.03912 Da

Table S2 - Number of negatively charged residues found within a 5Å radius sphere around the adducted residues

Adducted residue	n. of negative residues	Adducted residue	n. of negative residues
Arg 10	5	Lys 276	2
Arg 117	2	Lys 281	2
Arg 144	1	Lys 313	2
Arg 145	1	Lys 323	2
Arg 209	1	Lys 351	2
Arg 218	1	Lys 359	2
Arg 257	1	Lys 372	3
Arg 337	2	Lys 378	4
Arg 428	2	Lys 389	2
Arg 472	4	Lys 402	1
Arg 484	0	Lys 414	2
Lys 12	2	Lys 432	2
Lys 20	5	Lys 436	2
Lys 41	3	Lys 466	1
Lys 51	2	Lys 475	1
Lys 106	2	Lys 500	2
Lys 162	2	Lys 519	2
Lys 174	1	Lys 525	3
Lys 195	1	Lys 541	2
Lys 205	1	Lys 545	3
Lys 212	1	Lys 560	3
Lys 225	2	Lys 564	3
Lys 233	1	Lys 573	2
Lys 240	3	Lys 574	2
Lys 262	3		
Lys 274	3		

Chapter VI: Analysis of AGEs/ALEs in plasma samples

This Chapter will be submitted to *Free Radical Research* entitled: “Identification of low-abundant AGEs/ALEs in plasma of heart-failure patients using Orbitrap Fusion.”.

Publication expected: December 2019.

Chapter VI – Analysis of AGEs/ALEs in plasma samples

Abstract

Advanced Glycation/Lipoxidation End Products (AGEs/ALEs) are protein adducts arising from oxidative degradation pathways and have been described in the onset/progress of many pathologies, including diabetes and cardiovascular diseases. Many techniques have been set up already in order to identify and characterize AGEs/ALEs, nonetheless it remains very challenging since they are contained in very low amounts in plasma samples. Previously, we set up the VC1 pull-down, based on the Receptor for Advanced Glycation End Products (RAGE), to enrich AGEs/ALEs in-vitro. This project focused on validating the use of this technique for ex-vivo samples, such as healthy human plasma oxidized by the radical initiator AAPH, or incubated with RCS directly to produce AGEs/ALEs. Unfortunately, the VC1 pull-down with the current methods was not sufficient for identifying AGEs/ALEs. Therefore, other parameters were optimized throughout the sample preparation and analysis, including the use of the newest generation MS and solely focusing on HSA. For this purpose, plasma of heart failure patients was used, characterized by an increase of circulating AGEs/ALEs, and we determined 21 unique AGEs/ALEs in heart failure patients compared to control subjects. In conclusion, this project describes for the first time a large number of identified protein adducts in plasma samples.

6.1. Introduction

The identification and characterization of Post-Translational modifications (PTMs) has become more important over the last decades due to increasing exogenous influences, including exposure to UV light, tobacco smoke, exhaust fumes and ingestion of processed foods. Exposure to UV light causes direct oxidation, whereas tobacco smoke, exhaust fumes and processed foods contain many reactive carbonyl species (RCS) and/or reducing sugars. These compounds can adduct for example proteins, forming the so-called Advanced Glycation/Lipoxidation End Products (AGEs/ALEs). AGEs/ALEs can lead to detrimental effects as described already in many pathologies, such as diabetes, cardiovascular and neurodegenerative diseases. Therefore, much research is focused on optimizing methods for easier detection of AGEs/ALEs, since they are present in very low amounts, yet can contribute to disease onset and/or progression. Due to the low presence, various enrichment techniques have been described to aid the identification, like the aldehyde reactive probe (ARP) which have been shown to be successful in enriching carbonylated proteins/peptides from samples [1]. However, AGEs/ALEs also contain chemical moieties without a carbonyl and therefore will be missed by this enrichment. Previously, we have set-up a functional enrichment procedure, based on an affinity chromatography technique using

the Receptor for Advanced Glycation End Products (RAGE) [2]. This enrichment technique, the VC1 pull-down assay, has shown positive results for enriching well-known in-vitro produced AGEs/ALEs [3]. Nevertheless, it is still unclear whether circulating AGEs/ALEs in plasma can be enriched using this technique. Furthermore, it remains to be elucidated which proteins turning into AGEs/ALEs become a binder for RAGE and most likely contribute to the particular pathology.

Besides enrichment strategies, very sensitive mass spectrometers are vital in order to obtain a comprehensive characterization of AGEs/ALEs. Much progress has been made since the introduction of the most sensitive mass analyzer available, the orbitrap, yet another improvement has increased the sensitivity of identifying peptides with the introduction of the newest generation of tribrid mass spectrometers [4]. The Orbitrap Fusion provides besides the increased resolution, also faster MS detectors, parallel scanning and detection mechanisms and multiple fragmentation technique, which can aid the identification of PTMs. This combination makes the Orbitrap tribid MS by far the best instrument for identifying and characterizing AGEs/ALEs.

Good models are essential for validating the use of new enrichment techniques or instruments. Such as inducing the production of AGEs/ALEs in healthy human plasma in-vitro. 2,2'-Azobis(2-amidinopropane) dihydrochloride (AAPH) is a radical initiator and could potentially lead to the production of RCS in plasma and the subsequent adduction to proteins forming AGEs/ALEs. Likewise, plasma could be directly incubated with the most abundant RCS known, such as 4-hydroxy-2-nonenal (HNE), malondialdehyde (MDA) and acrolein (ACR). Preferably, plasma samples from different pathologies would be the best model, known to have an increase in AGEs/ALEs, since forcing oxidation in-vitro could lead to an excess of AGEs/ALEs, and/or non-physiological AGEs/ALEs. For this purpose, plasma samples from heart-failure (HF) patients would be more accurate to use for better validation of the methods, due to the physiological increase of AGEs/ALEs in these patients [5]. HF is characterized by the decrease in blood flow due to degeneration of the heart muscle that can be caused by various reasons, including myocardial infarction, coronary artery disease, high blood pressure and more. AGEs can contribute to the disease either via cross-links of extracellular matrix proteins or by interacting with AGE-receptors.

This study aimed to validate the enrichment technique, VC1 Pull-Down, and to identify novel AGEs/ALEs as RAGE binders. Furthermore, the Orbitrap Fusion was used for extensive mapping of AGEs/ALEs due to the better performance of the instrument.

6.2. Materials and methods

6.2.1. Reagents

Formic acid (FA), trifluoroacetic acid (TFA) and acetonitrile (ACN) were LC-MS grade; sodium dodecyl sulfate (SDS), ammonium bicarbonate, malondialdehyde tetrabutylammonium salt (MDA), acrolein (ACR), glyoxal (GO), methylglyoxal (MG), HEPES, NaCl, sodium dihydrophosphate, disodium phosphate, 2′,7′-Dichlorofluorescin diacetate (DCFH-DA), 2,2'-Azobis(2-amidinopropane) dihydrochloride (AAPH) and all other chemicals were analytical grade and purchased from Sigma-Aldrich (Milan, Italy). 4-Hydroxy-2-trans-nonenal dimethylacetal (HNE-DMA, catalog Number H9538) and recombinant HSA expressed in *P. pastoris* were purchased from Sigma Aldrich (Milan, Italy). Streptavidin- coated magnetic beads (Streptavidin Mag Sepharose™) were purchased from GE Healthcare (Milan, Italy). Protein carbonyl fluorometric assay kit and protein carbonyl immunoblot kit were purchased from Cell Biolabs-OxiSelect™ (San Diego, USA). Ultrapure water was prepared by a Milli-Q purification system (Millipore, Bedford, MA, USA). Any KD ™ Mini Protean® TGX ™ precast gel, Standard Precision Plus prestained protein standards, Laemmli sample buffer (2 ×/ 4 ×), Running buffer and Bio-Safe Coomassie, together with the threo-1,4- Dimercapto-2,3-butanediol (DTT) and iodoacetamide (IAA) were supplied by Bio-Rad Laboratories, Inc. Pierce™ Albumin Depletion Kit was purchased from Thermo Fisher Scientific (Milam, Italy). Trypsin and chymotrypsin sequencing grade was purchased from Roche Diagnostics SpA (Monza, Italy). Digestion buffer was 50mM ammonium bicarbonate; destaining solution was prepared mixing acetonitrile with digestion buffer (1:1 v/ v); reducing solution was 10 mM DTT in digestion buffer; alkylating solution was 55 mM iodoacetamide in digestion buffer; extraction solution was prepared as follows: 3% TFA/30% ACN in H_2O MilliQ.

6.2.3 Blood collection

Blood was collected from a subset of healthy subjects (8) and HF stage III patients (9) matched according to their age, sex, and clinical characteristics. Blood was collected into pre-cooled sample tubes containing EDTA and immediately spun down for 10 minutes, 2000 × g, at 4 °C to obtain plasma as supernatant. Plasma of healthy individuals was pooled and marked as control. Also plasma of HF patients was pooled and marked as HF.

6.2.4 In-vitro oxidation of plasma

Blood was collected from two healthy individuals into pre-cooled sample tubes containing EDTA and immediately spun down for 10 minutes, 2000 × g, at 4 °C to obtain plasma as supernatant. Plasma samples were pooled and diluted in PBS containing different concentrations of AAPH and incubated in the dark at 37°C while shaking at 450 rpm. At different timepoints, the reactions were

stopped by removing excess of AAPH by ultrafiltration using Amicon Ultra filter units 0.5 ml, cut-off 3 kDa (Millipore). Bradford assay was used to determine protein concentration, and samples were used immediately or stored at -80°C.

6.2.5 Plasma incubation with RCS

Different concentrations of HNE, ACR, GO, MG and MDA were added to plasma samples separately and incubated in the dark at 37°C while shaking at 450 rpm. After 6 hours, the reactions were stopped by removing excess of each RCS by ultrafiltration using Amicon Ultra filter units 0.5 ml, cut-off 3 kDa (Millipore). Differently treated plasma samples were pooled together and Bradford assay was used to determine protein concentration. Samples were used immediately or stored at -80°C.

6.2.6 Measurement of plasma oxidation

Plasma oxidation was measured fluorometrically using DCFH [6]. DCFH was prepared from DCFH-DA by basic hydrolysis. Briefly 500 µl of DCFH-DA stock solution (1 mM) was mixed with 2 ml of NaOH (0.01 N at 4°C) for 20 min. while protected from the light. The mixture was then neutralized with 2 ml of HCl (0.01 N), diluted with PBS to a final concentration of 10 µM and stored in ice for no longer than 8 h (working solution); an aliquot of 20 µl was added to 40 µl of plasma and then diluted to a final volume of 200 µl PBS containing different concentrations of AAPH in triplicate in a 96-well plate. Plasma oxidation was measured monitoring the 2-electron oxidation of DCFH to the highly fluorescent compound 2',7'-dichlorofluorescein (DCF). Fluorescence was measured at different timepoints using a multilabel, multitask plate reader (Victor-1420 Multilabel Counter; Wallac, Turku, Finland) and excitation wavelength (λex) was set at 485 nm and emission (λem) at 535 nm.

6.2.7 Protein carbonyl measurement

Oxidized plasma samples were analyzed for protein carbonyl content using two different commercial assays, protein carbonyl fluorometric assay kit and protein carbonyl immunoblot kit from Cell Biolabs-OxiSelect^{TM} (San Diego, USA). Protein carbonyls were determined fluorometrically (485 nm excitation/535 nm emission) following manufacturer's instructions. Protein carbonyls were also determined by immunoblotting according to the manufacturer's protocol.

6.2.8 VC1 pull-down assay

VC1-His-Strep was expressed and purified from Pichia pastoris culture supernatant as previously described [7]. The recombinant protein was immobilized on streptavidin-coated magnetic beads

by exploiting the affinity of the Strep tag towards streptavidin. In order to obtain the VC1-resin, 100 µg of purified VC1-His-Strep in 340 µl of 20 mM HEPES pH 7.1, 100 mM NaCl were added to 10 µl of packed streptavidin coated-beads, previously equilibrated with the same buffer. A volume of 340 µl of 20 mM HEPES pH 7.1, 100 mM NaCl were added to the same amount of beads in a different tube in order to obtain the Control-resin. After 1 h of incubation at 4 °C on a rotary mixer, the unbound material was carefully removed and the magnetic beads were washed twice with 500 µl of buffer (20 mM HEPES pH 7.1, 100 mM NaCl). The VC1- and Control- resin were incubated for 1 h at 4 °C with 320 µl of plasma or plasma treated with RCS at the concentration of 5 mg ml−1 in 20 mM HEPES pH 7.1, 100 mM NaCl. The unbound material was carefully removed and the beads were washed three times with 500 µl of Buffer (20 mM HEPES pH 7.1, 100 mM NaCl). The elution was performed by boiling the beads for 5 min in 15 µl of Laemmli Sample Buffer 4x mixed with 400 mM DTT, then with other 15 µl of buffer (20 mM HEPES pH 7.1, 100 mM NaCl). The two eluates were pooled.

6.2.9 HSA extraction

HSA extraction was performed using the Pierce™ Albumin Depletion Kit according to the manufacturer's recommendations. Briefly, 50µL of plasma was applied to equilibrated resin (25mM Tris-HCl, 75mM NaCl, pH 7.5 (equilibration/ washing buffer)) supplied in the kit and incubated for 2 min. at RT. Flow through was collected by centrifugation at 12,000 x g for 1 min. and reapplied to the column. Column was washed with 50 µL of buffer for 5 times. To elute bound albumin, resin was washed with 200µL of 20mM sodium phosphate, 250mM sodium thiocyanate, pH 7.2. Beads were spun at 12,000 x g for 1 min. and F-T was collected. This was repeated 4 additional times. All fractions were collected and analyzed by SDS-PAGE.

6.2.10 Reduction with sodium borohydride

Extracted HSA was diluted to 20 µM with PBS and incubated with sodium borohydride at a final concentration of 5 mM. The reaction was then incubated at room temperature for 60 min. The reaction was stopped by removing excess of sodium borohydride by ultrafiltration using Amicon Ultra filter units 0.5 ml, cut-off 3 kDa (Millipore), followed by in-solution digestion.

6.2.11 Intact protein analysis by MS

Plasma was analyzed by direct infusion on a triple-quadrupole (TQ) mass spectrometer (Finnigan TSQ Quantum Ultra, ThermoQuest, Milan, Italy) equipped with an Electrospray Finnigan Ion Max source. For MS analyses, samples were desalted by using Amicon Ultra filter units 0.5 ml, cut-off 10 kDa (Millipore) and washed three times with water. Samples were then diluted to 1 mg/ml with a final composition of $CH_3CN–H_2O–HCOOH$ (30 : 70 : 0.1, v/v/v). Aliquots of 50 µl were injected

into the mass spectrometer at a flow rate of 25 µl min^{-1} by using a ThermoQuest autosampler. Each sample was analyzed for 5 minutes under the following instrumental conditions: positive-ion mode; ESI voltage 3.5 kV, capillary temperature 350 °C, Q3 scan range 1200–1500 m/z, Q3 power 0.4 amu, scan time 1 s, Q2 gas pressure 1.5 Torr, skimmer offset 10 V, microscan set to 3. Full instrument control and ESI mass spectra acquisitions were carried out by Xcalibur software (version 2.0.7, Thermo Fisher Scientific, Rodano, MI, Italy). Mass spectra deconvolution was performed using MagTran software (version 1.02) [8].

6.2.12 In-gel and in-solution digestion

In-gel digestion; protein bands were excised from gels using a scalpel, finely chopped, transferred to a new eppendorf and washed with 200 µl of digestion buffer. An aliquot of 200 µl of destaining solution was added to each gel portion and heated at 37 °C for 10 min in the thermomixer (1400 rpm); the destaining solution was then discarded and this step was repeated until destaining was completed. In-solution digestion; extracted HSA was diluted to 1 µg/µl with ammonium bicarbonate buffer. Afterwards, gel pieces or extracted HSA were incubated with 10 mM DTT at 56 °C for 1 h and then with 55 mM iodocetamide at room temperature for 45 min in the dark. Digestion was performed by overnight-incubation at 37°C with sequencing-grade trypsin (Roche) dissolved in digestion buffer. Samples could also be subjected to a second digestion by a sequencing-grade chymotrypsin for 4 h at 25 °C in the presence of calcium chloride (10 mM). In-solution digestion was stopped by adding 1% formic acid and desalted using µ-C18 ZipTip. In-gel digestion was proceeded with peptide extraction by a 10 min-incubation with extraction solution and by an additional 10 min-incubation with pure acetonitrile. The two in-gel digested extracts were combined and dried in a vacuum concentrator (Martin Christ.). Digested peptide mixtures were then dissolved in an appropriate volume (10 µl) of 0.1% formic acid for sample cleaning with µ-C18 ZipTip.

6.2.13 Mass spectrometry analyses

Peptides were analyzed using a Dionex Ultimate 3000 nano-LC system (Sunnyvale CA, USA) connected to an Orbitrap FusionTM TribridTM Mass Spectrometer (Thermo Scientific, Bremen, Germany) equipped with a nano-electrospray ion source. Peptide mixtures were pre-concentrated onto an Acclaim PepMap 100 – 100 µm x 2 cm C18 and separated on EASY-Spray column, 15 cm x 75 µm ID packed with Thermo Scientific Acclaim PepMap RSLC C18, 3 µm, 100 Å. The temperature was set to 35 °C and the flow rate was 300 nL min−1. Mobile phases were the following: 0.1% Formic acid (FA) in water (solvent A); 0.1% FA in water/acetonitrile (solvent B) with 2/8 ratio. Peptides were eluted from the column with the following gradient: 4% to 28% of B

for 90 min and then 28% to 40% of B in 10 min, and to 95% within the following 6 min to rinse the column. Column was re-equilibrated for 20 min. Total run time was 130 min. One blank was run between duplicates to prevent sample carryover. MS spectra were collected over an m/z range of 375-1500 Da at 120,000 resolutions, operating in the data dependent mode, cycle time 3 sec between master scans. Higher-energy collisional dissociation (HCD) was performed with collision energy set at 35 eV.

6.2.14 Identification and localization of protein adducts

The software Proteome Discoverer (version 2.2.0.388, Thermo Scientific, USA), implemented with the algorithms SEQUEST, was used to compare the experimental full and tandem mass spectra with the theoretical ones obtained by the in-silico digestion of the human database from human canonical UniProtKB/Swiss-Prot database (released in 2017-07). Trypsin was selected as the cleaving protease, allowing a maximum of 2 missed cleavages. Peptide and fragment ion tolerances were set to 10 ppm and 0.6 Da, respectively. Cysteine carbamidomethylation was set as fixed modification while methionine oxidation as dynamic modification in combination with a list of dynamic modifications as listed in Table S1.

As a quality filter, only peptides with an Xcore value grater then 2.2 were considered as genuine peptide identifications. To ensure the lowest number of false positives, the mass values experimentally recorded were further processed through a combined search with the Database Decoy, where the protein sequences are inverted and randomized. This operation allows the calculation of the false discovery rate (FDR) for each match, so that all the proteins out of range of FDR between to 0.01 (strict) and 0.05 (relaxed) were rejected.

For the localization of AGE/ALE-deriving modifications, the MS/MS spectra of modified peptides were manually inspected; for the confident mapping of the modification sites, spectra were requested to match the expected ions (b and/or y) neighboring the modified amino acid residue both at the N- and C-termini.

6.2.15 pFind

All MS/MS data were analyzed using pFind 3.1.5 in this study, in which the Open-pFind workflow was adopted [3]. Open-pFind consists of two search steps, one open and one restricted. First, a sequence tag-based strategy is used to match spectra to a much larger set of possible peptide sequences in the open search, and no modifications are specified initially. After this step, a restricted search is then performed where several key parameters, including modification types and protein sequence entries, are automatically set by semi-supervised machine learning based on the open search results. Finally, the results from both open search and restricted search are

merged together and reranked based on a new semi- supervised machine learning model similar to Percolator. All datasets were searched against the human database from human canonical UniProtKB/Swiss-Prot database (released in 2018-12) consisting of 20,408 protein sequences. The target-decoy approach was used to control the False Discovery Rate (FDR). Where the decoys were generated by reversing the target protein sequences. The Open-pFind PSM results were FDR controlled to be less than 1% for peptides and at the protein group level. Mass tolerances of precursor ions was set as ± 10 ppm and fragment ions were set as ± 20 ppm. For the restricted search, cysteine carbamidomethylation was set as fixed modification; methionine oxidation, asparagine and glutamine deamidation, and acetylation at the protein N-terminus were set as variable modifications.

6.3. Results

6.3.1 Oxidizability of healthy human plasma

In order to identify proteins prone to be modified due to oxidative pathways, and possibly serve as biomarker, healthy human plasma was oxidized using the radical initiator AAPH. Plasma contains a huge number of antioxidants, maintaining the oxidative balance in blood. Using DCFH as a marker of the oxidative reaction, it could be determined at which point the anti-oxidants are consumed after addition of AAPH (Fig. 1A). After 80 minutes of plasma incubation with 20 mM AAPH, there is an increase in relative green fluorescence, corresponding to the oxidation of DCFH to the fluorescent compound DCF. A plateau is reached around 130 min. after addition of AAPH to plasma. Therefore, protein carbonyl groups, an index of protein oxidation, were measured at different timepoints. Plasma was incubated with 20 mM AAPH and after 0, 80, 100, 130 and 180 min. the reaction was stopped by removing AAPH by ultrafiltration. Protein carbonyl content was evaluated using a protein carbonyl fluorometric assay and a protein carbonyl blot. The fluorometric assay shows an increase, although not correlated over time, in protein carbonyl content, the protein carbonyl blot shows no difference before or after oxidation (Fig. 1B and C). To determine the type of modification, intact protein analysis by direct infusion MS was performed to understand the modifications induced on HSA. Figure 1D shows the deconvoluted spectra of plasma-HSA incubated with AAPH for different incubation times. In non-treated plasma, t=0, the peak at 66,443 Da corresponds to HSA, with two smaller peaks at 66,566 and 66,607 Da, approximately the mass shift of a cysteinylated form (+ 123, theoretical increment +119 Da) and glycated form (+ 164, theoretical increment + 162) respectively. When incubated with AAPH, at all timepoints, roughly the same peak at 66,479 Da is apparent, +36, which corresponds to the addition of 2 oxygen atoms (theoretical increment + 32). Since the intensity of the cysteinylated peak remain unchanged, it is likely that Cysteine 34, the only free cysteine in HSA, is oxidized into a sulfinic

acid. These data suggest that oxidation is occurring in the plasma samples, however, there is no formation of AGEs/ALEs yet.

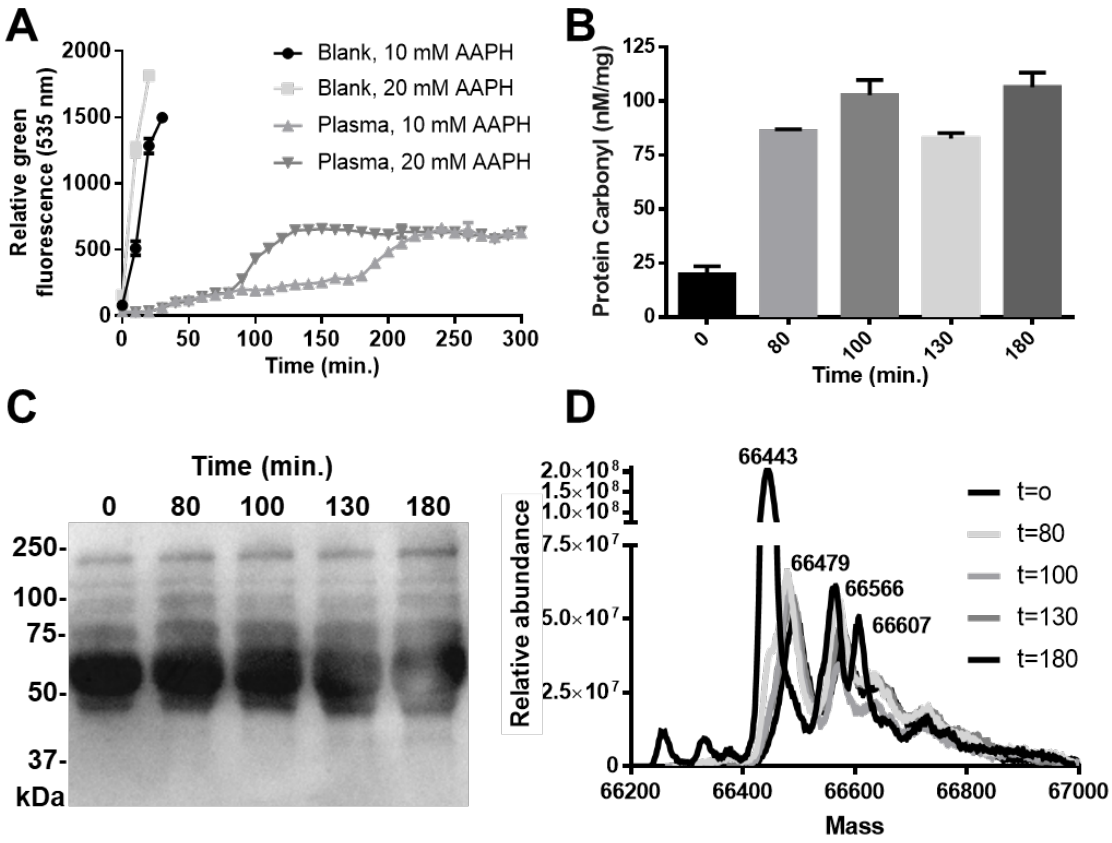

Figure 1. Oxidation of plasma content using AAPH. A) Oxidation of DCFH to DCF induced by AAPH. The reaction mixture consisted of DCFH, the azo-compound and human plasma (1:5 with PBS). Samples were incubated at 37°C in the dark and at fixed times the DCF content was measured by fluorescence (λex 485 nm, λem 535 nm). Values are mean ± SEM. B and C) At different timepoints protein carbonyl content was measured using a fluorometric assay (B, values are mean ± SEM) and by western blot (C). D) Direct infusion ESI-MS analysis of plasma and AAPH-treated plasma. Deconvoluted spectrum reports a peak at 66,443 Da, corresponding to HSA. Cysteinylated (66,566 Da) and glycated (66,607 Da) form of HSA are present in all samples. AAPH treated plasma shows an additional peak around 66,479 Da, suggesting the oxidation of HSA.

6.3.2 Longer incubations with AAPH

AAPH has proven to be successful in depleting anti-oxidants in plasma, and oxidizing plasma proteins, however the production of AGEs/ALEs was not observed. Therefore, an attempt was made at increasing the concentration of AAPH, as well as longer incubation times. Similarly, protein carbonyl content was evaluated using the fluorometric assay and protein carbonyl blot. As

can be seen from fig. 2, protein carbonyl groups are tremendously increased in AAPH treated plasma. Moreover, the higher the concentration of AAPH and the longer the incubation time, the higher the content of protein carbonyl groups in the sample.

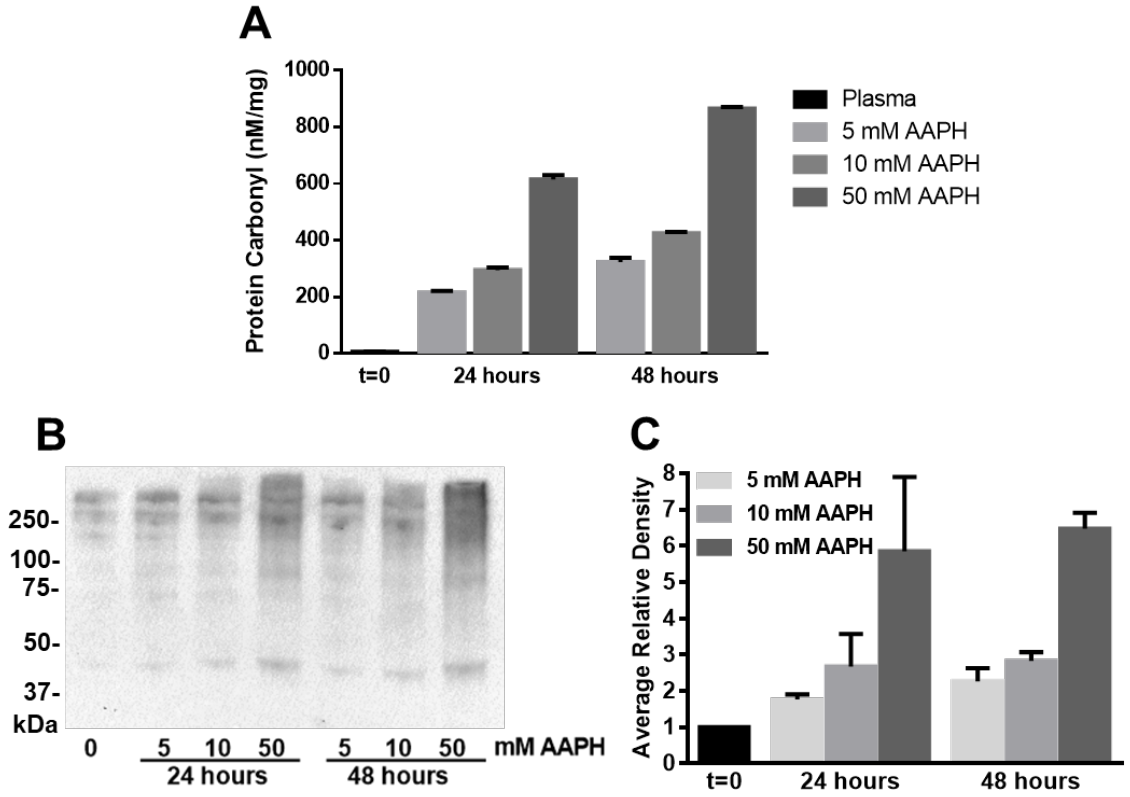

Figure 2. Oxidation of plasma content using different concentrations AAPH and longer incubation times. At different concentrations AAPH and timepoints protein carbonyl content was measured using a fluorometric assay (A, values are mean ± SEM) and by western blot (B, C, values are mean ± SEM).

6.3.3 Intact protein analysis

To link the protein carbonyl groups to the formation of AGEs/ALEs, intact protein analysis was performed again, focusing on HSA. Figure 3 represents the mass spectra of plasma and AAPH-treated plasma (mass range between *m/z* 1400 and 1500) characterized by the three sharp multicharged ions at m/z 1414.83, 1445.59 and 1477.71 relative to the three multicharged ions at 47+, 46+ and 45+ associated to HSA. When plasma was incubated with 5 mM AAPH for 24 hours, the main peaks have shifted and in addition, many new peaks can be detected. After deconvolution, the HSA peak has shifted 47 Da, which could suggest a trioxidation of the free cysteine group. At increasing concentrations of AAPH and prolonged incubation times, the spectra

cannot be deconvoluted due to the extent of modification. Moreover, the MS spectra lose resolution and become flat due to the presence of multiple adducts.

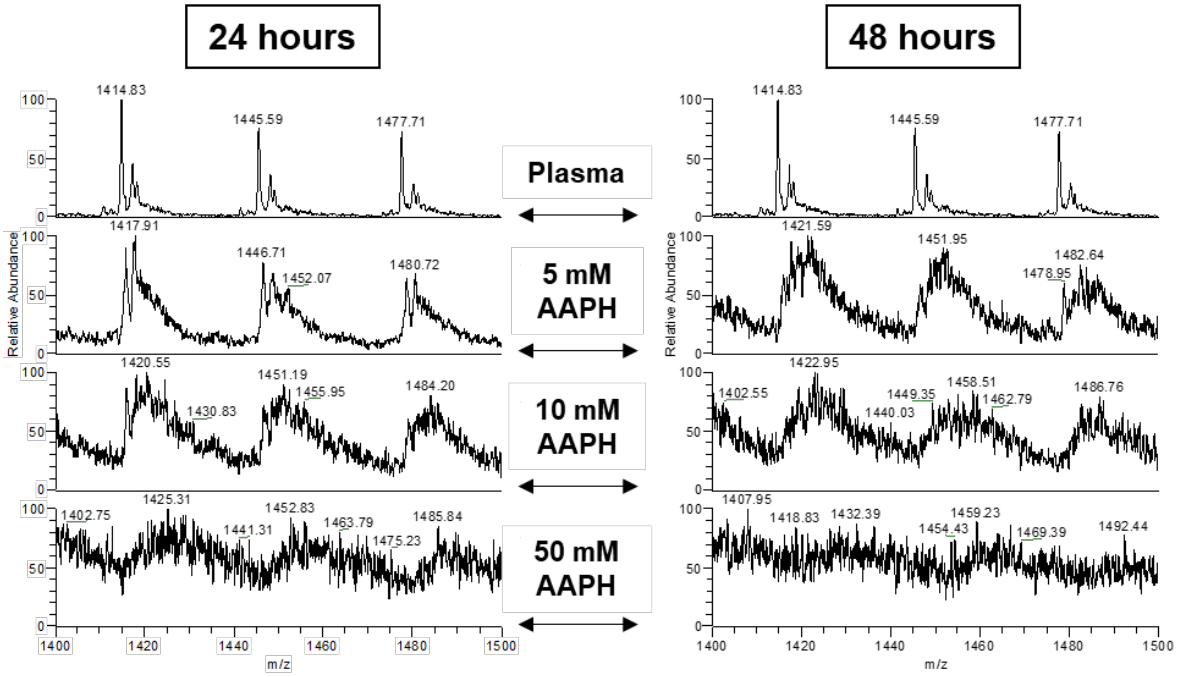

Figure 3. Direct infusion ESI-MS analysis of plasma and AAPH-treated plasma. Mass spectra of HSA recorded in a mass range between m/z 1400 and 1500. Native HSA shows sharp intense peaks referred to the charge ions 47+, 46+ and 45+ in untreated plasma. After incubation with increasing concentrations AAPH, the HSA peaks disappears due to the extent of modification.

6.3.4 Spectral counting

Due to the heterogeneity of the modified HSA, it could not be determined if AGEs/ALEs were present in the sample. Therefore, we proceeded to a bottom-up analysis to fully characterize the modifications present in AAPH treated plasma. Samples were run on SDS PAGE (Supplementary fig. 1), and in-gel digestion with trypsin and chymotrypsin was performed for digestion. Peptide mixtures were then analyzed using high resolution LC-MS/MS in data dependent mode. Firstly, data analysis was performed on Proteome Discover using a targeted method, meaning, only known modifications present in the database were searched for. Modifications included adducts by ACR, MDA, HNE, GO, MG and sugars, see full list in supplementary table 1. Surprisingly, we did not find an increased production of AGEs/ALEs corresponding to the increasing concentration of AAPH. However, data analysis demonstrated many oxidation products on amino side chains, such as methionine oxidation. In order to obtain a schematic overview of the induced modifications by AAPH, the software pFind was used. This is a search engine allowing the identification of

protein modifications recorded in the database of Unimod. Unimod is a comprehensive database with modifications that is community supported and displays accurate mass differences related to the modification. Results were analyzed by spectral counting; the percentage of peptide spectra matches (PSMs) with the specific modification was calculated compared to the total PSMs in that specific sample. Figure 4 shows a few examples of different oxidative products on various amino acids showing the same trend, increasing percentage of identified PSMs correlating to increasing concentration of AAPH. Oxidation of methionine was very abundant, with 8-15% of peptides containing the modification. Trioxidation on cysteine was also relative abundant, with 50 mM AAPH being very excessive in inducing oxidation on the cysteine containing peptides. Moreover, the percentage of identified PSMs with carbamidomethylation on cysteine are reported to validate the approach, since there should not be variability between samples as it is a sample preparation induced modification. Indeed, the graph shows minor variation between different treated plasma samples.

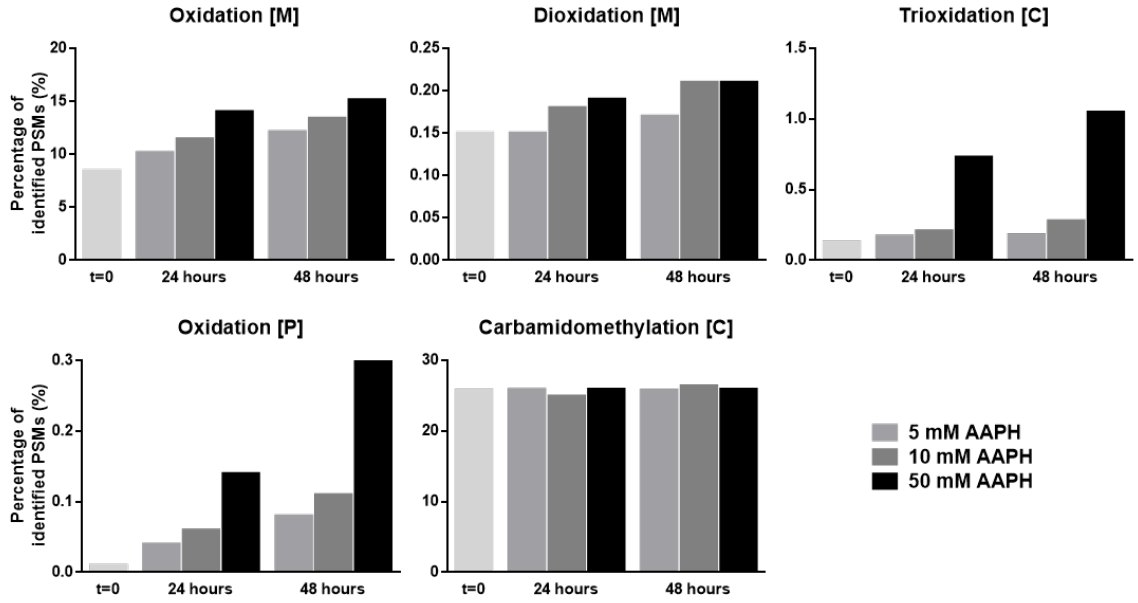

Figure 4. Spectral counting shows increased oxidation correlated over time and concentration of AAPH. Shown are the percentages of identified PSMs from the indicated modifications.

6.3.5 Plasma incubation with RCS

Using this approach, oxidizing plasma with AAPH, we did not obtain the formation of AGEs/ALEs, but rather amino acid side chain oxidation products. Therefore, to produce AGEs/ALEs, plasma was directly incubated with various concentrations of different RCS, including HNE, ACR, MDA, GO and MG. After 6 hours incubation, the reaction was stopped by removing RCS by ultrafiltration.

To confirm adducts formation, intact protein analysis was performed to visualize HSA. Figure 5 represents mass spectra of HSA incubated with either ACR or MDA to illustrate the formation of adducts. Regarding ACR, at increasing concentrations the native HSA peak almost disappears, confirming the formation of new species. Simultaneously a new peak appears around 66,500 Da, depicting the adduct of ACR with HSA. Similarly, incubation with MDA shows the formation of an adduct around 66,500 Da and the reduction in intensity of native HSA, though to a less extent.

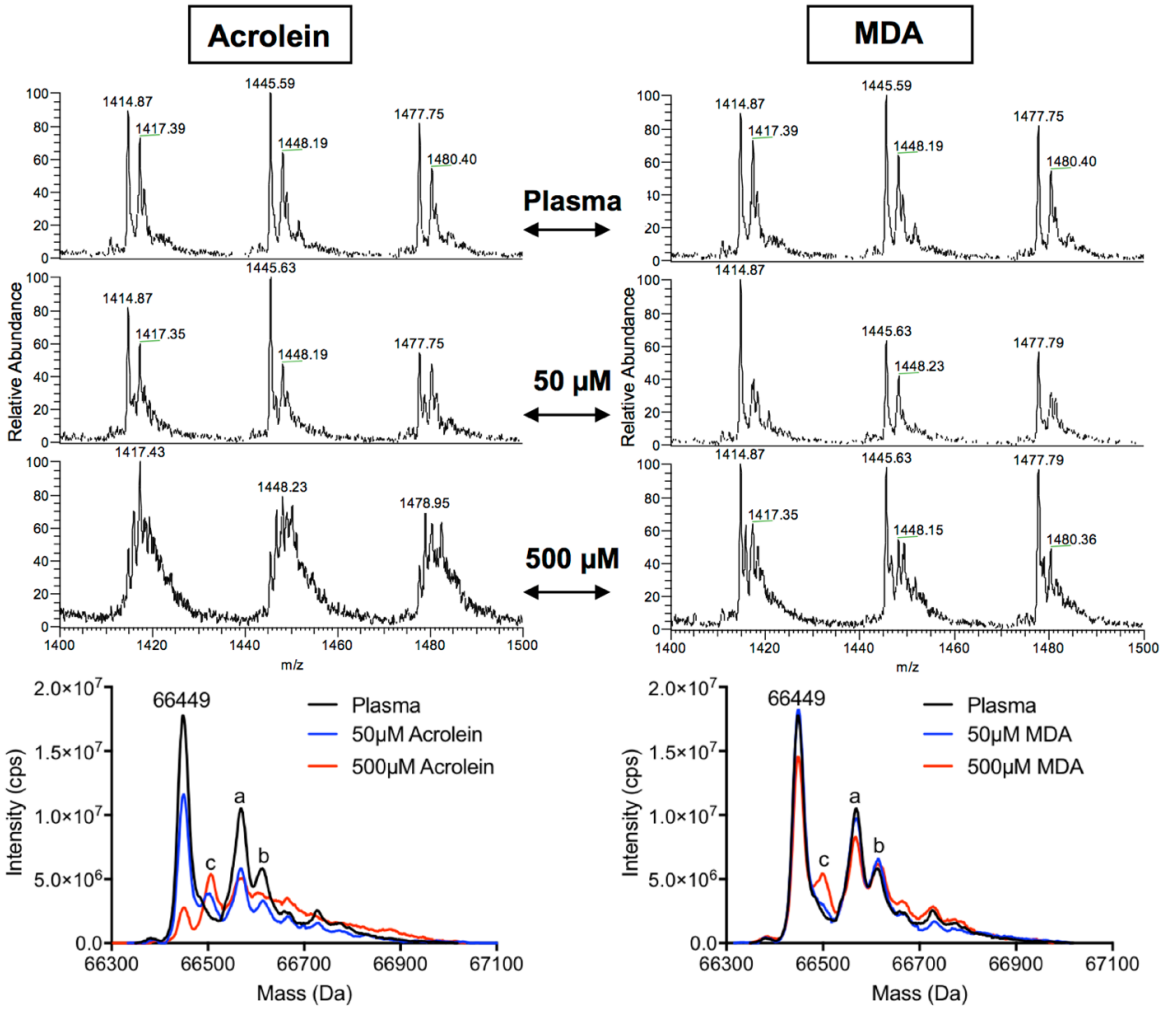

Figure 5. Direct infusion ESI-MS analysis of plasma and plasma incubated with ACR or MDA. Mass spectra of HSA recorded in a mass range between m/z 1400 and 1500. Native HSA shows sharp intense peaks referred to the charge ions 47+, 46+ and 45+ in untreated plasma; the deconvoluted spectrum reports a MW 66,449 Da. After incubation with increasing concentrations of ACR or MDA, spectra lose resolution due to the formation of new peaks. The HSA peak diminishes in the deconvoluted spectra when incubated with RCS. Shown are the cysteinylated form (a) of HSA, glycated form (b) and the formation of an adduct (c) with ACR or MDA.

6.3.6 VC1 Pull-Down assay

This time it was evident that AGEs/ALEs were formed by treating plasma directly with different RCS, due to the formation of an adduct between HSA and ACR or MDA. In order to elucidate the main proteins involved in AGEs/ALEs formation, and to identify AGEs/ALEs that become binder of RAGE, different AGEs/ALEs were pooled (plasma treated with 10 or 200 μM HNE, ACR, MDA, GO and MG separately) and subjected to a VC1 pull-down assay as previously described [2]. Figure 6 represents the three different VC1 pull-down assays performed on plasma and RCS treated plasma. At first sight, hardly any differences can be detected between the three different assays, therefore we moved forward to bottom-up MS in order to identify the AGEs/ALEs retained by VC1. Although in the previous chapter it was demonstrated that the VC1 pull-down assay was successful in retaining AGEs/ALEs when using a pure protein, HSA, in a complex mixture like plasma, no AGEs/ALEs were identified using MS.

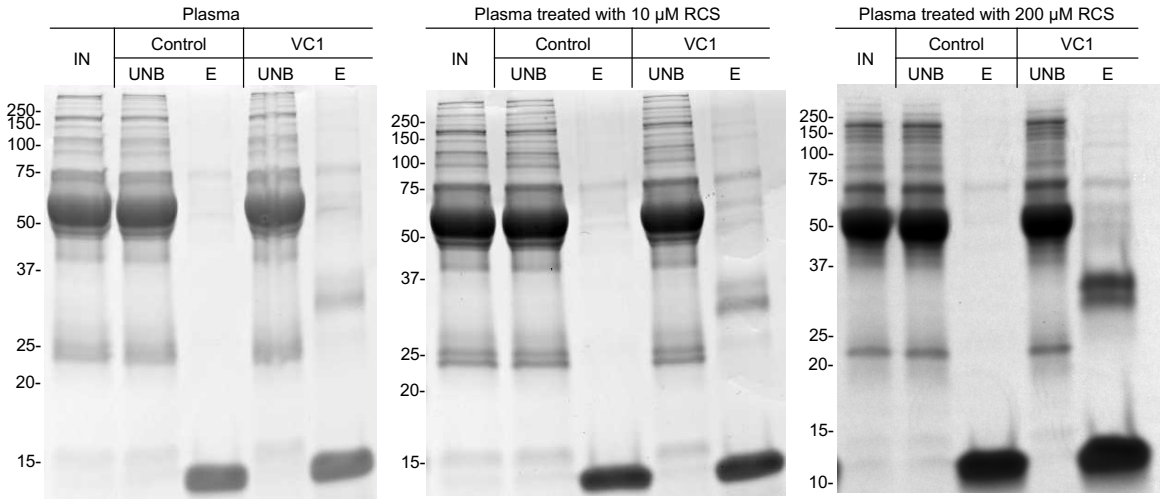

Figure 6. VC1 pull-down assay on plasma and plasma incubated with different ratios of RCS. The input fractions (IN), the unbound fractions (UNB) and eluates (E) were analyzed by SDS-PAGE followed by Coomassie staining. The gels show the same elution profile compared between plasma and plasma treated with RCS with some proteins retained by VC1 around 60 and 75 kDa, and to a less extent by the control resin. Since the elution is performed in denaturing conditions, this step removes any associated molecule from the resin, including the two VC1 glycovariants (34 and 36 kDa) and streptavidin (14 kDa).

6.3.7 HSA extraction

Since the VC1 pull-down assay was not sufficient to enrich AGEs/ALEs from plasma samples, the experimental set-up was evaluated. Firstly, focus was shifted from identifying AGEs/ALEs from the whole plasma proteome to the most abundant protein present in plasma, HSA. Secondly,

protein adducts can be quite unstable and can be lost during sample preparation. Therefore, sodium borohydride was used to reduce protein adducts in order to stabilize them for easier identification. Lastly, an even higher resolution mass spectrometer was used compared to the Orbitrap LTQ XL used until now, Fusion Tribrid. This new generation MS has faster scanning detectors, and allows parallel isolation and detection modes, increasing the coverage of analyzed peptides.

To make the plasma sample less complex, HSA was extracted using the Pierce™ Albumin Depletion Kit. Figure 7 shows the extraction of HSA from plasma, where the flow-through (FT) shows almost complete depletion of HSA from plasma, and the elution (E) indicates that HSA can be recovered in a less complex matrix.

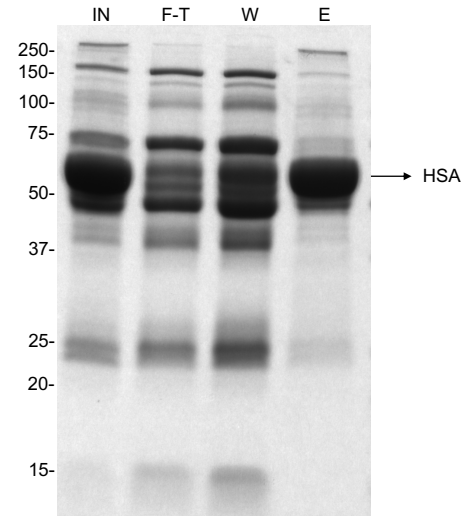

Figure 7. HSA extraction from plasma. The input fraction (IN), the flow-through fraction (F-T), the wash fraction (W) and eluate (E) were analyzed by SDS-PAGE followed by Coomassie staining.

6.3.8 Heart failure stage III samples

Instead of forcing AGEs/ALEs formation in-vitro, we chose to use a more physiological approach being plasma samples from heart failure patients. Plasma from heart failure patients is characterized by an increase of circulating AGEs/ALEs, making it a suitable model for the set-up of a sensitive method for the identification and characterization of protein adducts presumably involved in the onset and progression of the disease. Plasma samples were collected from healthy individuals and patients with heart failure stage III. These patients are characterized by marked limitation of physical activity and suffer fatigue, palpitation or dyspnea. A pool of healthy individuals (8) and heart failure patients (9) were used. HSA was extracted as described before, reduced using $NaBH_4$ and digested using trypsin. Peptides were then analyzed using high resolution LC-MS/MS on the Orbitrap Fusion and protein adducts were identified using Proteome Discoverer.

This new approach permitted us to identify many AGEs/ALEs in both healthy human plasma samples, but also AGEs/ALEs only present in plasma of heart failure patients (Fig. 8). Glycation, and the break-down product glyoxal, were the main modifications identified (30 different modification sites), present in both healthy (3 different modification sites) and heart failure plasma samples (11 different modification sites). Important is the HNE Michael adduct, specifically identified in only heart failure samples. Moreover, the importance of stabilizing adducts is underlined by the fact that the acrolein adduct could only be identified after reduction with $NaBH_4$. Overall, there are a substantial number of modifications present only in heart failure patients which could be important in understanding the progression of the disease.

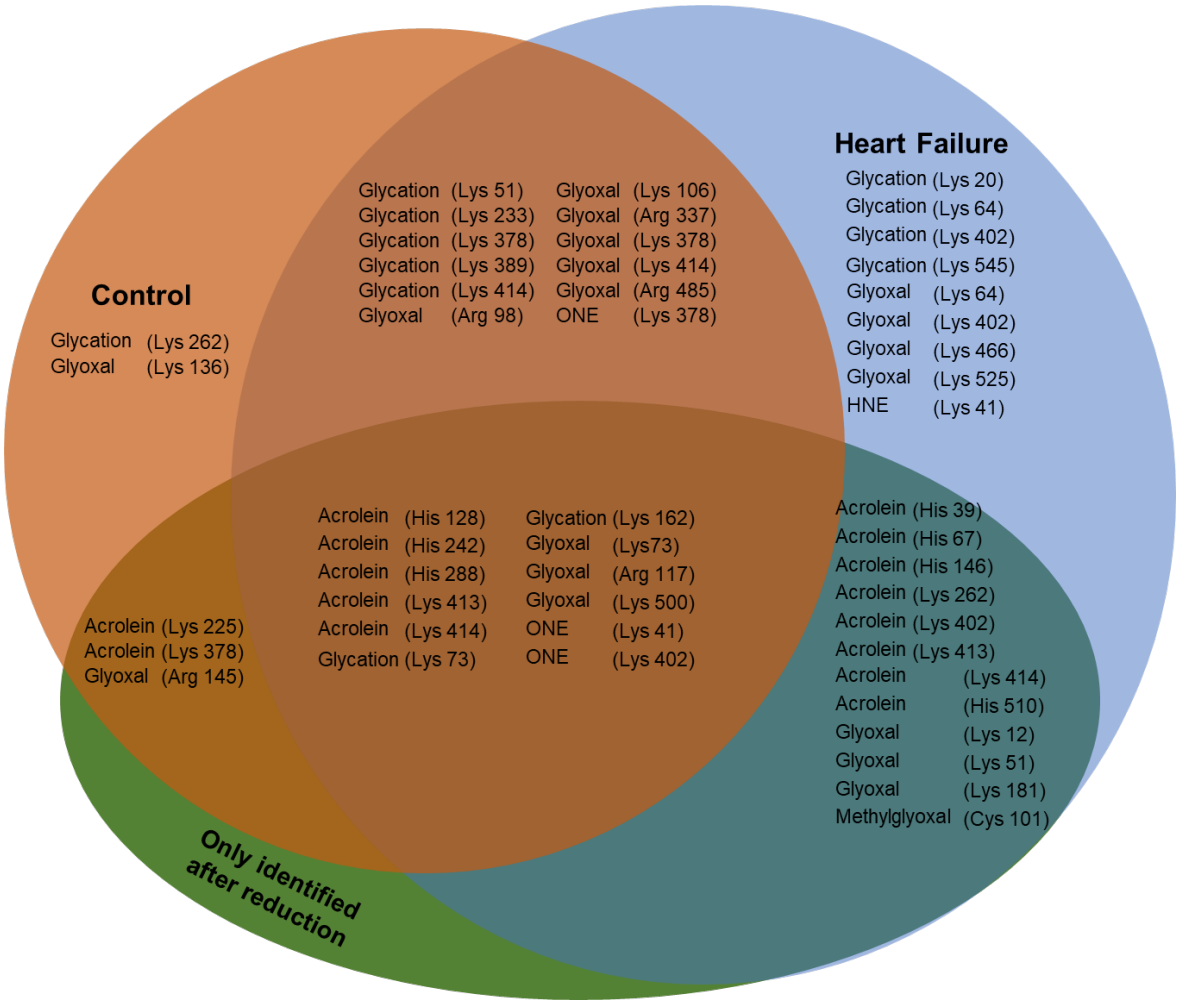

Figure 8. Venn diagrams of the identified AGEs/ALEs in healthy individuals and heart failure patients, as well as if they were identified only after reduction with $NaBH_4$. Reported are the type of modification followed by the site of adduction on HSA.

6.3.9 Validation of identified AGEs/ALEs

Lastly, it should be stressed that every modification identified was confirmed by manually checking the MS^2 spectra. Using Proteome Discoverer, a list of identified b- and y-ions is available as well as the instrumental MS^2 spectra with the annotation of identified b- and y-ions. Thereby, allowing us to manually check whether the annotated ions are true positives, and showing the relative abundance of the ions. Figure 9 shows a good identification of a glyoxal modification on a lysine residue of the HSA peptide K*VPQVSTPTLVEVSR. Most of the b- and y-ions are identified and are the main intense peaks in the spectra. Moreover, another indication that the annotated modification and peptide are true is the fact that the immonium ion is present of lysine with the glyoxal modification, the peak at m/z 187.10744. All identified modifications were validated using this approach.

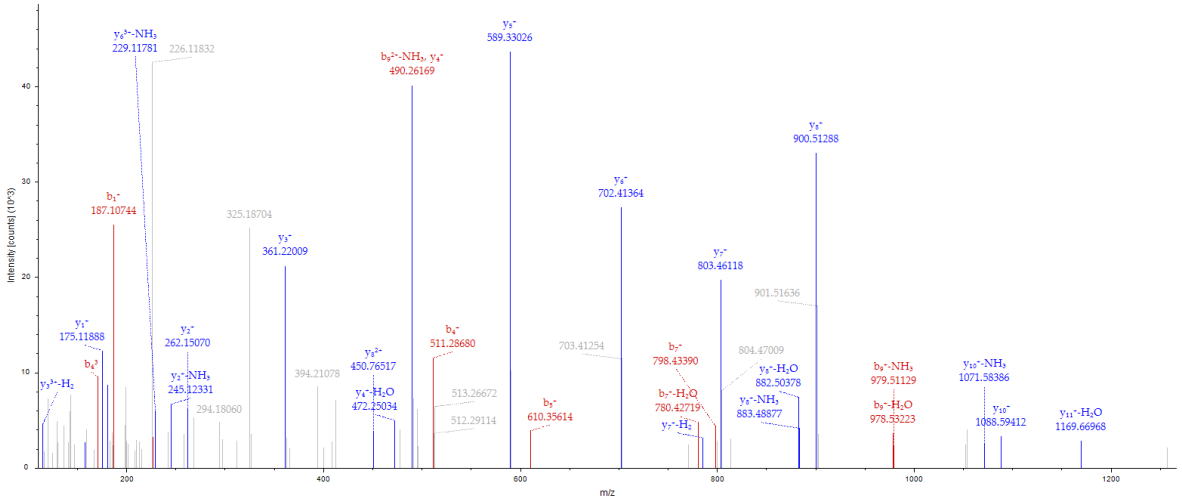

Figure 9. MS^2 spectrum with the b- and y-series of a peptide containing a glyoxal modification. The peak at 187.10744 represents the immonium ion of a lysine residue with a glyoxal adduct.

6.4. Discussion

Many pathologies have been reported to have an increase in circulating AGEs/ALEs contributing to disease progression, emphasizing the need for sensitive techniques to allow easier identification. Furthermore, full characterization is necessary for understanding the role each AGE/ALE play in the mechanisms leading to the onset and/or progression of the disease. Low abundance, heterogeneity and complex chemical structures make this a very challenging exercise. Therefore, many enrichment strategies have been explored, including the VC1 Pull-Down assay described in our previous papers [2, 3]. To validate the use of this technique for enriching low abundant AGEs/ALEs in plasma samples, healthy human plasma was oxidized using AAPH to identify which proteins are prone to modification, as well as the type of modification.

Since AAPH is a radical initiator, we hypothesized the attack of lipids, causing break-down products leading to the formation of ALEs. Unfortunately, only protein side chain oxidation products were identified, rendering the use of AAPH not suitable for the production of AGEs/ALEs. Incubating plasma directly with RCS did lead to the formation of protein adducts, however, using the VC1 Pull-Down assay we were not able to enrich AGEs/ALEs from plasma, indicating the need for more sensitive methods/equipment.

Multiple enrichment strategies are available optimized for in-vitro use or only a certain group of chemical structures and ex-vivo enrichment of AGEs/ALEs remains challenging as presented in this section and by many other papers. Besides an enrichment step, very sensitive equipment is a must in order to characterize AGEs/ALEs. Therefore, sample analysis was switched from the Orbitrap LTQ XL to Orbitrap Fusion. Orbitrap Fusion is a third generation MS providing even higher resolution, faster MS detectors and parallel isolation and detection increasing protein coverage and chance to detect PTMs. Indeed, PTM identification have shown to be more successful using the Orbitrap Fusion as shown by the identification of phosphorylation sites and protein glycosylation [9, 10]. Furthermore, sample preparation was optimized by only focusing on HSA and by reducing protein adducts using sodium borohydride. Reducing protein adducts is a necessary step in the sample preparation, since there are a variety of adducts unstable during the sample preparation process and can be lost during analysis. Moreover, some adducts are reversible like the retro Michael adduct of acrolein. Therefore, the reducing step will not only stabilize the adducts during sample preparation, but also inhibit reversible adducts. On the other hand, we only focused on HSA, since it is the most abundant protein in plasma and the main nucleophilic target [11]. Moreover, HSA protein adducts have been shown to contribute to the progression of heart failure, such as glycated HSA [12, 13].

To set up the new strategy, we used plasma samples from healthy individuals and heart failure patients stage III, since these plasma samples are known to have an increase in AGEs/ALEs content, making it the perfect model to investigate whether the strategy is sensitive enough for mapping AGEs/ALEs. Indeed, many protein adducts were identified, especially in heart failure samples and mainly coming from sugar oxidation pathways, such as glycation sites and the break-down products glyoxal and methyl glyoxal. This can be explained by the fact that many heart failure patients are also presented with higher sugars levels, or even diabetes complications [14]. Besides that, reducing protein adducts also showed an increase in identifying adducts, especially adducts with acrolein, that only could be identified after stabilizing the Michael adduct, indicating the importance of reducing adducts. The majority of acrolein adducts were identified in heart failure patients, implicating a possible role of this adduct in the onset or progression of the disease.

Particularly, His 146, already described as one of the key targets of HSA, could be a potential biomarker [15]. To validate the use of biomarkers, the next step will be the set-up of a selected ion monitoring (SIM) approach to elucidate whether the specific modifications can be targeted in each individual. The precursor ion will be fixed at the m/z of the detected peptide with modification described before. Using this approach, a fast and reliable method can be set up for the identification and characterization of AGEs/ALEs in plasma samples from different pathologies.
In conclusion, this is the first technique to our knowledge, describing the identification and characterization of disease specific HSA adducts by using the newest generation of orbitrap MS instruments in combination with focusing on HSA and reducing protein adducts. This approach could be used in combination with enrichment techniques, including the VC1 Pull-Down, to perform a plasma wide AGEs/ALEs search.

References

[1] R.C. Bollineni, M. Fedorova, M. Blüher, R. Hoffmann, Carbonylated plasma proteins as potential biomarkers of obesity induced type 2 diabetes mellitus, J Proteome Res 13(11) (2014) 5081-93.
[2] G. Degani, A.A. Altomare, M. Colzani, C. Martino, A. Mazzolari, G. Fritz, G. Vistoli, L. Popolo, G. Aldini, A capture method based on the VC1 domain reveals new binding properties of the human receptor for advanced glycation end products (RAGE), Redox Biol 11 (2017) 275-285.
[3] M. Mol, G. Degani, C. Coppa, G. Baron, L. Popolo, M. Carini, G. Aldini, G. Vistoli, A. Altomare, Advanced lipoxidation end products (ALEs) as RAGE binders: Mass spectrometric and computational studies to explain the reasons why, Redox Biol (2018) 101083.
[4] S. Eliuk, A. Makarov, Evolution of Orbitrap Mass Spectrometry Instrumentation, Annu Rev Anal Chem (Palo Alto Calif) 8 (2015) 61-80.
[5] J.W. Hartog, A.A. Voors, S.J. Bakker, A.J. Smit, D.J. van Veldhuisen, Advanced glycation end-products (AGEs) and heart failure: pathophysiology and clinical implications, Eur J Heart Fail 9(12) (2007) 1146-55.
[6] M. Carini, G. Aldini, M. Piccone, R.M. Facino, Fluorescent probes as markers of oxidative stress in keratinocyte cell lines following UVB exposure, Farmaco 55(8) (2000) 526-34.
[7] G. Degani, M. Colzani, A. Tettamanzi, L. Sorrentino, A. Aliverti, G. Fritz, G. Aldini, L. Popolo, An improved expression system for the VC1 ligand binding domain of the receptor for advanced glycation end products in Pichia pastoris, Protein Expr Purif 114 (2015) 48-57.
[8] Z. Zhang, A.G. Marshall, A universal algorithm for fast and automated charge state deconvolution of electrospray mass-to-charge ratio spectra, J Am Soc Mass Spectrom 9(3) (1998) 225-33.

[9] C.M. Woo, A. Felix, L. Zhang, J.E. Elias, C.R. Bertozzi, Isotope-targeted glycoproteomics (IsoTaG) analysis of sialylated N- and O-glycopeptides on an Orbitrap Fusion Tribrid using azido and alkynyl sugars, Anal Bioanal Chem 409(2) (2017) 579-588.
[10] S. Ferries, S. Perkins, P.J. Brownridge, A. Campbell, P.A. Eyers, A.R. Jones, C.E. Eyers, Evaluation of Parameters for Confident Phosphorylation Site Localization Using an Orbitrap Fusion Tribrid Mass Spectrometer, J Proteome Res 16(9) (2017) 3448-3459.
[11] G. Aldini, G. Vistoli, L. Regazzoni, L. Gamberoni, R.M. Facino, S. Yamaguchi, K. Uchida, M. Carini, Albumin is the main nucleophilic target of human plasma: a protective role against pro-atherogenic electrophilic reactive carbonyl species?, Chem Res Toxicol 21(4) (2008) 824-35.
[12] B. Paradela-Dobarro, S.B. Bravo, A. Rozados-Luís, M. González-Peteiro, A. Varela-Román, J.R. González-Juanatey, J. García-Seara, E. Alvarez, Inflammatory effects of in vivo glycated albumin from cardiovascular patients, Biomed Pharmacother 113 (2019) 108763.
[13] E. Selvin, A.M. Rawlings, P.L. Lutsey, N. Maruthur, J.S. Pankow, M. Steffes, J. Coresh, Fructosamine and Glycated Albumin and the Risk of Cardiovascular Outcomes and Death, Circulation 132(4) (2015) 269-77.
[14] M. Lehrke, N. Marx, Diabetes Mellitus and Heart Failure, Am J Cardiol 120(1S) (2017) S37-S47.
[15] G. Aldini, L. Regazzoni, M. Orioli, I. Rimoldi, R.M. Facino, M. Carini, A tandem MS precursor-ion scan approach to identify variable covalent modification of albumin Cys34: a new tool for studying vascular carbonylation, J Mass Spectrom 43(11) (2008) 1470-81.

Appendix

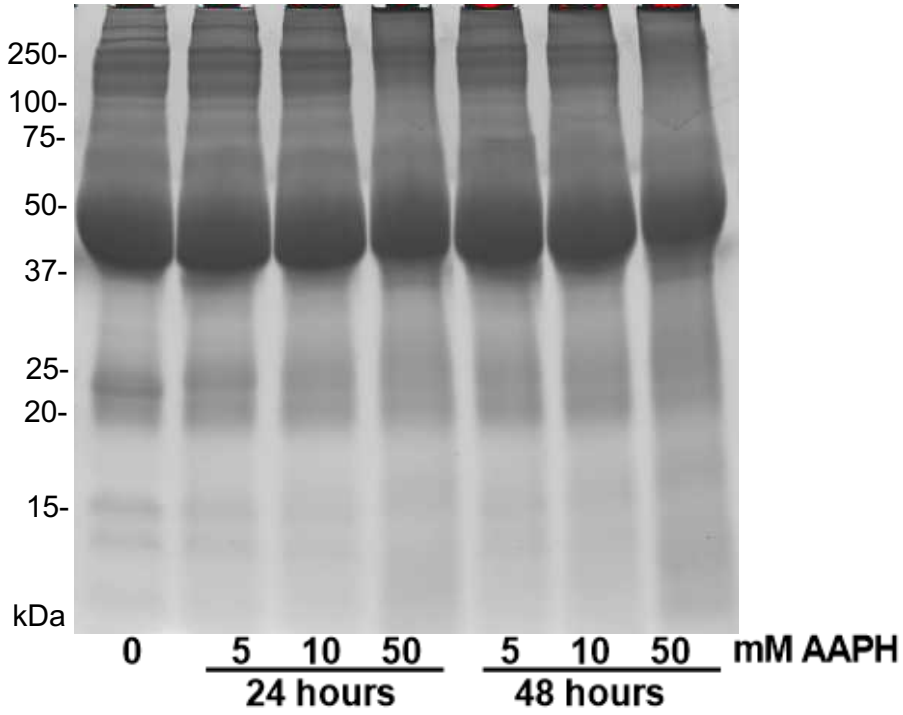

Supplementary figure 1: Protein gel of plasma treated with different concentrations of AAPH and different timepoints.

Table S1. Known (literature based) covalent adducts induced by HNE, MDA, ACR, MG, GO, ONE and sugars set as variable modifications within the PD parameters for the identification and localization of ALE-deriving adducts.

HNE

PTM	AA Res. Involved	ΔM
Michael adduct	Cys His Lys Arg	+ 156.110502 Da
Schiff Base	Lys Arg	+ 138.01446 Da
2-pentilpyrrole	Lys Arg	+ 120.0939 Da
Dehydropentylfuran	Cys His Lys Arg	+ 138.10446 Da

MDA

PTM	AA Res. Involved	ΔM
N-propenal-Lysine	Lys	+ 54.01056 Da
Di-dihydropyridine-lysine	Lys	+ 134.03678 Da
Malondialdehyde argpyrimidine	Arg	+ 36.0000 Da

ACR

PTM	AA Res. Involved	ΔM
Michael Adduct (propanal derivative)	Cys Lys His	+ 56.02621 Da
Hydroxy-tetra-hydropyrimidine (Propane-arginine)	Arg	+ 56.02621 Da
Double Michael Adduct	Lys	+ 112.05243 Da
Schiff Base	Lys	+ 38.01565 Da
Formyl-dehydro-piperidyl-lysine	Lys	+ 94.04186 Da
Methylpyridine-lysine	Lys	+ 77.03912 Da

MG

PTM	AA Res. Involved	ΔM
Carboxy-ethyl	Cys Lys Arg	+ 72.021 Da

Methylimidazolone	Arg	+ 54.011 Da
Pyrimidine	Arg	+ 80.026 Da
Tetra-hydro-pyrimidine	Arg	+ 144.042 Da

GO

PTM	AA Res. Involved	ΔM
Carboxy-methyl	Lys Arg	+ 58.005 Da
Imidazolone	Arg	+ 39.995 Da

ONE

PTM	AA Res. Involved	ΔM
Michael adduct	Cys His Lys Arg	+ 154.099 Da
Pentylfuran	Cys His Lys Arg	+ 136.089 Da

Sugars

PTM	AA Res. Involved	ΔM
Glycation	Lys Arg	+ 162.053 Da
Imidazolone	Arg	+ 144.042 Da
Pyraline	Lys	+ 108.172 Da

Table S2. Known (literature based) reduced covalent adducts induced by HNE, MDA, ACR, MG, GO, ONE and sugars set as variable modifications within the PD parameters for the identification and localization of ALE-deriving adducts.

HNE

PTM	AA Res. Involved	ΔM
Michael adduct Reduced	Cys His Lys Arg	+ 158.131 Da
Schiff Base Reduced	Lys Arg	+ 140.120 Da

MDA

PTM	AA Res. Involved	ΔM
N-propenal-Lysine	Lys	+ 56.026 Da
Di-dihydropyridine-lysine	Lys	+ 138.068 Da

ACR

PTM	AA Res. Involved	ΔM
Michael Adduct (propanal derivative) Reduced	Cys Lys His	+ 58.042 Da
Double Michael Adduct Reduced	Lys	+ 116.084 Da
Schiff Base Reduced	Lys	+ 40.031 Da
Formyl-dehydro-piperidyl-lysine Reduced	Lys	+ 96.058 Da

ONE

PTM	AA Res. Involved	ΔM
Michael adduct Reduced	Cys His Lys Arg	+ 158.131 Da
Schiff Base Reduced	Cys His Lys Arg	+ 140.120 Da

Chapter VII: Effect of AGEs and ALEs on NF-κB activity

Chapter VII: Effect of AGEs and ALEs on NF-κB activity

Abstract

Advanced Glycation/Lipoxidation End Products (AGEs/ALEs) are pathogenic factors coming from oxidative degradation pathways and have been described in the onset/progress of many pathologies, including diabetes and cardiovascular diseases. AGEs/ALEs exert their damaging activity through different mechanisms and one of them is to bind to the receptor for AGEs (RAGE). The AGE-RAGE axis has already been described extensively, however there is no evidence of how ALEs can induce pro-inflammatory activity. Since previously we described the mechanisms of ALEs as binder of RAGE, we sought to determine whether ALEs can bind and induce a pro-inflammatory activity through RAGE. We set up a cellular model with and without the expression of RAGE and the presence of a NF-κB gene reporter. Due to limitations of the cellular model, a RAGE dependent mechanism for NF-κB activation could not be set up. However, it was evident that both AGEs and ALEs activated the NF-κB pathway independent of RAGE. Furthermore, ALEs showed an increase in reducing potential of the cells most likely related to activation of the nrf2 pathway. Further studies are necessary to elucidate the effect of AGEs/ALEs on NF-κB activation.

7.1. Introduction

Advanced Glycation/Lipoxidation End Products (AGEs/ALEs) are pathogenic factors implicated in many different diseases, including cardiovascular diseases, chronic renal failure, diabetes and neurological disorders [1-4]. AGEs and ALEs are similar compounds, proteins adducted by oxidative degradation products, and exert damaging activity directly on the protein itself, as well as through signaling pathways. Regarding AGEs, the involvement of the Receptor for Advanced Glycation End Products (RAGE) and the signaling mechanisms are well described. In contrast, ALEs have also been shown to induce down-stream signaling pathways, but up to date no receptor has been described for this event. Naturally, RAGE could be the most prominent candidate, considering AGEs/ALEs share a common chemical structure. In fact, our previous paper described the mechanisms necessary for ALEs to become a binder of RAGE [5].

RAGE is a multi-ligand receptor that consist of multiple isomers, including a membrane bound form and a soluble form. The membrane bound receptor contains an intracellular signaling domain, able to activate different pathways leading to a pro- or anti-inflammatory immune response [6]. One of the main pathways involved is the NF-κB pathway followed by the increase in expression of cytokines, growth factors, as well as the upregulation of the receptor itself [7]. Besides AGEs, well-known ligands of the receptor are HMGB-1 and S100 proteins. In addition to

AGEs/ALEs, RAGE has also been implicated in many different pathologies, like Parkinson's disease, Alzheimer's disease, pulmonary inflammatory responses and inflammatory diseases in general [8-11]. Combining the data of sustained inflammatory activity of AGEs/ALEs and the receptor, it can be assumed that the NF-κB pathway is chronically activated. However, the exact molecular mechanisms leading to these cellular events are still not well understood. This project aimed to understand whether besides AGEs, also ALEs induce downstream signalling pathways either through RAGE or as such by utilizing a cell line with a NF-κB gene reporter.

7.2. Materials and Methods

7.2.1 Chemicals and reagents

Bradford reagent, protease inhibitors, IL-1α, HSA, bardoxolone and all other chemicals were purchased from Sigma-Aldrich (Milan, Italy). ONE-Glo Luciferase Assay System and RealTime-Glo MT Cell Viability Assay were purchased from Promega (USA).

7.2.2 Cell Culture and Lentiviral Transduction

HEK293T and R3/1 clones were grown in Dulbecco modified Eagle medium (DMEM; Lonza, Verviers, Belgium) supplemented with 10% fetal bovine serum (FBS; Gibco), 1% glutamine (Lonza), and 1% penicillin/streptomycin (Gibco, USA). R3/1-pLXSN (hereinafter referred to as R3/1 Control) or R3/1-FL-RAGE (hereinafter referred to as R3/1 RAGE) cells were generated as described in Sessa et al. [12]. For lentivirus production, $9 \bullet 10^6$ HEK293T cells were seeded in 15 cm plate, medium was discarded after 16 hours and substituted with Iscove's Modified Dulbecco's Medium (IMDM; Lonza), 10% FBS, 1% penicillin/streptomicin and 1% glutamine 100U/mL. Transfection was performed using calcium phosphate precipitation method using lentiviral package vectors (7 µg pDM2-VSVG and 28 µg pCMV-ΔR8.91) and 32 µg pGreenFire-NF-κB-Puro (a kind gift of Dr. Darius Widera, University of Reading, UK [13]). Medium was changes 16 hours later with complete IMDM and butyrate sodium (1 µg/ml; Sigma, St Louis, USA) and virus particles were harvested after 36 h. Medium containing virus particles was centrifuged at 1500 rpm for 5 minutes and filtered through 0.22 µm filter (Merck, Germany) before centrifugation at 20000 rpm for 2 hours at 4 °C. Supernatant was discarded and virus particles were resuspended in 40 µl of sterile cold PBS and left in ice with gentle agitation for 30 minutes. Aliquots were stored at -80°C. For lentiviral transduction, 60.000 R3/1 Control or R3/1 RAGE cells were seeded in a 12 well-plate and the day after medium was replaced with fresh medium containing 6 µl (MOI 10) or 12 µl (MOI 20) of virus particles solution for 24 h. Medium was changed 24 hours later and cells were selected with 1 µg/ml of puromycin for 4 days.

7.2.3 Western blot

R3/1 cells were harvested in RIPA buffer in the presence of proteases inhibitors, incubated in ice for 30 min and centrifuged at 12.000 x g for 15 minutes at 4°C. Supernatants were collected and protein concentration was determined. Protein extracts were separated by SDS-PAGE and transferred to Amersham Hybond ECL Nitrocellulose membranes (GE Healthcare, Little Chalfont, United Kingdom). Membranes were incubated with a goat anti-human RAGE (1 µg/ml; cat. AF1145; R&D Systems Minneapolis, MN, USA) or an antibody against GAPDH (0.2 µg/mL, sc-25778, Santa Cruz Biotechnology). Proteins were visualized by the Amersham ECL Western Blotting Detection Reagents (GE Healthcare).

7.2.4 Preparation of AGE/ALE albumins and natural extracts

Recombinant human serum albumin (HSA) expressed in *P. pastoris* (Cat no. A7736) was obtained from Sigma. To obtain AGEs, HSA was incubated with glucose for 3 months or with fructose for 4 months. After incubation, unreacted sugar was removed by diafiltration using Amicon Ultra-0.5 ml (Cut off 10 K) filters. To obtain ALEs, HSA was incubated at various ratios separately with HNE, MDA or ACR for 24 hours. After incubation, unreacted RCS were removed by diafiltration using Amicon Ultra-0.5 ml (Cut off 10 K) filters and same ratios different RCS were pooled together.

7.2.5 Stimulation of Cells

Cells for pro-inflammatory activity were stimulated with 10 ng/ml human recombinant IL-1α (Sigma-Aldrich), 500 µg/ml HSA or AGEs, or 10 µg/ml HMGB-1 in serum-free medium at different timepoints. For proliferation assays, cells were treated with 500 µg/ml HSA, AGEs/ALEs, or various concentrations of ALEs for 72 hours in complete medium. To assess the anti-inflammatory activity, cells were pre-treated with different compounds at different concentrations for 18 hours in complete medium, followed by a 6-hour stimulation with 10 ng/ml IL-1α. Experiments were assayed by NF-κB luciferase activity, RealTime-Glo assay or an MTT assay.

7.2.6 NF-κB luciferase activity assay

After treatment, cells were washed twice with cold PBS followed by a freeze-thaw cycle with reporter lysis buffer (Promega) for complete cell lysis. Experiments in 6 wells plates; protein lysate was collected and spun for 10 min. at 15.000 x g to remove debris. Luciferase activity was then measured by adding 100 µl ONE-Glo Luciferase Assay Substrate (Promega) to 50 µl protein lysate in a white 96-wells plate followed by a luciferase measurement performed using a luminometer (WALLAC 1420, Multilabel counter, Perkin Elmer life and Analytical Sciences). Experiments in 96-wells plates; after the freeze-thaw cycle, 100 µl ONE-Glo Luciferase Assay Substrate (Promega)

was directly added to the wells, followed by a luciferase measurement performed using a luminometer (WALLAC 1420, Multilabel counter, Perkin Elmer life and Analytical Sciences).

7.2.7 RealTime-Glo assay

RealTime-Glo assay was performed following manufacturer's instructions. In brief, for continuous measurement, medium containing RealTime-Glo reagents and compounds to test were added simultaneously to the wells containing cells. Luciferase was then measured hourly up to 72 hours. For end-point measurements, medium containing compounds was removed and replaced with medium containing RealTime-Glo reagents, incubated for 30 min., and luciferase was measured.

7.2.8 MTT assay

After stimulation, 10 µl 5 mg/ml MTT reagent was added for 4 hours. Afterwards, medium was removed, and cells were lysed and MTT was solubilized by adding 100 µl DMSO. 96-wells plate was shaken for 1 minute, followed by an absorbance measurement at 490 nm using a plate reader (BioTek's PowerWave HT, USA). Cells incubated with respective concentration of DMSO (<0.1%) were used as a control for 100% cell proliferation. Statistical analysis was performed in the GraphPad software. Experiments were performed with biological and technical replicates.

7.3. Results

7.3.1 Transduction of the cell line

In order to obtain a fast and sensitive method for assessing binding of RAGE and the subsequent activation of the NF-κB pathway, R3/1 Control and R3/1 RAGE cells were lentivirally transduced with a lentiviral NF-κB-driven reporter encoding for luciferase. Firstly, transduced cells were tested for the expression of RAGE (Fig. 1A). This blot shows clearly that R3/1 RAGE transduced cells well express the receptor and that there is no expression of RAGE in R3/1 Control cells. Next, different clones were produced with two different mode of infections (MOI), 10 and 20. When stimulated with IL-1α, a potent inducer of the pro-inflammatory pathway through NF-κB, control cells showed negligible luciferase luminescence. By contrast, transduced cells with both MOI showed a huge increase in production of luminescence signal, with MOI 20 being superior to MOI 10. Therefore, experiments were continued with R3/1 cells with NF-κB-Luc MOI 20. Moreover, IL-1α induced a higher inflammatory response through NF-κB than untreated cells, confirming the success of this assay.

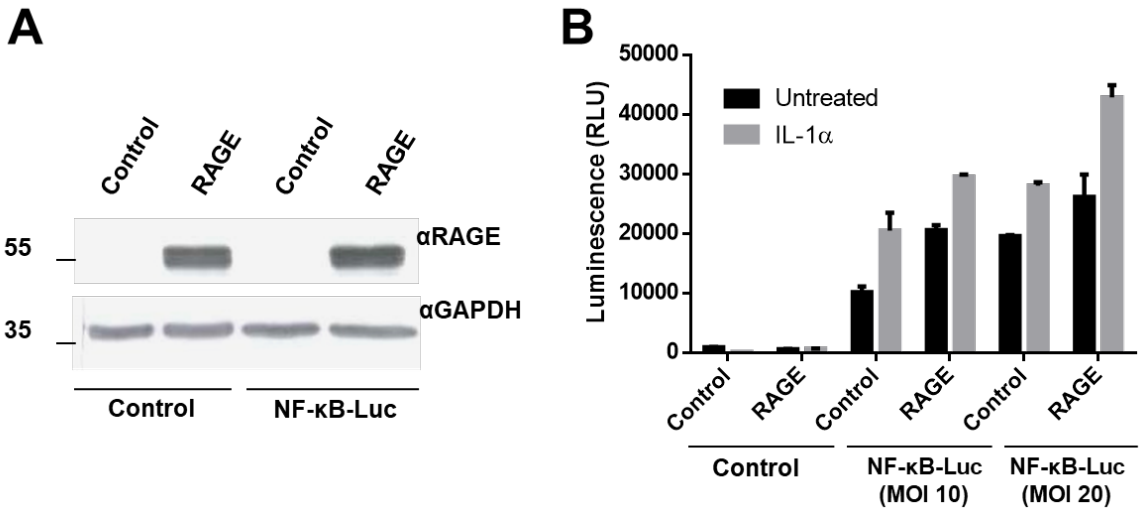

Figure 1. Luciferase expression in R3/1 clones. A) Expression of RAGE in R3/1 Control or R3/1 RAGE (Control or NF-κB-Luc) was determined with a specific antibody against the extracellular domain of RAGE. GAPDH detection was used as normalizer. B) Cells were stimulated for 24 hours with and without IL-1α in starvation medium. Control cells (no NF-κB-Luc) show no luminescence at all, whereas the transfected cells show a clear production of luminescence, increased at higher MOI. Shown are mean ± SEM.

7.3.2 Validating a RAGE-dependent mechanism

A good cell model was obtained for detecting pro-inflammatory activity, thus the next step was to explore the possibility of detecting a RAGE-dependent mechanism of the NF-κB pathway activation. To achieve this, ligands of RAGE were used known to activate the NF-κB pathway. Established ligands of RAGE are HMGB1 and AGEs, primarily HSA modified with fructose or glucose. Cells were treated with different compounds for 24 hours in medium without serum. Microscopical analysis was performed to identify cytotoxicity of the compounds, none was observed. Then, cells were harvested and lysed, followed by protein concentration determination to correct for the measured luciferase luminescence. Figure 2 shows that untreated RAGE cells already significantly express a higher basal level of NF-κB-dependent luciferase activity. IL-1α works very well as a positive control and the negative control for AGEs, HSA, does not induce a cellular response. The AGE, HSA modified with fructose, demonstrated an increased level in luminescence, however this is not RAGE dependent. Furthermore, NF-κB activity is increased in RAGE cells upon stimulation with HMGB1, nevertheless this is comparable with untreated cells.

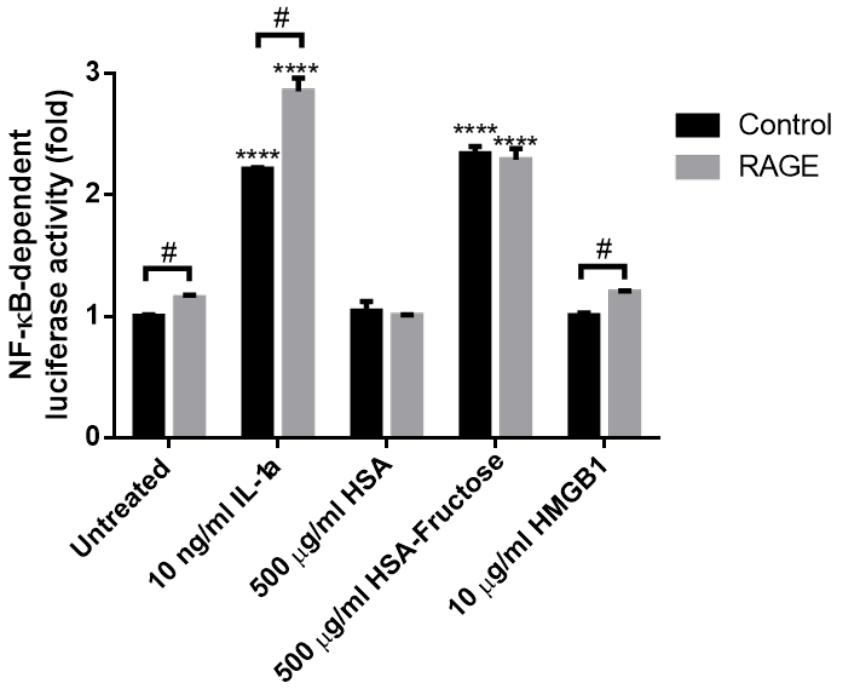

Figure 2. Treatment with known ligands of RAGE. Cells were treated 24 hours with indicated compounds. Results shown were corrected on protein concentration and compared to untreated control cells. Mean ± SEM analyzed using two-way ANOVA with Holm-Sidak correction (**p < 0.0001 was considered significant, CI 95%) to compare against untreated control cells or an unpaired Student's t-test (#p < 0.05, two-tailed, CI 95%) to compare between control and RAGE cells.**

7.3.3 Effects of AGEs/ALEs on control cells

An attempt was made to optimize the experiment to gain better results. Different timepoints were tested from 2 to 72 hours, various concentrations of AGEs were considered, and cells were starved before adding compounds to adopt to medium without serum. It should be taken into account that compounds were added in medium without serum considering that FBS contains high amount of oxidation products, and most likely also AGEs and/or ALEs. Moreover, different AGEs were tested for a RAGE-dependent NF-κB activity, such as HSA modified with fructose, glucose or commercially available glycated HSA. Unfortunately, we were unable to detect a RAGE-dependent mechanism for assessing NF-κB activity, suggesting that this experimental set-up is not suitable to identify RAGE ligands. Despite that, we observed that AGEs, as well as ALEs, were able to induce pro-inflammatory activity in R3/1 control cells independent of RAGE. Representative bar graphs are shown in figure 3. ALEs were produced by incubating HSA with different ratios, from 0.1 to 10X of RCS (HNE, ACR and MDA), and were pooled afterwards. Every

compound tested for NF-κB activity was also tested for cytotoxicity using an MTT assay, which clearly shows no toxic effect when compared to untreated. On the contrary, when treated, both AGEs and ALEs significantly increased cell viability, which can be explained by the fact that these compounds can be utilized by cells in absence of serum. NF-κB-dependent luciferase activity is also clearly increased when cells were stimulated with different AGEs, with emphasis on glycated HSA. Moreover, increasing ratio of RCS versus HSA also showed an increased NF-κB-dependent luciferase activity.

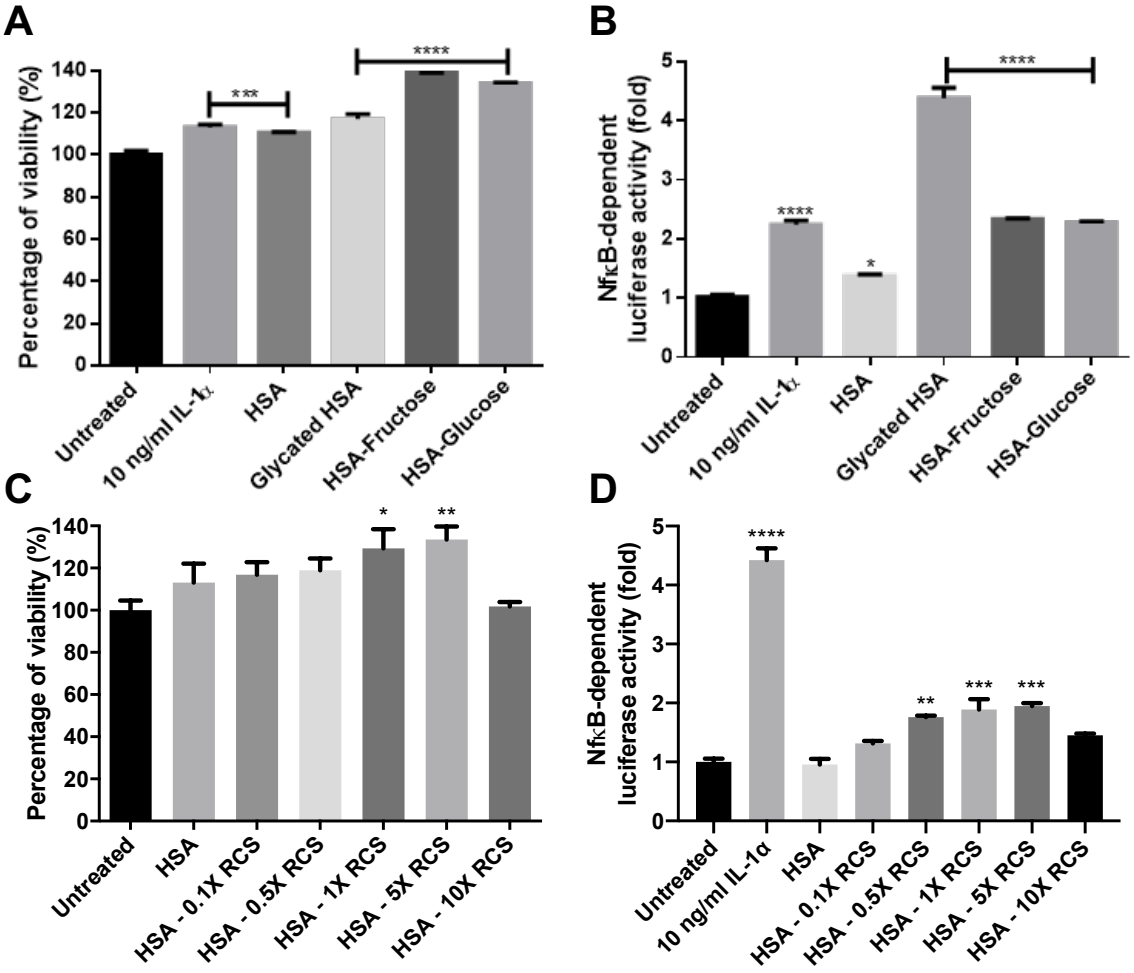

Figure 3. Increased NF-κB activity through different AGEs/ALEs. Cells were stimulated for 6 hours with indicated compounds, HSA and AGEs (top) or ALEs (bottom) were added at 500 µg/ml. Followed by an MTT assay (A,C) or by a luciferase luminescence measurement (B,D). Compared to untreated, mean ± SEM analyzed using ANOVA with Bonferroni correction (∗p < 0.05, ∗p < 0.01 ∗∗∗p < 0.001 and ∗∗∗∗p < 0.0001 were considered significant, CI 95%).

7.3.4 Proliferating effect of ALEs on control cells

Since both AGEs and ALEs showed an increase in proliferation, we sought to determine the effect of AGEs and ALEs on cell proliferation using the RealTime-Glo™ MT Cell Viability Assay from Promega. This assay allows us to monitor cell proliferation continuously up to 72 hours. The assay is based on the reduction of a substrate into a NanoLuc® substrate by viable cells, which is consumed by a NanoLuc® Enzyme to produce a luminescent signal. Non-viable cells are not able to produce this substrate and therefore no luminescent signal is produced. Figure 4 shows various assays, where AGEs demonstrate to have no effect on cell proliferation. Interestingly, ALEs did induce faster cell proliferation correlated to the amount of modification. The value for HSA – 10X RCS is out of range due to the high increase of the output of the assay. Figure 4C also shows a concentration dependent correlation with HSA modified with 1X RCS. To confirm this data, cells were incubated with the same compounds, and manually counted after 70 hours. Surprisingly, this data showed no increase in cell number, in contrast with the other assay. It was hypothesized, that ALEs do not increase cell proliferation, yet it increases the reduction potential of the cells. For example, via the upregulation of reducing enzymes due to activation of the nrf2 pathway.

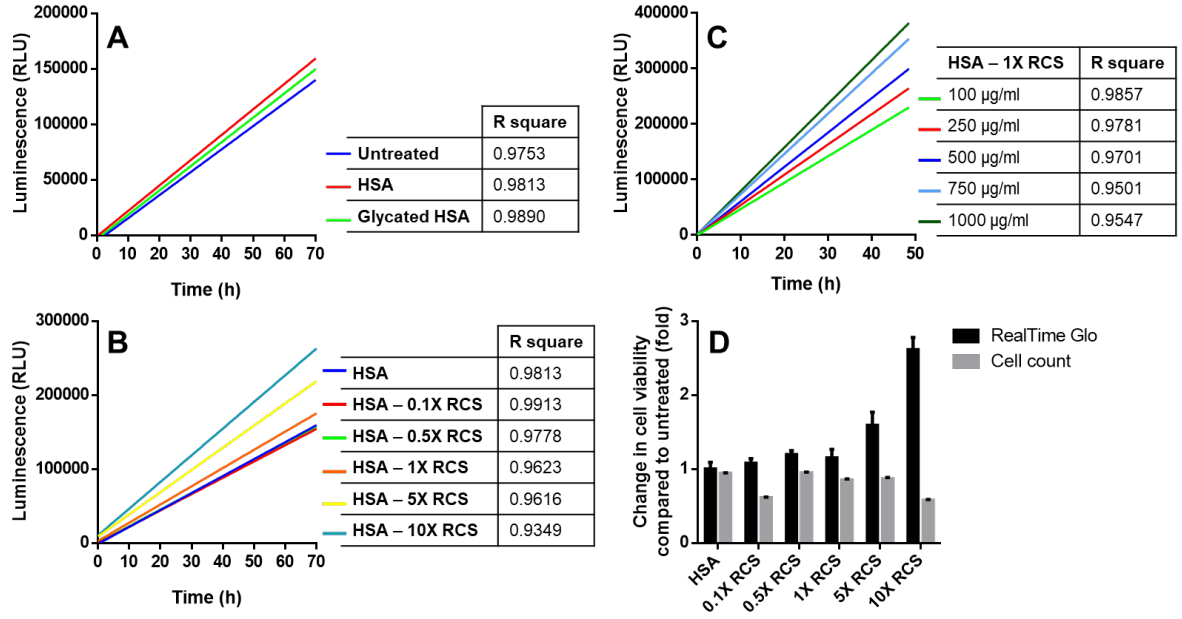

Figure 4. ALEs increase cell proliferation. A) R3/1 control cells were incubated with 500 µg/ml compounds in complete medium. Using RealTime-Glo™ MT Cell Viability Assay, luminescence was continuously monitored. Linear regression line was fitted and R square values were calculated. B) R3/1 control cells were incubated with 500 µg/ml increasing modified HSA with RCS. Linear regression line was fitted and R square values were calculated. C) Different concentrations of HSA – 1X RCS were tested for proliferation. Linear regression line was fitted and R square values were

calculated. D) Cells were incubated with the same compounds at 500 µg/ml and counted manually after 70 hours. Change in cell viability compared to HSA was plotted, together with the results from the RealTime-Glo assay after 70 hours.

To support the hypothesis of increased reducing potential of cells, an experiment was set-up to elaborately increase reducing enzymes in the cells. Bardoxolone is a known activator of the nrf2 pathway, which is activated to detoxify toxic compounds such as oxidants and RCS partly by the upregulation of reducing enzymes like aldo-keto reductases. This enzyme could be capable of reducing the cell viability substrate of RealTime-Glo and give a false positive signal in cell proliferation. Indeed, low concentrations of bardoxolone were able to increase the luminescence signal of the RealTime-Glo assay 5-fold, whereas MTT and cell count showed no increase in cell proliferation (Fig. 5).

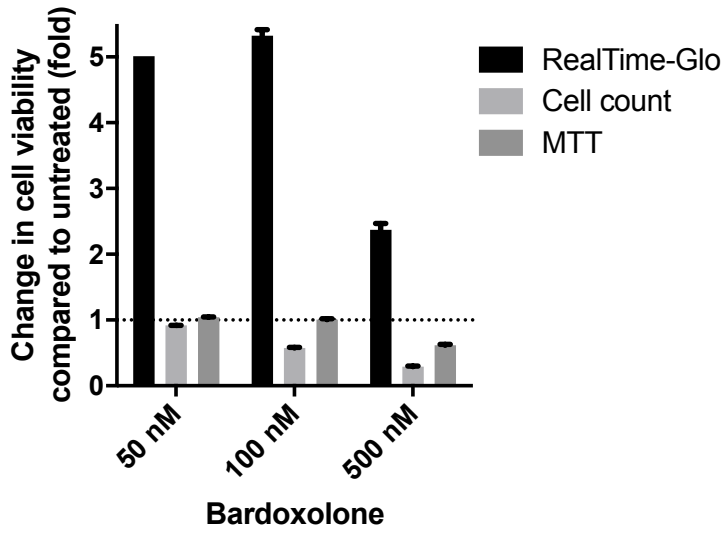

Figure 5. Bardoxolone increases the production of reducing enzymes. R3/1 control cells were incubated with different concentrations of bardoxolone for 24 hours, followed by the assessment of three different assays to determine cell proliferation. Compared to untreated of the relative assay, shown are mean ± SEM.

7.4. Discussion

AGEs are well known ligands of RAGE able to induce pro-inflammatory and pro-fibrotic activity through the NF-κB pathway [14-17]. ALEs, having great similarity to AGEs, have also been shown to induce pro-inflammatory and pro-fibrotic responses [18]. However, no specific receptor has yet been described to this cellular event. Since AGEs and ALEs are produced by similar pathways, oxidative degradation of either sugars or lipids forming protein adducts, the involvement of RAGE is very likely. Indeed, we have been able to demonstrate already using MS techniques and

molecular modelling studies that a specific set of ALEs can bind RAGE [5]. Therefore, we aimed to determine whether ALEs, like AGEs, can bind RAGE and induce a pro-inflammatory and pro-fibrotic response. To this end, we tried to set-up a cellular model for determining a RAGE-dependent activation of the NF-κB pathway. Although the cellular model was efficient in evaluating activation of the NF-κB pathway, the assay could not distinguish the involvement of RAGE using well-known ligands. This could be explained by the fact that the cell line overexpressing RAGE already shows a higher basal level of luciferase dependent NF-κB activity, suggesting that the cells are more vulnerable. Secondly, experiments were carried out in serum-free medium due to the high presence of oxidation products in fetal bovine serum, hence the incubation time was relatively short since cells do not respond well in serum-free medium. It is believed that the activation of RAGE needs long-term steady-state binding and activation for inducing down-stream signaling pathways, making this assay incompatible to study the effects of ALEs on RAGE binding and activation. Lastly, since the cells do not express RAGE by itself and had to be lentivirally transduced it is plausible to think that some key cellular components in the downstream pathway are missing. To circumvent this problem, future studies could instead focus on silencing the gene for RAGE in a cell line having basal expression of RAGE, like the human pulmonary epithelial cell line A549, to evaluate a RAGE dependent mechanism of NF-κB activation through ALEs [19].

Nevertheless, increased NF-κB activity was detected independently of RAGE in the presence of different AGEs, either suggesting a role for other receptors or no receptor involvement at all. Studies have shown already that the presence of AGEs induce a chronic state of inflammation and further studies are necessary to elucidate the mechanisms behind sustained NF-κB activity [20]. Proteomic wide studies are necessary to discover which cellular pathways are involved when cells are treated with AGEs. ALEs, besides showing an increased NF-κB activity as well, also showed an increase in RealTime Glo activity. This assay is originally intended to use for cell proliferation/cytotoxicity assays. Nonetheless, we observed an increase in this assay that was not related to the increase of cell number when manually counted. Indicating another mechanism potentially increasing luciferase dependent RealTime Glo activity. The assay is based on the reduction of a substrate by viable cells which is a company secret. The reduced substrate can then be converted into a compound producing light by the luciferase enzyme. The increase in luciferase activity could therefore be explained by the simple fact that other pathways are activated increasing the production of reducing enzymes. One of these pathways is the nrf2 pathway, activated under oxidative stress increasing the upregulation of anti-oxidant enzymes able to reduce oxidized biomolecules. Bardoxolone is a well-known activator of this pathway [21], and indeed showed a huge increase in RealTime Glo activity, confirming the suspicion of increased

reducing potential of the cells instead of actual cell proliferation. ALEs, but not AGEs, showed an increase using this assay, suggesting the capability of ALEs to activate the nrf2 pathway. RCS are activators of the nrf2 pathway, implying the release of RCS during incubation, via a retro-Michael mechanism, and sustained activation of the nrf2 pathway. Specific assays are necessary, like the nrf2 translocation assay or proteomic studies, to confirm the activation of this pathway.
In conclusion, due to limitations of the cellular model, a RAGE-dependent activity of AGEs/ALEs on the NF-κB pathway could not be determined. However, it can be used for determining pro-inflammatory activity. Furthermore, ALEs showed activation of the NF-κB pathway, a pro-inflammatory effect, as well as the nrf2 pathway, an anti-inflammatory effect. This contrary effect is likely concentration and/or type of ALEs based.

References

[1] S. Del Turco, G. Basta, An update on advanced glycation endproducts and atherosclerosis, Biofactors 38(4) (2012) 266-74.
[2] S. Sugiyama, T. Miyata, R. Inagi, K. Kurokawa, Implication of the glycoxidation and lipoxidation reactions in the pathogenesis of dialysis-related amyloidosis (Review), Int J Mol Med 2(5) (1998) 561-5.
[3] F.Y. Yap, P. Kantharidis, M.T. Coughlan, R. Slattery, J.M. Forbes, Advanced glycation end products as environmental risk factors for the development of type 1 diabetes, Curr Drug Targets 13(4) (2012) 526-40.
[4] J. Li, D. Liu, L. Sun, Y. Lu, Z. Zhang, Advanced glycation end products and neurodegenerative diseases: mechanisms and perspective, J Neurol Sci 317(1-2) (2012) 1-5.
[5] M. Mol, G. Degani, C. Coppa, G. Baron, L. Popolo, M. Carini, G. Aldini, G. Vistoli, A. Altomare, Advanced lipoxidation end products (ALEs) as RAGE binders: Mass spectrometric and computational studies to explain the reasons why, Redox Biol (2018) 101083.
[6] I. González, J. Romero, B.L. Rodríguez, R. Pérez-Castro, A. Rojas, The immunobiology of the receptor of advanced glycation end-products: trends and challenges, Immunobiology 218(5) (2013) 790-7.
[7] C. Ott, K. Jacobs, E. Haucke, A. Navarrete Santos, T. Grune, A. Simm, Role of advanced glycation end products in cellular signaling, Redox Biol 2 (2014) 411-29.
[8] X. Jiang, X. Wang, M. Tuo, J. Ma, A. Xie, RAGE and its emerging role in the pathogenesis of Parkinson's disease, Neurosci Lett 672 (2018) 65-69.
[9] K. Prasad, AGE-RAGE stress: a changing landscape in pathology and treatment of Alzheimer's disease, Mol Cell Biochem (2019).

[10] E.A. Oczypok, T.N. Perkins, T.D. Oury, All the "RAGE" in lung disease: The receptor for advanced glycation endproducts (RAGE) is a major mediator of pulmonary inflammatory responses, Paediatr Respir Rev 23 (2017) 40-49.
[11] B.I. Hudson, M.E. Lippman, Targeting RAGE Signaling in Inflammatory Disease, Annu Rev Med 69 (2018) 349-364.
[12] L. Sessa, E. Gatti, F. Zeni, A. Antonelli, A. Catucci, M. Koch, G. Pompilio, G. Fritz, A. Raucci, M.E. Bianchi, The receptor for advanced glycation end-products (RAGE) is only present in mammals, and belongs to a family of cell adhesion molecules (CAMs), PLoS One 9(1) (2014) e86903.
[13] M.T. Zeuner, T. Vallance, S. Vaiyapuri, G.S. Cottrell, D. Widera, Development and Characterisation of a Novel NF-, Mediators Inflamm 2017 (2017) 6209865.
[14] C.A. Downs, N.M. Johnson, G. Tsaprailis, M.N. Helms, RAGE-induced changes in the proteome of alveolar epithelial cells, J Proteomics 177 (2018) 11-20.
[15] S.S. Nah, I.Y. Choi, C.K. Lee, J.S. Oh, Y.G. Kim, H.B. Moon, B. Yoo, Effects of advanced glycation end products on the expression of COX-2, PGE2 and NO in human osteoarthritic chondrocytes, Rheumatology (Oxford) 47(4) (2008) 425-31.
[16] T. Okamoto, S. Yamagishi, Y. Inagaki, S. Amano, K. Koga, R. Abe, M. Takeuchi, S. Ohno, A. Yoshimura, Z. Makita, Angiogenesis induced by advanced glycation end products and its prevention by cerivastatin, FASEB J 16(14) (2002) 1928-30.
[17] H.M. Lander, J.M. Tauras, J.S. Ogiste, O. Hori, R.A. Moss, A.M. Schmidt, Activation of the receptor for advanced glycation end products triggers a p21(ras)-dependent mitogen-activated protein kinase pathway regulated by oxidant stress, J Biol Chem 272(28) (1997) 17810-4.
[18] N. Shanmugam, J.L. Figarola, Y. Li, P.M. Swiderski, S. Rahbar, R. Natarajan, Proinflammatory effects of advanced lipoxidation end products in monocytes, Diabetes 57(4) (2008) 879-88.
[19] N. Nakano, K. Fukuhara-Takaki, T. Jono, K. Nakajou, N. Eto, S. Horiuchi, M. Takeya, R. Nagai, Association of advanced glycation end products with A549 cells, a human pulmonary epithelial cell line, is mediated by a receptor distinct from the scavenger receptor family and RAGE, J Biochem 139(5) (2006) 821-9.
[20] M.W. Poulsen, R.V. Hedegaard, J.M. Andersen, B. de Courten, S. Bügel, J. Nielsen, L.H. Skibsted, L.O. Dragsted, Advanced glycation endproducts in food and their effects on health, Food Chem Toxicol 60 (2013) 10-37.

[21] S.A. Reisman, G.M. Chertow, S. Hebbar, N.D. Vaziri, K.W. Ward, C.J. Meyer, Bardoxolone methyl decreases megalin and activates nrf2 in the kidney, J Am Soc Nephrol 23(10) (2012) 1663-73.

Chapter VIII: General discussion

Chapter VIII: General discussion

Involvement of AGEs and ALEs in a wide variety of pathologies have been clearly described in the past decades and have become an important area of research due to the increasing exogenous sources as well as new techniques becoming available providing new information. Much focus has therefore been on elucidating the molecular mechanisms behind the formation of AGEs/ALEs, and the role they play in particular pathologies. The formation of AGEs/ALEs have been extensively described already [1], however this is a just a tip of the iceberg, and many more RCS are involved. Combining that with the whole proteome that can be adducted, sensitive, fast and reliable methods are necessary to understand what the molecular entities are leading to inflammation. Many methods have been set up already in addressing this matter, from MS methods to biochemistry and immunological techniques. The most used biochemistry technique is the derivatization with DNPH, and subsequent spectrophotometric methods to identify protein carbonyls [2]. Immunological techniques include the identification of specific adducts, such as protein carbonyls in general or HNE adducts, to give an example, using ELISA or western blotting [2-4]. These methods provide a general overview of the protein adducts present, despite that, no information can be obtained about the exact nature of the modification and the localization. Hence the use of MS methods, by far the most powerful and popular technique to characterize and localize protein adducts. Many MS methods have already been set up for in-vitro use for mapping adducts of model proteins with certain RCS [5-9]. Although these methods have been contributing to the discovery of AGEs/ALEs, very few methods have been able to translate this to physiological samples with low abundant AGEs/ALEs. For this purpose, enrichment techniques have been explored, including the VC1 pull-down, based on RAGE [10]. RAGE is also a key player in the signaling pathways of AGEs and their effect on cells in different pathologies, such as diabetes and atherosclerosis [11, 12]. Therefore, the thread of this thesis is to explore RAGE as a stationary phase for enriching AGEs/ALEs, to discover the molecular mechanisms of RAGE binding and the effect of AGEs/ALEs on cellular signaling pathways through RAGE.

AGEs and ALEs are very similar compounds, making it plausible to believe that besides AGEs, RAGE is also able to bind ALEs. The VC1 pull-down has already been shown to successfully capture AGEs, and the first part of the project was therefore focused on elucidating if this technique could also be used for capturing ALEs. Indeed, by using an integrated MS and computational approach, we discovered that RAGE is able to bind ALEs coming from HSA protein adducts with HNE, MDA and ACR. Specifically, those adducts that reduce the basicity of the target amino acid and the basic amino acid should be at the center of a set of carboxylic acids which,

once the residue is modified, become available to freely contact the RAGE positive residues. Consequently, we revealed a mechanism in which ALEs are able to bind RAGE, making the VC1 pull-down an even more promising technique in enriching AGEs/ALEs from samples. Apart from that, RAGE could also be involved in the signaling pathways that ALEs have been described in [13, 14].

Since a suitable enrichment strategy was obtained and validated to enrich functionally relevant AGEs/ALEs, we aimed to translate this to physiological samples where AGEs/ALEs are present in low amounts. We started by oxidizing healthy human plasma in-vitro to obtain a controllable model of plasma samples with AGEs/ALEs. AAPH was not suitable for producing AGEs/ALEs, although it did increase the presence of protein carbonyls significantly. Suggested is the direct oxidation of amino acids that can generate protein carbonyl groups as reviewed by Weber et al [15]. We advanced with the direct incubation of plasma with different RCS. HSA protein adduct formation was confirmed using intact protein analysis, unfortunately the VC1 pull-down was not able to enrich for AGEs/ALEs. This can be due to the interference and higher affinity of other proteins in plasma samples, such as prothrombin, which seems to be a strong binder of RAGE [unpublished data]. Other explanations could be the involvement of low molecular compounds present in plasma masking the molecular entities responsible for binding RAGE. Or the methods used for characterization, such as the MS used, are not sensitive enough for identifying low abundant AGEs/ALEs. Future studies will explore the possibilities of using the VC1 pull-down in tissue samples or cellular extracts.

The last argument leads us to the next part of the project, which was to improve other variables throughout the sample process and characterization. In particular, the use of the newest generation MS, the tribrid MS. In combination with the albuminomic approach and stabilizing certain adducts by means of reduction, we were able to identify a significant number of AGEs/ALEs present in healthy subject and heart failure patients. This is one of the first proofs of a huge number of identified AGEs/ALEs in plasma samples without the need of an enrichment step, hence very little sample preparation by using a high-resolution MS, Orbitrap Fusion. This demonstrates how powerful the tribrid orbitrap MS is when comparing it to other MS instruments, making it by far the most sensitive approach for characterizing AGEs/ALEs and perhaps many other PTMs. Considering that each and single AGE/ALE identified in heart failure patients and not in the control subjects could be a potential biomarker, we aim at setting up a targeted MS method, SIM, to validate the use of this approach and for future purposes.

Having demonstrated that ALEs are binder of RAGE, we also investigated whether ALEs can bind RAGE in a cellular model and activate the down-stream signaling pathways. The cellular model

containing a NF-κB gene reporter was successfully set-up, nonetheless the assay could not be validated by using well-known ligands of the receptor. Perhaps key cellular components of the downstream signaling pathways of RAGE are missing since the cell lines were transduced with the receptor. Thus a RAGE dependent NF-κB activation could not be determined, but AGEs/ALEs did activate the NF-κB pathway by other means. AGEs have been shown already to activate the NF-κB pathway [16], however the molecular mechanisms are still unclear and although one paper suggest the inhibition of autophagy resulting in NF-κB activation [17]. Our results also showed an increase in NF-κB activity upon stimulation with ALEs, not reported before. On the other hand, ALEs also increased the reducing potential of the cells, most likely related to the activation of the nrf2 pathway, a protective mechanism. This suggest that ALEs can either have a pro- or anti-inflammatory effect, most likely depending on the concentration and type of ALE. Proteomic studies are vital in understanding the pathways leading up to this.

In conclusion, besides AGEs, ALEs have been discovered as RAGE binders and the mechanism of action was deciphered using a computational approach. However, using RAGE as an enrichment technique was not sufficient for identifying low abundant AGEs/ALEs in plasma. Regardless, using the newest generation MS, for the first time a high number of AGEs/ALEs were identified with little sample preparation in plasma of healthy subjects and heart failure patients. Lastly, a RAGE dependent cellular activity could not be determined and more studies are necessary to understand the role of AGEs/ALEs on NF-κB activation.

References

[1] G. Vistoli, D. De Maddis, A. Cipak, N. Zarkovic, M. Carini, G. Aldini, Advanced glycoxidation and lipoxidation end products (AGEs and ALEs): an overview of their mechanisms of formation, Free Radic Res 47 Suppl 1 (2013) 3-27.

[2] G. Colombo, M. Clerici, M.E. Garavaglia, D. Giustarini, R. Rossi, A. Milzani, I. Dalle-Donne, A step-by-step protocol for assaying protein carbonylation in biological samples, J Chromatogr B Analyt Technol Biomed Life Sci 1019 (2016) 178-90.

[3] D. Weber, L. Milkovic, S.J. Bennett, H.R. Griffiths, N. Zarkovic, T. Grune, Measurement of HNE-protein adducts in human plasma and serum by ELISA-Comparison of two primary antibodies, Redox Biol 1 (2013) 226-33.

[4] J. Wu, X. Luo, L.J. Yan, Two dimensional blue native/SDS-PAGE to identify mitochondrial complex I subunits modified by 4-hydroxynonenal (HNE), Front Physiol 6 (2015) 98.

[5] C.B. Afonso, B.C. Sousa, A.R. Pitt, C.M. Spickett, A mass spectrometry approach for the identification and localization of small aldehyde modifications of proteins, Arch Biochem Biophys 646 (2018) 38-45.
[6] G. Aldini, I. Dalle-Donne, G. Vistoli, R. Maffei Facino, M. Carini, Covalent modification of actin by 4-hydroxy-trans-2-nonenal (HNE): LC-ESI-MS/MS evidence for Cys374 Michael adduction, J Mass Spectrom 40(7) (2005) 946-54.
[7] G. Aldini, L. Gamberoni, M. Orioli, G. Beretta, L. Regazzoni, R. Maffei Facino, M. Carini, Mass spectrometric characterization of covalent modification of human serum albumin by 4-hydroxy-trans-2-nonenal, J Mass Spectrom 41(9) (2006) 1149-61.
[8] G. Aldini, M. Orioli, M. Carini, Alpha,beta-unsaturated aldehydes adducts to actin and albumin as potential biomarkers of carbonylation damage, Redox Rep 12(1) (2007) 20-5.
[9] C.M. Spickett, A. Reis, A.R. Pitt, Use of narrow mass-window, high-resolution extracted product ion chromatograms for the sensitive and selective identification of protein modifications, Anal Chem 85(9) (2013) 4621-7.
[10] G. Degani, A.A. Altomare, M. Colzani, C. Martino, A. Mazzolari, G. Fritz, G. Vistoli, L. Popolo, G. Aldini, A capture method based on the VC1 domain reveals new binding properties of the human receptor for advanced glycation end products (RAGE), Redox Biol 11 (2017) 275-285.
[11] A.M. Kay, C.L. Simpson, J.A. Stewart, The Role of AGE/RAGE Signaling in Diabetes-Mediated Vascular Calcification, J Diabetes Res 2016 (2016) 6809703.
[12] E. McNair, M. Qureshi, K. Prasad, C. Pearce, Atherosclerosis and the Hypercholesterolemic AGE-RAGE Axis, Int J Angiol 25(2) (2016) 110-6.
[13] N. Shanmugam, J.L. Figarola, Y. Li, P.M. Swiderski, S. Rahbar, R. Natarajan, Proinflammatory effects of advanced lipoxidation end products in monocytes, Diabetes 57(4) (2008) 879-88.
[14] U. Hardt, A. Larsson, I. Gunnarsson, R.M. Clancy, M. Petri, J.P. Buyon, G.J. Silverman, E. Svenungsson, C. Grönwall, Autoimmune reactivity to malondialdehyde adducts in systemic lupus erythematosus is associated with disease activity and nephritis, Arthritis Res Ther 20(1) (2018) 36.
[15] D. Weber, M.J. Davies, T. Grune, Determination of protein carbonyls in plasma, cell extracts, tissue homogenates, isolated proteins: Focus on sample preparation and derivatization conditions, Redox Biol 5 (2015) 367-380.
[16] B.K. Rodiño-Janeiro, B. Paradela-Dobarro, S. Raposeiras-Roubín, M. González-Peteiro, J.R. González-Juanatey, E. Álvarez, Glycated human serum albumin induces NF-κB activation

and endothelial nitric oxide synthase uncoupling in human umbilical vein endothelial cells, J Diabetes Complications 29(8) (2015) 984-92.
[17] Y.M. Song, S.O. Song, Y.H. You, K.H. Yoon, E.S. Kang, B.S. Cha, H.C. Lee, J.W. Kim, B.W. Lee, Glycated albumin causes pancreatic β-cells dysfunction through autophagy dysfunction, Endocrinology 154(8) (2013) 2626-39.

Appendix I: Anti-inflammatory activity

Appendix I: Anti-inflammatory activity

1. Introduction

Sustained NF-κB activation has been shown to lead to chronic inflammatory diseases and in search of preventive and/or curative medicine, natural compounds could be a key candidate due to the presence of many anti-oxidants [1]. Advantages of natural compounds are that they are freely available, new compounds can be discovered compared to standard combinatorial chemistry and less toxic effects compared to synthesized compounds. Since the NF-κB pathway is a good model of evaluating the pro- or anti-inflammatory response, we sought to determine the anti-inflammatory effect of natural compounds, known to have a high antioxidant property. Natural compounds such as apple, bergamot and artichoke have a very high content of polyphenols and have been positively linked in mediating chronic inflammatory diseases [2-5]. Inflammation is often accompanied by an increase in ROS which can exceed the anti-oxidant capacity available in the body. Therefore, the intake of natural antioxidant sources can prevent or mediate the increase in ROS and related inflammatory activity.

Polyphenols are very diverse compounds containing two or more phenol rings, and aid in the protection of plants against pathogens and UV radiation. This group of compounds have been researched extensively due to the fact that they contain different chemical properties, however, the mechanism of action remains largely unknown and the efficacy is often low. Fractionating polyphenol extracts could lead to the discovery of new compounds, and can be tested directly by evaluating the anti-inflammatory effect mediated by the NF-κB pathway. Therefore, this part of the project was to investigate the anti-inflammatory role of crude or purified extracts of natural occurring compounds in preventing sustained inflammation through the activation of the NF-κB pathway using the cellular model set-up previously.

2. Material and Methods

2.1 Chemicals and reagents

IL-1α, rosiglitazone and all other chemicals were purchased from Sigma-Aldrich (Milan, Italy). ONE-Glo Luciferase Assay System and RealTime-Glo MT Cell Viability Assay were purchased from Promega (USA).

2.2 Cell Culture

R3/1 control cells containing the NF-κB reporter gene were grown in Dulbecco modified Eagle medium (DMEM; Lonza, Verviers, Belgium) supplemented with 10% fetal bovine serum (FBS; Gibco). Cells were seeded at 3.000 cells/well in a 96-wells plate for the assessment of anti-inflammatory activity and incubated overnight before stimulation.

2.3 Preparation of natural extracts

Both bergamot juice and apple pulp extract were obtained by an enrichment of the phenolic fraction by using a polystyrene resin column (Mitsubishi). The elution was carried out by a mild KOH solution (pH = 8.5). A cationic resin at acid pH was used to neutralize the extract, that was then dried under vacuum. The so obtained extract were then weighed and dissolved in DMSO or directly in DMEM for the tests.

2.4 Stimulation of Cells

To assess the anti-inflammatory activity, cells were pre-treated with different compounds at different concentrations for 18 hours in complete medium, followed by a 6-hour stimulation with 10 ng/ml IL-1α. Experiments were assayed by NF-κB luciferase activity, RealTime-Glo assay or an MTT assay.

2.5 NF-κB luciferase activity assay

After treatment, cells were washed twice with cold PBS followed by a freeze-thaw cycle with reporter lysis buffer (Promega) for complete cell lysis. After the freeze-thaw cycle, 100 µl ONE-Glo Luciferase Assay Substrate (Promega) was directly added to the wells, followed by a luciferase measurement performed using a luminometer (WALLAC 1420, Multilabel counter, Perkin Elmer life and Analytical Sciences).

2.6 RealTime-Glo assay

RealTime-Glo assay was performed following manufacturer's instructions. In brief, for end-point measurements, medium containing compounds was removed and replaced with medium containing RealTime-Glo reagents, incubated for 30 min. at 37°C and luciferase was measured using a luminometer (WALLAC 1420, Multilabel counter, Perkin Elmer life and Analytical Sciences).

2.7 MTT assay

After stimulation, 10 µl 5 mg/ml MTT reagent was added for 4 hours. Afterwards, medium was removed, and cells were lysed and MTT was solubilized by adding 100 µl DMSO. 96-wells plate was shaken for 1 minute, followed by an absorbance measurement at 490 nm using a plate reader (BioTek's PowerWave HT, USA). Cells incubated with respective concentration of DMSO (<0.1%) were used as a control for 100% cell proliferation. Statistical analysis was performed in the GraphPad software. Experiments were performed with biological and technical replicates.

3. Results

3.1 Rosiglitazone as NF-κB inhibitor

Since an indication was obtained in chapter 7 that bardoxolone is able to increase the reducing potential of cells, and potentially providing protection to the cells, we were also interested to see if this compound would be able to decrease inflammatory activity. Accordingly, cells were incubated for 18 hours with bardoxolone, followed by a 6-hour stimulation with IL-1α. Lower concentrations of bardoxolone were used, due to the toxic effects of bardoxolone at higher concentrations. Where 10 and 50 nM significantly increased NF-κB dependent luciferase activity, 100 nM was efficiently in reducing the activity.

Considering that this assay was able to detect anti-inflammatory activity, an attempt was made to optimize this experiment using a compound that is known to possess anti-inflammatory activity through NF-κB, rosiglitazone [6]. Without doubt, rosiglitazone can reduce pro-inflammatory activity at all concentrations tested and does not show toxicity (Fig. 1). Moreover, we can state that it does not increase the reducing potential of the cell.

3.2 Natural compounds

Previous experiments with bardoxolone and rosiglitazone have shown that the cellular model can be utilized for other purposes than intended. Therefore, our interest was shifted to the identification of anti-inflammatory activity of polyphenolic natural compounds, including apple and bergamot fruit extracts (Fig. 2). Apple pulp extract demonstrated a significant increase in cell viability using the RealTime-Glo assay from 50 µg/ml, but not observed using the MTT assay, suggesting the increase in production of reducing enzymes. In fact, at the concentration of 500 µg/ml the MTT assay showed a significant toxic effect, while the RealTime-Glo assay is still significantly increased. Pulp extract of apple also showed an effect at 50 µg/ml onwards by the inhibition of the NF-κB pathway. At the same time, an extract of the bergamot fruit was assayed for the same activity. From 250 µg/ml a significant increase in cell viability was observed using the RealTime-Glo and MTT assay, while a significant decrease is already detected at 1 µg/ml regarding the inhibition of the NF-κB pathway.

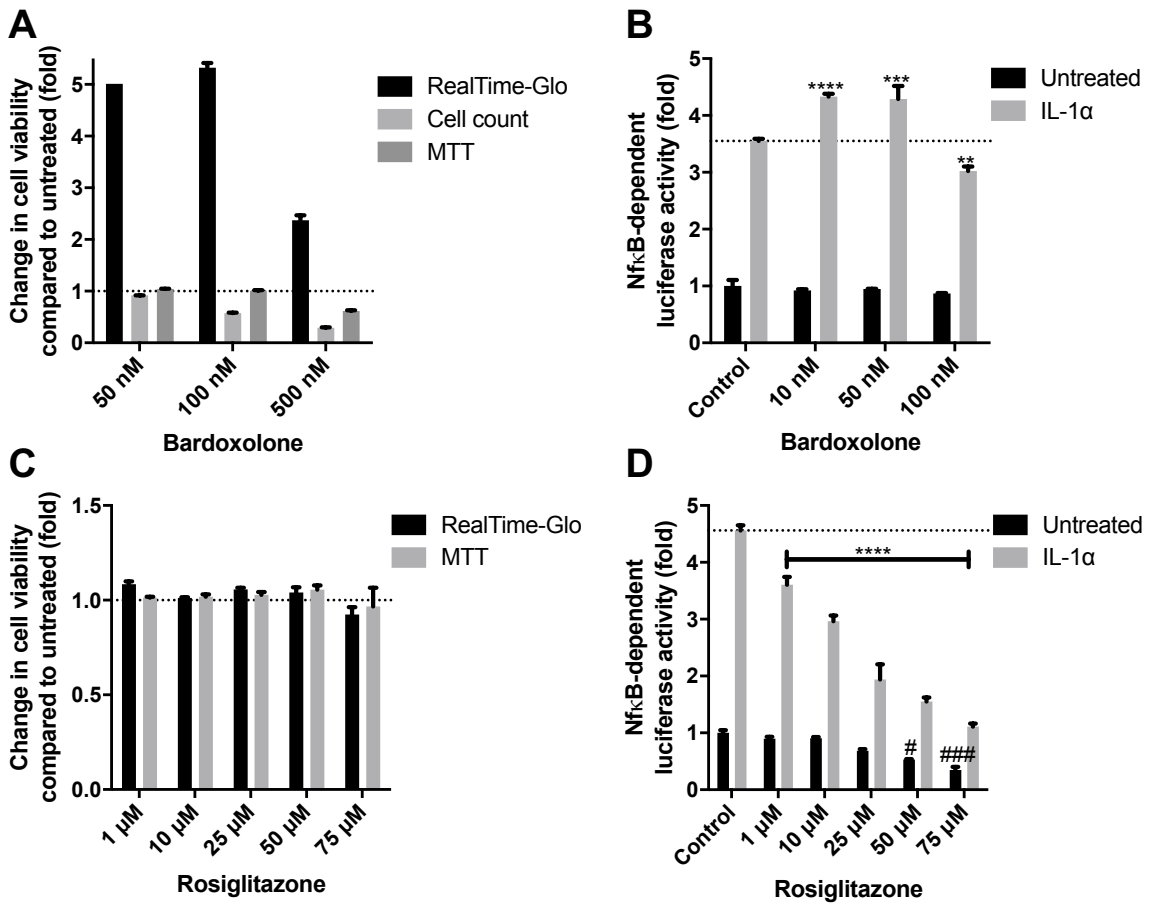

Figure 1. Bardoxolone increases the production of reducing enzymes and rosiglitazone is able to reduce NF-κB activity. A) R3/1 control cells were incubated with different concentrations of bardoxolone for 24 hours, followed by the assessment of three different assays to determine cell proliferation. Compared to untreated of the relative assay, shown are mean ± SEM. B) R3/1 control cells were incubated for 18 hours with different concentrations of bardoxolone, followed by a 6 hour stimulation with IL-1α. Then NF-κB dependent luciferase activity was measured. Compared to control untreated, mean ± SEM are shown. Analyzed using two-way ANOVA with Bonferroni correction (compared to control IL-1α, **p < 0.01, ***p < 0.001 and ****p < 0.0001 were considered significant, CI 95%). C) R3/1 control cells were incubated with different concentrations of rosiglitazone for 24 hours, followed by the assessment of cell viability using MTT and RealTime-Glo. Compared to untreated of the relative assay, shown are mean ± SEM. D) R3/1 control cells were incubated for 18 hours with different concentrations of rosiglitazone, followed by a 6 hour stimulation with IL-1α. Then NF-κB dependent luciferase activity was measured. Compared to control untreated, mean ± SEM are shown. Analyzed using two-way ANOVA with Bonferroni correction (compared to control untreated, #p < 0.05 and ###p < 0.001, compared to control IL-1α, ****p < 0.0001 were considered significant, CI 95%).

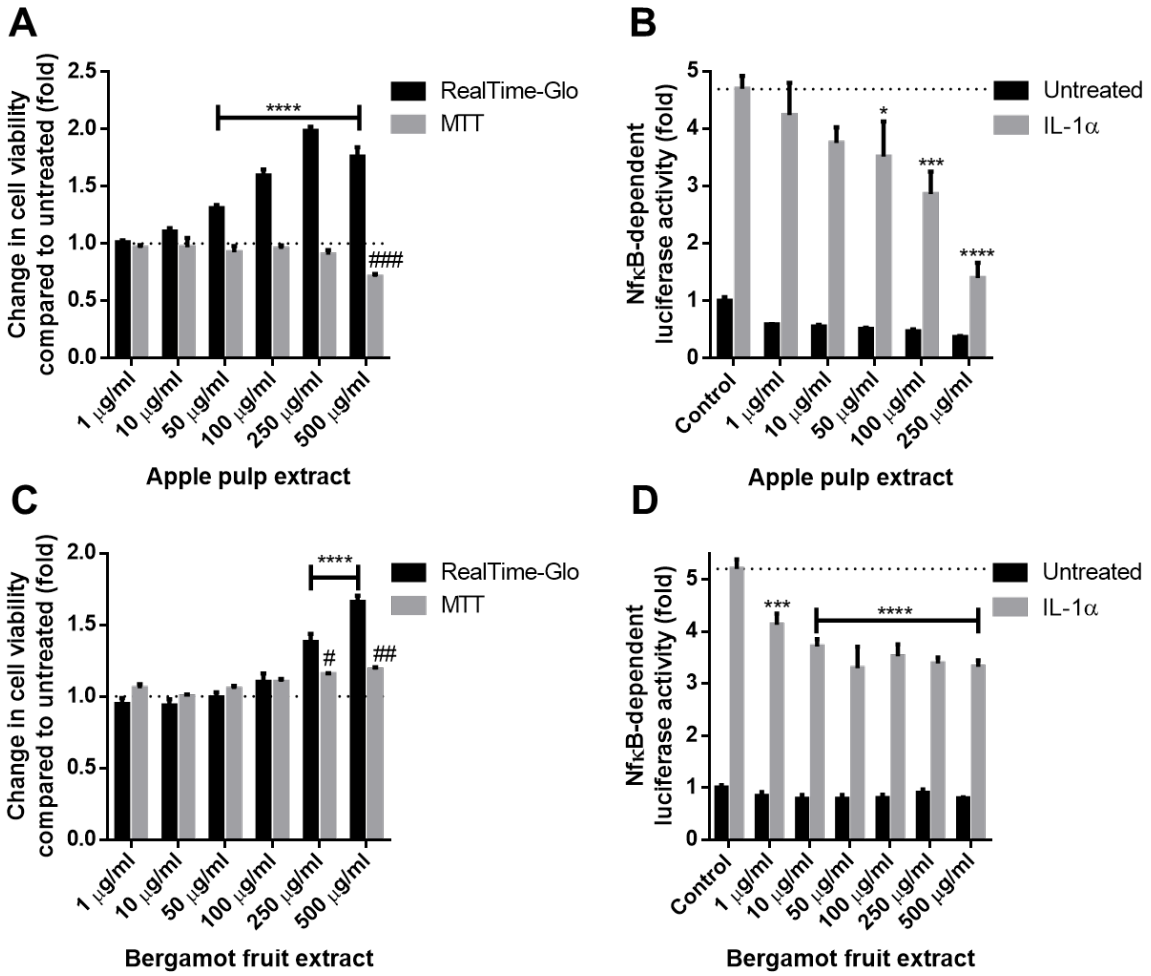

Figure 2. Polyphenolic compounds are able to increase the reduction potential of R3/1 cells and decrease pro-inflammatory activity through the NF-κB pathway. A and C) R3/1 control cells were incubated with different concentrations of apple pulp extract (A) or bergamot fruit extract (C) for 24 hours, followed by the assessment of cell proliferation using MTT and RealTime-Glo. Compared to untreated of the relative assay, shown are mean ± SEM. Analyzed using two-way ANOVA with Bonferroni correction (compared to untreated RealTime-Glo, ∗∗∗∗p < 0.0001, compared to untreated MTT, #p < 0.05, ##p < 0.01 and ###p < 0.001 were considered significant, CI 95%). B and D) R3/1 control cells were incubated for 18 hours with different concentrations of apple pulp extract (B) or bergamot fruit extract (D), followed by a 6 hour stimulation with IL-1α. Then NF-κB dependent luciferase activity was measured. Compared to control untreated, mean ± SEM are shown. Analyzed using two-way ANOVA with Bonferroni correction (compared to control IL-1α, ∗p < 0.05, ∗∗∗p < 0.001 and ∗∗∗∗p < 0.0001 were considered significant, CI 95%).

4. Discussion

Since the activation of the nrf2 pathway is a cellular defense mechanism aiming to reduce inflammatory activity, we sought to determine if this cellular model could be utilized for determining anti-inflammatory activity through the NF-κB pathway. For this purpose, cells were pre-treated with rosiglitazone, to validate the assay since it is known to reduce NF-κB activity [7], and subsequently treated with IL-1α, used to induce NF-κB activity. In fact, low concentrations of rosiglitazone successfully reduced NF-κB activity in the cells. To link the upregulation of the nrf2 pathway and reduction in NF-κB activity together, we explored the possibilities of natural compounds with high content of polyphenols and anti-oxidant activity. This area of research, using natural compounds as medicine, is extensively investigated due to the many advantages compared to synthesized compounds. Several natural compounds and extracts were obtained and tested for anti-inflammatory activity, as well as for the increase in RealTime Glo activity, most likely related to activation of the nrf2 pathway. Apple and bergamot fruits did show the potential of using natural compounds for reducing inflammatory activity through the NF-κB pathway, as already shown by many different papers [2, 8]. However, the herein described cellular model could be utilized as a high-throughput assay able to test the anti-inflammatory activity in a fast and sensitive manner, together with the assessment of a possible link with the nrf2 pathway. Further studies are necessary to validate the use of this strategy.

References

[1] M.J. Killeen, M. Linder, P. Pontoniere, R. Crea, NF-κβ signaling and chronic inflammatory diseases: exploring the potential of natural products to drive new therapeutic opportunities, Drug Discov Today 19(4) (2014) 373-8.

[2] R. Risitano, M. Currò, S. Cirmi, N. Ferlazzo, P. Campiglia, D. Caccamo, R. Ientile, M. Navarra, Flavonoid fraction of Bergamot juice reduces LPS-induced inflammatory response through SIRT1-mediated NF-κB inhibition in THP-1 monocytes, PLoS One 9(9) (2014) e107431.

[3] X.J. Li, Z. Zhu, S.L. Han, Z.L. Zhang, Bergapten exerts inhibitory effects on diabetes-related osteoporosis via the regulation of the PI3K/AKT, JNK/MAPK and NF-κB signaling pathways in osteoprotegerin knockout mice, Int J Mol Med 38(6) (2016) 1661-1672.

[4] W.C. Huang, C.L. Lai, Y.T. Liang, H.C. Hung, H.C. Liu, C.J. Liou, Phloretin attenuates LPS-induced acute lung injury in mice via modulation of the NF-κB and MAPK pathways, Int Immunopharmacol 40 (2016) 98-105.

[5] P. Arulselvan, M.T. Fard, W.S. Tan, S. Gothai, S. Fakurazi, M.E. Norhaizan, S.S. Kumar, Role of Antioxidants and Natural Products in Inflammation, Oxid Med Cell Longev 2016 (2016) 5276130.
[6] Y.F. Zhang, X.L. Zou, J. Wu, X.Q. Yu, X. Yang, Rosiglitazone, a Peroxisome Proliferator-Activated Receptor (PPAR)-γ Agonist, Attenuates Inflammation Via NF-κB Inhibition in Lipopolysaccharide-Induced Peritonitis, Inflammation 38(6) (2015) 2105-15.
[7] J.W. Mao, H.Y. Tang, Y.D. Wang, Influence of Rosiglitazone on the Expression of PPARγ, NF-κB, and TNF-α in Rat Model of Ulcerative Colitis, Gastroenterol Res Pract 2012 (2012) 845672.
[8] D. Zhang, M. Mi, F. Jiang, Y. Sun, Y. Li, L. Yang, L. Fan, Q. Li, J. Meng, Z. Yue, L. Liu, Q. Mei, Apple polysaccharide reduces NF-Kb mediated colitis-associated colon carcinogenesis, Nutr Cancer 67(1) (2015) 177-90.